UNIVERSITAT DE VALÈNCIA

FACULTAT DE MEDICINA I ODONTOLOGIA

DEPARTAMENT DE FARMACOLOGIA

MITOCHONDRIA AND ENDOPLASMIC RETICULUM INTERPLAY AT THE CORE OF EFAVIRENZ-INDUCED HEPATIC EFFECTS

Tesis doctoral

MIRIAM POLO PEÑALVER

Directores:

Dr. Juan Vicente Esplugues Mota

Dra. Nadezda Apostolova

Dr. Víctor Manuel Víctor González

Valencia, 2016

UNIVERSITAT DE VALÈNCIA
FACULTAT DE MEDICINA I ODONTOLOGIA
DEPARTAMENT DE FARMACOLOGIA

Dr. JUAN VICENTE ESPLUGUES MOTA, Catedrático de Universidad en el Departamento de Farmacología de la Universidad de Valencia,

Dra. NADEZDA APOSTOLOVA, Profesor Ayudante Doctor en el Departamento de Farmacología de la Universidad de Valencia y

Dr. VICTOR MANUEL VICTOR GONZÁLEZ, Investigador en FISABIO-Hospital Dr. Peset y Profesor Asociado en el Departamento de Fisiología de la Universidad de Valencia,

CERTIFICAN:

Que el trabajo titulado "Mitochondria and endoplasmic reticulum interplay at the core of efavirenz-induced hepatic effects", presentado por la Licenciada en Biotecnología **Dña. Miriam Polo Peñalver,** ha sido realizado bajo nuestra dirección y asesoramiento en el Departamento de Farmacología de la Facultad de Medicina y Odontología de la Universidad de Valencia.

Concluido el trabajo experimental y bibliográfico, autorizamos la presentación y la defensa de esta Tesis Doctoral.

Para que así conste a los efectos oportunos, se expide la presente certificación en Valencia, a 1 de Diciembre de 2016.

Fdo. Dr. Juan Vicente Esplugues Mota **Fdo. Dra. Nadezda Apostolova**

Fdo. Dr. Víctor Manuel Víctor González

This doctoral thesis has been supported by the following grants and projects:

- Predoctoral trainee research grant Vali+d (ACIF/2013/136) from Conselleria d'Educació, Cultura i Esport, Generalitat Valenciana.
- Predoctoral trainee research grant for a stay in a research center out of Valencian Community (BEFPI/2015/004), Conselleria d'Educació, Cultura i Esport, Generalitat Valenciana.
- “Experimental pharmacology of the digestive tract" (PROMETEO/2010/060). Aid program for the development of I+D actions by research groups of excellence. PI: Juan Vicente Esplugues Mota. Funding body: Conselleria d'Educació, Cultura i Esport, Generalitat Valenciana. Duration: 5 years (2010 – 2014).
- "Characterization of new cellular mechanisms of antiretroviral hepatotoxicity" (PI11/00237). PI: Juan Vicente Esplugues Mota. Funding body: Ministry of economy and competitiveness. Duration: 3 years (2012 – 2014).
- "Influence of autophagy and endoplasmic reticulum stress on hepatotoxicity induced by antiretrovirals" (UV-INV-PRECOMP12-80613). PI: Nadezda Apostolova. Funding body: University of Valencia. Duration: 1 year (2012 – 2013).
- “Autophagy, mitochondrial dysfunction and endoplasmic reticulum stress: keys to understand the hepatic toxicity induced by the antiretroviral drug Efavirenz” (GV/2014/118). PI: Nadezda Apostolova. Funding body: Conselleria d'Educació, Cultura i Esport, Generalitat Valenciana. Duration: 2 years (2014 – 2015).
- “Pharmacology of the digestive tract and inflammation” (PROMETEOII/2014/035). PI: Juan Vicente Esplugues Mota. Funding body: Conselleria d'Educació, Cultura i Esport, Generalitat Valenciana. Duration: 4 years (2014 – 2017).
- “Role of anti-HIV drugs in the onset and/or progression of non-alcoholic fatty liver disease” (PI14/00312). PI: Nadezda Apostolova. Funding body: Instituto de Salud Carlos III, Ministry of economy and competitiveness. Duration: 3 years (2015 – 2017).

“Trabajar duro por algo que no nos interesa se llama estrés, trabajar duro por algo que amamos se llama pasión”

-Peter Drucker-

A mi familia

ACKNOWLEDGEMENTS

La elección de una carrera universitaria es una de las decisiones más importantes en la vida de cualquier estudiante. Elegí la Licenciatura de Biotecnología porque siempre me ha gustado la investigación científica y, desde que empecé la carrera, hacer una tesis doctoral era algo que me llamaba la atención. Gracias a la realización del trabajo final de máster en un grupo de investigación de excelencia tuve la oportunidad de conseguir una beca predoctoral, y ya han pasado casi cuatro años desde entonces. Prácticamente, sin haberme dado cuenta, he finalizado esta etapa de mi vida que ha sido dura pero a la vez maravillosa. En estos años he aprendido a confiar más en mí misma, a ser independiente y a trabajar en equipo, a defender mis ideas y aceptar las críticas, a trabajar duro y sobre todo a valorar la suerte que he tenido de poder trabajar en lo que me gusta. En definitiva, estos años me han enseñado tantas cosas a nivel personal y profesional, que me gustaría compartir el mérito de esta tesis con todas aquellas personas que he tenido el placer de conocer en todo este tiempo y que, sin duda alguna, han influido en mi vida.

En primer lugar, me gustaría dar las gracias a mis directores de tesis. Al Dr. Juan Vicente Esplugues, a la Dra. Nadezda Apostolova y al Dr. Víctor Manuel Víctor por la dirección y asesoramiento. Muchas gracias Juan Vicente por haber confiado en mí y por darme la oportunidad de formar parte de tu grupo de investigación. También quiero dar las gracias a Nade por todo el trabajo y tiempo invertido en mí, por transmitirme su pasión por la ciencia, por confiar en mí siempre, por enseñarme a ser crítica con mi trabajo, por ayudarme a crecer tanto a nivel personal como profesional, por sus consejos, por su paciencia; en definitiva, gracias Nade por haber hecho que la tesis sea una etapa tan positiva para mí. También quiero agradecerle a Víctor su apoyo a la hora de pedir la beca predoctoral, muchas gracias por confiar en mí.

Sin duda alguna, quiero dar las gracias a mi “Liver Team” porque sin ellos la tesis no hubiera sido lo mismo. A Haryes por enseñarme y apoyarme en mis comienzos, por sus consejos y sus ánimos, y por ser tan buena persona. Haryes, ha sido un placer trabajar contigo, te echamos mucho de menos. Gracias Ana por tu apoyo, por tus consejos y por esa alegría que transmites cada día en el laboratorio. Qué pena que durante el

último año hayamos coincidido tan poquito. A mis chicos preferidos, Nando y Alberto, que más que compañeros son amigos. Desde luego que hacer la tesis ha merecido la pena solo por conocer a personas como vosotros. Muchísimas gracias por estar siempre cuando lo necesitaba, por vuestra ayuda, apoyo, consejos, por las risas a diario; sois increíbles!!! (como dice Bisbal, jejeje). Alberto, "serranico", no cambies nunca. Nos queda pendiente la excursión por nuestros pueblos!!! Nando, "Poison" jajaja, empezamos la tesis juntos y la terminamos también casi a la vez. No tengo palabras para agradecerte todo lo que me has ayudado, ha sido un placer trabajar contigo. No me olvido de María, muchísimas gracias guapa por tu ayuda, gente tan trabajadora como tú hay poca. Gracias por el buen rollo que transmites, por tu sentido del humor y por alegrar el laboratorio cada día.

Por supuesto, quiero dar las gracias a Dulce e Isa por todos los buenos momentos que hemos pasado, por las risas y los cotilleos que tanto nos gustan, jejeje. Ajonjolinas, estoy segura de que todavía nos quedan muy buenos momentos por pasar juntas ☺. También me gustaría dar las gracias a Dolo, Raquel, Lara, Amelia, Pedro, Ángela, Olga, Antonio, Edu, Tati, Jorge, César, Patri, Victor, Laura, Fernando, Nicole, Samu, Mariam y Ainhoa por hacer el día a día en el laboratorio mucho más fácil. A Jesús, por todos los buenos momentos que hemos vivido desde la carrera hasta ahora, gracias por tus consejos, ánimos y por tu ayuda. A Raúl y Dora por facilitarnos el trabajo experimental en el laboratorio. También a Loles, Ángeles, Sara, Carlos, Mª Ángeles y Miguel por sus consejos y por demostrar su dedicación y pasión por la ciencia. Gracias Brian por hacernos las cosas del laboratorio mucho más fáciles y por tu ayuda con el inglés. A todas las personas que componen el Departamento de Farmacología, muchísimas gracias por todo.

Durante la realización de la tesis he tenido la oportunidad de disfrutar de una estancia predoctoral en Módena que me ha aportado mucho a nivel personal y profesional. Me gustaría darle las gracias al Dr. Andrea Cossarizza por haberme permitido disfrutar de la estancia en su laboratorio. A toda la gente del laboratorio, Marcello, Milena, Sara, Lara, Simone, Elena y Regina, por toda la ayuda recibida, vuestra paciencia y por hacerme fácil el trabajo en vuestro laboratorio, grazie mille!

También me gustaría darle las gracias al Dr. Ricardo Flores por permitirme llevar a cabo el fracionamiento subcelular en su laboratorio, gracias por su ayuda y asesoramiento.

Muchísimas gracias a todos mis amigos de la carrera y, sobre todo, a mis Campeñ@s por todos los momentos que hemos vivido, y los que nos quedan por vivir juntos. Muchísimas gracias por vuestro apoyo incondicional, los consejos y los ánimos recibidos desde que os conozco. También le quiero dar las gracias a mi cuñada por ser tan buena persona, por sus ánimos y por su apoyo, muchas gracias Lidia por estar siempre que lo he necesitado.

Para finalizar, me gustaría dar las gracias a mi familia, a la que le dedico esta tesis y sin la cual su realización no hubiera sido posible. A mis padres y a mi hermano por apoyarme y estar pendientes de mí en todo momento, muchísimas gracias por creer siempre en mí. A mis abuelos, por todo su cariño y todo lo que han hecho por mí a lo largo de mi vida. A mis tios y primos por sus ánimos y confiar en mí. Y, especialmente, me gustaría agredecerle a Víctor su apoyo incondicional desde que le conozco, hace ya más de 10 años. Muchas gracias Kari por sacarme siempre una sonrisa, por estar siempre dispuesto a ayudarme, por tus ánimos, tus consejos; en definitiva, gracias por ser como eres, a tu lado soy la mujer más feliz del mundo. Os quiero muchísimo a todos!!

ABBREVIATIONS

2-DG	2-Deoxy-D-glucose
3TC	Lamivudine
A	Ampere
ABC	Abacavir
Aco2	Aconitase
ACTB	β-actin
ADP	Adenosine diphosphate
AIDS	Acquired immunodeficiency syndrome
ALAS-1	5-aminolevulinic acid synthase
AMP	Adenosine monophosphate
APS	Ammonium persulfate
ASC	Apoptosis-associated speck-like protein
ASK1	Apoptosis signal-regulating kinase 1
ATF4	Activating transcription factor-4
ATF6	Activating transcription factor-6
ATFS-1	Activating transcription factor associated with stress-1
ATP	Adenosine triphosphate
ATPase	ATP synthase
ATV	Atazanavir
ATV/COBI	ATV enhanced with COBI
ATV/r	ATV enhanced with RTV
AZT	Azidothymidine
BAPTA	1,2-bis(o-aminophenoxy)ethane-N,N,N’,N’-tetraacetic acid
BCA	Bicinchoninic acid
Bcl-2	B-cell lymphoma 2
BiP	Binding immunoglobulin protein
BSA	Bovine serum albumin
CI	Complex I
CII	Complex II
CIII	Complex III
CIV	Complex IV

CV	Complex V
cART	Combined antiretroviral therapy
CAV1	Caveolin-1
CBS	Cystathionine β-synthase
CCCP	Protonophore carbonyl cyanide m-chloro phenyl hydrazone
CDK1	Cyclin B1/cyclin-dependent kinase 1
cDNA	Complementary DNA
ChIP	Chromatin immunoprecipitation
CHOP	C/EBP homologous protein (or GADD153)
ClpX	Caseinolytic protease X
C_{max}	Maximum concentration
C_{min}	Minimum concentration
CNX	Calnexin
CoA	Coenzyme A
COBI	Cobicistat
CSIC	Consejo superior de investigaciones científicas
CYP	Cytochrome P450
CYPA	Cyclophylin A
Cyt *c*	Cytochrome *c*
d4T	Stavudine
ddI	Didanosine
DMEM	Dulbecco's modified eagle's medium
DMSO	Dimethylsulfoxide
DNA	Deoxyribonucleic acid
dNTP	Deoxynucleotide triphosphate
Drp1	Dynamin-related protein 1
DRV	Darunavir
DRV/COBI	DRV enhanced with COBI
DRV/r	DRV enhanced with RTV
dsRNA	Double-stranded RNA
DTG	Dolutegravir

DTT	Dithiothreitol
EDTA	Ethylenediaminetetraacetic acid
EFV	Efavirenz
EGTA	Ethylene glycol tetraacetic acid
eIF2α	Eukaryotic initiation factor 2α
EIs	Entry Inhibitors
ER	Endoplasmic reticulum
ERAD	ER-associated degradation
Ero1α	ER oxidoreductase 1 alpha
EtBr	Ethidium bromide
ETC	Electron transport chain
ETR	Etravirine
EVG	Elvitegravir
EVG/COBI	EVG enhanced with COBI
FACL4	Long chain acyl-CoA synthetase
FAM82A2	Family with sequence similarity 82, member A2
FBS	Foetal bovine serum
FDA	Food and drug administration
FIs	Fusion inhibitors
Fis1	Fission 1
FPV	Fosamprenavir
FTC	Emtricitabine
GADD153	Growth arrest- and DNA damage-inducible gene 153
GAPDH	Glyceraldehyde 3-phosphate dehydrogenase
GDP	Guanosine diphosphate
GESIDA	Grupo de estudio del SIDA (AIDS study group)
GLS-1	Glutaminase C
Grp75	Glucose-regulated protein 75
Grp78	78 kDa glucose-regulated protein (or BiP)
GTP	Guanosine triphosphate
HAART	Highly active antiretroviral therapy

HBSS	Hank's balanced salt solution
HBV	Hepatitis B virus
HCl	Hydrochloric acid
HCV	Hepatitis C virus
HEPES	4-(2-hydroxyethyl)-1-piperazineethanesulfonic acid
HIF-1	Hypoxia-inducible factor 1
HIV	Human immunodeficiency virus
HO.	Hydroxyl radical
Hoechst 33342	Bisbenzimide H 33342 trihydrochloride
HPRT1	Hypoxanthine phosphoribosyltransferase 1
HSCs	Hepatic stellate cells
HSP	Heat shock protein
HSP90AA1	HSP90 alpha class A member 1
HSP90AB1	HSP90 alpha class B member 1
HSP90B1	HSP90 beta member 1
IB	Isolation buffer
IBM	Inner boundary membrane
IBMCP	Instituto de Biología Molecular y Celular de Plantas
IDV	Indinavir
IgG	Immunoglobulin G
IIs	Integrase inhibitors
IMM	Inner mitochondrial membrane
IMS	Mitochondrial intermembrane space
IP_3	Inositol-1,4,5-triphosphate
IP_3Rs	IP_3 receptors
IRE1	Inositol-requiring transmembrane kinase/endoribonuclease 1
kDa	Kilodalton
L-NAME	Nω-Nitro-L-arginine methyl ester
LDH	Lactate dehydrogenase
LONP1	Mitochondrial Lon protease
LONP2	Peroxisomal Lon protease

LPV	Lopinavir
Lys	Lysine
MAMs	Mitochondria-associated membranes
MAVS	Mitochondrial antiviral-signalling protein
MEFs	Mouse embryonic fibroblasts
MELAS	Mitochondrial encephalomyopathy, lactic acidosis, and stroke-like episodes
MEM	Minimum essential medium
MERRFs	Myoclonic epilepsy with ragged-red fibres
Mff	Mitochondrial fission factor
Mfn1	Mitofusin 1
Mfn2	Mitofusin 2
MiD49	Mitochondrial dynamics proteins of 49 kDa
MiD51	Mitochondrial dynamics proteins of 51 kDa
MM	Mitochondrial matrix
MRB	Mitochondria resuspending buffer
mRNA	Messenger RNA
mtDNA	Mitochondrial DNA
MTS	Mitochondrial targeting sequence
MVC	Maraviroc
MW	Molecular weight
N/A	Not reported or available
NAD	Nicotinamide adenine dinucleotide
NADH	Reduced NAD
NAO	10-N-nonyl-acridine-orange-chloride
NEAA	Non-essential amino acids
NF-κB	Nuclear factor-kappa B
NFV	Nelfinavir
NLRP3	Nod-like receptor family, pyrin domain containing 3
NNRTIs	Non-nucleoside reverse transcriptase inhibitors
NOS	Nitric oxide synthase

NRF-2	Nuclear respiratory factor 2
NRTIs	Nucleoside reverse transcriptase inhibitors
NVP	Nevirapine
$O_2.^-$	Superoxide
OMM	Outer mitochondrial membrane
$ONOO^-$	Peroxynitrite
OPA1	Optic atrophy protein 1
OxPhos	Oxidative phosphorylation
PACS-2	Phosphofurin acidic cluster sorting protein 2
PBS	Phosphate-buffered saline
PC	Phosphatidylcholine
PCR	Polymerase chain reaction
PDI	Protein disulphide isomerase
PE	Phosphatidylethanolamine
PERK	RNA-dependent protein kinase-like eIF2α kinase
PEs	Pharmacokinetic enhancers
P_i	Inorganic phosphate
PI	Propidium iodide
PINK1	PTEN-induced putative kinase-1
PIs	Protease inhibitors
PMA	Phorbol-12-myristate-13-acetate
Pol-γ	Polymerase-γ
PQC	Protein quality control
PS	Phosphatidylserine
PS2	Presenilin-2
PTEN	Phosphatase and tensin homolog
PTPIP51	Protein tyrosine phosphatase-interacting protein 51 (or FAM82A2)
RAL	Raltegravir
RIG-I	Retinoic acid inducible gene I
RNA	Ribonucleic acid
$RO_2.$	Peroxyl radical

ROS	Reactive oxygen species
Rot	Rotenone
RPMI	Roswell park memorial institute
RPV	Rilpivirine
rRNA	Ribosomal RNA
RT	Room temperature
RT-PCR	Reverse transcription PCR
RTV	Ritonavir
RyRs	Ryanodine receptors
SDS	Sodium dodecyl sulfate
SDS-PAGE	Sodium dodecyl sulphate-polyacrylamide gel electrophoresis
Ser	Serine
SERCA	Sarco-endoplasmic reticulum Ca^{2+}-ATPase
SIG-1R	Sigma1-receptor
siRNA	Small interfering RNA
SIRT3	Sirtuin 3
SQV	Saquinavir
StAR	Steroidogenic acute regulatory protein
STS	Staurosporine
T-20	Enfuvirtide
TAE	Tris-acetate-EDTA
TBS	Tris-buffered saline
TBS-T	TBS-Tween
TDF	Tenofovir disoproxil fumarate
TE	Tris-EDTA
TEMED	N,N,N´,N´-Tetramethylethylendiamine
TFAM	Mitochondrial transcription factor A
TG	Thapsigargin
TMRM	Tetramethylrhodamine methyl ester perchlorate
TOM20	Translocase of OMM 20
TPV	Tipranavir

Tris	2-Amino-2-hydroxymethyl-propane-1,3-diol
tRNA	Transfer RNA
TXNIP	Thioredoxin-interacting protein
UCIM	Unidad central de investigación de medicina
UCP	Uncoupling protein
UNAIDS	Joint united nations programme on HIV/AIDS
UPR	Unfolded protein response
UPRmt	Mitochondrial unfolded protein response
UPV	Universidad politécnica de Valencia
V	Volts
VAP-B/C	Vesicle-associated membrane protein-associated protein B/C
VDAC1	Voltage-dependent anion channel 1
Veh	Vehicle
WB	Western blot
WHO	World health organization
WT	Wild-type
ZDV	Zidovudine
Δp	Proton electrochemical gradient potential
$\Delta\Psi_m$	Mitochondrial membrane potential

LIST OF FIGURES

LIST OF TABLES

ABSTRACT

The non-nucleoside analogue reverse transcriptase inhibitor efavirenz (EFV) is among the most widely used drugs in the combined antiretroviral therapy (cART) employed in the treatment of human immunodeficiency virus (HIV) infection. Although generally considered safe, there is a concern about the side effects induced by EFV-containing therapies. It has been associated with hepatic toxicity and metabolic disturbances and, although the mechanisms involved are not clear, recent evidence has pinpointed a specific mitochondrial action of EFV accompanied by the induction of an endoplasmic reticulum (ER) stress/unfolded protein response in cultured human hepatic cells.

In the present work, in order to understand the role of mitochondria in the effects of EFV, firstly, we have assessed the cellular actions of this drug in a model of hepatic cells that lack functional mitochondria (rho^{o} cells generated in Hep3B background). In addition, we have studied mitochondrial dynamics, in wild-type Hep3B cells, which depends among other processes on the interaction between mitochondria and ER. This interaction has also been analysed by evaluation of mitochondria-associated membranes (MAMs). Finally, in order to further link the two effects of EFV (mitochondria and ER), we have analysed the expression of LONP1, a highly conserved mitochondrial protease whose activation is an adaptive mechanism in both oxidative and ER stress. Throughout the manuscript, the effects of EFV have been compared to those induced by the classic pharmacological inducer of ER stress thapsigargin (TG), the typical mitotoxic agent rotenone (Rot) - a standard complex I inhibitor - and the uncoupler of OxPhos CCCP.

On the one hand, EFV-treated rho^{o} cells exhibited a substantial reduction in parameters indicative of mitochondrial interference, such as increased superoxide production, mitochondrial mass/morphology alterations and enhanced expression of LONP1. In line with these results, the cytotoxic effect (cell number, chromatin condensation, cell cycle alterations and induction of apoptosis) of EFV was less pronounced in Hep3B respiration-depleted cells than in wild-type cells. The effect of EFV was both similar and different from those of two distinct mitochondrial stressors, TG and Rot, depending on the parameter studied.

On the other hand, markers of mitochondrial dynamics were expressed differentially with the stimuli used (EFV, TG, Rot and CCCP), which points to a specificity of the dual

ER/mitochondrial stress induced by EFV. EFV treatment enhanced mitochondria/ER interorganelle interaction, as shown by co-immunoprecipitation experiments of MAMs protein partners. In addition, LONP1 was upregulated at mRNA and protein levels under all conditions. Surprisingly, upon treatment with EFV, its extramitochondrial presence (ER and MAMs) increased.

In conclusion, hepatic cells lacking normal mitochondria (rho^{o}) are less vulnerable to EFV. This finding may account for the idiosyncratic hepatic reactions triggered by anti-HIV drugs and may also explain the different degrees of susceptibility to liver damage seen in patients undergoing antiretroviral therapy. The specific dual mitochondria-ER effect induced by EFV enhances MAMs content and this is associated with increased extramitochondrial LONP1 expression. This is the first report of this phenomenon in mammalian cells and suggests a novel MAMs-linked function of LONP1.

RESUMEN

El inhibidor de la transcriptasa inversa no análogo de nucleósido efavirenz (EFV) es uno de los fármacos más utilizados en la terapia antirretroviral combinada (TARc) empleada en el tratamiento de la infección por el virus de la inmunodeficiencia humana (VIH). Aunque en general se ha considerado seguro, existe una gran preocupación acerca de los efectos secundarios inducidos por las terapias que contienen EFV. Este fármaco se ha asociado con toxicidad hepática y trastornos metabólicos y, aunque los mecanismos implicados no están claros, evidencias recientes han señalado una acción mitocondrial específica de EFV acompañada por la inducción de estrés de retículo endoplasmático (RE)/respuesta a proteínas desplegadas en células hepáticas humanas cultivadas.

En el presente trabajo, con el objetivo de entender el papel de la mitocondria en los efectos inducidos por EFV, en primer lugar, hemos evaluado las acciones celulares de este fármaco en un modelo de células hepáticas que carecen de mitocondrias funcionales (células rho^{o} generadas en el fondo Hep3B). Además, hemos estudiado la dinámica mitocondrial, en células Hep3B *wild-type*, que depende entre otros procesos de la interacción entre las mitocondrias y el RE. Esta interacción también se ha analizado mediante la evaluación de las membranas asociadas a las mitocondrias (MAMs). Por último, con el fin de vincular aún más los dos efectos de EFV (mitocondria y RE), hemos analizado la expresión de LONP1, una proteasa mitocondrial altamente conservada cuya activación es un mecanismo adaptativo tanto en el estrés oxidativo como en el de RE. A lo largo del manuscrito, los efectos de EFV se han comparado con los inducidos por un inductor farmacológico clásico del estrés de RE, tapsigargina (TG), el agente mitotóxico típico rotenona (Rot) - un inhibidor estándar del complejo I - y el desacoplador de la OxPhos, CCCP.

Por un lado, las células rho^{o} tratadas con EFV mostraron una reducción importante en los parámetros indicativos de interferencia mitocondrial, tales como aumento de la producción de superóxido, alteraciones en la morfología y masa mitocondrial, y aumento de la expresión de LONP1. En consonancia con estos resultados, el efecto citotóxico (número de células, condensación de la cromatina, alteraciones del ciclo celular e inducción de la apoptosis) de EFV fue menos pronunciado en las células Hep3B deficientes de respiración que en las células *wild-type*. El efecto de EFV fue

tanto similar como diferente de los efectos producidos por dos factores distintos de estrés mitocondrial, TG y Rot, dependiendo del parámetro estudiado.

Por otro lado, los marcadores de la dinámica mitocondrial se expresaron de forma diferente con los estímulos utilizados (EFV, TG, Rot y CCCP), lo que apunta a una especificidad del doble estrés mitocondrial/RE inducido por EFV. El tratamiento con EFV potenció la interacción entre las mitocondrias y el RE, como se muestra por los experimentos de co-inmunoprecipitación de los complejos proteicos de las MAMs. Además, LONP1 fue regulado positivamente tanto a nivel de ARNm como de proteína en todas las condiciones. Sorprendentemente, tras el tratamiento con EFV, su presencia extramitocondrial (RE y MAMs) aumentó.

En conclusión, las células hepáticas que carecen de mitocondrias normales (rho^{o}) son menos vulnerables a EFV. Este hallazgo puede explicar las reacciones hepáticas idiosincrásicas desencadenadas por los fármacos anti-VIH y también los diferentes grados de susceptibilidad al daño hepático observados en pacientes sometidos a terapia antirretroviral. El doble efecto mitocondria-RE específico inducido por EFV aumenta el contenido de MAMs y esto está asociado con el aumento de la expresión extramitocondrial de LONP1. Este es el primer informe de este fenómeno en células de mamífero y sugiere una función novedosa de LONP1 relacionada con las MAMs.

INDEX

I. INTRODUCTION

1. OVERVIEW OF THE HUMAN IMMUNODEFICIENCY VIRUS INFECTION

The human immunodeficiency virus (HIV), classified within the genus *Lentivirus, Retroviridae* family, is the causative agent of acquired immunodeficiency syndrome (AIDS) (Barre-Sinoussi F. *et al*., 1983). Two types of genetically different HIV has been described, HIV-1 and HIV-2 which have similar epidemiological characteristics; although HIV-1 is more widespread and is responsible for most cases of infection and HIV-2, less transmissible and pathogenic, is found mainly in West Africa (De Cock K.M. *et al*., 1993). According to WHO and UNAIDS, at the end of 2015 there were in the world about 36.7 million people infected with HIV. That same year, about 2.1 million people became newly infected and around 1.1 million died from AIDS-related causes (WHO and UNAIDS, 2016).

1.1. Life cycle and infection by the human immunodeficiency virus

HIV can infect a variety of immune cells such as CD4+ T cells, macrophages and microglial cells where viral replication occurs. Lentiviruses are transmitted as single-stranded enveloped RNA viruses; upon entry into the target cell, the viral RNA genome is converted into double-stranded DNA by a virally encoded reverse transcriptase enzyme. The resulting viral DNA is integrated into the human genome by a virally encoded integrase and uses the cell machinery for its expression (Smith J.A. and Daniel R., 2006).

The HIV life cycle is carried out in several steps (Fig.I.1). It begins with the entry in the cell by associating the virus with a CD4 receptor and a co-receptor on the CD4+ T cell surface, followed by fusion of the viral envelope with the cell membrane and the release of the HIV capsid into the cell. After reverse transcription of viral RNA into viral DNA by HIV reverse transcriptase, the viral DNA is integrated into the host cell's genome by the viral integrase. After transcription and translation, some RNAs function as new copies of the virus genome, while others function as mRNAs to produce structural proteins. The final step of the viral cycle is the assembly, with the action of the viral protease, of new mature HIV virions which are able to infect another cell (Zheng Y.H. *et al*., 2005; Smith J. A. and Daniel R., 2006).

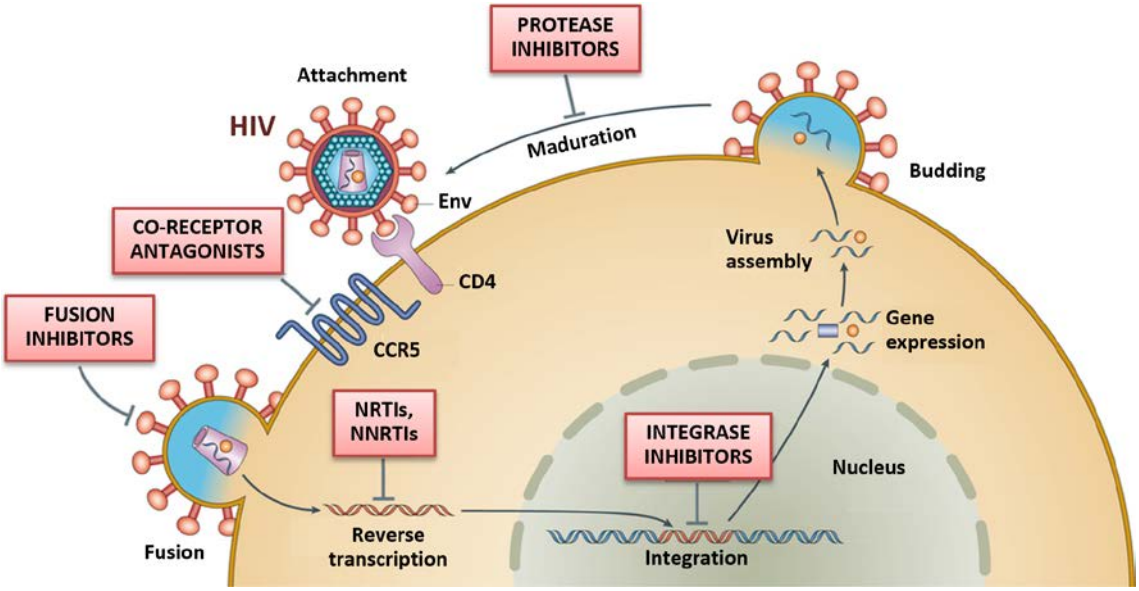

Figure I.1. Schematic representation of the HIV life cycle (modified from Laskey S.B. and Siliciano R.F., 2014). The boxes represent the different classes of antiretroviral drugs and blue arrows show the site of the viral cycle on which they act. NRTIs and NNRTIs: nucleoside and non-nucleoside reverse transcriptase inhibitors.

HIV transmission is only possible through contact between body fluids that have a high viral concentration, such as sexual contact, parenteral exposure to blood or contaminated blood products, and vertical transmission from mother to foetus or neonate during birth or through breast milk (Crandall K.A., 2001).

HIV infection develops in several stages identified by a set of symptoms and clinical indicators. Although it may be highly variable among patients, is characterized by a brief acute phase associated with high levels of viral load; followed by a clinical latency stage, asymptomatic, in which a gradual deterioration of the immune system occurs with a great production of new viral particles and a decrease in the number of CD4+ T cells; finally culminating with the development of AIDS. This critical stage of HIV infection occurs when the immune system is unable to replace CD4+ T lymphocytes lost during the virus attack, so that plasma levels of these cells fall below $2x10^5$ cells/mL of blood. This phenomenon makes the host vulnerable to opportunistic infections (Pantaleo G. *et al.,* 1993).

2. ANTIRETROVIRAL THERAPY

Zidovudine (ZDV), also known as azidothymidine (AZT), was the first effective antiretroviral drug against HIV. It was synthesized by Jerome Horwitz in 1964 as a false nucleoside to be used as an antineoplastic. In 1985 it was found that AZT was effective against HIV *in vitro* (Mitsuya H. *et al*., 1985) and the U.S. FDA (Food and Drug Administration) approved its use for the treatment of this infection in 1987 (Fischl M.A. *et al*., 1987).

The treatment of HIV was revolutionized in the mid-1990s with the development of the first compounds of new pharmacological families, and the introduction of drug regimens that combined these agents, called highly active antiretroviral therapy (HAART) or combined antiretroviral therapy (cART). The increased efficacy of these combined treatments is due to the increased number of obstacles for viral replication, which leads to reduction in plasma viral load resulting in a significant reconstitution of the immune system (Autran B. *et al*. 1997; Komanduri K.V. *et al*. 1998; Lederman M.M. *et al*. 1998). Antiretroviral agents individually do not suppress HIV long term, therefore they should be used in combination regimen to achieve the greatest possible benefit, the better tolerability and compliance, and reduce the risk of resistance development (De Clercq E., 2009). cART has resulted in longer survival in infected patients due to the restoration and preservation of their immune functions, which leads to reduced mortality and morbidity, improving their quality of life (Mocroft A. *et al*., 2003; Panos G. *et al*., 2008). The drawback is that the viral genome in the host tissue cannot be eradicated, meaning an immunological and clinical deterioration of infected people.

Currently, 26 antiviral drugs are approved by FDA for HIV treatment (Tab.I.1) and classified in seven families according to the mechanism by they which interfere with the replicative cycle of the virus (Fig.I.1):

- Nucleoside Reverse Transcriptase Inhibitors (NRTIs)
- Non-Nucleoside Reverse Transcriptase Inhibitors (NNRTIs)
- Protease Inhibitors (PIs)
- Fusion Inhibitors (FIs)
- Entry Inhibitors (EIs) or CCR5 co-receptor antagonists

- Integrase Inhibitors (IIs)
- Pharmacokinetic Enhancers (PEs)

2.1. Nucleoside Reverse Transcriptase Inhibitors (NRTIs)

NRTIs were the first approved anti-HIV drugs and their mechanism of action is based on inhibiting the activity of HIV reverse transcriptase (Balzarini J., 1994). They are analogues of the naturally occurring deoxynucleotides (adenosine, cytidine, guanosine and thymidine) needed to synthesize the viral DNA. NRTIs are administered as prodrugs; once inside the cell, they must be activated (phosphorylated) to generate 5'-triphosphate which is incorporated into cellular DNA as alternative substrate, except for tenofovir, which is a nucleotide analogue (has an activated phosphate group in its chemical structure and therefore does not require this chemical process). The incorporation of NRTIs leads to the termination of the growing viral DNA chain because of the lack of a 3'-OH terminus that prevents the addition of more nucleotides (Hao Z. *et al*., 1990; De Clercq E., 2002).

2.2. Non-Nucleoside Reverse Transcriptase Inhibitors (NNRTIs)

These agents inhibit HIV reverse transcriptase by non-competitively binding to a hydrophobic pocket near its catalytic site, which alters the spatial conformation of the substrate-binding site and reduces the enzyme´s polymerase activity (De Clercq E., 2009). They are characterized by a long half-life in plasma, which allows the administration in a single daily dose. Because they are metabolised through the P450 pathway and the fact that there is great variability in the isozymes involved for each compound, their plasma levels can change and may also be influenced by the interactions with other drugs metabolised through the same pathway. These anti-HIV drugs are also characterized by a low barrier to resistance (Blas-Garcia A. *et al.,* 2011).

2.3. Protease Inhibitors (PIs)

PIs interfere with the last step of the viral replication cycle by blocking the action of the viral protease and thus preventing the formation of infectious viral particles. These drugs are similar to the substrates of HIV protease, an enzyme responsible for the

cleavage of the viral polyprotein precursors during virion maturation (Wensing A.M. *et al.,* 2010).

DRUG CLASS	GENERIC NAME	BRAND NAME	FDA APPROVAL DATE
NRTIs	Abacavir (ABC)	Ziagen	December 17, 1998
	Didanosine (ddI)	Videx	October 9, 1991
	Emtricitabine (FTC)	Emtriva	July 2, 2003
	Lamivudine (3TC)	Epivir	November 17, 1995
	Stavudine (d4T)	Zerit	June 24, 1994
	Tenofovir disoproxil fumarate (TDF)	Viread	October 26, 2001
	Zidovudine (ZDV)	Retrovir	March 19, 1987
NNRTIs	Efavirenz (EFV)	Sustiva	September 17, 1998
	Etravirine (ETR)	Intelence	January 18, 2008
	Nevirapine (NVP)	Viramune	June 21, 1996
	Rilpivirine (RPV)	Edurant	May 20, 2011
PIs	Atazanavir (ATV)	Reyataz	June 20, 2003
	Darunavir (DRV)	Prezista	June 23, 2006
	Fosamprenavir (FPV)	Lexiva	October 20, 2003
	Indinavir (IDV)	Crixivan	March 13, 1996
	Nelfinavir (NFV)	Viracept	March 14, 1997
	Ritonavir (RTV)	Norvir	March 1, 1996
	Saquinavir (SQV)	Invirase	December 6, 1995
	Tipranavir (TPV)	Aptivus	June 22, 2005
	Lopinavir (LPV)	Kaletra*	September 15, 2000
FIs	Enfuvirtide (T-20)	Fuzeon	March 13, 2003
CCR5 Antagonist	Maraviroc (MVC)	Selzentry	August 6, 2007
IIs	Dolutegravir (DTG)	Tivicay	August 13, 2013
	Elvitegravir (EVG)	Vitekta	September 24, 2014
	Raltegravir (RAL)	Isentress	October 12, 2007
PEs	Cobicistat (COBI)	Tybost	September 24, 2014

Table I.1. FDA-approved HIV drugs (AIDSinfo, 2016). *Ritonavir-boosted lopinavir.

2.4. Fusion Inhibitors (FIs)

FIs were designed to prevent virus entry into the host cell by binding to the gp41 protein located in the viral envelope. The binding prevents conformational changes required for the fusion of the viral envelope with the cell membrane, and hence virus entry. Enfurvirtide (T-20) is the only FI drug available (Matthews T. *et al*., 2004).

2.5. CCR5 co-receptor antagonists

CCR5 antagonists bind to hydrophobic pockets within the transmembrane helices of the CCR5 receptor (Dragic T. *et al*. 2000; Tsamis F. *et al*. 2003). Drug binding they induce and stabilize a receptor conformation, preventing the virus entry into the host cell. Maraviroc (MVC), the only CCR5 inhibitor available, is only active against HIV which has tropism for this receptor, and lacks effect against HIV with tropism for the CXCR4 receptor or mixed tropism (CCR5/CXCR4) (Ghebremedhin B., 2012).

2.6. Integrase Inhibitors (IIs)

This group of drugs inhibits the catalytic activity of HIV integrase preventing the insertion of the HIV genome into the DNA of the host cell, an essential step in the HIV replication cycle. Until three years ago, raltegravir (RAL) was the only integrase inhibitor used commercially. Currently, elvitegravir (EVG) and dolutegravir (DTG) are being used as part of a fixed dose combination (Pandey K.K., 2011; Raffi F. *et al*., 2016; GESIDA, 2016).

2.7. Pharmacokinetic Enhancers (PEs)

PEs are used to increase the plasma levels of other anti-HIV drugs making them more effective. Whereas the PI ritonavir (RTV) has been the only available PE for more than a decade, cobicistat (COBI) has recently emerged as an alternative boosting agent. COBI, not an HIV drug itself, is used as a PE of atazanavir (ATV) or darunavir (DRV) in combination with other antiretroviral agents in the treatment of HIV infection (Marzolini C. *et al*., 2016; Crutchley R.D. *et al*., 2016).

2.8. Guidelines on antiretroviral therapy

Since the introduction of cART in 1996, antiretroviral multitherapy has become increasingly effective in inhibiting HIV replication and in limiting the viral resistance, making it widely accepted. Combination of three (or more) anti-HIV compounds is aimed at these goals: (i) to obtain synergism between different compounds acting at different molecular targets; (ii) to lower the individual drug dosages in order to reduce their adverse effects; and (iii) to diminish the development of drug resistance (De Clercq E., 2009).

Although some antiretroviral drugs are less used because of their limited effectiveness, its cumbersome management guidelines and/or the appearance of adverse effects, the variety of compounds available offer numerous options to obtain the most appropriate combination depending on the requirements of each person. The selection of a regimen should be individualized based on virologic efficacy, potential adverse effects, pill burden, dosing frequency, drug-drug interaction potential, comorbid conditions, cost, and resistance test results. cART strategies are frequently updated and according to current guidelines (GESIDA, 2016), the initial treatment for HIV-1 consists of a combination of three drugs that include two NRTIs associated with a NNRTI, an II or an enhanced PI (Tab.I.2). These combinations are effective in lowering plasma viral load below 50 copies/mL in more than 75% of cases at 48 weeks (Clumeck N. *et al*., 2008; GESIDA, 2016).

In the last decade, cART has dramatically improved the natural course of HIV infection. cART does not eradicate HIV, but the disease can be controlled if the treatment continues throughout the patient's life. Chronic exposure to these drugs has led to the emergence of adverse long-term effects, which can affect the health of patients and often require discontinuation of the treatment. Due to the special characteristics of this disease, the development of antiretroviral drugs was particularly fast and focused primarily on clinical efficacy, which is the reduction of mortality. However, once the disease has been controlled, adverse effects associated to therapy and mechanisms of toxicity caused by drugs used in it have become very important in the last years (Blas-García A. *et al*., 2011).

RECOMMENDATIONS	HAART REGIMENS		
	NRTI	**NRTI**	**3rd DRUG**
PREFERENTIAL	ABC	3TC	**II:** DTG
	TDF	FTC	**II**: DTG or RAL
	TAF	FTC	**II**: EVG/COBI
ALTERNATIVE	TDF	FTC	**NNRTI**: RPV or EFV
	TDF	FTC	**II**: EVG/COBI
	ABC	3TC	**II**: RAL
	TDF	FTC	**Enhanced PI** DRV/COBI or DRV/r ATV/COBI or ATV/r
	ABC	3TC	**PI**: ATV/COBI or ATV/r

Table I.2. Combinations of antiretroviral drugs recommended for triple therapy in patients starting HIV treatment (GESIDA, 2016). TAF is a new formulation of tenofovir, which instead of difumarate uses alafenamide. PI/r: PI enhanced with ritonavir (RTV).

3. ADVERSE EFFECTS OF ANTIRETROVIRAL THERAPY

The immediate adverse effects, which are well defined, can be anticipated and are usually easy to control; mainly affect the gastrointestinal tract, the skin and the SNC. Many of these effects disappear in a few weeks and most patients overcome them. However, if symptoms persist over longer times, they are more difficult to predict and control. Also, they enhance the effects of chronic diseases associated with aging and affect the functioning of organs and systems. The most common adverse effects generated by long-term cART include metabolic syndrome, lipodystrophy, hyperlipidaemia, insulin resistance and toxicities in the liver, heart, kidney, bone marrow, retina, ear and skin (Hofman P. and Nelson A.M., 2006). Although some of these side effects have been described for cART generally, there are also certain drug toxicities related to specific pharmacological families or to a particular compound (Maggiolo F., 2009, Blas-García A. *et al*, 2010; Caron-Debarle M. *et al*, 2010; Apostolova N. *et al*, 2011b). The main adverse effects associated with each antiretroviral drug are described in Tab.I.3.

There are several factors that influence the presence/absence of toxicity associated with antiretroviral drugs, such as adherence to therapy, concurrent diseases, drug interactions as well as interindividual variations caused by age, sex, nutritional status and especially genetic variation responsible principally for the variability in the response to therapy (Evans W.E. and McLeod H.L., 2003; Rodriguez-Novoa S. *et al*., 2005).

The overall benefits of viral suppression and improved immune function as a result of effective antiretroviral therapy far outweigh the risks associated with the adverse effects of some antiretroviral drugs. However, in patients at high risk or with chronic illnesses already diagnosed, the effect of certain antiretroviral drugs may contribute to trigger or advance such chronic diseases.

DRUG	SEVERE ADVERSE EFFECT	COMMON ADVERSE EFFECT (> 5%)
NRTIs		
ABC	Myocardial infarction, dyslipidaemia, hypersensitivity reaction, pancreatitis	N/A
ddI	Pancreatitis, insulin resistance, hepatic steatosis, lactic acidosis, peripheral neuropathy, retinal changes	Nausea and vomiting
FTC	Hyperpigmentation	N/A
3TC	N/A	N/A
d4T	Insulin resistance, hyperlipidaemia, hepatic steatosis, lactic acidosis, pancreatitis	Lipoatrophy, peripheral neuropathy
TDF	Loss of bone mineral density, renal insufficiency	N/A
AZT	Anaemia, neutropenia, insulin resistance, hyperlipidaemia, hepatic steatosis, lactic acidosis, lipoatrophy, myopathy	Nausea and vomiting, headache, asthenia, nail pigmentation
NNRTIs		
EFV	Hyperlipidaemia, hepatotoxicity, rash, teratogenic in human foetus	Neuropsychiatric symptoms, serum transaminase elevations
ETR	Rash	Nausea
NVP	Hepatotoxicity, hypersensitivity syndrome, rash, Stevens-Johnson syndrome	Serum transaminase elevations

RPV	Rash, hepatotoxicity, neuropsychiatric symptoms	N/A
PIs		
ATV	Cardiovascular risks with RTV, cholelithiasis, hyperlipidaemia with RTV, rash, renal effects	Diarrhoea with RTV, indirect hyperbilirubinemia
DRV	Hyperlipidaemia, hepatotoxicity, Stevens-Johnson syndrome	Rash
FPV	Hyperlipidaemia, Stevens-Johnson syndrome, nephrolithiasis	Rash
IDV	Hyperlipidaemia, indirect hyperbilirubinemia, nephrolithiasis, hyperglycaemia	Gastrointestinal effects, headache, asthenia
NFV	Hyperlipidaemia, hyperglycaemia	Diarrhoea
RTV	Hyperlipidaemia, hepatotoxicity, hyperglycaemia	Gastrointestinal effects
SQV	Cardiovascular risks with RTV, hyperglycaemia, hyperlipidaemia	Gastrointestinal effects, headache
TPV	Intracranial haemorrhages, hepatotoxicity	Nausea, diarrhoea, rash
LPV/RTV	Cardiovascular risks, hepatotoxicity, pancreatitis, insulin resistance, hyperlipidaemia, hyperglycaemia	Diarrhoea, nausea, vomiting
FIs		
T-20	Rash, elevated serum transaminases	Local injection site reactions, increased incidence of bacterial pneumonia
CCR5 Antagonists		
MVC	Hepatotoxicity, hypersensitivity reaction, rash, musculoskeletal symptoms	Abdominal pain, upper respiratory tract infections
IIs		
DTG	Hypersensitivity reaction	Insomnia, headache
EVG	N/A	Nausea, diarrhoea
RAL	Myopathy, rash, Stevens-Johnson syndrome	N/A

Table I.3. Antiretroviral therapy-associated common and/or severe adverse effects (AIDSinfo, 2016). N/A indicates either that there are not reported cases for the particular side effect or that data for the specific ARV drug class are not available.

3.1. Antiretroviral therapy-related hepatotoxicity

Liver toxicity is one of the most relevant adverse effects of cART, owing to its frequency, the fact that it can lead to interruption of therapy (Soriano V. *et al*., 2008),

and that most of antiretroviral drugs are potentially hepatotoxic (Stern J.O. *et al*., 2003; Sulkowski M.S., 2004; Blas-Garcia A. *et al*., 2011). Most studies have found that the incidence of elevated liver enzyme levels after six or more months of cART is approximately 2-18% (Bonfanti P. *et al*., 2000; Sulkowski M.S. *et al*., 2002; Wit F.W. *et al*., 2002).

Data from clinical studies show that the second cause of mortality in patients treated with antiretrovirals is the liver disease (Weber R. *et al*., 2006; Price J.C. and Thio C.L., 2010), preceded only by the mortality directly associated with AIDS. Among the factors that can increase the risk of hepatotoxicity due to anti-HIV drugs include: the presence of other infections such as hepatitis B or C virus (HBV or HCV), age, past history of liver damage, alcohol or drug abuse, obesity and taking other drugs that can cause liver damage (Joshi D. *et al*., 2011).

The clinical spectrum of hepatotoxicity produced by cART is varied and covers: asymptomatic and transient elevations of liver enzymes, hepatitis, steatosis, steatohepatitis, fibrosis and portal hypertension, and rarely, acute fulminant hepatitis (Pineda J.A. *et al*., 2010; Domingo P. and Lozano F., 2011). Liver toxicity caused by cART can be inflicted through several mechanisms, such as hypersensitivity reactions, direct mitochondrial inhibition, disturbances of lipid/sugar metabolism and steatosis, direct cell stress, and immune reconstitution in the presence of viral hepatitis coinfection (Núñez M., 2010).

3.2. Mitochondrial toxicity

The mitochondrion is a major target of drug-induced cytotoxicity, which occurs through a wide variety of mechanisms such as inhibition or uncoupling of oxidative phosphorylation (OxPhos), oxidative stress and/or opening of the mitochondrial permeability transition pore (Labbe G. *et al*., 2008). Many important adverse effects associated with cART are known to be the consequence of mitochondrial toxicity, but they have been mainly attributed to the inhibition by NRTI of DNA polymerase-γ (Pol-γ), the enzyme responsible for mtDNA replication (Martin J.L *et al*., 1994; Walker U.A. *et al*., 2002; Apostolova N. *et al*., 2011b). mtDNA encodes 13 subunits of the electron transport chain (ETC) essential to OxPhos, so decreased levels of mtDNA and

polypeptides encoded by it leads to mitochondrial dysfunction (Kohler J.J. and Lewis W., 2007; Chiao S.K. *et al*, 2009).

The effects on mitochondria of NNRTIs, which do not inhibit Pol-γ, are less well documented, though some elements of the toxicity attributed to these drugs resemble disorders induced by mitochondrial dysfunction (Sato N., 2007; Abdul-Ghani M.A. and DeFronzo R.A., 2008).

Classically, symptoms of mitochondria affect the tissues with high-energy demand (e.g. the muscles) and are mostly manifested as myopathy, peripheral neuropathy, hepatotoxicity, hyperlactatemia and lactic acidosis. However, other alterations have also been related to mitochondrial dysfunction, such as disturbances in the lipid metabolism (a complex syndrome often termed HIV-related lipodystrophy) and nephropathy, although the mechanisms implicated and the extent to which mitochondria are involved in these effects vary greatly (Petit F. *et al.*, 2005; Hammer S.M. *et al.*, 2008; Maagaard A. and Kvale D., 2009; Feeney E.R. and Mallon P.W., 2010; 2011).

4. EFAVIRENZ (EFV)

The NNRTI efavirenz (EFV), chemically described as (S)-6-chloro-4-(cyclopropylethynyl)-1,4-dihydro4-(trifluoromethyl)-2H-3,1-benzoxazin-2-one (Fig.I.2), is among the most widely used drugs in cART. The long half-life of EFV (44 - 55 h) allows its prolonged effect on the reduction of viral RNA with a daily dose (600 mg in adults), what makes it highly effective (Smith P.F. *et al*., 2001; Maggiolo F., 2009). After a single oral dose, plasma concentrations peak at 3 - 5 h and become steady at 6 – 7 days (Maggiolo F., 2009). A daily dose of 600 mg usually results in a C_{max} of 12.9 ± 3.7 µM and a C_{min} of 5.6 ± 3.2 µM (Starr S.E. *et al*., 1999; Staszewski S. *et al*., 1999), but important pharmacokinetic interindividual variability has been reported, with several studies reporting higher levels (30 - 50 µM) in as many as 20%-40% of patients (Marzolini C. *et al*., 2001; Taylor S. *et al*., 2001; Burger D. *et al*., 2006; Kwara A. *et al*., 2009; van Luin M. *et al*., 2009; Carr D.F. *et al*., 2010; Gounden V. *et al*., 2010) and as high as 80 µM in some studies (Kwara A. *et al*., 2009; Van Luin M. *et al*., 2009; Gounden V. *et al*., 2010).

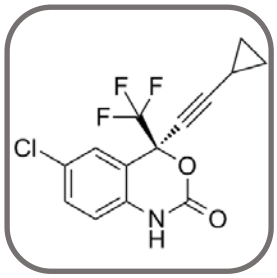

Figure I.2. Quemical structure of efavirenz (EFV, $C_{14}H_9ClF_3NO_2$).

EFV is metabolised mainly in the liver by the cytochrome P450 system (CYP) into inactive hydroxylated metabolites. CYP2B6 is the mainly isoenzyme responsible for the metabolism of EFV, although CYP3A4 and CYP2A6 are also involved (Ward B.A. *et al*., 2003). Many *in vitro* and clinical studies have revealed that genetic polymorphisms of CYP2B6 strongly influence EFV pharmacokinetics, leading to marked differences in drug's plasma concentrations which depend on the individual's genetics (Bumpus N.N. *et al*., 2006; Desta Z. *et al*., 2007, King J. and Aberg J.A., 2008).

Although generally considered safe, there is a concern about the side effects induced by EFV-containing therapies, such as rash, neuropsychiatric disturbances, lipid and metabolic alterations, and hepatotoxicity (Tashima K.T. *et al*., 2003; Gutiérrez F. *et al*., 2005; Maggiolo F., 2009; Loko M.A. *et al*., 2011; Echenique I.A. and Rich J.D., 2013; Patil R. *et al*., 2015). In particular, there is a growing concern whether lifelong treatment with this and/or other drugs used in cART leads to accumulative hepatotoxicity as liver-related complications are the second cause of mortality among AIDS patients (Jones M. and Núñez M., 2012). The mechanisms behind this liver damage are unclear, but it has been reported the presence of acute mitochondrial dysfunction in cultured human hepatocytes treated with clinically relevant concentrations of EFV. Studies with the human hepatoma cell line Hep3B and primary cultures of human hepatocytes have revealed that the mitochondrial effect of EFV involves specific inhibition of complex I of the electron transport chain (ETC), which leads to reduced oxygen (O_2) consumption, decreased mitochondrial membrane potential ($\Delta\Psi_m$), bioenergetic changes and elevated reactive oxygen species (ROS) generation (Apostolova N. *et al*., 2010; 2011c; Blas-García A. *et al*., 2010). Parallel to these manifestations, EFV triggers endoplasmic reticulum (ER) stress and activates the

unfolded protein response (UPR) observed as altered ER morphology and increased expression of several UPR genes (Apostolova N. *et al*., 2013).

5. MITOCHONDRION

5.1. Mitochondrial structure

Mitochondria are organelles found in all eukaryotic cells (except in mature erythrocytes). They range from 0.5 to 1 μm in diameter and collectively can occupy as much as 25% of the volume of the cell; their shape, number, size and subcellular location depend on the energy needs of the cell (Lodish H. *et al*., 2003).

These organelles possess a double membrane whose architecture was revealed in the 1950s by electron microscopy imaging (Palade G.E., 1953). The outer mitochondrial membrane (OMM) has integral membrane proteins (porins) that allow the passage of molecules of up to 5000 Da. The inner membrane (IMM) is organized in characteristic folds that protrude into the matrix (MM), named cristae, which accommodate the respiratory chain complexes. Unlike the OMM, the IMM is much less permeable, but it has various transport proteins that allow the movement of impermeable molecules across the membrane. The region between the cristae is known as inner boundary membrane (IBM) (Zick M. *et al*., 2009). IMM and the OMM generate two distinct and very specific compartments: the MM and the mitochondrial intermembrane space (IMS) (Fig.I.3). The morphology and size of these organelles, as well as their behaviour and location in the cell, are variable and depend on interactions between outer surface proteins and cytoskeletal components, suggesting that mitochondria are dynamic, interconnected structures that respond to environmental and developmental signals to satisfy cellular needs.

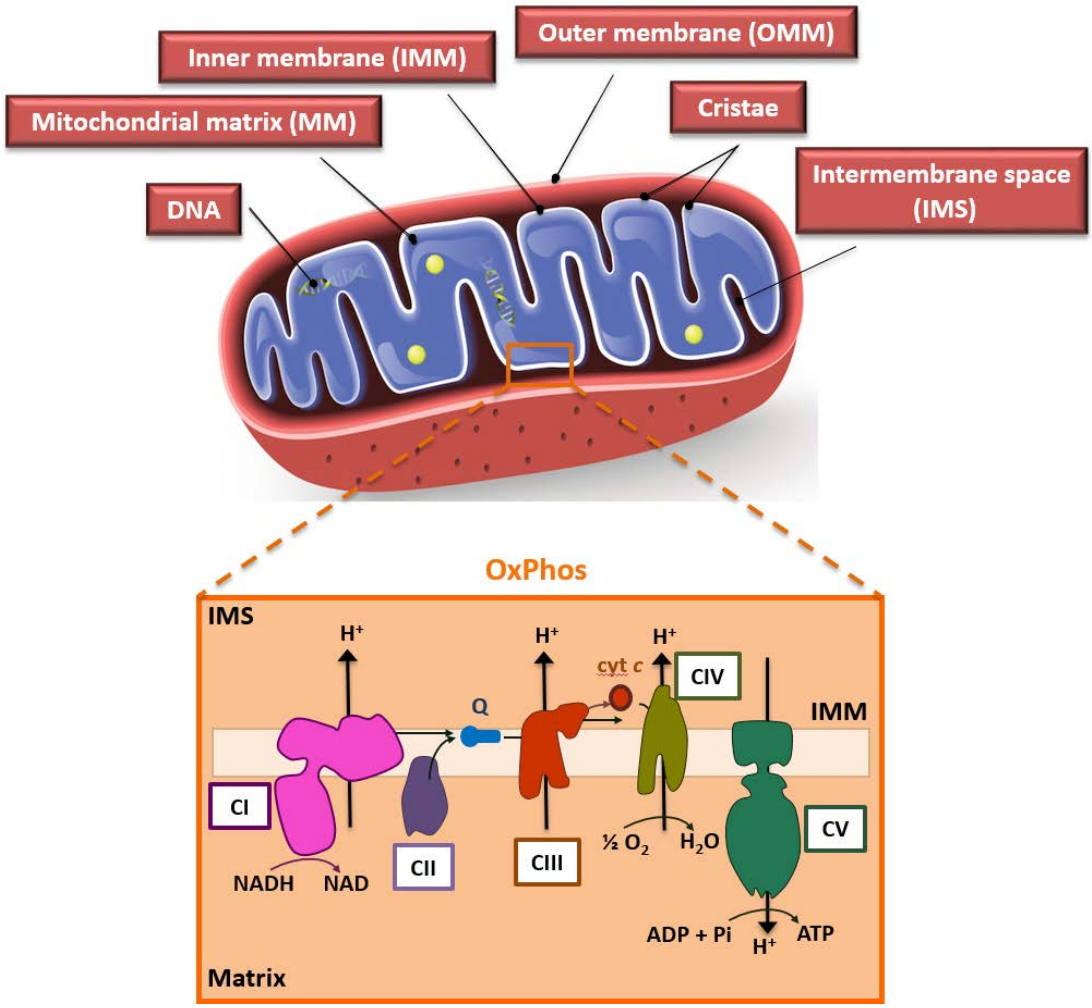

Figure I.3. Representative scheme of the mitochondria structure with its main components. The foremost role of mitochondria is the generation of ATP (adenosine triphosphate) through OxPhos, carried out by five protein complexes (I-V) which form the ETC (Smith R.A. *et al.*, 2012). NADH-ubiquinone oxidoreductase (CI) catalyses the transfer of electrons from the NADH to the coenzyme Q or ubiquinone. This electron flow causes four protons to be pumped into the IMS. Coenzyme Q is also the acceptor of the electrons that come from the succinate dehydrogenase (CII), acting as an alternative point of entry of electrons to the ETC. This electron transfer is not coupled to proton translocation. The cytochrome *c* reductase (CIII) transfers electrons from reduced ubiquinone to cytochrome *c* (cyt *c*), producing a new flow of protons into the IMS. The third proton pump is the cyt *c* oxidase (CIV) that oxidizes cyt *c* and transfers the electrons to O_2 to form H_2O (Poyton R.O. *et al.*, 2009). The proton gradient between the MM and the IMS is used by the ATP synthase (ATPase or CV) to synthesize ATP from ADP (adenosine diphosphate) and P_i (inorganic phosphate) (Poyton R.O. *et al.*, 2009).

Mitochondria are semi-autonomous organelles that contain their own genome and protein synthesis machinery; however, the vast majority of mitochondrial proteins are encoded by nuclear genes and thus imported into mitochondria post-translation. The

mitochondrial genome (mtDNA) is a circular DNA molecule of about 16 kb that possesses 37 genes necessary for assembly of the OxPhos machinery: 13 for subunits of respiratory complexes, 22 for mitochondrial transfer RNA (tRNA) and 2 for ribosomal RNA (rRNA) (Anderson S. *et al*., 1981). Mitochondria replicate their DNA and divide mainly in response to the energy needs of the cell, rather than in phase with the cell cycle, thus tissues with a high energy demand such as brain, liver, heart and skeletal muscle have a high content of mitochondria (Amacher D.E., 2005).

5.2. Mitochondrial dynamics

For several decades, there was a general understanding of mitochondria as solitary and static organelles; however, live-cell microscopy studies in the 1980s suggested a new view of these organelles as highly dynamic structures that construct large, branched, interconnected network called the mitochondrial reticulum (Bereiter-Hahn J., 1990). This structure involves continuous and balancing fusion and fission events that regulate mitochondrial morphology. Mitochondrial numbers are increased by the process of mitochondrial biogenesis. Abnormal mitochondria (or portions of mitochondria) can be eliminated through a quality control process called mitophagy (Twig G. *et al*., 2008). Mitochondrial movement along the microtubules allows its intracellular transport (trafficking). All these functions together are referred to as mitochondrial dynamics (Youle R.J. and van der Bliek A.M., 2012).

Fission creates a greater number of discrete non-networked mitochondria, whereas fusion increases connectivity, thereby allowing sharing of matrix proteins and mitochondrial DNA among these organelles (Santel A. *et al*., 2003). The causes and consequences of mitochondrial fission and fusion are highly contextual. Fission may be either a physiological step in the process of mitosis (mitotic fission), the beginning of programmed cell death (apoptosis) or a normal part of a cell's quality control mechanism, allowing elimination of dysfunctional mitochondria (by mitophagy) (Taguchi N. *et al*., 2007; Twig G. *et al*., 2008; Mitra K. *et al*., 2009). Mitochondrial dynamics also alters the network in order to fulfil the specific metabolic and energetic demands of the cell and participates in cell cycle progression, apoptosis, production of O_2-derived free radicals, mitochondrial DNA stability, O_2 sensing and the cell's stress response (Chan D.C., 2012; Archer S.L., 2013). Acquired, pathological alterations in

mitochondrial dynamics contribute to many human diseases, including cardiovascular diseases, such as pulmonary arterial hypertension, degenerative neurological diseases, such as Parkinson's disease, ischaemia/reperfusion injury and cancer (Archer S.L., 2013). Moreover, disorders of mitochondrial dynamics are emerging as mechanisms of pathogenesis in diseases that had not classically been linked to mitochondria.

The opposing process, fusion, allows for the mixing of mitochondrial contents between organelles for maintenance of a homogeneous mitochondrial network (Chen H. *et al*., 2005). Fusion also allows a healthy mitochondrion to compensate for oxidative damage in a failing mitochondrion by admixture of its healthy mitochondrial proteins and mtDNA (Youle R.J. and van der Bliek A.M., 2012). When fusion is no longer adequate to compensate for accumulated damage, the diseased portion of the mitochondria depolarizes and undergoes fission, with a simultaneous suppression of fusion. This isolates damaged sections of mitochondria, allowing their removal in a mitophagic vacuole, thereby protecting the cell (Twig G. *et al*., 2008).

5.2.1. Mitochondrial fusion

Although mitochondrial fusion can be simply defined as the joining of two organelles into one, it requires the coordination of two distinct steps: fusion of the OMM followed by fusion of the IMM (Fig.I.4). OMM fusion is mediated by mitofusin proteins (Mfn1 and Mfn2), large transmembrane GTPases embedded in the OMM (Santel A. and Fuller M.T., 2001; Rojo M. *et al*., 2002). IMM fusion is mediated by optic atrophy protein 1 (OPA1), a dynamin-related GTPase associated with the IMM or intermembrane space (Meeusen S. *et al*., 2006; Song Z. *et al*., 2009). Similar to many IMM proteins, OPA1´s primary structure consists of an N-terminal mitochondrial targeting sequence (MTS) and transmembrane domain. While MTS is constitutively cleaved upon import into the organelle, an N-terminal transmembrane domain remains and anchors this form to the membrane, referred to as the long-form (l-OPA1). Two proteases (Oma1 and Yme1L) have the capacity to cleave OPA1 from its N-terminal transmembrane domain, producing a short (s-OPA1), soluble form that has a more characteristic topology to other dynamin family members (Fig.I.4). These proteases appear to be highly regulated, responding to various aspects of mitochondrial biology. Oma1 is strongly activated by depolarization of the IMM, as

well as by apoptotic stimuli; while Yme1L activity can be controlled by ATP levels, OxPhos and translational stress (Ishihara N. *et al*., 2006; Ehses S. *et al*., 2009; Rainbolt T.K. *et al*., 2013; Mishra P. *et al*., 2014). These mechanisms allow tuning of mitochondrial fusion rates to the organellar and cellular bioenergetics. In particular, it appears that a balance of long and short forms of OPA1, as well as proteolysis itself is required for fusion activity (McQuibban G.A. *et al*., 2003; Song Z. *et al*., 2007; Mishra P. *et al*., 2014), although recent studies have challenged this viewpoint by implicating l-OPA1 as the primary fusion mediator (Anand R. *et al*., 2014).

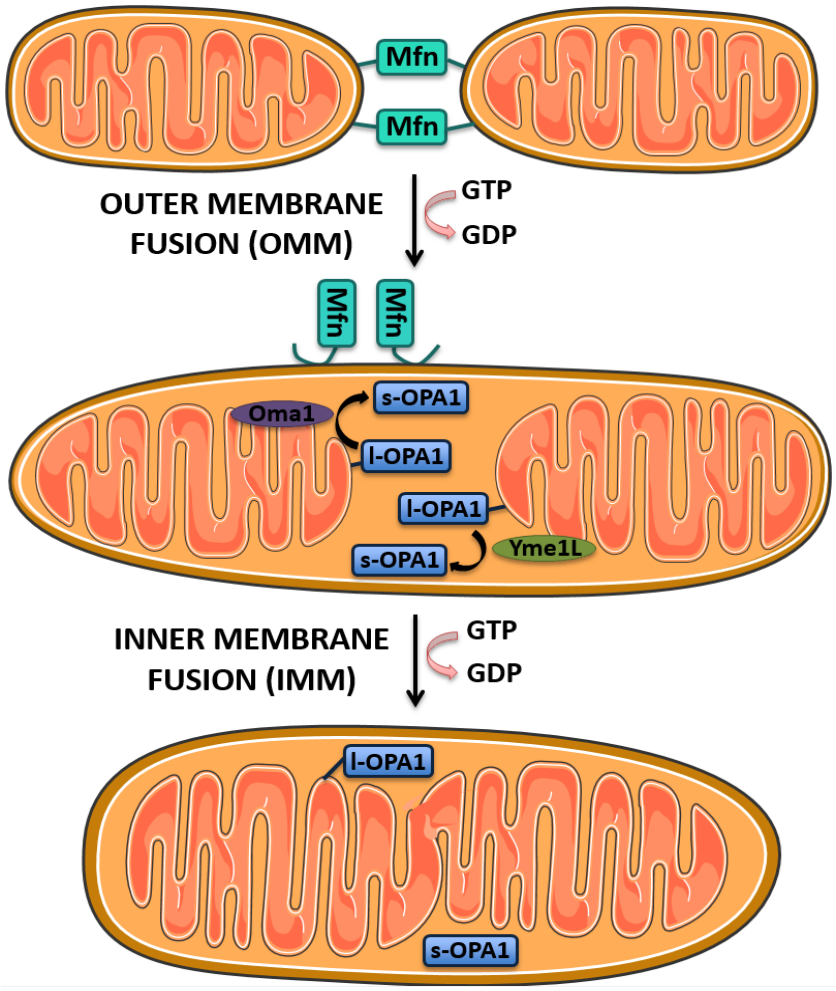

Figure I.4. Schematic representation of the process of mitochondrial fusion (modified from Mishra P., 2016). It is a two-step process consisting of OMM fusion, mediated by Mfn1 and Mfn2 GTPases, followed by IMM fusion, mediated by OPA1 GTPase. OPA1 is present in two forms, a long form (l-OPA1) which is an integral membrane form, and a shorter, processed form (s-OPA1). Proteolytic processing of OPA1 can be achieved via either the Oma1 or Yme1L proteases.

5.2.2. Mitochondrial fission

The mitochondrial fission machinery has two major components: dynamin-related protein 1 (Drp1) and its adaptor proteins (Fig.I.5). Drp1 is a member of the dynamin GTPase family and is homologous with dynamin, the mitochondrial fission mediator in yeast (Smirnova E. *et al*., 2001). Drp1 has an essential role in fission and mice lacking Drp1 die before birth (Ishihara N. *et al* 2009). Fluorescent microscopy provides evidence that Drp1 is recruited from the cytosol to the mitochondrial surface to mediate fission (Frank S. *et al*., 2001). A number of recruitment proteins have been identified including fission 1 (Fis1), mitochondrial fission factor (Mff) and the newly discovered mitochondrial dynamics proteins of 49 kDa and 51 kDa (MiD49 and MiD51), all of which are localized to the OMM (Gandre-Babbe S. and van der Bliek A.M., 2008; Loson O.C. *et al*., 2013).

In the cytosol, Drp1 exists as a dimer or tetramer and only assembles into higher-order complexes when it binds to the OMM (Zhu P.P. *et al*., 2004; Chang C.R. and Blackstone C., 2007). In most models, Drp1 translocates to and oligomerizes on the mitochondrial surface, forming a ring which constricts the organelle and eventually leads to fission (Fig.I.5). However, the involvement of other auxiliary factors has been suggested. In particular, the role of the ER has come to the forefront (Friedman J.R. *et al*., 2011; Rowland A.A. and Voeltz G.K., 2012). In this model, ER tubules actually wrap around mitochondria, facilitate constriction and perhaps the final fission event. Interestingly, this process appears to utilize localized actin-myosin based contraction to generate the pre-constriction forces (Hatch A.L. *et al*., 2014). Therefore, the dynamic behaviour of these two organelles directly influence one another and this evidence highlights the importance of mitochondrial-ER interactions.

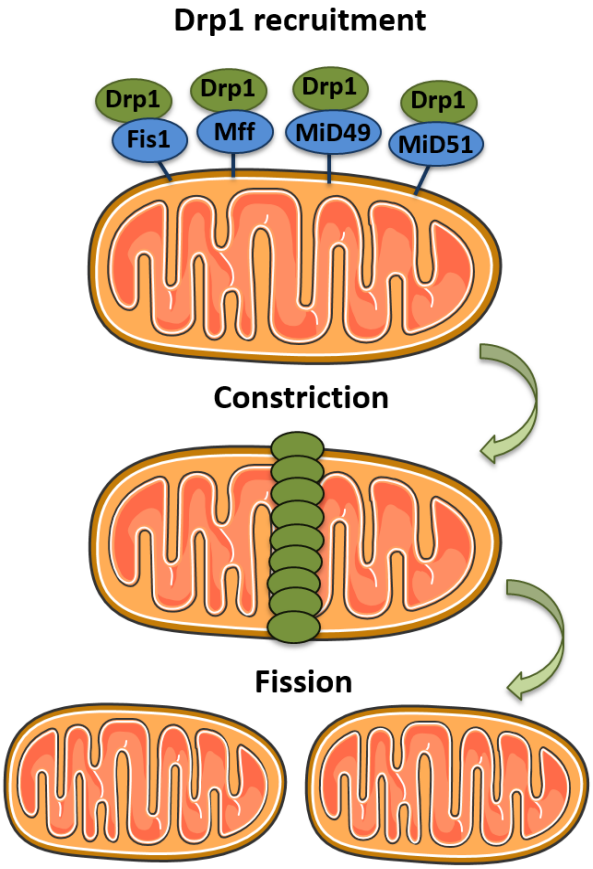

Figure I.5. Schematic representation of the process of mitochondrial fission (modified from Mishra P. and Chan D.C., 2014). Drp1 is recruited to mitochondria surface where it oligomerizes into a ring-like structure and promotes scission of the mitochondrial membrane. Four recruitment proteins have been identified, Fis1, Mff, MiD49 and MiD51.

Mitochondrial fission is highly regulated by post-translational modifications of Drp1, including SUMO(small ubiquitin-like modifier)ylation, or phosphorylation that can either activate or inactivate its GTPases activity and fission (Wasiak S. *et al.*, 2007; Cribbs J.T. and Strack S., 2007). Drp1 is inhibited by phosphorylation at Ser^{637} and activated by phosphorylation at Ser^{616} (Taguchi N. *et al.*, 2007; Cribbs J.T. and Strack S., 2007). Dephosphorylation of Drp1 at Ser^{637} is necessary for Mff interaction with Drp1 (Zhang Z. *et al.*, 2016), whereas MiDs can bind the phosphorylated form of Drp1 at Ser^{637} (Loson O.C. *et al.*, 2013). The mitotic fission results in part from cyclin B1/cyclin-dependent kinase 1 (CDK1), which simultaneously triggers mitosis and fission by phosphorylation of Drp1 at Ser^{616} (Marsboom G. *et al.*, 2012; Rehman J. *et al.*, 2012). The interaction of Drp1 with its binding partner Fis1 contributes to mitotic fission (Lee S. *et al.*, 2014). Under oxidative stress conditions, protein kinase Cδ mediates phosphorylation of Ser^{579} in human Drp1 isoform 3 (corresponding to Ser^{616} in the

human Drp1 isoform 1), leading to mitochondrial fragmentation and impaired mitochondrial function, which contributes to hypertension-induced brain injury (Qi X. *et al*., 2011). Under nutrient starvation conditions, for example, mitochondrial fission is repressed by phosphorylation of Drp1-Ser^{637} and coincident dephosphorylation of Drp1-Ser^{616} to protect mitochondria from autophagosomal degradation and sustain cell viability (Rambold A.S. *et al*., 2011).

5.3. Mitochondrial membrane potential ($\Delta\Psi_m$)

It is a fundamental mitochondrial physiological parameter because it directly controls three crucial cellular processes, ATP synthesis, mitochondrial calcium (Ca^{2+}) sequestration and generation of ROS, and is therefore often regarded as a key indicator of cell health (Perry S.W. *et al*., 2011). As shown in Fig.I.3, mitochondria generate ATP by utilizing the proton electrochemical gradient potential, or electrochemical proton motive force (Δp), generated by serial reduction of electrons through the ETC. Under normal circumstances, the accumulation of protons in the IMS can be dissipated by the synthesis of ATP o through uncoupling proteins (UCP), which can modulate the loss of protons through the IMM decreasing the electrochemical potential and favouring heat dissipation (Argilés J.M. *et al*., 2002). The uncoupling of the OxPhos allows protons to go directly back to the MM producing heat but not ATP (Amacher D.E., 2005).

A fast $\Delta\Psi_m$ collapse occurs with the opening of the transition pore of the mitochondrial permeability resulting from an exposure to mitochondrial toxins or conditions which can increase mitochondrial Ca^{2+} levels, especially if they are accompanied by additional factors such as oxidative stress (Lecoeur H. *et al*., 2004). This phenomenon associated with the impaired mitochondrial integrity leads to the permeabilization of the OMM and the translocation of pro-apoptotic proteins to the cytosol, ending in cell death by apoptosis (Novo E. and Parola M., 2008). The loss of $\Delta\Psi_m$ may be an early event in some apoptotic processes or, depending on the apoptotic model, also a consequence of the apoptosis-signalling pathway (Ly J.D. *et al*., 2003).

There are numerous well-known uncouplers and inhibitors of OxPhos, such as the protonophore carbonyl cyanide m-chloro phenyl hydrazone (CCCP) that causes an uncoupling of the proton gradient (Lou P.H. *et al*., 2007), and rotenone, a pesticide that prevents the transfer of electrons from CI to ubiquinone blocking the ubiquinone-binding site (Li N. *et al*., 2003).

5.4. Reactive oxygen species (ROS) and oxidative stress

Mitochondria is where 99% of the molecular O_2 in the cell is reduced, thereby producing H_2O. Thus, it is not a surprise that these organelles are main cellular generators of ROS, mostly synthesised in the form of superoxide ($O_2.^-$) resulting from irregular side reactions and incomplete reduction of O_2 during the electron transport at the ETC (Cadenas E. and Davies K.J., 2000). ROS are mainly produced within the complexes I and III and roughly $3x10^7$ molecules of $O_2.^-$ are generated in a single mitochondrion per day. Besides ETC as a notorious ROS producer, additional mitochondrial sources of ROS have been reported including enzymes of the Krebs cycle (Boveris A. and Cadenas E., 1997; Sauer H. *et al*., 2001). Under normal conditions, from 0.15% to 0.4 % of the totally consumed O_2 is converted into $O_2.^-$ but this yield can be drastically augmented in many physiological and pathological circumstances (Hansford R.G. *et al*., 1997; St-Pierre J. *et al*., 2002). ROS is a collective term for several free radical and non-radical molecules such as $O_2.^-$, hydroxyl (HO.) and peroxyl ($RO_2.$) radicals, and hydrogen peroxide (H_2O_2) (Halliwell B. and Cross C.E., 1994). $O_2.^-$ can react with nitric oxide (NO) thus generating peroxynitrite ($ONOO^-$), a very potent oxidant and it also inhibits aconitase, a key enzyme in the control of NADH generation providing a feedback mechanism to control electron flow through ETC. Also, $O_2.^-$ is a precursor of H_2O_2 which is a substrate of several mitochondrial enzymes (Jones D.P., 2008). Moreover, H_2O_2 can be converted into the highly oxidative and cytotoxic HO.. Mitochondrial ROS are important second messengers that act as signalling molecules between these organelles and the cytosol. However, under many physiological and pathological circumstances mitochondria overproduce ROS which tend to be scavenged by the mitochondrial antioxidant defence machinery (Le Bras M. *et al*., 2005). Still, this detoxifying system can be overwhelmed which occurs in circumstances of impaired electron transport, decreased O_2 availability, etc. The overproduction of

ROS and/or the failure of the intrinsic cellular antioxidant system to scavenge them, leads to a state known as oxidative stress. As a result of their intrinsic high reactivity, ROS react almost with all macromolecules within the mitochondrion. Oxidative damage of mitochondrial lipids, proteins and mtDNA results in abnormal mitochondrial protein synthesis and folding as well as altered protein complex assembly which ultimately compromises mitochondrial function. Oxidative stress is also characterized by changes in the redox state of the mitochondrion that has important consequences for signalling (Apostolova N. *et al*., 2011a).

Oxidative stress has been given major clinical importance over recent years and a vast body of evidence has pointed to its role in a wide variety of pathological situations, both inherited and acquired, from ischaemia/reperfusion and cardiovascular diseases, to diabetes, cancer, infectious diseases, neurodegeneration and aging (Duchen M.R. and Szabadkai G., 2010). It is evident that increases in ROS can determine cell fate (survival vs. cell death). All mammalian cells possess intrinsic programs which determine progression to cell death and several distinct models of cell death have been described: apoptosis, necrosis, autophagy-related, etc. (Orrenius S. *et al*., 2007). Moderate increases in ROS may generate mild mitochondrial damage and thus induce mitophagic removal of these organelles. Depending on the duration and the intensity of this stimulus, mitophagy can promote cell survival or can lead to autophagy-related cell death. Greater increases in ROS can lead to apoptotic or necrotic cell death (Lemasters J.J., 2005; Yen W.L. and Klionsky D.J., 2008).

5.5. Mitochondrial stress response

Mitochondria are the main energy producers in the cell, and are essential mediators of cell death as sources and targets of ROS, and as regulators of ATP levels and calcium homeostasis. For this reason, the preservation of mitochondrial function and integrity is critical for cell viability. In a cellular environment, especially under stress conditions, proteins are at risk for being inactivated by misfolding or aggregation (Dobson C.M., 2003). To prevent the accumulation of these toxic protein aggregates within the cell, organisms have co-evolved complex protein quality control (PQC) networks composed of molecular chaperones and proteases (Hartl F.U. *et al*., 2011; Mogk A. *et al*., 2011; Powers E.T. and Balch W.E., 2013). Molecular chaperones are not only responsible for

the *de novo* folding of proteins but also for their refolding after stress. Proteolytic machines on the other hand, are responsible for the removal of damaged or unwanted proteins.

There is growing evidence that points to an important role of mitochondrial protein defects in the pathogenesis of human diseases such as neurological disorders, aging, cancer and various neuromuscular syndromes (Schapira A.H., 1999; Wallace D.C., 1999; Turner C. and Schapira A.H., 2001). Mitochondrial stress raises when unfolded, misfolded or damaged proteins accumulate in a certain compartment interfering with OxPhos and normal mitochondrial functions. Protein overload triggers the mitochondrial unfolded protein response (UPRmt), which is the first mechanism to be engaged to restore mitochondrial proteostasis. During the UPRmt, mitochondrial stress is signalled to the nucleus to promote the expression of mitochondrial-associated chaperones and proteases to repair and refold misfolded proteins when damage is reversible and/or to remove proteins when damage is irreversible (Gibellini L. *et al*., 2016). The UPRmt was initially identified in a monkey cell line (Zhao Q. *et al*., 2002) and has been extensively investigated in *C. elegans* while this pathway is only poorly understood in mammals (Haynes C.M. *et al*., 2007; 2010; Nargund A.M. *et al*., 2012). It has been suggested that the subcellular distribution of activating transcription factor associated with stress-1 (ATFS-1) is a key regulatory branch-point in the pathway. Under non-stress conditions, ATFS-1 is directed to the MM where it is rapidly degraded by the AAA+ protease, Lon. In the presence of protein overload however, ATFS-1 is not imported into mitochondria but accumulates in the cytosol and then translocates into the nucleus, where it activates the transcription of specific genes (Nargund A.M. *et al*., 2012). Significantly, the redistribution of ATFS-1 to the nucleus is dependent on the IMM embedded ABC-family peptide transporter Haf-1 (Haf transporter 1). Furthermore, both ClpX and ClpP from *C. elegans* have been experimentally implicated as direct components of the UPRmt signal transduction pathway (Haynes C.M. *et al*., 2007; 2010). Interestingly, Haynes and colleagues proposed a model, whereby stress within the MM is signalled across the IMM (via Haf-1) by a factor that is generated by the ClpXP protease (Haynes C.M. *et al*., 2010). Hence a ClpXP-dependent degradation product may regulate ATFS-1 trafficking.

In mammalian mitochondria, the PQC network contains key chaperones such as heat shock protein-70 (HSP70, also known as HSPA9 and mortalin) and HSP60 (also known as HSPD1) and their cofactors, and five different AAA+ proteases (Fig.I.6). Two of these proteases, Lon (also known as LONP1) and ClpXP, are located in the MM while IMS-facing Yme1L1 (also known as *i*-AAA protease) and two different matrix-facing *m*-AAA protease complexes are anchored to the IMM (Szklarczyk R. *et al*., 2014; Quiros, P.M. *et al*., 2015).

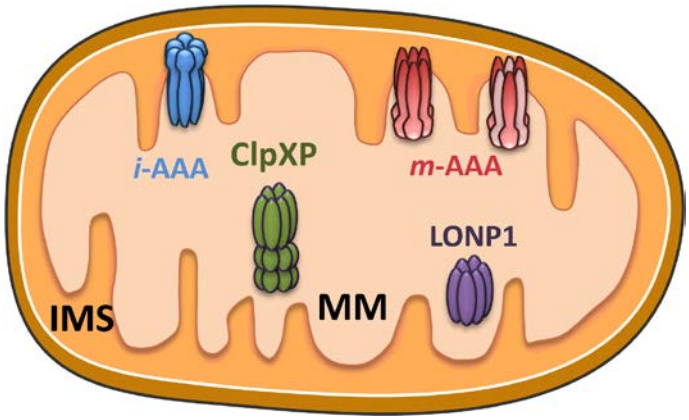

Figure I.6. Mitochondrial AAA+ proteases. LONP1 and ClpXP localize in the mitochondrial matrix (MM), whereas *i*-AAA and *m*-AAA are anchored to the inner membrane (IMM). *m*-AAA proteases expose their catalytic site to the MM and *i*-AAA to the intermembrane space (IMS). Figure modified from Matsushima Y. and Kaguni L.S., 2012.

Beyond UPRmt, mitochondrial fusion provides an additional level of quality control in the mitochondrial stress response that is triggered when ETC functions are temporarily impaired and $\Delta\Psi_m$ is reduced (Chan D.C., 2006). The late-stage quality control mechanism is characterized by mitophagy, which is the engulfment of mitochondria within double-membraned vesicles and subsequent deliver to lysosomes (Kim I. *et al*., 2007; He C. and Klionsky D.J., 2009). In humans, mitophagy is preceded by mitochondrial fission and is driven by two proteins: PTEN (phosphatase and tensin homolog)-induced putative kinase-1 (PINK1) and Parkin, an E3 ubiquitin ligase (Geisler S. *et al*., 2010; Westermann B., 2010). Therefore, depending on the duration and the intensity of stresses, several mechanisms can be engaged to repair damage and restore mitochondrial function (Fig.I.7). Mitochondrial proteases are not only involved in the UPRmt, but actively participate at multiple levels in the stress-response system (Gibellini L. *et al*., 2016).

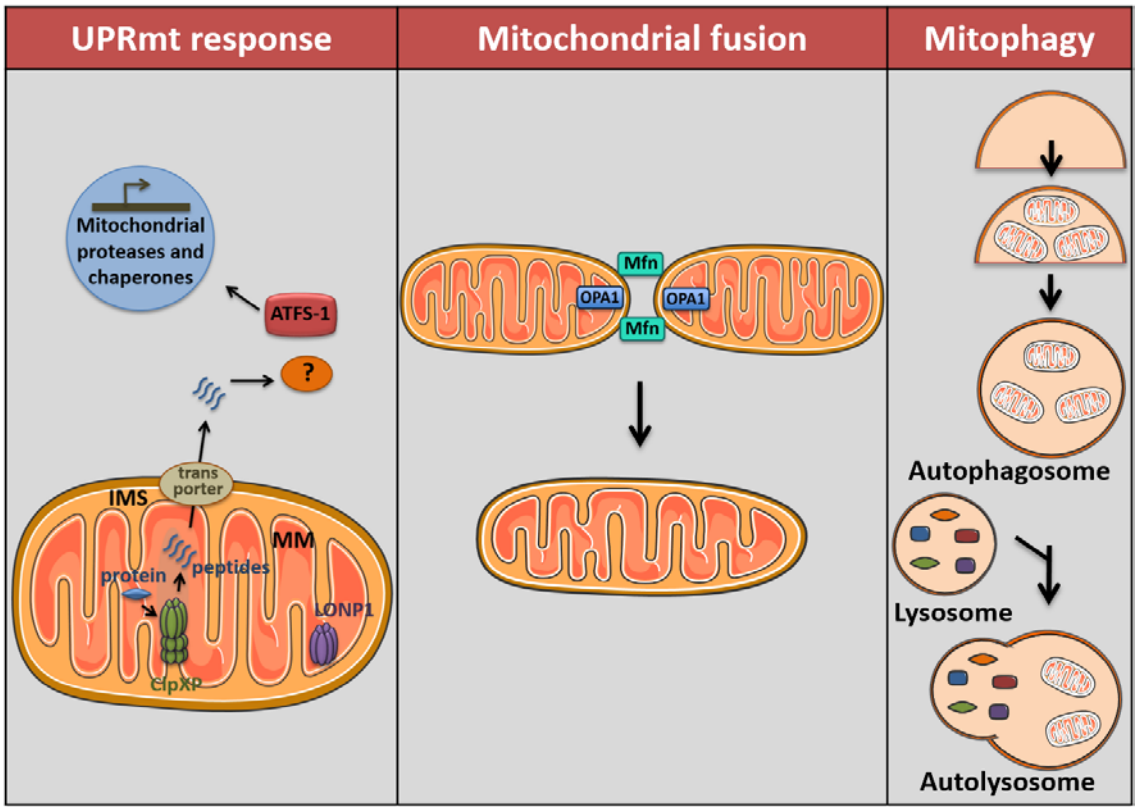

Figure I.7. Mitochondrial stress response. This process can involve different mechanisms: the mitochondrial unfolded protein response (UPRmt) which promotes the expression of mitochondrial-associated chaperones and proteases, such as LONP1 and ClpXP (left panel); mitochondrial fusion (middle panel) and mitophagy (right panel). Figure modified from Gibellini L. *et al.*, 2016.

5.5.1. Mitochondrial Lon protease

Mitochondrial Lon protease (LONP1) is a highly conserved and ubiquitous serine protease of the MM (Wang N. *et al.*, 1993). It is encoded by the *LONP1* gene (PRSS15), situated on chromosome 19, as a 107 kDa pre-protein which is then processed in a 100 kDa mature enzyme (Wang N. *et al.*, 1994). It is widely expressed in multiple human tissues – with the highest levels in the most metabolically active organs – heart, brain, liver and skeletal muscle (Wang N. *et al.*, 1993). There is also a peroxisomal form of the Lon protease, called LONP2; despite apparent similarities to LONP1 in proteolytic functions, the peroxisomal LONP2 is encoded by a completely different nuclear gene, and is regulated independently of LONP1 (Pomatto L.C. *et al.*, 2016).

LONP1 is regulated both at the post-transcriptional level, as at least three splicing variants have been described, and at the post-translational level, through acetylation/deacetylation at Lys917 (Gibellini L. *et al.*, 2014a). The mature protein

consists of three domains (Fig.I.8): an N-terminal domain, which is involved in substrate binding and oligomeric assembling, an ATPase AAA+ domain, and a C-terminal proteolytic domain, which contains a serine-lysine catalytic dyad (Rotanova T.V. *et al*., 2004). Data obtained through crystallography suggest that the proteolytic domain is inactive when LONP1 is in the monomeric form, to avoid uncontrolled proteolysis, and that its activation requires LONP1 oligomerization in hexamers (Garcia-Nafria J. *et al*., 2010).

Figure I.8. Domain structure of mitochondrial Lon protease (LONP1). It comprises three domains, an N-terminal domain, a central AAA+ ATPase domain and a C-terminal protease domain. The N-terminal domain is involved in oligomerization and protein substrate binding. The AAA+ domain contributes ATP binding and hydrolysis. The C-terminal protease domain contains a serine and lysine dyad in the active site.

In human cells, LONP1 is involved in several aspects of mitochondrial biology, by interacting with proteins involved in various functions of the organelle (Fig.I.9). LONP1 belongs to the mitochondrial proteolytic systems, degrading misfolded and damaged proteins (Pinti M. *et al*., 2015). In this context, six substrates of LONP1 have been identified: oxidatively modified aconitase (Aco2) (Bota D.A. and Davies K.J., 2002), mitochondrial transcription factor A (TFAM) (Matsushima Y. *et al*., 2010; Lu B. *et al*., 2013), steroidogenic acute regulatory protein (StAR) (Granot Z. *et al*., 2007), glutaminase C (GLS-1) (Kita K. *et al*., 2012), cystathionine β-synthase (CBS) (Teng H. *et al*., 2013) and 5-aminolevulinic acid synthase (ALAS-1) (Tian Q. *et al*., 2011). The fact that LONP1 downregulation leads to PINK1 accumulation in mammalian cells, suggests that also PINK1 could be target of LONP1 activity (Jin S.M. and Youle R.J., 2013). This protease also is involved in mtDNA maintenance through direct binding to mtDNA and proteolytic degradation of TFAM. LONP1 silencing in colon carcinoma cells affected OxPhos and Krebs cycle proteins (Gibellini L. *et al*., 2014b). In addition, LONP1 downregulation led to a decrease in the levels of several other proteins in the MM, including those involved in energetic metabolism, mitochondrial architecture, ribosome assembly, mtDNA metabolism and stress response (Gibellini L. *et al*., 2014b).

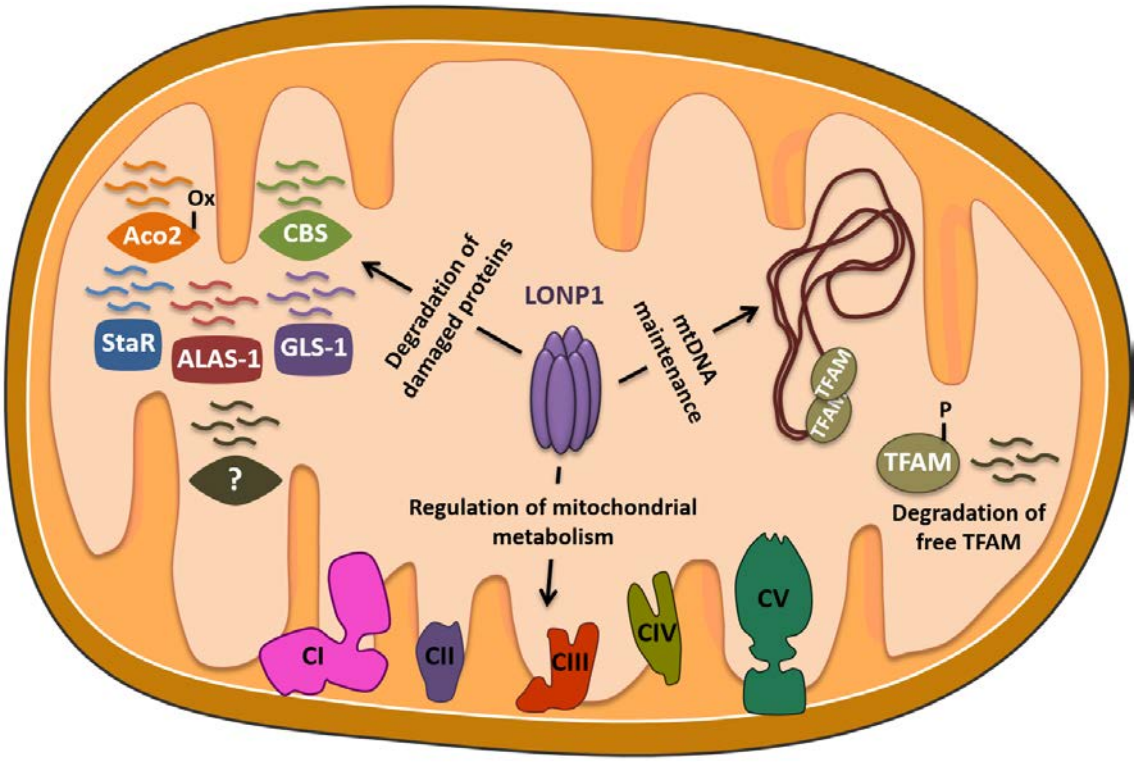

Figure I.9. Main functions of LONP1 in mitochondria of human cells. LONP1 is involved in (i) the degradation of damaged or oxidized proteins, such as aconitase (Aco2), steroidogenic acute regulatory protein (StAR), glutaminase C (GLS-1), cystathionine β-synthase (CBS) and 5-aminolevulinic acid synthase (ALAS-1); (ii) mitochondrial metabolism regulation by selective degradation of, and interaction with some subunits of OxPhos complexes and (iii) maintenance of mtDNA by degrading p-TFAM. Figure modified from Pinti M. *et al*., 2015.

LONP1 is one of the most important cellular stress-responsive proteins (Ngo J.K. and Davies K.J., 2009). Acute stressors, such as heat shock, serum starvation, mitochondrial protein overload, high levels of ROS and ER stress lead to its upregulation (Hori O. *et al*., 2002; Ngo J.K. and Davies K.J., 2009; Pinti M. *et al*., 2010; 2011; Bahat A. *et al*., 2015). The functional characterization of *LONP1* promoter has revealed the presence of several potential binding sites for stress-responsive transcription factors, such as nuclear respiratory factor 2 (NRF-2), nuclear factor-kappa B (NF-κB), Nkx-2 and the lymphoid transcription factor (Lyf-1) (Pinti M. *et al*., 2011). The *LONP1* promoter region -623/+1 contains a NRF-2 consensus binding site which is essential for response to ROS. The ability of NRF-2 to regulate LONP1 expression is a key factor in its ability to promote the expression of key components of the mtDNA transcription and replication machinery, as well as of genes encoding respiratory subunits (Scarpulla R.C., 2002). More recently, the analysis of transcriptional regulation of *LONP1* in HEK293 cells has

identified three binding sites for NRF-2 at the position -196, -183 and -150 of *LONP1* promoter (Bahat A. *et al*., 2015). Another very important transcriptional site in the promoter of this gene is the region -2023/-1230 that contains a putative binding site for NF-κB (Pinti M. *et al*., 2011). The presence of an NF-κB binding site further consolidate LONP1's role as a stress protein (Ngo J.K. and Davies K.J., 2009). LONP1 expression is also significantly induced by hypoxia-inducible factor 1 (HIF-1) (Fukuda R. *et al*., 2007). Furthermore, LONP1 is regulated at a post-translational level. The NAD^+-dependent mitochondrial deacetylase sirtuin 3 (SIRT3) mediates LONP1 deacetylation, and SIRT3 silencing causes an increase of LONP1 protein levels but not of LONP1 mRNA (Gibellini L. *et al*., 2014a).

As essential regulator of mitochondrial biology, LONP1 is emerging as an important element of mitochondrial alterations that can be observed in several human deseases in which the most active organs are involved (Tab.I.4) (Bota D.A. and Davies K.J., 2016). In addition, chronic upregulation of LONP1 has been associated with tumorigenesis. Malignant transformation and oncogenic growth are highly dependent on adaptation to new sources of energy and to hypoxia, which explains the important role LONP1 plays in a variety of malignancies including colon cancer (Quiros P.M. *et al*., 2014), diffuse large cell lymphoma (Bernstein S.H. *et al*., 2012), mammary epithelial, cervical cancer (Nie X. *et al*., 2013), bladder cancer (Liu Y. *et al*., 2014), etc. As LONP1 is upregulated by acute oxidative stress, it is also involved in a number of conditions caused by the ingestion of toxins and drugs which cause damage via generation of ROS or nitrogen species such $O_2^{\cdot -}$, H_2O_2, and $ONOO^-$, as in different tissues involved in detoxification such as the kidney and adipose tissues (Bota D.A. and Davies K.J., 2016). In conclusion, LONP1 is a major controller of several mitochondrial functions. Thus, it is not surprising that it is associated with the development of human diseases including cancer.

CATEGORY	DISEASES	REFERENCES
Impaired proteolytic activity and oligomerization of LONP1 caused by mutations in the encoding gene	Cerebral, ocular, dental, auricular, skeletal (CODAS) syndrome	Dikoglu E. *et al*., 2015; Strauss K.A. *et al*., 2015
Lower LONP1 expression	Hereditary spastic paraplegia	Hansen J. *et al*., 2008
Increased LONP1 levels with mtDNA mutated	Mitochondrial encephalomyopathy, lactic acidosis, and stroke-like episodes (MELAS)	Felk S. *et al*., 2010
LONP1 overexpression and increased proteolytic activity	Friedreich´s ataxia	Guillon B. *et al*., 2009
	HAART-related lipodystrophy	Pinti M. *et al*., 2010
LONP1 overexpression but decreased LONP1 proteolytic activity	Myoclonic epilepsy with ragged-red fibres (MERRFs)	Wu S.B. *et al*., 2010
	Cardiac ischemia and heart failure	Kuo C.Y. *et al*., 2015

Table I.4. Classification of human diseases in which LONP1 expression is modified. Table modified from Pinti M. *et al*., 2015.

5.5.2. ClpXP

ClpP is a serine protease whose functional form is a heptamer that assembles into a tetradecamer in the presence of caseinolytic protease X (ClpX) (Kang S.G. *et al*., 2005). ClpP is encoded by the nuclear gene *CLPP*, located in the chromosome 19. The transcription and translation of *CLPP* result in the synthesis of a precursor protein of approximately 37 kDa, which is then processed in the mature form of 32 kDa (Corydon T.J. *et al*., 1998). The AAA+ ATPase ClpX (37 kDa) is encoded by the *CLPX* gene, located on chromosome 15; together with ClpP it forms the ClpXP complex, an ATP-dependent protease which degrades damaged and misfolded proteins in mitochondria (Baker T.A. and Sauer R.T., 2012). As mentioned above, ClpXP acts by inducing the UPRmt in *C.*

elegans (Haynes C.M. *et al*., 2010). In mammalian cellular models, the overexpression of ClpXP is also associated with the upregulation of nuclear genes involved in UPRmt, but the mechanism of this signalling is still a matter of debate (Al-Furoukh N. *et al*., 2015).

5.5.3. Heat-shock proteins

Heat-shock proteins (HSPs), or heat stress proteins, are highly conserved chaperones that play crucial roles in folding/unfolding of proteins, assembly of multiprotein complexes, transport/sorting of proteins into correct subcellular compartments, cell-cycle control and signalling, protection of cells against stress/apoptosis and antigen presentation (Li Z. and Srivastava P., 2004). HSPs constitute a large family of proteins that are often classified based on their molecular weight: HSP10, HSP40, HSP60, HSP70, HSP90, etc. HSP90 is located in the cytosol and consists of N-terminal ATP binding domain, substrate-interacting middle domain, and C-terminal dimerization domain (Jackson S.E., 2013). There are 2 major cytosolic HSP90 proteins: HSP90AA1 (Hsp90α), an inducible form, and HSP90AB1 (Hsp90β), a constitutive form. Other HSP90 proteins are found in the ER (HSP90B1) and mitochondria (TRAP1) (Chen B. *et al*., 2005). Despite high conservation between Hsp90α and Hsp90β, these proteins display different functions (Zuehlke A.D. *et al*., 2015). Unlike Hsp90α, Hsp90β is essential in mammals, suggesting that Hsp90β is involved in processes that maintain viability, whereas Hsp90α is involved in more adaptive roles (Voss A.K. *et al*., 2000; Grad I. *et al*., 2010). On the other hand, HSP90B1 plays critical roles in folding proteins in the secretory pathway such as toll-like receptors and integrins (Randow F. and Seed B., 2001; Yang Y. *et al*., 2007). It is considered an essential immune chaperone to regulate both innate and adaptive immunity (Schild H. and Rammensee H.G., 2000).

6. APOPTOTIC CELL DEATH

Apoptosis is a (patho)physiological phenomenon of enormous biological importance (Perl M. *et al*., 2005). It is a type of cell death characterized by membrane blebbing, shrinkage of the cell, chromatin condensation and nuclear fragmentation. Intense research over the last 20 years has revealed that this process is necessary for

development and homeostasis of multicellular organisms. It is also related to many pathological processes; increased apoptosis is a prominent feature of numerous neurodegenerative diseases (Alzheimer's disease, Parkinson´s disease and Huntington´s disease), whereas apoptosis below the physiological rate is associated with cancer. Disturbances of apoptosis are also believed to be implicated in a long list of clinical conditions such as ischaemia/reperfusion, diabetes and infectious diseases (Perl M. *et al*., 2005).

Two major apoptotic pathways have been recognized: the extrinsic, which is originated at the death receptors on the cell membrane and the intrinsic, in which mitochondria are major players (Elmore S., 2007). Importantly, certain stimuli can activate both pathways. Additionally, these pathways are interconnected and converge on the same caspase effectors, as caspase activity has been found in practically all cases of apoptosis. Mitochondrial apoptosis can also be induced as a secondary event upon triggering of the extrinsic pathway (Wang X., 2001; Ekert P.G. and Vaux D.L., 2005). Since mitochondria were related to apoptosis in the 1990s, several hypotheses regarding the mechanisms of their implication have emerged including disruption of the $\Delta\Psi_m$, opening of the voltage-gated ion channel, regulation of the proton flux and pore-forming by B-cell lymphoma 2 (Bcl-2) proteins and release of pro-apoptotic proteins (Elmore S., 2007).

At present, there is a general consensus that OMM permeabilization is a key event in apoptosis. This process enables the release of pro-apoptotic factors from the IMS to the cytosol, which triggers downstream cell death pathways. Indeed, the first solid evidence regarding mitochondrial implication in apoptosis was the discovery that cyt *c*, a well-known member of the ETC, is released during mitochondrial apoptosis and activates down-stream caspases in the cytosol (Liu X. *et al*., 1996; Yang J. *et al*., 1997).

7. AUTOPHAGY

In contrast to apoptosis, autophagy is primarily a cell survival/defence mechanism that is essential for the eliminations of damaged organelles, misfolded proteins and intracellular microbes. It is implicated in important biological functions such as cell survival, cell death, metabolism, development, aging, infections and immunity. For this

reason, alterations in its functioning have been associated with the aetiology of many human diseases such as cancer, neurodegenerative and muscular diseases, metabolic, hepatic and cardiovascular disorders, infections by microorganisms, diabetes and obesity (Mizushima N. *et al*., 2008; Meijer A.J. and Codogno P., 2009; Shen H.M. and Codogno P., 2011).

This complex biological phenomenon, first described 50 years ago (De Duve C. and Wattiaux R., 1966), consists of selective and controlled degradation of cellular components and can be divided into 3 types depending on how the cytoplasmatic material for degradation is delivered to the lysosome: macroautophagy (or simply denominated autophagy), microautophagy and chaperone-mediated autophagy. In macroautophagy, this content is sequestered in a double-membrane vesicle called autophagosome. The autophagic pathways seem to be very complex but the core machinery generally involves two ubiquitin-like conjugation systems (Ohsumi Y., 2001; Klionsky D.J., 2007). In the first, the ubiquitin-like protein Atg12 and Atg5 generate a complex which interacts with Atg16 to form a multimer complex that is localized in the membrane of the early autophagosome. In the second system, the ubiquitin-like protein Atg8, also known as microtubule-associated protein 1 light chain 2 (LC3), is cleaved by Atg4 and then conjugated to phosphatidylethanolamine giving rise to LC3-II. This conjugated form is targeted to the autophagosomal membrane. While the Atg5/Atg12/Atg16 complex detaches from mature autophagosomes once the membrane extension has terminated, Atg8/LC3-II is associated with the autophagosome throughout the entire process, until its degradation by the lysosome. This is why this protein is used as a universal marker of autophagy.

Although most of the cytosol can be randomly "sequestered" through autophagy, in many cases autophagy has substrate specificity. For example, ubiquitinated protein aggregates and unnecessary or damaged organelles are selectively chosen for autophagy degradation (He C. and Klionsky D.J., 2009). Different terms have been used to describe the selectivity of each process according to the element to be degraded, such as autophagic degradation of mitochondria (mitophagy) (Kim I. *et al*., 2007), ribosomes (ribophagy) (Kraft C. *et al*., 2008), peroxisomes (pexophagy) (Dunn W.A. Jr. *et al*., 2005) and ER (reticulophagy) (Bernales S. *et al*., 2006; Klionsky D.J. *et al*., 2007).

8. ENDOPLASMIC RETICULUM (ER)

The endoplasmic reticulum (ER) is a cellular organelle that forms an interconnected network of flattened, membrane-enclosed sacs or tube-like structures known as cisternae, which are continuous with the outer nuclear membrane. There are two types of ER, rough, studded with ribosomes, and smooth-extended through the cell (Lodish H. *et al*., 2003).

The ER is the main site of synthesis, storing, modifying and transport of newly synthesized proteins (Lodish H. *et al*., 2003), as well as the main centre of storage, signalling and regulation of intracellular Ca^{2+}. In addition, this organelle performs other functions such as detoxification of xenobiotics and biosynthesis of steroids, cholesterol and other lipids (Rao R.V. *et al*., 2004; Deegan S. *et al*., 2013).

The lumen of the ER constitutes a unique cellular environment, possessing the highest Ca^{2+} concentrations of the cell due to the active transport of Ca^{2+} ATPases. In addition, because of its role in protein folding and transport in the secretory pathway, it is rich in Ca^{2+}-dependent chaperones such as the 78 kDa glucose-regulated protein (called Grp78, BiP or HSPA5), Grp94 (also known as HSP90B1) and calreticulin, which helps to stabilize proteins that are not completely folded. On the other hand, the lumen of the ER is a highly oxidizing environment, crucial for the formation of disulphide bonds mediated by the protein disulphide isomerase (PDI) and for the correct folding and modification of many proteins destined for secretion or anchorage in the cell surface (Kim I. *et al*., 2008).

The molecular profile of the ER reflects its signalling role and is strongly dominated by components of the Ca^{2+} signalling pathway. It contains the inositol-1,4,5-triphosphate (IP_3) receptors (IP_3Rs) and ryanodine receptors (RyRs) responsible for releasing Ca^{2+} in response to the input signals (Patel S. *et al*., 1999; Patterson R.L. *et al*., 2004; Mikoshiba K., 2006). Both the regulated release and the leak of Ca^{2+} are counteracted by the sarco-endoplasmic reticulum Ca^{2+}-ATPase (SERCA) whose function is to maintain the internal store of Ca^{2+}. SERCA transfers Ca^{2+} from the cytosol of the cell to the lumen of the ER at the expense of ATP hydrolysis (Clapham D.E., 2007). The luminal Ca^{2+}-binding proteins such as calnexin (CNX) and calreticulin play an important

role in regulating the SERCA activity and maintenance of a constant luminal level of Ca^{2+} (John L.M. *et al*., 1998).

A wide variety of alterations such as hypoxia, lack of nutrients, redox imbalance, changes in Ca^{2+} homeostasis, increased protein translation, virus infections, chemical substances and mutations can generate an imbalance between the capacity of ER folding and the amount of proteins to be folded, causing the accumulation of unfolded or poorly folded proteins and thus generating ER stress. The resulting fate of the cell is either survival or apoptosis, depending on the cellular response to the stress. When misfolded proteins accumulate in the ER lumen, cells activate a self-protective mechanism, termed the unfolded protein response (UPR) (Xu C. *et al*., 2005; Hussain S.G. and Ramaiah K.V., 2007; Cnop M. *et al*., 2012).

8.1. Unfolded protein response (UPR)

The UPR of eukaryotic cells consists of three different mechanisms: (i) translational attenuation to limit further protein loads (Harding H.P. *et al*., 1999), (ii) transcriptional activation of genes encoding factors involved in ER protein folding and degradation (Gething M.J. and Sambrook J., 1992) and (iii) ER-associated degradation (ERAD), which restores the folding capacity through the clearance of unfolded or misfolded proteins by enabling their retrotranslocation from the ER into the cytosol via the ubiquitin-proteasome system (Mori K., 2000).

In mammals, the UPR signalling pathway is initiated by three ER membrane-associated sensors: activating transcription factor-6 (ATF6), inositol-requiring transmembrane kinase/endoribonuclease 1 (IRE1) and double-stranded RNA-dependent protein kinase (PKR)-like eukaryotic initiation factor 2α (eIF2α) kinase (PERK) (Fig.I.10). If the survival signal is insufficient to relieve the cells from ER stress, apoptosis is triggered in order to remove ER stress-damaged cells. Many reports have shown that several molecules, including IRE1 (Urano F. *et al*., 2000; Iwawaki T. *et al*., 2001), apoptosis signal-regulating kinase 1 (ASK1) (Nishitoh H. *et al*., 2002), Bax/Bak (Wei M.C. *et al*., 2001; Scorrano L. *et al*., 2003; Hetz C. *et al*., 2006), PERK, eIF2α-activating transcription factor-4 (ATF4) (Rutkowski D.T. *et al*., 2006), and CCAAT enhancer-binding protein (C/EBP) homologous protein (CHOP, also known as a growth arrest- and DNA damage-

inducible gene 153 (GADD153)) (Zinszner H. *et al*., 1998; Oyadomari S. *et al*., 2002), are related to ER stress-induced apoptosis signalling pathways.

Dysfunction of the UPR, or prolonged ER stress, disrupts ER homeostasis. A large number of groups have described the relation between ER stress responses and a variety of human diseases, including neurodegenerative disease, metabolic disease, inflammatory disease, diabetes mellitus, cancer and cardiovascular disease (Kaufman R.J., 2002; Tabas I. and Ron D., 2011).

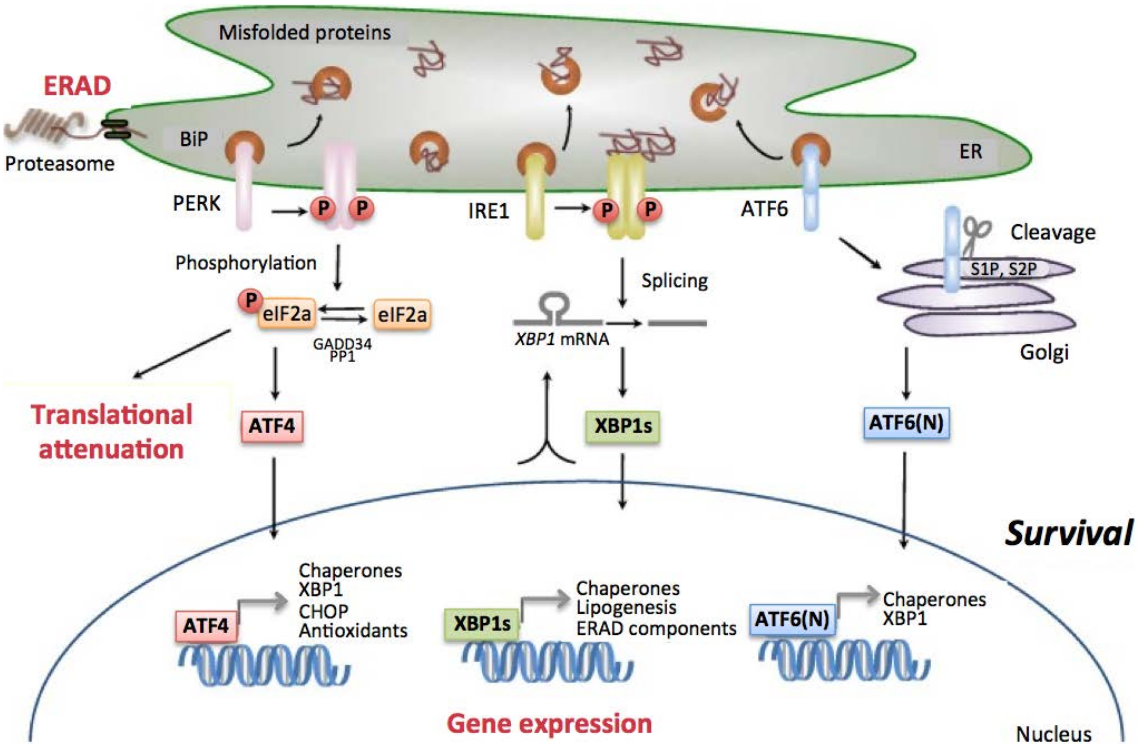

Figure I.10. Survival signalling under ER stress conditions. The accumulation of misfolded proteins activates three ER stress sensors: activating transcription factor-6 (ATF6), inositol-requiring transmembrane kinase/endoribonuclease 1 (IRE1), and double-stranded RNA-dependent protein kinase (PKR)-like eukaryotic initiation factor 2α (eIF2α) kinase (PERK). ATF6 is activated following cleavage with S1P and S2P, after transport to the Golgi. Activated ATF6 (ATF6(N)) induces the expression of ER chaperones and XBP1. Activated IRE1 induces the splicing of *XBP1* mRNA, and the resulting spliced XBP1 protein (XBP1s) controls the transcription of ER-resident chaperones and genes involved in lipogenesis and ER-associated degradation (ERAD). Activated PERK enables the translation of activating transcription factor-4 (ATF4) which induces the transcription of many genes required for ER quality control (Kadowaki H. and Nishitoh H., 2013).

8.2. ER stress in the liver

The liver is one of the main secretory organs of the organism. Its multiple functions include synthesis and secretion of plasma proteins, regulation of glucose homeostasis, and metabolism of lipids and xenobiotics. Hepatocytes, like other secretory cells, have a highly active and well-developed ER structure that represents about 50% of the cellular content. Due to the great importance of ER function in liver metabolism, ER stress and UPR have been associated with almost all forms of acute and chronic liver diseases, with special relevance in steatosis, steatohepatitis, hyperhomocysteinemia, viral hepatitis, ischemia/reperfusion injury and drug-induced toxicity (Ji C., 2008; Malhi H. and Kaufman R.J., 2011).

The use of some drugs and the development of hepatic toxicity have been associated with ER stress, such as the case of high-dose acetaminophen in mouse liver (Nagy G. *et al*., 2007; 2010) and metapyrylene in rats (Craig A. *et al*., 2006; Auman J.T. *et al*., 2007). Some PIs used in HIV treatment such as SQV, ATV and RTV also induce ER stress associated with hepatotoxicity, as this effect has been seen in human hepatocyte cell lines and primary rodent hepatocytes (Parker R.A. *et al*., 2005; Zhou H. *et al*., 2006; Flint O.P. *et al*., 2009).

9. LINK BETWEEN ER AND MITOCHONDRIA

9.1. Mitochondria-associated membranes (MAMs)

The presence of a physical connection between the ER and mitochondria was hinted for many decades and indicated by pioneering electron microscopic observations which revealed a possible interplay between the OMM and the ER membrane in 1969 (Ruby J.R. *et al*., 1969). However, mitochondria-associated membranes (MAMs) were not discovered as a biochemical entity until 1990, when Jean Vance isolated a membrane structure through cell fractionation, which she defined as the contact site between the ER and the mitochondria (Vance J.E., 1990). MAMs represent ER membranes closely apposed to mitochondria, which can be purified as distinct structures. A breakthrough in the functional characterization of the MAMs only came up at the turn of the millennium, mainly through the work of Rizzuto R. *et al*., 1998.

They showed that the mitochondria are exposed to higher Ca^{2+} concentrations than the cytosol after Ca^{2+} release from the ER, suggesting the existence of microdomains of high Ca^{2+} concentrations and transfer between the ER and mitochondria that required a physical, proteinaceous linkage between these two organelles. At this time, Vance's lab followed up its initial discovery by exploring the function of the MAMs in lipid homeostasis in rat liver cells (Shiao Y.J. *et al*., 1998). Similar findings highlighting the key role MAMs play in lipid synthesis were also soon reported in yeast cells (Achleitner G. *et al*., 1999), indicating the evolutionary conserved functions of these ER-mitochondria contact sites. In the last decades through the continuous advances in live-cell imaging techniques allowing 3D reconstitutions of ER and mitochondria networks, the total surface area of mitochondria juxtaposed to the ER has been estimated at around 5-20% (Rizzuto R. *et al*., 1998). Therefore, MAMs provide more than just a proteinaceous link between these two organelles; they rather enable functional transit of metabolites and signalling molecules with relevant implications in homeostatic functions within the cell and beyond (van Vliet A.R. *et al*., 2014).

MAMs seem to be a highly flexible collection of proteins that is able to recruit a variety of signalling components according to the cell's need. In spite of the increasingly large number of proteins recognized to participate in this complex, a core subset of ER and mitochondria associated proteins has been identified that seem to form the basic components of the MAMs (Fig.I.11). These proteins include Ca^{2+} ion channels located at the ER or at the OMM, like the IP_3R (Furuichi T. *et al*., 1989) and voltage-dependent anion channel 1 (VDAC1, also known as porin) (Szabadkai G. *et al*., 2006); enzymes of the lipid biosynthetic pathways and lipid transfer proteins like long chain acyl-CoA synthetase (FACL4) (Voelker D.R., 2005); various chaperones, like the glucose-regulated protein 75 (Grp75) physically associated to VDAC1 (Szabadkai G. *et al*., 2006), the ER chaperone CNX (Lynes E.M. *et al*., 2012) and the sigma1-receptor (SIG-1R) (Hayashi T. and Su T.P., 2003; 2007); enzymes involved in ER redox regulation, like the ER oxidoreductase 1 alpha (Ero1α) (Anelli T. *et al*., 2012); protein kinases, like PERK (Verfaillie T. *et al*., 2012); and proteins involved in the regulation of ER-vesicular sorting, like phosphofurin acidic cluster sorting protein 2 (PACS-2) (Simmen T. *et al*., 2005) and vesicle-associated membrane protein-associated protein B/C (VAP-B/C)

associated with protein tyrosine phosphatase-interacting protein 51 (PTPIP51) that is involved in cellular Ca^{2+} homeostasis (De Vos K.J. *et al*., 2012). In addition, proteins regulating mitochondrial shape and fusion/fission, like Mfn2, Mfn1, Fis1 and Drp1 have been found in the MAMs (De Brito O.M. and Scorrano L., 2008; Iwasawa R. *et al*., 2011). Mfn2 is one of the best studied MAMs-resident proteins, whose effects on MAMs structure and function have been reported in different studies (Chen H. *et al*., 2003; De Brito O.M. and Scorrano L., 2008; Munoz J.P. *et al*., 2013). This GTPase, which is located on both the OMM and the ER membranes, is able to establish homotypic as well as heterotypic (with the OMM-associated Mfn1) ER–mitochondria interactions, which provide stability to the interface between these organelles. In line with this, Mfn2 ablation in murine fibroblasts and HeLa cells led to the disruption of the ER-mitochondria contact sites, increasing the distance between these organelles, and caused a change in both the ER and mitochondrial morphology. Importantly, loss of Mfn2 also caused a defective mitochondrial Ca^{2+} uptake (De Brito O.M. and Scorrano L., 2008), demonstrating how disruption of the ER-mitochondria contact sites may profoundly affect Ca^{2+} buffering capacity of the mitochondria and overall calcium homeostasis, with vital consequences on the cellular fate.

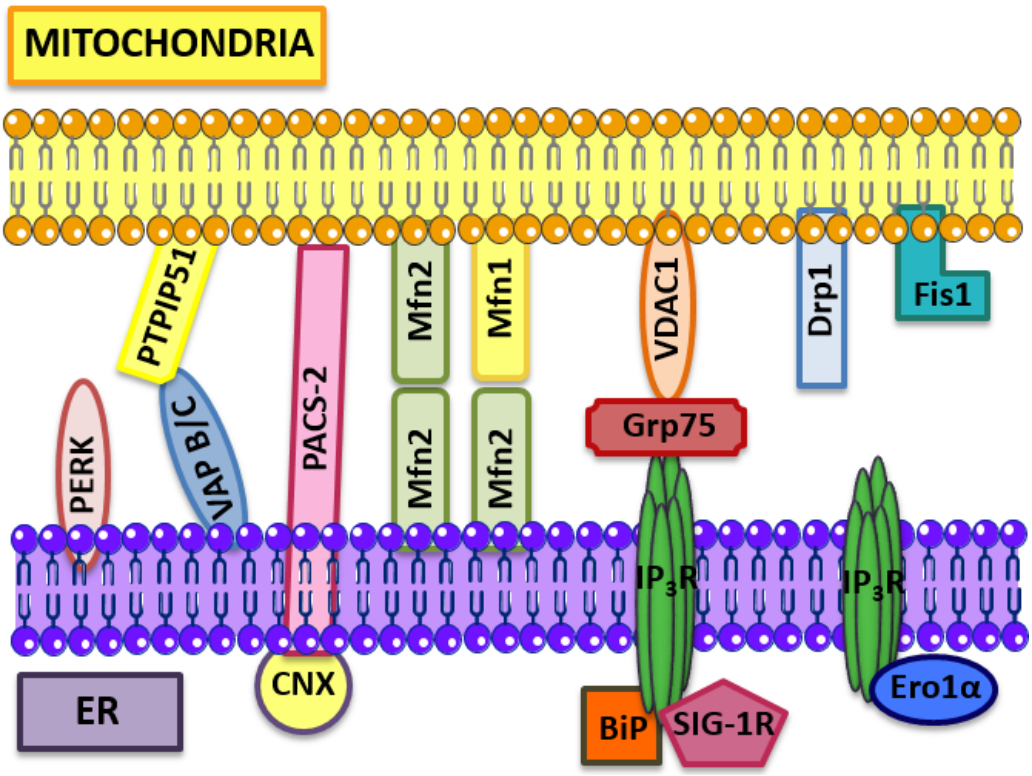

Figure I.11. Summary of MAMs protein composition. These proteins include Ca^{2+} ion channels located at the ER or at the OMM, like the inositol-1,4,5-triphosphate receptor (IP_3R) and voltage-dependent anion channel 1 (VDAC1); proteins that regulate mitochondrial shape and fusion/fission, like Mfn2, Mfn1, Fis1 and Drp1; various chaperones, like binding immunoglobulin protein (BiP) also known as 78 kDa glucose-regulated protein (Grp78), the glucose-regulated protein 75 (Grp75) physically associated to VDAC1, the ER chaperone calnexin (CNX) and the sigma1-receptor (SIG-1R); enzymes involved in ER redox regulation, like the ER oxidoreductase 1 alpha (Ero1α); protein kinases, like PERK; and proteins involved in the regulation of ER-vesicular sorting, like phosphofurin acidic cluster sorting protein 2 (PACS-2) and vesicle-associated membrane protein-associated protein B/C (VAP-B/C) associated with protein tyrosine phosphatase-interacting protein 51 (PTPIP51).

9.2. The function of the ER-mitochondria tethering

Eukaryotic cells contain membrane-bound organelles with unique identities and specialized functions. Communication and cooperation between ER and mitochondria take place in order to maintain a variety of physiological functions (Fig.I.12). This communication requires short distances between membranes to connect them, and allowing ions, metabolites and lipids exchange.

9.2.1. Ca^{2+} exchange

Cyclical Ca^{2+} exchange between ER and mitochondria is essential for cell life and death (Patergnani S. *et al*., 2011). ER Ca^{2+} determines the correct functioning of numerous ER enzymes involved in the manufacture of secretory proteins (Michalak M. *et al*., 2002). Intramitochondrial Ca^{2+} activate numerous mitochondrial enzymes such as enzymes catalyzing OxPhos (Gellerich F.N. *et al.*, 2010). The apposition of the ER with mitochondria is a prerequisite for Ca^{2+} exchange. After their intracellular release from the ER, free Ca^{2+} ions cannot travel further than 100-500 nm before they typically encounter a Ca^{2+}-binding protein (Allbritton N.L. *et al*., 1992). This high concentration of Ca^{2+}-binding proteins creates microdomains in the proximity of ER Ca^{2+} release channels (Parker I. and Yao Y., 1996). Fluorescence microscopy with Ca^{2+}-sensitive photoproteins showed that mitochondrial movement is slowest when cytosolic Ca^{2+} concentrations are high (Yi M. *et al*., 2004). Ca^{2+}-sensitive probes attached to the OMM have further demonstrated that mitochondria specifically approach the ER where capacitive Ca^{2+} influx occurs (Giacomello M. *et al*., 2010; Csordas G. *et al*., 2010).

Low or very high cytosolic Ca^{2+} concentrations diminish IP_3R opening and hence reduce ER Ca^{2+} release (Bezprozvanny I. *et al*., 1991). With this, Ca^{2+} released from the ER serves to autoregulate its release from this storage compartment. These findings also predict a central role of the extent of ER-mitochondria apposition in cytosolic Ca^{2+} homeostasis. Thus, ER-mitochondria Ca^{2+} signalling and exchange have to work interdependently to determine the Ca^{2+} concentrations and the correct functioning of both the ER and mitochondria.

Once released from mitochondria, Ca^{2+} is efficiently taken up into the ER by Ca^{2+} pumps of the SERCA family, which close the circle of intracellular Ca^{2+} signalling between the ER and mitochondria (Vangheluwe P. *et al*., 2005). The SERCA inhibitor thapsigargin (TG) produces high cytosolic Ca^{2+} concentrations which cause mitochondrial Ca^{2+} overload (Beaver J.P. and Waring P., 1996). This condition ultimately provokes the irreversible opening of IP_3Rs through the binding of mitochondrial cyt *c* at MAMs, triggering apoptosis. Thus MAMs can also accommodate a massive transfer of Ca^{2+} from the ER to mitochondria to promote cell death

(Boehning D. *et al*., 2003) and therefore not only determines ER-mitochondria Ca^{2+} signalling, but also the speed of apoptosis onset (Simmen T. *et al*., 2005; De Brito O.M. and Scorrano L., 2008).

9.2.2. Lipid metabolism

MAMs were initially described as an ER subdomain enriched in proteins involved in lipid metabolism. Early biochemical studies on triacylglycerol, phosphatidylcholine (PC) and phosphatidylethanolamine (PE) showed that the synthesis of these lipids requires enzymatic activity associated with both the ER and mitochondria, thus postulating a transport and transfer of lipids between the ER and mitochondria (Dennis E.A. and Kennedy E.P., 1972; Jelsema C.L. and Morre D.J., 1978; Bell R.M. *et al*., 1981). FACL4 which mediates the ligation of fatty acids to coenzyme A (CoA) and is involved in triacylglycerol synthesis, is used today as one of the most reliable MAMs marker proteins (Voelker D.R., 2005). Also, acyl-CoA:cholesterol acyltransferase-1 (ACAT1/SOAT1) is a MAMs marker protein, since its enzymatic activity is among the most enriched on the MAMs (Rusinol A.E. *et al*., 1994). All of this suggests that MAMs provide a tight platform for lipid synthesis and lipid transfer between the ER and mitochondria.

Interestingly, the accumulation of lipid metabolism enzymes in the MAMs suggest that lipid synthesis and exchange at the MAMs generate an ER subdomain with unique properties (Sano R. *et al*., 2009). Studies indicate that the MAMs-localized lipid handling may have a profound impact on mitochondrial metabolism, since yeast cells defective in phosphatidylserine (PS) biosynthesis become respiration-deficient (Birner R. *et al*., 2001) and mouse PS decarboxylase knockout cells show altered mitochondrial membrane dynamics (Steenbergen R. *et al*., 2005).

9.2.3. Mitochondrial morphology

Several proteins involved in mitochondrial movement along microtubules, such as dynein and kinesin, are tightly regulated by increases in Ca^{2+} levels at the MAMs (Yi M. *et al*., 2004; Pizzo P. *et al*., 2012). Reduced mitochondrial motility induces an increase in their association to the MAMs, thus enhancing their Ca^{2+} uptake and buffering capacity (Yi M. *et al*., 2004; Pizzo P. and Pozzan T., 2007). Miro family of proteins

(Miro1 and 2) is one of the master regulators of mitochondrial motility, based on local Ca^{2+} levels. It has been shown that these proteins have an important role in tethering the mitochondria to the cytoskeleton by binding kinesin, thus leading to the movement of this organelle (Fransson S. *et al*., 2006; Saotome M. *et al*., 2008).

Beyond the regulation of mitochondrial motility, MAMs participate in the regulation of mitochondrial morphology (Scorrano L., 2013). In 2011, Friedman and co-workers demonstrated in yeast that mitochondrial fission occurs at positions where ER tubules contact and constrict mitochondria. These constrictions would facilitate Drp1 recruitment (Friedman J.R. *et al*., 2011). As mentioned above, Mff and Fis1 are important for Drp1 recruitment to mitochondrial fission sites and both proteins have also been localized to the MAMs (Loson O.C. *et al*., 2013). Mff localizes in a Drp1-independent manner to mitochondrial constrictions at sites of ER contact (Loson O.C. *et al*., 2013). All these findings suggest that the recruitment of the mitochondrial fission machinery to the MAMs is crucial for mitochondrial morphology.

9.2.4. Autophagy

As mentioned above, autophagy is a degradative process in which cytosolic components and damaged organelles, but also invading pathogens, are engulfed in double-membrane vesicles and delivered to lysosomes for their degradation (Klionsky D.J., 2007). It has been described that the ER-mitochondrial contacts are essential for autophagosome formation. Different proteins involved in autophagy were found to be enriched in MAMs after starvation-induced autophagy (Hamasaki M. *et al*., 2013): ATG14 (autophagy related 14), ATG5 and DFC1 (double FYVE-domain containing protein 1) transfer and assemble in a MAMs complex. Interestingly, the disruption of ER-mitochondrial contacts by knocking down PACS-2 or Mfn2 decreases the number of autophagosomes, suggesting that MAMs integrity is a requirement for autophagosome formation. The impact of ER-mitochondria contact on autophagy is also evident when the autophagic membranes originate from mitochondria. According to this model, disruption of ER-mitochondria contacts by ablation of Mfn2 inhibits lipid transfer and starvation-induced autophagy, by inhibiting the PS transfer from ER into mitochondria-derived autophagosomes (Hailey D.W. *et al*., 2010). These studies highlight the importance of ER-mitochondria tethering in the progression of the starvation-induced

autophagy. MAMs serve as platform for autophagosome formation (Hamasaki M. *et al*., 2013) and are indispensable for lipid transfer from ER to mitochondria and eventual autophagosome formation on the surface of mitochondria (Hailey D.W. *et al*., 2010). However, it remains unclear whether autophagosome originate only at MAMs and whether this localization is important only in starvation-induced autophagy.

9.2.5. Apoptosis

During apoptosis, mitochondrial fragmentation increases due to recruitment of the fission protein Drp1 to the OMM. In this particular location, Drp1 also stimulates Bax (Bcl2-associated X protein, a pro-apoptotic OMM protein) to form oligomeric pores that cause OMM permeabilization (OMMP), causing the release of cyt *c* and other pro-apoptotic factors to the cytosol (Hoppins S. and Nunnari J., 2012). Conversely, when mitochondrial fusion is increased, apoptosis is attenuated.

Apoptosis is intimately connected to the mitochondrial Ca^{2+} levels. Excessive mitochondrial Ca^{2+} accumulation often leads to OMMP and finally the induction of apoptosis (Pinton P. *et al*., 2008). Several studies have associated MAMs and a higher ER-mitochondria Ca^{2+} transfer with mitochondrial dysfunction and apoptosis. It has been shown that IP_3R activity is regulated by several interacting proteins. In fact, it has been shown that cyt *c* binds to IP_3R channels during apoptosis, blocking the Ca^{2+}-dependent inhibition of IP_3R function and promotes apoptotic Ca^{2+} release (Pinton P. *et al*., 2008). Indeed, PTEN has also been reported to be located at the MAMs and enhances Ca^{2+} signalling to the mitochondria in situations of increased ER stress and pro-apoptotic signalling (Bononi A. *et al*., 2013).

9.2.6. Inflammatory response

The inflammasome is a multiprotein complex of the innate immune response that regulates the activation of caspase-1 and triggers the processing and maturation of proinflammatory cytokines (Schroder K. and Tschopp J., 2010; Franchi L. *et al*., 2010). NLRP3 (Nod-like receptor family, pyrin domain containing 3) is the most thoroughly characterized inflammasome and comprises the NLR protein NLRP3, the adapter apoptosis-associated speck-like protein (ASC) and pro-caspase-1 (Jin C. and Flavell R.A., 2010). NLRP3 colocalizes with ASC proteins at the MAMs fraction and ASC

translocation to the MAMs seems to be NLRP3-dependent (Zhou R. *et al*., 2011).

The generation of mitochondrial ROS appears to be common to many activators of the NLRP3 inflammasome (Dostert C. *et al*., 2008). It has been described that VDAC is ultimately required for mitochondrial ROS production. In this regard, the downregulation of VDAC significantly impairs NLRP3 inflammasome activation (Zhou R. *et al*., 2011). The critical role of MAMs in NLRP3 inflammasome activation is still unclear. However, all these findings suggested the crucial role of the MAMs in the coordination of cell non-autonomous functions, like inflammation. Moreover, another NLRP3 binding partner, thioredoxin-interacting protein (TXNIP), redistributes to MAMs/mitochondria in response to oxidative stress (Saxena G. *et al*., 2010) or NLRP3 inflammasome activation (Zhou R. *et al*., 2011). NLRP3 and IRE1α signalling pathways are required for TXNIP induction under ER stress (Oslowski C.M. *et al*., 2012).

9.2.7. Modulation of ER stress

During early phases of ER stress, ER–mitochondrial connection is enriched in the perinuclear zone of cells (Bravo R. *et al*., 2011). In this cellular context, it would be feasible that connections between ER and mitochondria participate in the regulation of ER stress.

In ROS-mediated ER stress, it was shown that PERK localizes in the MAMs, being required for the regulation of interorganellar communication during ROS-induced cell death in immortalized mouse embryonic fibroblasts (MEFs) (Verfaillie T. *et al*., 2012). Furthermore, genetic ablation of *PERK* decreased mitochondrial Ca^{2+} uptake, conferring mitochondrial protection against apoptosis (Verfaillie T. *et al*., 2012). It has been reported in MEFs cells that the mitochondrial protein Mfn2 physically interacts with PERK and this binding is required for the proper regulation of cellular homeostasis upon ER stress (Munoz J.P. *et al*., 2013).

BiP/Grp78, apart from its role in protein folding, is involved in Ca^{2+} buffering in the ER lumen (Lièvremont J.P. *et al*., 1997). In this regard, it has been shown that BiP forms a complex with the ER protein SIG-1R, to control the mitochondrial Ca^{2+} signalling at MAMs. These authors observed that ER stress induction by TG treatment induces

dissociation between BiP and SIG-1R and the translocation of SIG-1R from the MAMs to other ER regions in Chinese hamster ovary (CHO) cells (Hayashi T. and Su T.P., 2007).

9.2.8. Antiviral signalling

During viral infection, the RNA helicase RIG-I (retinoic acid inducible gene I) recognizes dsRNA (a viral replication signature) as non-self and is recruited to its adaptor protein MAVS (mitochondrial antiviral-signalling protein), initiating the cellular antiviral response (Kumar H. *et al*., 2006). Interestingly, this transmembrane protein is localized to both peroxisomes and mitochondria (Seth R.B. *et al*., 2005; Dixit E. *et al*., 2010), as well as to the MAMs (Horner S.M. *et al*., 2011). The specific location of the RIG-I-MAVS complex at the MAMs is driven by the tethering factor Mfn2 (Horner S.M. *et al*., 2011).

In addition, HCV is sensed by RIG-I (Saito T. *et al*., 2008), however this virus uses its NS3/4A protease to cleave MAVS, avoiding antiviral induction (Meylan E. *et al*., 2005). Interestingly, NS3/4A is able to process MAMs-associated MAVS, but not mitochondrial-associated MAVS (Horner S.M. *et al*., 2011), indicating that MAVS subpopulation located at this certain cellular hub is critical for the antiviral signalling against HCV (Horner S.M., 2014). Recent proteomic studies have identified at MAMs new proteins during RNA virus replication, such as RAB1B (member RAS oncogene family 1B), VTN (vitronectin) and LONP1 (Horner S.M. *et al*., 2015). Therefore, the importance of the MAMs in the innate immune response to RNA viruses would rely on its function as a key cellular platform, contributing to the dynamic relocalization of protein complexes to initiate antiviral signalling.

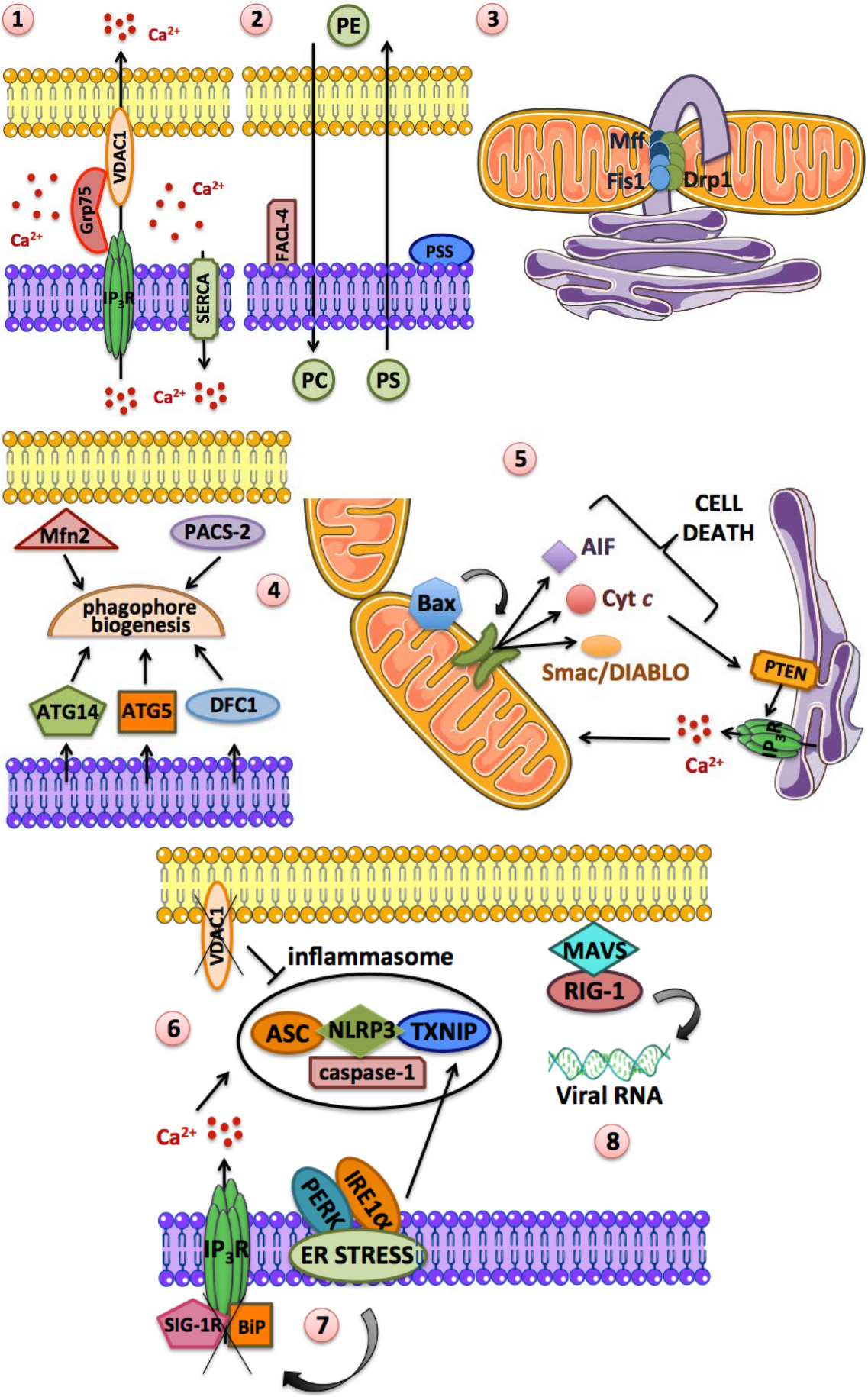
1
Ca2+
VDAC1
Grp75
Ca2+
Ca2+
IP3R
SERCA
Ca2+
2
PE
FACL-4
PSS
PC
PS
3
Mff
Fis1
Drp1
Mfn2
PACS-2
4
phagophore biogenesis
ATG14
ATG5
DFC1
5
CELL DEATH
AIF
Bax
Cyt c
Smac/DIABLO
PTEN
IP3R
Ca2+
VDAC1
inflammasome
6
ASC
NLRP3
TXNIP
caspase-1
Ca2+
MAVS
RIG-1
Viral RNA
8
PERK
IRE1α
ER STRESS
IP3R
SIG-1R
BiP
7

Figure I.12. Schematic representation of MAMs and the major pathways they regulate. (1) Ca^{2+} EXCHANGE. The ER releases Ca^{2+} through specialized channels (IP_3R) and pumps it back through SERCA. Mitochondria uptakes this Ca^{2+} by channels like VDAC1. (2) LIPID METABOLISM. MAMs also allow the transfer of lipids, such as phosphatidylcholine (PC), phosphatidylethanolamine (PE) and phosphatidylserine (PS), between ER and mitochondria. Enzymes of the lipid biosynthetic pathways like long chain acyl-CoA synthetase (FACL4) and phosphatidylserine synthase (PSS) are localized at MAMs. (3) MITOCHONDRIAL MORPHOLOGY. Mitochondrial fission occurs at positions where ER tubules contact and constrict mitochondria. These constrictions facilitate Drp1 recruitment by Mff and Fis1 to mitochondrial fission sites and both proteins have been localized to the MAMs. (4) AUTOPHAGY. Proteins involved in autophagy, such as ATG14, ATG5 and DFC1 (double FYVE-domain containing protein 1), have been found in MAMs. In addition, PACS-2 and Mfn2 are also required for autophagosome formation. (5) APOPTOSIS. During apoptosis, Drp1 induces mitochondrial fission and also stimulates Bcl2-associated X protein (Bax) causing OMM permeabilization (OMMP) and the release of cyt *c* and other pro-apoptotic factors to the cytosol. Cyt *c* binding to IP_3R channels can block the Ca^{2+}-dependent inhibition of IP_3R function and promote apoptotic Ca^{2+} release. Indeed, PTEN enhances Ca^{2+} signalling to the mitochondria in situations of increased ER stress and pro-apoptotic signalling. (6) INFLAMMATORY RESPONSE. Nod-like receptor family, pyrin domain containing 3 (NLRP3), the adapter apoptosis-associated speck-like protein (ASC), pro-caspase-1 and thioredoxin-interacting protein (TXNIP) localize at MAMs. VDAC1 (mitochondrial ROS producton) and IRE1α (ER stress) are involved in NLRP3 inflammasome activation. (7) ER STRESS. ER stress induces dissociation between BiP and SIG-1R that control the mitochondrial Ca^{2+} signalling at MAMs. PERK localizes at MAMs under ER stress. (8) ANTIVIRAL SIGNALLING. Retinoic acid inducible gene I (RIG-1) recognizes viral RNA and is recruited to its adaptor protein MAVS (mitochondrial antiviral-signalling protein), initiating the cellular antiviral response. Figure modified from Bravo-Sagua R. *et al*., 2013 and Marchi S. *et al*., 2014.

9.3. MAMs in health and disease

The vast implications of Ca^{2+} in various intracellular signalling mechanisms demonstrate the importance of the MAMs for metabolism and cellular lifespan. Not surprisingly, MAMs have been proposed as a site that is affected in neurodegenerative diseases (Schon E.A. and Area-Gomez E., 2010). The role of the MAMs in diabetes has also been reported (Zorzano A. *et al*., 2009; Sebastian D. *et al*., 2012). Proteins implicated in cancer like PML (Pinton P. *et al*., 2011), in the viral manipulation of cellular metabolism (Williamson C.D. and Colberg-Poley A.M., 2009) and in inflammation (Tschopp J., 2011; Zhou R. *et al*., 2011) have been detected on the MAMs as well, evidencing the huge potential of future studies in the field to further

understanding of human disease.

Neuronal cells require very large amounts of energy for their activities and rely almost exclusively on mitochondria as a provider, in particular in axons and dendrites (Kann O. and Kovacs R., 2007). Thus, the distribution and morphology of mitochondria is a critical determinant of neuronal survival (Knott A.B. and Bossy-Wetzel E., 2008; Knott A.B. *et al*., 2008). Consistent with this, a number of structural proteins can give rise to neuronal defects if mutated. For example, mutations in *MFN2*, which is essential for the transport of mitochondria along the axons (Misko A. *et al*., 2010), lead to Charcot Marie Tooth type 2A disease, a peripheral neuropathy (Cartoni R. and Martinou J.C., 2009), wherein the longest neurons in patients die (Zuchner S. and Vance J.M., 2006). Another neurodegenerative disease tied to the MAMs is Alzheimer's disease (Schon E.A. and Area-Gomez E., 2010). Alzheimer's disease-associated mutations in the MAMs protein presenilin-2 (PS2) lead to reduced ER Ca^{2+} content and even further increased ER–mitochondria Ca^{2+} transfer when compared to wild type overexpression (Zampese E. *et al*., 2011a; 2011b). In Parkinson's disease, mutations in PINK1 and Parkin lead to increased mitochondrial fragmentation catalysed by Drp1 that also coincides with an arrest of mitochondrial motility (Wang X. *et al*., 2011; Yu W. *et al*., 2011).

On the other hand, MAMs are involved in different metabolic processes, including steroid metabolism. Caveolin-1 (CAV1) has been recently identified as an integral component of hepatic MAMs, which determine the relative cholesterol content of these ER subdomains (Sala-Vila A. *et al*., 2016). A detailed comparative proteomics analysis between MAMs from wild type and CAV1-deficient mice (CAV1KO) suggests that functional CAV1 contributes to the recruitment and regulation of intracellular steroid and lipoprotein metabolism-related processes accrued at MAMs (Sala-Vila A. *et al*., 2016). In humans, CAV1 mutations result in lipodystrophies and CAV1KO display a phenotype of partial lipodystrophy and resistance to obesity. In the liver, CAV1KO show an important intracellular lipid imbalance, decreased formation of lipid droplets and a cholesterol-promoted mitochondrial dysfunction (Frank P.G. *et al*., 2008; Bosch M. *et al*., 2011; Sala-Vila A. *et al*., 2016). Another recent study using genetic and dietary murine models of obesity has revealed that in the liver, obesity drives an abnormal increase in MAMs formation, which results in increased Ca^{2+} flux from the ER

to mitochondria. The mitochondrial Ca^{2+} overload is accompanied by increased mitochondrial ROS production and impairment of metabolic homeostasis (Arruda A.P. *et al*., 2014). Suppression of two distinct proteins critical for ER-mitochondrial apposition and Ca^{2+} flux, IP_3R_1 and PACS-2, resulted in improved cellular homeostasis and glucose metabolism in obese animals, suggesting that this mechanism is critical for metabolic health and could represent a new therapeutic target for metabolic disease (Arruda A.P. *et al*., 2014).

The association of a number of MAMs proteins with cancer and tumorigenesis has also been seen. For example, PACS-2 which maintains MAMs integrity and ER-mitochondria Ca^{2+} exchange, is mutated in as much as 40% of sporadic colorectal cancer biopsies and could thus act as a tumour suppressor (Anderson G.R. *et al*., 2001). However, the maintenance of the MAMs and their Ca^{2+} signalling platform is not a clear hallmark of cancer, since the tumour suppressor PML actually promotes the opposite: PML interacts with IP_3R_3, which results in reduced ER–mitochondria Ca^{2+} flux and apoptosis resistance (Pinton P. *et al*., 2011). Similarly, the suspected tumour suppressor trichoplein/mitostatin (TpMs) inhibits Mfn2 and hence MAMs formation, but it is downregulated or mutated in a number of types of cancer (Vecchione A. *et al*., 2009; Fassan M. *et al*., 2011). Thus, future research will have to elucidate which functional aspect of the MAMs is most critical for tumorigenesis: apoptosis onset or the maintenance of cancer cell metabolism.

Another important group of MAMs regulatory proteins are chaperones and oxidoreductases of the ER such as BiP/Grp78, ERp44, Ero1α, and CNX. All of these are central players in ER–mitochondria Ca^{2+} flux (Simmen T. *et al*., 2010). In mouse models, it has been shown that loss of Ero1α function leads to reduced peak amplitude of cardiomyocyte Ca^{2+} transients, resulting in a partial resistance to progressive heart failure (Chin K.T. *et al*., 2011). This latter aspect is also important for the MAMs-associated regulation of Ca^{2+} signalling by SERCA. The cellular redox state plays an important role in the regulation of SERCA activity, whereas mild oxidation increases pump activity (Lancel S. *et al*., 2009), chronic oxidation results in a complete stop of calcium pumping (Lancel S. *et al*., 2010). These results indicate how cellular redox and

redox-sensitive enzymes could directly modulate the Ca^{2+} signalling function of the MAMs.

In addition to modulating MAMs Ca^{2+} signalling, Tschopp´s laboratory has discovered that ROS lead to the activation of NLRP3 inflammasomes in a human monocytic cell line (Zhou R. *et al*., 2011). This activation coincides with the shift of TXNIP from cytosolic thioredoxin 1 to the NLRP3 inflammasome on the MAMs. Increased ROS production inside mitochondria due to extra- or intracellular stress triggers is a prerequisite for this observation (Tschopp J., 2011). Interestingly, the MAMs structural component VDAC is integral to this response, since RNAi-mediated VDAC1/2 knockdown abrogates inflammasome formation in response to monosodium urate, alum or nigericin. Similar to apoptosome formation that requires the release of mitochondrial cyt *c*, ROS-triggered inflammasome activation might require the release of mitochondrial DNA, providing an additional potential role for the MAMs (Nakahira K. *et al*., 2011).

Given these important roles of the MAMs for Ca^{2+} signalling, apoptosis and inflammasome activation, it comes as no surprise that numerous viral proteins target this structure. One prominent and well-described example is the human cytomegalovirus glycoprotein UL37 exon 1 (Bozidis P. *et al*., 2010). This glycoprotein is targeted to the MAMs by means of its two MTS (Williamson C.D. and Colberg-Poley A.M., 2010) and is able to reduce ER Ca^{2+} content, possibly by increasing the targeting of Grp75 (Bozidis P. *et al*., 2010) or by modulating the amount of Ca^{2+}-regulating chaperones and oxido-reductases such as BiP on the MAMs (Zhang A. *et al*., 2011). As mentioned above, MAMs also house RIG-1 that triggers an immunity signalling cascade upon viral infection. In addition, HIV-1 Vpr has been suggested to disrupt MAMs by reducing Mfn2 and Drp1 protein levels in human embryonic kidney cells and human CD4+ T cells (Huang C.Y. *et al*., 2012).

II. AIMS

The general aim of this study was to investigate the involvement of mitochondria in the efavirenz-induced effects in cultured human hepatic cells and, specifically, to understand the mitochondria-ER interplay.

Specific aims were:

1. **To evaluate the effects of efavirenz on hepatic cells lacking functional mitochondria (rho^{o} cells).**
2. **To study the effect of efavirenz on mitochondrial dynamics, a phenomenon that depends among other processes on the interaction between ER and mitochondria.**
3. **To analyse the influence of efavirenz on the interaction between mitochondria and ER and, in particular, regarding mitochondria-associated membranes (MAMs).**
4. **To assess the expression and subcellular location of LONP1 under dual ER stress/mitochondrial dysfunction such as that induced by efavirenz.**
5. **To compare the effect of efavirenz with those induced by other antiretroviral drugs regarding LONP1 expression in hepatic cells.**

III. MATERIALS AND METHODS

1. REAGENTS

1.1. Antiretroviral drugs

The antiretroviral drugs used were purchased from Sequoia Research Products (Pangbourne, UK) and were dissolved in their respective vehicles before use (Tab.III.1).

DRUG	TRADE NAME	VEHICLE
Efavirenz (EFV)	Sustiva®	Methanol
Lopinavir (LPV)	Kaletra®	Methanol
Ritonavir (RTV)	Norvir®	Methanol
Rilpivirine (RPV)	Edurant®	DMSO
Darunavir (DRV)	Prezista®	DMSO
Raltegravir (RAL)	Isentress®	DMSO
Abacavir (ABC)	Ziagen®	Distilled water
Didanosine (ddI)	Videx®	Distilled water

Table III.1. List of antiretroviral drugs used with their corresponding trade names and vehicles in which they were dissolved.

1.2. General chemical reagents

All reagents used in this study were of analytical grade. The general chemical reagents were purchased from Sigma-Aldrich Chemicals (Stenheim, Germany), Roche Applied Science (Penzberg, Germany), Merck (Darmstadt, Germany) and Panreac Química S.A. (Barcelona, Spain).

Fluorescent probes, tetramethylrhodamine methyl ester perchlorate (TMRM), 10-N-nonyl-acridine-orange-chloride (NAO) and MitoSOX^{TM}, were acquired from Molecular Probes (Thermo Fisher Scientific, Waltham, MA, USA); propidium iodide (PI) and annexin V-fluorescein (Annexin V-FITC Apoptosis detection kit) were from Abcam (Cambridge, UK) and bisbenzimide H 33342 trihydrochloride (Hoechst 33342) from Sigma-Aldrich Chemicals.

The primary antibodies used in Western Blot experiments were purchased from Sigma-Aldrich Chemicals, Thermo Fisher Scientific, Abcam, Proteintech (Rosemont, IL, USA), Cell Signaling (Danvers, MA, USA), BD Biosciences (Franklin Lakes, NJ, USA) and Santa Cruz Biotechnology (Heidelberg, Germany). The secondary antibodies were obtained from Thermo Fisher Scientific and Vector laboratories (Burlingame, CA, USA).

1.3. Reagents for cell culture

Media and supplements for cell culture were purchased from Gibco (Thermo Fisher Scientific) including minimum essential medium (MEM), Dulbecco's modified eagle's medium (DMEM), Roswell Park memorial institute (RPMI) medium, sodium pyruvate, non-essential amino acids (NEAA), trypsin-EDTA, penicillin/streptomycin, L-glutamine, phosphate-buffered saline (PBS). Foetal bovine serum (FBS) was acquired from Lonza (Basel, Switzerland), and Hank's balanced salt solution (HBSS), uridine, phorbol-12-myristate-13-acetate (PMA) and William's medium E were from Sigma-Aldrich Chemicals.

2. CELL CULTURE

2.1. Cell lines

Experiments were performed with the human hepatoblastoma cell line Hep3B (ATCC HB-8064), which displays certain degree of cytochrome P450 activity (specifically CYP2B6) capable of metabolizing EFV (Zhu X.H. *et al*., 2007; Lin J. *et al*., 2012). Several confirmatory experiments were performed using HepaRG cells, terminally differentiated hepatic cells derived from a human hepatic progenitor cell line with many characteristics of primary human hepatocytes (Anthérieu S. *et al*., 2010). Finally, the human glioma cell line U-251MG (CLS 300385), human hepatic stellate cells (HSCs) LX2 and U937 human monocytes (European Collection of Cell Culture, Salisbury, UK) were also used in some experiments. HSCs LX2 were kindly provided by Dr. Scott L. Friedman (Icahn School of Medicine at Mount Sinai, NY, USA).

Hep3B cells were cultured in MEM supplemented with 10% heat-inactivated FBS, 2 mM L-glutamine, 1 mM sodium pyruvate, 1 mM NEAA, penicillin (50 U/mL) and streptomycin (50 μg/mL).

Undifferentiated HepaRG cells (HPRGC10), purchased from Gibco, were firstly grown at a density of 2.7 x 10^4 cell/cm^2 in William's medium E supplemented with 2 mM L-glutamine, 50 µM hydrocortisone hemisuccinate (Sigma-Aldrich Chemicals), 5 µg/mL bovine insulin, 10% FBS, 100 U/mL penicillin and 100 µg/mL streptomycin. In order to induce cell differentiation, 2% DMSO was added to the medium after 2 weeks of culture and cells were further cultured in its presence for another 2 weeks (Anthérieu S. *et al.*, 2010). After that, differentiated hepatocyte-like cells were selectively collected through mild trypsinization (trypsin-EDTA 0.125%) and reseeded at a density of 7-9 x 10^4 cells/cm^2 in medium containing 2% DMSO. Treatments were performed in DMSO-free medium.

Human immortalized HSCs LX2 were cultured in DMEM and U-251MG cells in DMEM with 4.5 g/L glucose. U937 human monocytes were maintained in RPMI medium and were differentiated into macrophages by incubation with PMA 10 nM during 48 h, when they were used for the experiments.

All cell cultures, except U937 human monocytes, were subcultured once they reached 90-95% confluence, using trypsin-EDTA to detach them, and were re-fed with fresh medium every 2-3 days. Cell cultures were maintained in an incubator (IGO 150, Jouan, Saint-Herblain Cedes, France) at 37 °C, in a humidified atmosphere with 5% CO_2/95% air (AirLiquide Medicinal, Valencia, Spain).

2.2. Generation and maintenance of rho^o cells

In order to generate rho^o cells in Hep3B background, wild-type (WT) cells were treated for 8 weeks with ethidium bromide (EtBr, 500 ng/mL) to deplete mtDNA, in medium supplemented with 50 µg/mL uridine (King M.P. and Attardi G., 1989). Taken into account that rho^o cells have a slower proliferation rate compared to the parental cells, the two cell types were seeded at different cell density (in the case of 48-well plates, 50.000 cells per well for rho^o cells and 30.000 cells per well for WT) in order to ensure the same cell density when the drug was added.

3. TREATMENTS

Unless otherwise stated, experiments were performed using clinically relevant concentrations of drugs which were chosen by considering the important interindividual variability in their pharmacokinetics. For this, in order to analyse the concentration-dependence of the results we used 3 concentrations of each drug within and above the therapeutic range. In each experiment, we used a control of the vehicle used in the treatment and a negative control (untreated cells).

In some experiments, the effect of EFV was compared to those induced by the classical ER-stress inductor thapsigargin (TG, 2 µM) (Thastrup O. *et al*., 1990) and two widely employed mitochondrial stressors: rotenone (Rot, 10-25 µM), a common pharmacological inhibitor of Complex I of the ETC (Li N. *et al*., 2003), and the protonophore carbonyl cyanide m-chloro phenyl hydrazone CCCP (10 µM), a potent chemical uncoupler of OxPhos (Lou P.H. *et al*., 2007).

In order to assess whether the observed changes were dependent on Ca^{2+}, we pre-treated cells with an intracellular Ca^{2+} chelator, 10 µM BAPTA (1,2-bis(o-aminophenoxy)ethane-N,N,N',N'-tetraacetic acid) from Abcam, 1 h before the treatment.

To study apoptosis, cells were treated with the inducer of apoptosis staurosporine (STS 1 µM, from Sigma-Aldrich Chemicals), which was used as a positive control.

The non-specific nitric oxide synthase (NOS) inhibitor L-N^G-nitroarginine methyl ester (L-NAME 50 µM, Cayman Chemical, MI, USA) was used to evaluate the influence of NOS activity.

4. TRANSFECTION EXPERIMENTS: *CHOP* and *LONP1* silencing

Transient transfections were performed by small interfering RNA (siRNA) using LipofectAMINE™ 2000 (Thermo Fisher Scientific) and following the protocol supplied by the manufacturer. For control experiments, SignalSilence® unconjugated control siRNA (Cell Signaling) was employed.

Both for *CHOP* and *LONP1* silencing, cells were seeded the day before the experiment in t-25 flasks at cell density of approximately 90%. siRNA/Lipofectamine complexes were formed in serum-free OptiMEM (Gibco), using 50 nM of *GADD153 siRNA(h)* from Santa Cruz Biotechnology or 10 nM *LONP1 siRNA(h)* from Ambion® (Thermo Fisher Scientific). Transfections were performed in complete cell culture medium without antibiotics, over 24 h for *CHOP* silencing and 48 h for *LONP1*, and then cells were re-fed with fresh complete medium containing antibiotics.

5. ELECTROCHEMICAL MEASUREMENT OF OXYGEN CONSUMPTION

Cellular oxygen (O_2) consumption was measured using a Clark-type electrode (Oxytherm, Hansatech Instruments, Norfolk, UK), based on a membrane polarographic O_2 detector, first described by Lewis C. Clark (Clark L.C. *et al*., 1953; Severinghaus J.W. and Astrup P.B., 1986). The system consists of a two electrode cell, a permeable membrane to O_2 and an electrolyte. The electrodes are a silver/silver chloride anode and a platinum cathode, and conduction between both occurs by an electrolyte (3M KCl) in which they are immersed. Molecular O_2 diffuses through the Teflon membrane which is permeable to gases into the sensor of the electrode. Applying a polarizing voltage (700 mV) the electrolyte ionizes and initiates a current flow and a series of electrochemical reactions (Fig.III.1):

Platinum cathode $\quad \mathbf{O_2 + 2e^- + 2H_2O \longrightarrow H_2O_2 + 2OH^- \ (reduction)}$

Silver anode $\quad \mathbf{4Ag + 4Cl^- \longrightarrow 4AgCl + 4e^- \ (oxidation)}$

Figure III.1. Electrochemical reactions taking place in the Clark-type oxygen (O_2) electrode. Oxidation of atmospheric O_2 is the principle of the chemical reaction.

O_2 is consumed during the reaction, being its concentration in the respiration buffer (HBSS) proportional to the magnitude of current flow. O_2 reduction generates a current which is the basis of the measurement and the trace obtained is thus a measure of the O_2 consumption of the reaction mixture. The electrode is coupled with an integral thermoelectric temperature control that allows measurements at constant temperature.

Before performing the measurement, the electrode was calibrated in air-saturated respiration buffer, considering the atmospheric O_2 concentration as maximal (200 µM O_2). Electrode zero setting was performed by adding excess of the reducing agent sodium dithionite ($Na_2S_2O_4$, Panreac) to the chamber. Mitochondrial respiration specificity was confirmed by adding directly to the chamber 1 mM potassium cyanide (KCN), an OxPhos specific inhibitor which inhibited O_2 consumption induced by the treatments. The electrode is connected to a PC (Fig.III.2) for instrument control and data analysis with a Custom Windows® software, allowing to monitor O_2 concentration in real time as well as the rate of consumption over different time periods.

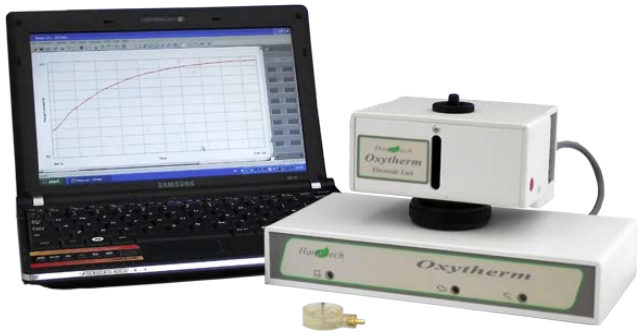

Figure III.2. Clark-type O_2 electrode.

O_2 consumption was evaluated in intact cells. For this, cells were detached by trypsinization immediately before the measurement and counted using hemacytometer (Bright Line Counting Improved Neubauer Chamber, Hausser Scientific, Horsham, PA, USA). Then, 4 million cells were resuspended in 1 mL HBSS and taken to the respiration chamber where the suspension is constantly stirred and maintained at 37 °C.

6. MEASUREMENT OF ATP CONCENTRATION

Intracellular ATP concentration was assessed with a bioluminescent assay based on the luciferin oxidation to oxyluciferin, as described in Fig.III.3.

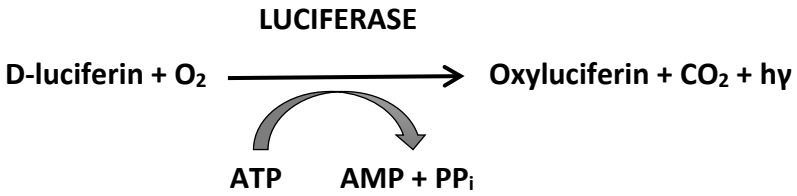

Figure III.3. Luciferase-mediated oxidation of luciferin to oxyluciferin. ATP concentration in the samples is directly proportional to the light emitted by this reaction (hγ).

We used the "ATP Bioluminescence kit" (Roche Applied Science) and the assay was performed according to the manufacturer's protocol. Briefly, cells were seeded in t-25 flasks and treated (with 80% confluence) for 24 h with EFV, vehicle, TG, Rot, or a combination of these with the glucose analogue 2-Deoxy-D-glucose (2-DG, 10 mM) that inhibits glycolysis (Wick A.N. *et al*., 1957). Afterwards, cells were detached by trypsinization and centrifuged at 500 g for 5 min in a microcentrifuge (5415-R, Eppendorf, Hamburg, Germany) at 4 °C; cell pellets were then resuspended in 100 µL of dilution buffer provided by the kit. ATP standard curve was prepared (10^{-11}-10^{-2} M) using ATP stock solution (10 mg/mL) provided by the kit and dilution buffer in order to minimize the background luminescence. Then, 20 µL of the standard solution or 25 µL of the sample were applied per well in a black 96-well plate with light bottom, in triplicate. Next, 20 or 25 µL of cell lysis buffer provided by the kit were added to each well (with standard or sample, respectively) and the plate was incubated for 5 min at RT. Luminescence was detected with plate reader Fluoroscan Ascent FL (Thermo Fisher Scientific) immediately after injecting 30 µL/well of the luciferase reagent by the luminoscan dispenser.

In order to normalize the ATP concentration values with the protein amount of each sample, 10 µL/well of the cell lysate were removed before reading and total protein concentration was determined using the "BCA Protein Assay Kit" (Pierce Chemicals, Bouler, CO, USA, see section "7.2. Protein quantification: bicinchoninic acid (BCA) assay").

7. ANALYSIS OF PROTEIN EXPRESSION

For the protein expression analysis, cells were seeded in t-25 flasks and treatment was performed with 80%-confluent cultures. After this, cells were collected on ice to prevent protein degradation by the following procedure: medium was removed, cells were washed with 5 mL of PBS and immediately after detached with 0.5 mL of trypsin (1 min, 37 °C). In order to stop trypsinization, medium was added and the resulting cell suspension was centrifuged for 3 min at 500 g. Then, cell pellets were washed with cold PBS and centrifuged in a microcentrifuge, at 4 °C, for 5 min, at 500 g. Supernatants were discarded and cell pellets were stored at -80 °C until use.

7.1. Protein extracts

7.1.1. Whole-cell extracts

Cell pellets were resuspended in 50-100 µL (depending on the size of the cell pellet) of complete lysis buffer whose composition was: 20 mM HEPES pH 7.4, 400 mM NaCl, 20% (v/v) glycerol, 0.1 mM EDTA, 10 µM Na_2MoO_4 and 10 mM NaF. Immediately prior to use, 1 mM DTT, protease inhibitors ("Complete Mini" protease inhibitor cocktail, and "Pefabloc", both purchased from Roche Applied Science) and 0.05% NP-40 were added. Thereafter, samples were vortexed at maximum speed, for 20 sec, incubated on ice, for 15 min, vortexed again at maximum speed, for 10 sec and subsequently centrifuged in a microcentrifuge at 16,000 g, for 15 min, at 4 °C. Supernatants (whole-cell protein extracts) were collected and stored at -20 °C until future use.

7.1.2. Whole-cell extracts with preserved phosphorylation

In order to preserve phosphorylated proteins, cell pellets were lysed in 75-100 µL of PhosphoSafe (Novagen, Calbiochem, La Jolla, CA, USA), a lysis buffer which preserves the phosphorylation state of proteins, supplemented with 10X "Complete Mini" protease inhibitor cocktail. The resulting lysates were vortexed for 15 sec, incubated for 5 min at RT and centrifuged at 4 °C, for 5 min, at maximum speed. Supernatants (whole-cell extracts) were collected and stored at -20 °C until future use.

7.1.3. Mitochondria-enriched extracts

We used confluent cell cultures plated in t-75 flasks. After the treatment, cells were detached with trypsin and collected with ice-cold PBS as stated before. Cell pellets were resuspended in 0.5 mL fractionation buffer (10 mM Tris-HCl pH 7.5, 0.25 M sucrose and 1 mM EDTA) and lysed on ice by a passage through a 23-gauge needle in a 1 mL plastic syringe. Unbroken cells were pelleted by centrifugation at 4 °C, for 10 min, at 500 g. The supernatant was collected, transferred to a new eppendorf tube and centrifuged at 16,000 g, for 30 min, at 4 °C. The supernatant resulting from this centrifugation was collected representing the cytosolic fraction, whereas the pelleted mitochondrial fraction was washed with 1 mL fractionation buffer. Subsequently, another centrifugation step was performed, at 11,000 g for 10 min, and the pellet obtained was resuspended in 50 µL mitochondrial buffer (10 mM Tris-acetate pH 8.0, 5 mM $CaCl_2$, 0.5% NP-40, 1 mM DTT and protease inhibitor cocktail (Roche Applied Science)), thus giving rise to a mitochondria-enriched cellular fraction. Finally, obtained protein extracts were stored at -20 °C for further use.

7.1.4. Isolation of mitochondria-associated membranes (MAMs)

Subcellular fractioning, which included MAMs, was performed using cell pellets obtained from 12-14 confluent t-150 flasks per condition. Isolation was performed as described by Wieckowski M.R. *et al*., 2009 (Fig.III.4). Cells pellets were resuspended in 20 mL of ice-cold isolation buffer (IB)-1 (225 mM mannitol, 75 mM sucrose, 0.1 mM EGTA and 30 mM Tris-HCl pH 7.4) and homogenized with a Teflon pestle at 4 °C. Next, serial centrifugations (at 4 °C) were performed: the homogenate was centrifuged at 600 g for 5 min, the supernatant was then centrifuged again in the same conditions and the supernatant obtained was centrifuged at 7,000 g for 10 min. On the one hand, in order to proceed with further separation of cytosolic and ER fractions, the supernatant obtained was centrifuged at 20,000 g for 30 min at 4 °C. Further centrifugation of the obtained supernatant (100,000 g for 1 h) results in the isolation of ER (pellet) and cytosolic fraction (supernatant). On the other hand, the pellet containing mitochondria was resuspended gently in 20 mL of IB-2 (225 mM mannitol, 75 mM sucrose and 30 mM Tris-HCl pH 7.4) and the resulting suspension was centrifuged at 7,000 g for 10 min at 4 °C. The mitochondrial pellet obtained thereby

was resuspended in IB-2 as before and centrifuged (10,000 g, 10 min, 4 °C). Thereafter, the crude mitochondrial pellet was gently resuspended in 2 mL of ice-cold mitochondria resuspending buffer (MRB; 250 mM mannitol, 5 mM HEPES (pH 7.4) and 0.5 mM EGTA). The fractionation of crude mitochondria was performed with Percoll medium and centrifugation at 95,000 g for 30 min at 4 °C in a Beckman Coulter Optima L-100 XP ultracentrifuge (SW40 rotor, Beckman, Fullerton, CA, USA). MAMs and mitochondrial suspension were collected and centrifuged at 6,300 g for 10 min at 4 °C. Finally, the MAMs supernatant was centrifuged at 100,000 g for 1 h (70-Ti rotor, Beckman) at 4 °C and the mitochondrial pellet was resuspended in 20 mL of MRB and centrifuged at 6,300 g for 10 min at 4 °C. The pellet of MAMs and pure mitochondria were collected in MRB and stored at -20 °C for further use.

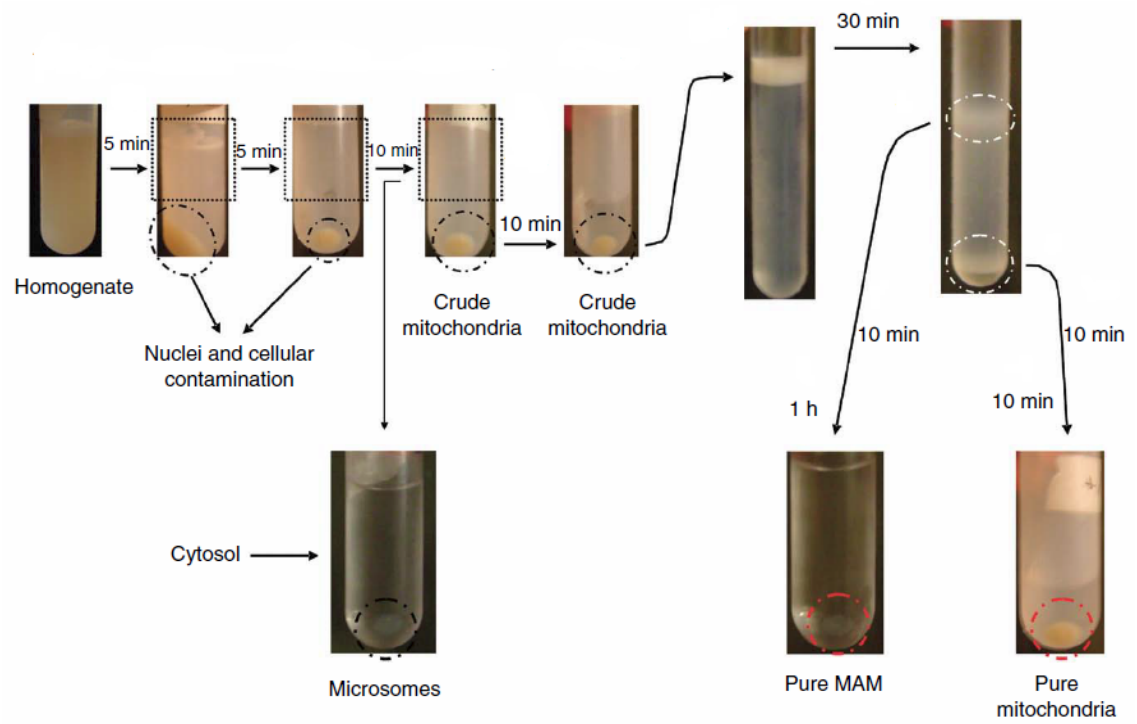

Figure III.4. Schematic representation of the workflow during MAMs isolation. Different kind of pellets and fractions obtained during the isolation process are shown (from Wieckowski M.R. *et al.*, 2009).

The obtained subcellular protein fractions (0.5-6 µg/µL) were analysed by WB (see section "7.3. Sodium dodecyl sulphate-polyacrylamide gel electrophoresis (SDS-PAGE) and Western blot (WB)").

These cellular subfractionation experiments were performed at Instituto de Biología Molecular y Celular de Plantas (IBMCP, UPV-CSIC, Valencia, Spain) with the assistance of Dr. Ricardo Flores Pedauyé (Research Professor, CSIC).

7.2. Protein quantification: bicinchoninic acid (BCA) assay

We used the bicinchoninic acid (BCA) assay to quantify the protein content in the cell extracts. This method is based on the well-known Biuret reaction (reduction of Cu^{2+} to Cu^{1+} by protein in an alkaline medium). Cu^{1+} ions bind to two molecules of BCA which generates purple-colored reaction product that exhibits a strong absorbance at 562 nm and is nearly linear with increasing protein concentrations over a broad working range (Smith P.K. *et al*., 1985).

"BCA Protein Assay Kit" (Pierce Chemicals) was used to perform the assay. In order to link the variation of absorbance with the amount of protein, a standard curve was prepared using bovine serum albumin (BSA, 2 mg/mL) with serial dilutions (1-0.0156 mg/mL) that were prepared in the same buffer as the samples to minimize the background absorbance. Both the standard dilutions and the samples were assayed in duplicate. For this, 20 µL of standard or samples were applied per well in a 96-well plate and 200 µL/well of working reagent were added. As suggested in the manufacturer's protocol, this reagent was always prepared fresh, mixing 50 parts of the BCA reagent A with 1 part of BCA reagent B. Then, the plate was incubated at 37 °C, for 30 min, with gentle shaking and protected from light. The absorbance was measured at 570 nm using a "Multiscan" plate-reader spectrophotometer (Thermo Fisher Scientific).

7.3. Sodium dodecyl sulphate-polyacrylamide gel electrophoresis (SDS-PAGE) and Western blot (WB)

SDS-PAGE and WB were performed using standard methods.

7.3.1. Polyacrylamide gel electrophoresis (PAGE)

SDS-PAGE was performed using "Mini-PROTEAN 3 Cell" System (Bio-Rad Laboratories, Hercules, CA, USA). Polyacrylamide gels were prepared with an acrylamide/bisacrylamide solution, ratio 37.5:1 (Sigma-Aldrich Chemicals). Resolving

gels, with different % of polyacrylamide, were prepared in 0.375 M Tris-HCl pH 8.8 and 0.1% SDS, whereas stacking gels, containing 3.75% polyacrylamide, were prepared in 0.125 M Tris-HCl pH 6.8 and 0.1% SDS. To catalyse the reaction of polymerization, we used ammonium persulfate (APS, Bio-rad) and N,N,N´,N´-Tetramethylethylendiamine (TEMED, Sigma-Aldrich Chemicals). Protein extracts, containing equal total protein amounts (20-50 µg), were prepared before loading by adding Laemmli loading buffer (0.5 mM Tris-HCl pH 6.8, 25% glycerol v/v, 0.5% v/v β-mercaptoethanol, 10% SDS and 0.5% bromophenol blue) and boiled at 99 °C for 5 min to enable protein denaturation (Laemmli U.K., 1970). In order to determine the molecular weight of the polypeptides, a commercial molecular weight marker was loaded in parallel ("Precision Plus Protein Standard-Kaleidoscope", Bio-Rad). Electrophoresis was performed with running buffer (25 mM Tris pH 8.3, 192 mM glycine and 0.1% SDS), at constant voltage of 120-150 V.

7.3.2. Protein transfer to nitrocellulose membrane

Resolved proteins were transferred from the polyacrylamide gel to a 0.2 µm Hybond ECL nitrocellulose membrane (Amersham, GE Healthcare, Little Chalfont, UK), using "Mini Trans-Blot Electrophoretic Transfer Cell" (Bio-Rad). The transfer was performed at 4 °C, during 1 h and constant electric current of 0.4 A, in transfer buffer (25 mM Tris pH 8.3, 192 mM glycine and 20% methanol).

After the transfer, the nitrocellulose membrane was incubated in Ponceau solution (Sigma-Aldrich Chemicals), which reversibly stains proteins and is used as control of the amount of protein loaded and transfer quality. After removing Ponceau staining with Milli Q water, the membrane was incubated in fresh-made blocking solution (fat-free milk powder or BSA, both at 5% in Tris-buffered saline-Tween (TBS-T)) with continuous gentle shaking, for 1 h, at RT. The composition of TBS-T was: 20 mM Tris-HCl pH 7.2, 150 mM NaCl and 0.1% v/v Tween-20. Then, the membrane was incubated with the primary antibody, prepared in blocking solution containing 0.02% sodium azide (NaN_3, Merck), overnight at 4 °C. Thereafter, the membrane was washed in TBS-T, 3x10 min, at RT with vigorous shaking in order to remove excess antibody and incubated with the secondary antibody, prepared fresh in blocking solution, for 1 h, at RT. After this incubation another washing step followed (same conditions). Details about the antibodies used are enclosed in Tab.III.2.

PRIMARY ANTIBODIES				
PROTEIN	**ANTIBODY**	**DILUTION**	**MW (kDa)**	**COMPANY**
CV subunit β	Mouse monoclonal	1:1000	56.5	Thermo Fisher
CIV subunit II	Mouse monoclonal	1:1000	25.5	Thermo Fisher
FACL4	Rabbit polyclonal	1:1000	79	Thermo Fisher
Porin	Rabbit polyclonal	1:1000	30	Abcam
LONP1	Rabbit polyclonal	1:1000	106	Abcam
FAM82A2	Rabbit polyclonal	1:2000	52	Abcam
Grp75	Rabbit polyclonal	1:1000	74	Abcam
ClpX	Rabbit monoclonal	1:1000	69	Abcam
Mitofusin 2	Mouse monoclonal	1:1000	86	Abcam
DDIT3/CHOP	Mouse monoclonal	1:1000	19	Abcam
CI subunit ND1	Rabbit polyclonal	1:600	36	Abcam
Actin	Rabbit polyclonal	1:1000	40	Sigma-Aldrich
Tubulin	Mouse monoclonal	1:1000	56	Sigma-Aldrich
TOM20	Rabbit polyclonal	1:1000	16	Proteintech
Drp1	Rabbit monoclonal	1:1000	82	Cell Signaling
p-Drp1(Ser^{616})	Rabbit polyclonal	1:1000	82	Cell Signaling
OPA1	Mouse monoclonal	1:1000	112	BD Biosciences
Cytochrome *c*	Mouse monoclonal	1:1000	12	BD Biosciences
IP_3R_3	Mouse monoclonal	1:1000	304	BD Biosciences
VAP B/C	Rabbit polyclonal	1:1000	27	Santa Cruz
LDH	Rabbit polyclonal	1:1000	37	Santa Cruz

SECONDARY ANTIBODIES		
ANTIBODY	**DILUTION**	**COMPANY**
Peroxidase-labeled goat anti-rabbit IgG	1:5000	Vector laboratories
Peroxidase-labeled goat anti-mouse IgG	1:2000	Thermo Fisher

Table III.2. Primary and secondary antibodies used in WB experiments.

7.3.3. Chemiluminescence detection

Immunolabeling was detected by enhanced chemiluminescent reagent (ECL from Amersham, GE Healthcare) or SuperSignal WestFemto (Pierce Chemicals) and visualized with a digital luminescent image analyser (FUJIFILM LAS 3000, Fujifilm, Tokio, Japan). Densitometric analyses were performed using Multi Gauge software.

7.3.4. Stripping

In order to probe the same membrane with other antibodies, we removed bound antibodies from the nitrocellulose membrane by a process called "stripping". For this, after the completed immunoblot and visualization of the proteins, the membrane was washed in TBS-T for 10 min, at RT and then incubated with 0.5 M glycine pH 2.5 (for 1 h, at RT and vigorous shaking) or stripping buffer (62.5 mM Tris-HCl pH 6.7, 100 mM β-mercaptoethanol and 2% SDS) for 30 min, at 56 °C and vigorous shaking. Subsequently, the membrane was washed 3x10 min in TBS-T, at RT. After this, WB continued as in the standard protocol, starting with blocking the membrane with fresh-made blocking solution for 1 h, at RT, followed by primary and secondary antibody incubation, as described above.

7.4. Immunoprecipitation and co-immunoprecipitation

Immunoprecipitation of FAM82A2 (PTPIP51) or Porin and co-immunoprecipitation of VAP B/C or Grp75 were performed by standard procedures. Firstly, t-150 flasks of cultured cells were treated for 24 h, cells were then trypsinized and cellular pellets collected. Whole-cell extracts were obtained and total protein amount in them determined, as described in chapter "7.1. Protein extracts". Then, whole-cell extracts containing 1-0.2 mg of total protein were diluted to 600 µL with complete lysis buffer and incubated with 1-2 µg of rabbit polyclonal antibody against FAM82A2 (Abcam) or against Porin (Proteintech), overnight, at 4 °C and with gentle shaking. Thereafter, the extracts were incubated with 60 µL of protein A-Sepharose CL-4B beads (GE Healthcare) for 4 h, at 4 °C and with gentle shaking. Further, the samples were centrifuged in a microcentrifuge at 300 g, for 1 min, at 4 °C and supernatant discarded. The obtained immunoprecipitates were then washed 3 times with 1 mL lysis buffer. Lastly, the samples were resuspended in 30 µL Laemmli loading buffer 2X and heated

at 99 °C, for 5 min and with shaking. After another centrifugation step (microcentrifuge, 300 g, 1 min, 4 °C), the supernatant was collected and loaded on a polyacrylamide gel. Next, a standard procedure for SDS-PAGE followed (see chapter "7.3. Sodium dodecyl sulphate-polyacrylamide gel electrophoresis (SDS-PAGE) and Western blot (WB)"). Immunoprecipitated and co-immunoprecipitated proteins were detected with the corresponding antibodies indicated in Tab.III.2. As a negative control, we used whole-cell extracts without immunoprecipitation.

8. CHROMATIN IMMUNOPRECIPITATION (ChIP) ASSAY

Analysis of the *LONP1* gene with MatInspector software (Genomatix, Munich, Germany) identified several NF-κB binding sites in the promoter region of *LONP1*. To examine the potential role of NF-κB in the expression of *LONP1,* ChIP assay was performed with an antibody directed against NF-κB.

In order to stabilize protein-DNA complexes, treated cell cultures (t-25 flasks) were crosslinked with 1% formaldehyde (at RT for 10 min and gentle agitation) and incubated with 0.125 M glycine (at RT for 2 min). Then, cells were washed three times and collected with ice-cold PBS. Next, cells were centrifuged (at 4 °C, for 5 min and 500 g) and pellets were resuspended in 0.3 mL of SDS sonication buffer (1% SDS, 5 mM EDTA, 50 mM Tris-HCl pH 8.0 and protease inhibitor cocktail (Roche Applied Science)) and sonicated three times for 20 s (40 s in between) at maximum speed (Branson Digital Sonifier, Emerson Electric Co., MO, USA). After centrifugation at maximum speed for 10 min at 4 °C, supernatants (ChIP extracts) were collected (50 µL of one of them as Input) and immunoprecipitation was performed overnight at 4 °C with anti-NF-κB antibody (3 µg/mL) or with control IgG antibody (secondary antibody for anti-NF-κB) both from Thermo Fisher Scientific. Thereafter, samples were incubated with 60 µL protein A-Sepharose CL-4B beads (GE Healthcare) overnight at 4 °C. After centrifugation at 1500 g for 2 min, precipitates were washed sequentially once with low-salt wash buffer (1 % Triton X-100, 2 mM EDTA, 20 mM Tris-HCl pH 8 and 150 mM NaCl), twice with high-salt wash buffer (1% Triton X-100, 2 mM EDTA, 20 mM Tris-HCl pH 8 and 500 mM NaCl) and once with LiCl wash buffer (0.25 mM LiCl, 1% NP-40, 0.1 % Tween 20, 1 mM EDTA and 10 mM Tris-HCl pH 8), for 5 min each. Precipitates were

then washed twice with TE buffer (10 mM Tris-HCl pH 8 and 1 mM EDTA) and extracted twice with elution buffer (1% SDS, 0.1 M $NaHCO_3$). To reverse crosslinking, eluates and the Input were heated at 65 °C for 16 h in presence of 0.25 M NaCl. Finally, DNA fragments were purified with the "PureLink™ Quick PCR purification kit" (Thermo Fisher Scientific) according to the manufacturer's protocol. Equal amounts of each sample were amplified using specific primers for the *LONP1* promoter region -121 to -307 (relative to the transcription starting site): 5'-CCACCAGCATCAACATCAG-3' (forward) and 5'-CGCATGCTCAAGATTCAGG-3' (reverse). PCR was performed using TaKaRa Taq™ (Takara Bio, Kusatsu, Japan). The reaction was performed as suggested in the manufacturer´s protocol, in 10 µL final volume and the presence of 0.05 µL of Takara Taq, 1X PCR Buffer, 0.2 mM dNTP mixture and 10 µM of each primer (F and R). The reaction mixture was incubated in a 24-well thermocycler (GeneAmp PCR System 2400, PerkinElmer, Waltham, MA, USA) under the following conditions: 95 °C for 4 min; 95 °C for 30 s, 55 °C for 30 s, 72 °C for 15 min (40 cycles); 72 °C for 10 min; 4 °C ∞. PCR products were then separated by electrophoresis in 2% agarose gel and binding was determined by the relative intensity of Goldview (Goldview DNA safe stain, UVAT Bio, Valencia, Spain) fluorescence compared to the input control.

9. PCR ANALYSES

9.1. Determination of mtDNA copy number

Total cellular DNA was isolated using the QIAamp® DNA Mini kit (Qiagen, Hilden, Germany) according to the manufacturer's instructions. Briefly, cell pellet ($4x10^6$ cells) was resuspended in PBS to a final volume of 200 µL and 20 µL of Proteinase K and 200 µL Buffer AL (provided with the kit) were added. After incubation at 56 °C for 10 min, ethanol (96-100%) was added to the samples in order to precipitate total cellular DNA. Next, the mixture was applied carefully to "QIAamp Spin Column" provided with the kit and, after several washings according to instructions, DNA was eluted with distilled water and quantified using the NanoDrop® ND-1000 spectrophotometer (NanoDrop Technologies, Wilmington, DE, USA). DNA purity was verified by standard electrophoresis using agarose gels.

For the amplification of mtDNA content, we used the following primers, which are complementary to sequences of the *NDR1* gene: mtF3212 5'-CACCCAAGAACAGGGTTTGT-3' (forward) and mtR3319 5'-TGGCCATGGGTATGTTGTTTA-3' (reverse). mtDNA content was quantified relative to nuclear DNA (nDNA), for the amplification of which we used primers complementary to sequences of the nuclear gene cyclophylin A (*CYPA*): CypAF 5'CGTCTCCTTTGAGCTGTTTG-3' (forward) and CypAR 5'TCTGGTCGTTCTTCTAGTGG-3' (reverse). PCR reactions were performed in a Carousel-based LightCycler® 2.0 Real Time PCR System (Roche Applied Science). Both PCR reactions of mtDNA and nDNA were performed using 100 ng of total DNA mixed with LightCycler® FastStart DNA MasterPLUS SYBR Green I master mix (Roche Applied Science) following the instructions in the manual. Forward and reverse primers (0.2 µM) were added in a final reaction volume of 10 µL. For mtDNA amplification, reactions were performed as follows: 5 min at 95 °C; 1 s at 95 °C, 5 s at 65 °C and 6 s at 72 °C (40 cycles). For nuclear DNA amplification, reactions were performed as follows: 10 min at 95 °C; 1 s at 95 °C, 5 s at 58 °C and 18 s at 72 °C (35 cycles). To quantify the amounts of the template, a standard curve for the analysed gene was included in each run. The specificity of the amplified products was verified by melting curve analysis and agarose gel electrophoresis. Data were calculated as number of DNA copies.

9.2. Real time quantitative RT-PCR

9.2.1. RNA isolation

The experiment was performed using mRNA of t-25 flask cell cultures. Total RNA was isolated using the "RNeasy Mini Kit" (Qiagen) according to manufacturer's instructions. Briefly, cellular pellets were resuspended in 350 µL lysis buffer and lysed by passage through a 20-gauge needle. Then, 350 µL of 70% ethanol was added and the samples were applied to a column which retains RNA. After the column had been washed appropriately, RNA was eluted in 30 µL of RNAse free-H_2O. The concentration of the total RNA obtained was determined using NanoDrop® ND-1000 spectrophotometer.

9.2.2. cDNA synthesis

Complementary DNA (cDNA) was synthetized using 2 µg of total RNA using "PrimeScript™ RT Reagent Kit" (Takara Bio). The reaction was performed as suggested

in the manufacturer´s protocol, in 20 µL final volume and the presence of 1X PrimeScript Buffer, 1 µL PrimeScript RT Enzyme Mix I, 25 pmol Oligo dT Primer and 50 pmol Random 6-mers. The reaction mixture was incubated in a 24-well thermocycler under the following conditions: 37 °C for 15 min, 85 °C for 5 s, 4 °C ∞.

9.2.3. Quantitative RT-PCR

Quantitative reverse transcriptase PCR (RT-PCR) was carried out in a Carousel-based LightCycler® 2.0 Real Time PCR System (Roche Applied Science), mixing 1 µL of cDNA with LightCycler® FastStart DNA MasterPLUS SYBR Green I master mix (Roche Applied Science) following the instructions in the manual. Forward and reverse primers (1 µM) were added in a final reaction volume of 10 µL. RT-PCRs were performed as follow: 30 s at 95 °C; 5 s at 95 °C, 20 s at 60 °C (60 cycles); 15 s at 65 °C and 30 s at 40 °C. All reactions were performed in duplicate and together with a negative control (H_2O instead of cDNA). The specificity of the amplified products was verified by melting curve analysis and standard electrophoresis on 1-2% agarose gels containing Goldview and using buffer TAE 1x (20 mM Tris, pH 7.8, 10 mM sodium acetate and 0.5 mM EDTA).

We used specific primers for the human genes *LONP1, ACTB, HSP90AA1, HASP90AB1, HSP90B1* (all of them from Integrated DNA Technologies, Coralville, IA, USA), *MFN1*, *MFN2*, *OPA1*, *FIS1* and *DRP1* (all of them synthesized by TIB Molbiol, Berlin, Germany). Primer sequences are shown in Tab.III.3.

GENE	PRIMER SEQUENCES
LONP1	F: 5´-ATGGAGGACGTCAAGAAACG-3´ R: 5´-GATCTCAGCCACGTCAGTCA-3´
MFN1	F: 5´-ACCGAGGAGGTGGCAAACAAAG-3´ R: 5´-GCTGGGTCTGAAGCACTAAGGC-3´
MFN2	F: 5´-GGTGCTCAACGCCAGGATTCAG-3´ R: 5´-TGCCGCTCTTCACGCATTTCC-3´
OPA1	F: 5´-GGCATGGCTCCTGACACAAAGG-3´ R: 5´-GCTGAATCCTGCTTGGACTGGC-3´
FIS1	F: 5´-AAGGGAGCAAGGAGGAACAGCG-3´ R: 5´-ACAGCAAGTCCGATGAGTCCGG-3´
DRP1	F: 5´-GACTTTGCTGATGCTTGTGGGC-3´ R: 5´-CTCTCCAGTTGCCTGTGGTTGG-3´
ACTB	F: 5´-GGACTTCGAGCAAGAGATGG-3´ R: 5´-AGCACTGTGTTGGCGTACAG-3´
HSP90AA1	F: 5´-ACATCTGCCTCTGGTGATGAG-3´ R: 5´-CCGAAGACGTTCCACAAAGG-3´
HASP90AB1	F: 5´-TTTAGATGCCTGAGGAAGTGC-3´ R: 5´-GCTCTCATAGCGAATCTTGTCC-3´
HSP90B1	F: 5´-TCTCCCCTTGAATGTTTCCCG-3´ R: 5´-TCATGTCCAGCGTTTTACGAAC-3´

Table III.3. Pairs of primers used for quantitative RT-PCR.

To quantify the expression of our target genes, we used the housekeeping gene *ACTB* (β-actin) and results were normalized taking into consideration its expression. Calculations were based on the comparison of the threshold values (C_t) at a constant level of fluorescence. The model of quantification is described in Fig.III.5.

$$R = 2^{-[\Delta Ct\ sample - \Delta Ct\ control]}$$

Figure III.5. Relative quantification model of gene expression.

9.3. Microarrays

The relative expression of different genes involved in inflammation and cellular stress (*AIM2*, *CASP1*, *CASP5*, *CCL7*, *CXCL1*, *CXCL2*, *HSP90AA1*, *HSP90AB1*, *HSP90B1*, *IL18*, *IL1B*, *IL33*, *IL6*, *MAP3K7*, *NAIP*, *NLRP1*, *NLRP3*, *NOD2*, *P2RX7*, *PANX1*, *PTGS2*, *PYCARD*, *RIPK2*, *TNFSF11* and *TRAF6*) (Tab.III.4) was analysed in LX2 cells using a pre-validated set of real time PCR assays (PrimePCR assays Bio-Rad) applied in 96-well plate, following the instructions provided. The expression of two housekeeping genes, *ACTB* and *GADPH*, was also analysed in the same plates, and *ACTB*, as the gene with more stable expression, was chosen as to normalize data. All reactions were performed in a CFX96 touch real-time PCR, and analysed with Biorad CFX Manager 3.1 software (Bio-Rad). Data are expressed as relative-fold change with respect to untreated (vehicle) sample, set to one.

The same method was used to analyse the mRNA expression of *CASP1, CCL2, CCL7, HSP90B1, IFNB1, IL18, IL1B, IRAK1, MAPK12, MAPK9, MEFV, MYD88, NAIP, NLRC4, NLRP12, NLRP3, P2RX7, PANX1, PSTPIP1, PTGS2, PYCARD, RIPK2, TNFA, TNFSF14* and *TNFSF4* in U937-derived macrophages (Tab.III.4). The mRNA levels of two housekeeping genes, *ACTB* and *HPRT1*, was also measured, and the later one was chosen to normalize data.

For the experiment, LX2 cells and macrophages were treated with vehicle, EFV 10 or 25 µM for 24 h. Total RNA isolation and cDNA synthesis were performed as described in chapters “9.2.1. RNA isolation” and “9.2.2. cDNA synthesis”. Finally, PCR was carried out following the instructions provided. Briefly, 1 µL of cDNA was mixed with 10 µL of 2x SsoAdvancedTM universal SYBR® Green supermix (Bio-Rad) in a final reaction volume of 20 µL. Then, the PCR reaction mix was transferred into the well of a 96-well plate containing lyophilized primers. PCRs were performed as follow: 2 min at 95 °C; 5 s at 95 °C, 30 s at 60 °C (40 cycles); 5 s/step at 65-95 °C (0.5 °C increments). All reactions were performed together a positive PCR control assay, a RT control assay, a DNA contamination control assay and RNA quality assay provided by the manufacturer.

REFSEQ	SYMBOL	NAME
NC_000001.10	*AIM2*	Absent in melanoma 2
NC_000011.9	*CASP1*	Caspase 1
NC_000011.9	*CASP5*	Caspase 5
NC_000017.10	*CCL2*	Chemokine (C-C motif) ligand 2
NC_000017.10	*CCL7*	Chemokine (C-C motif) ligand 7
NC_000004.11	*CXCL1*	Chemokine (C-X-C motif) ligand 1
NC_000004.11	*CXCL2*	Chemokine (C-X-C motif) ligand 2
NC_000012.11	*GADPH*	Glyceraldehyde-3-phosphate dehydrogenase
NC_000023.10	*HPRT1*	Hypoxanthine phosphoribosyltransferase 1
NC_000014.8	*HSP90AA1*	Heat shock protein 90kDa alpha (cytosolic), class A member 1
NC_000006.11	*HSP90AB1*	Heat shock protein 90kDa alpha (cytosolic), class B member 1
NC_000012.11	*HSP90B1*	Heat shock protein 90kDa beta (Grp94), member 1
NC_000009.11	*IFNB1*	Interferon, beta 1, fibroblast
NC_000002.11	*IL1B*	Interleukin 1, beta
NC_000007.13	*IL6*	Interleukin 6 (interferon, beta 2)
NC_000011.9	*IL18*	Interleukin 18 (interferon-gamma-inducing factor)
NC_000009.11	*IL33*	Interleukin 33
NC_000023.10	*IRAK1*	Interleukin-1 receptor-associated kinase 1
NC_000005.9	*MAPK9*	Mitogen-activated protein kinase 9
NC_000022.10	*MAPK12*	Mitogen-activated protein kinase 12
NC_000006.11	*MAP3K7*	Mitogen-activated protein kinase kinase kinase 7
NC_000016.9	*MEFV*	Mediterranean fever
NC_000003.11	*MYD88*	Myeloid differentiation primary response gene (88)
NC_000005.9	*NAIP*	NLR family, apoptosis inhibitory protein
NC_000002.11	*NLRC4*	NLR family, CARD domain containing 4
NC_000017.10	*NLRP1*	NLR family, pyrin domain containing 1

NC_000001.10	*NLRP3*	NLR family, pyrin domain containing 3
NC_000019.9	*NLRP12*	NLR family, pyrin domain containing 12
NC_000016.9	*NOD2*	Nucleotide-binding oligomerization domain containing 2
NC_000012.11	*P2RX7*	Purinergic receptor P2X, ligand-gated ion channel, 7
NC_000011.9	*PANX1*	Pannexin 1
NC_000015.9	*PSTPIP1*	Proline-serine-threonine phosphatase interacting protein 1
NC_000001.10	*PTGS2*	Prostaglandin-endoperoxide synthase 2
NC_000016.9	*PYCARD*	PYD and CARD domain containing
NC_000008.10	*RIPK2*	Receptor-interacting serine-threonine kinase 2
NC_000006.11	*TNFA*	Tumor necrosis factor
NC_000001.10	*TNFSF4*	Tumor necrosis factor (ligand) superfamily, member 4
NC_000013.10	*TNFSF11*	Tumor necrosis factor (ligand) superfamily, member 11
NC_000019.9	*TNFSF14*	Tumor necrosis factor (ligand) superfamily, member 14
NC_000011.9	*TRAF6*	TNF receptor-associated factor 6
NC_000007.13	*β-actin*	Actin, beta

Table III.4. Genes analysed in the PrimePCR assay.

These experiments were performed in the laboratory of Prof. Andrea Cossarizza, at University of Modena and Reggio Emilia (Modena, Italy), under the supervision of Prof. Marcello Pinti and Dr. Milena Nasi.

10. LIGHT MICROSCOPY

Cells were seeded in 48-well plates and, after the treatment, washed with HBSS. In order to analyse cellular morphology, bright field individual images (40x) of live-cells were captured with IX81 Olympus microscope (Olympus, Hamburg, Germany) using 'CellR' software v.2.8.

11. FLUORESCENCE MICROSCOPY AND STATIC CYTOMETRY

In order to avoid trypsinization and further manipulation of the cells which often provokes artefacts in flow cytometry, we employed a life cell fluorescence imaging method in which cells remain adherent and vital during the whole procedure. Fluorescence was detected with an IX81 Olympus fluorescence microscope and CellR software v.2.8 was employed to capture individual images. The fluorescent signal was quantified individually (per cell) by static cytometry software 'ScanR' version 2.03.2 (Olympus). This technique allows to analyse and quantify numerous cell parameters automatically.

All treatments were performed in duplicate in 48-well plates. Cells were then washed in HBSS and 16-30 images per well were immediately recorded. Nuclei were stained with the fluorochrome Hoechst 33342 (2.5 µM) for the last 30 min of the treatment, at 37 °C and darkness.

11.1. Cell proliferation/survival and cell cycle analysis

Cells were treated, allowed to proliferate exponentially (24 h) and then counted according to mean Hoechst fluorescence (2.5 µM Hoechst 33342, 25 images per well). Hoechst area and total intensity of its fluorescence were also recorded for analysis of nuclear area (nuclear size) and cell cycle.

11.2. Mitochondrial membrane potential ($\Delta\Psi_m$)

Cells were treated and in the last 30 min of treatment, fluorochrome 5 µM TMRM was added to assess $\Delta\Psi_m$. As control of the experiment, 10 µM CCCP was used (Lou P.H. *et al*., 2007). Detection filters used were 540/10 nm for excitation and 590 nm for emission.

11.3. Mitochondrial superoxide production

Cells were treated and in the last 30 min of treatment, 2.5 µM MitoSOX was added to assess mitochondrial superoxide production. This fluorochrome accumulates within mitochondria (as it is attracted by the $\Delta\Psi_m$ due to its positive charge) where it is oxidized by the superoxide ion only and not by other ROS, features that make it a

selective mitochondrial superoxide detector. As positive control we used 25 µM Rot. Detection filters used were 540/10 nm for excitation and 590 nm for emission.

11.4. Mitochondrial mass

To assess mitochondrial mass, 1 µM NAO was added in the last 30 min of treatment. This hydrophobic fluorescent probe binds specifically to cardiolipin which is located in the IMM, regardless of changes on the $\Delta\Psi_m$, marking specifically mitochondria of living cells (Wu C.W. *et al*., 2007). Detection filters used were 495 nm for excitation and 519 nm for emission.

11.5. Apoptosis

Apoptosis was studied as bivariate Annexin V/Propidium iodide (PI) analysis (apoptosis detection kit, Abcam). After the treatment, the medium in a 48-well plate was replaced with HBSS containing 0.9 µL per well of Annexin V fluorescein (to detect phosphatidylserine exteriorization) and 2.5 µM Hoechst 33342 (to mark nuclei). Following incubation at 37 °C and darkness (20 min), 0.3 µL per well of the chromatin-detecting dye PI was added (10 min) to label dead or damaged cells. Staurosporine (STS, 1 µM), a widely used protein kinase inhibitor, was employed as a positive pro-apoptotic control (Lakhani S.A. *et al*., 2006). Detection filters used were 495 nm for excitation and 519 for emission for Annexin V and 540/10 nm for excitation and 590 nm for emission for PI.

12. CONFOCAL FLUORESCENCE MICROSCOPY

We used a Leica TCS-SP2 confocal laser scanning unit (Leica Microsystems, Wetzlar, Germany) with argon and helium-neon laser beams and attached to a Leica DMIRBE inverted microscope. This equipment belongs to Unidad Central de Investigación de Medicina (UCIM, Universidad de Valencia, Valencia, Spain). Images were captured at 63x magnification with HCX PL APO 40.0 x 1.32 oil UV objective. Image J program was used to analyze the images and the colocalization analysis was performed with the Colocalization Colormap plugin.

12.1. Analysis of mitochondrial morphology

Cells plated on multi-well coverslips (Thermo Fisher Scientific) were treated and then stained with 2.5 µM Hoechst 33342 (to mark nuclei) and 1 µM NAO (to mark mitochondria) for the last 30 min of treatment. After washing with HBSS, life cell images were acquired.

12.2. Immunofluorescence analysis

After treatment in multi-well coverslips, cells were fixed with 4% formaldehyde for 15 min at RT, and then rinsed with PBS 3 times for 5 min each to eliminate the formaldehyde. After fixation and blocking for 60 min at RT with blocking solution (PBS, 5% normal goat serum and 0.3% Triton™ x-100), cells were incubated with primary antibodies, overnight at 4 °C. Samples were then rinsed 3 times with PBS for 5 min each and incubated with secondary antibodies (goat anti-rabbit Alexa Fluor 488 at 1:500 and goat anti-mouse Alexa Fluor 594 at 1:600, both from Thermo Fisher Scientific) for 1 h at RT in the dark. All antibodies were diluted in antibody dilution buffer (PBS, 1% BSA and 0.3% Triton™ x-100). To mark nuclei, 5 µM of the fluorochrome Hoechst 33342 was added for the last 30 min. After washing with PBS, 3 times for 5 min each, cells were maintained in HBSS and images were acquired.

12.2.1. Translocation of p-Drp1 to mitochondria

To analyse the translocation of p-Drp1 to mitochondria, after fixation and blocking, cells were incubated with the next primary antibodies: rabbit anti-phospho-Drp1 (Ser616) at 1:200 (Cell Signaling) and mouse anti-TOM20 at 1:250 to mark mitochondria (BD Biosciences).

12.2.2. Analysis of LONP1 presence in ER or mitochondria

To study the presence of LONP1 in ER or mitochondria, cells were incubated with primary antibodies after fixation and blocking. We used rabbit anti-LONP1 at 1:50 (Proteintech) and mouse anti-Calnexin at 1:750 to mark ER (Thermo Fisher Scientific) or mouse anti-TOM20 at 1:250 to mark mitochondria.

13. STATISTICAL ANALYSES

Data were analysed using GraphPad Prism 6.0 software (GraphPad Software, La Jolla, CA, USA). Statistical analysis was performed by Student's *t*-test or one-way ANOVA multiple comparison test followed by a Newman-Keuls test. In most cases, data are presented as % of control (untreated cells considered 100%). All values are expressed as a mean ± SEM (statistical significance in the case of EFV treatment was analysed vs. vehicle (MeOH) and represented as $^{*}P < 0.05$, $^{**}P < 0.01$ and $^{***}P < 0.001$, whereas TG, Rot, CCCP and STS were analysed separately and their significance was shown as: $^{\#}P < 0.05$, $^{\#\#}P < 0.01$ and $^{\#\#\#}P < 0.001$ vs. untreated cells or DMSO).

IV. RESULTS

SECTION 1: ANALYSIS OF THE INVOLVEMENT OF MITOCHONDRIA IN THE EFFECTS INDUCED BY EFV

1. Determination of the Hep3B rho^o phenotype

Our group has already reported that EFV not only disrupts mitochondrial function in hepatic cells but also induces ER stress with the consequent activation of UPR. Notably, the effect of EFV on ER has been shown to involve mitochondria as it is radically reduced in cells with respiration-deficient mitochondria (Apostolova N. *et al*., 2013). In order to better understand the implication of the mitochondria in the hepatic effect induced by EFV, we assessed the action of this drug on cells lacking functional mitochondria (rho^o phenotype), and compared it to that of the typical mitotoxic agent rotenone (Rot) and the widely employed ER stress inductor thapsigargin (TG).

Firstly, after generation of rho^o cells, we analysed several markers of this phenotype, which is characterized by the absence of fully functional mitochondria. Electrochemical measurements of O_2 consumption in intact cells using a Clark-type oxygen electrode revealed a major drop in the respiration of rho^o cells, which maintained only 15% of the basal levels recorded in WT cells (Fig.IV.1A). Also, the depletion of mtDNA and hence the rho^o state of these cells was controlled by quantitative genomic PCR analysis of the amount of mtDNA versus that of nuclear DNA. This experiment revealed that rho^o cells possessed roughly 30% of the mtDNA compared to WT cells (Fig.IV.1B), indicating a major depletion but meaning that they are not completely devoid of mtDNA or not fully “rho^o” cells (Fig.IV.1B).

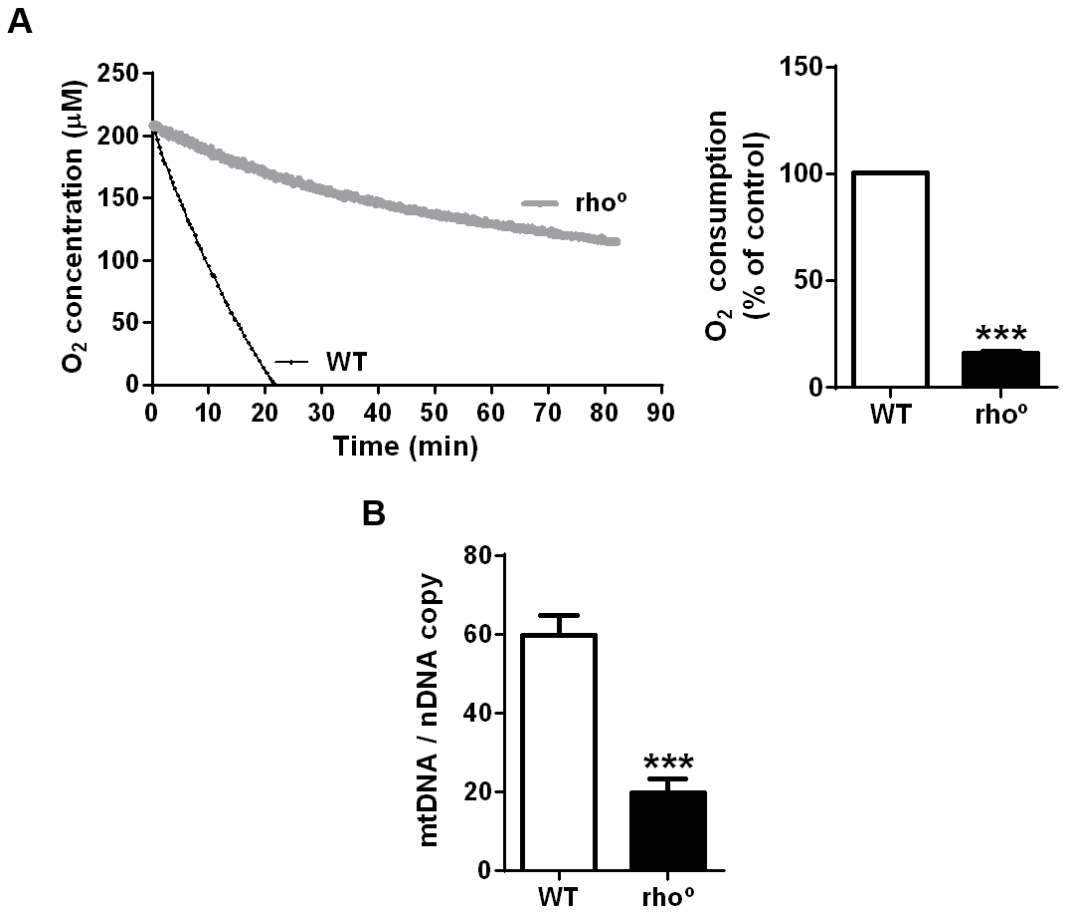

Figure IV.1. Determination of the Hep3B rho^{o} phenotype. (A) Electrochemical measurement of O_2 consumption with a Clark-type O_2 electrode. Representative traces and histogram showing O_2 consumption in intact rho^{+} and rho^{o} cells (4 × 10^{6} cells were employed in each run). (B) Quantitative genomic PCR used to quantify the relative ratio of mtDNA/nDNA in rho^{+} and rho^{o} cells. Data represent mean ± SEM, n = 4, and were analysed by Student's t-test (*P < 0.001 vs. WT cells).**

WB analysis using whole-cell protein extracts demonstrated the complete absence of subunit II of the mitochondrial Complex IV and a major reduction (80%) in expression of ND1, a Complex I subunit, both mtDNA-encoded proteins, while no alterations were observed in the expression of Porin and CV-β, mitochondrial proteins encoded by nuclear genes (Fig.IV.2).

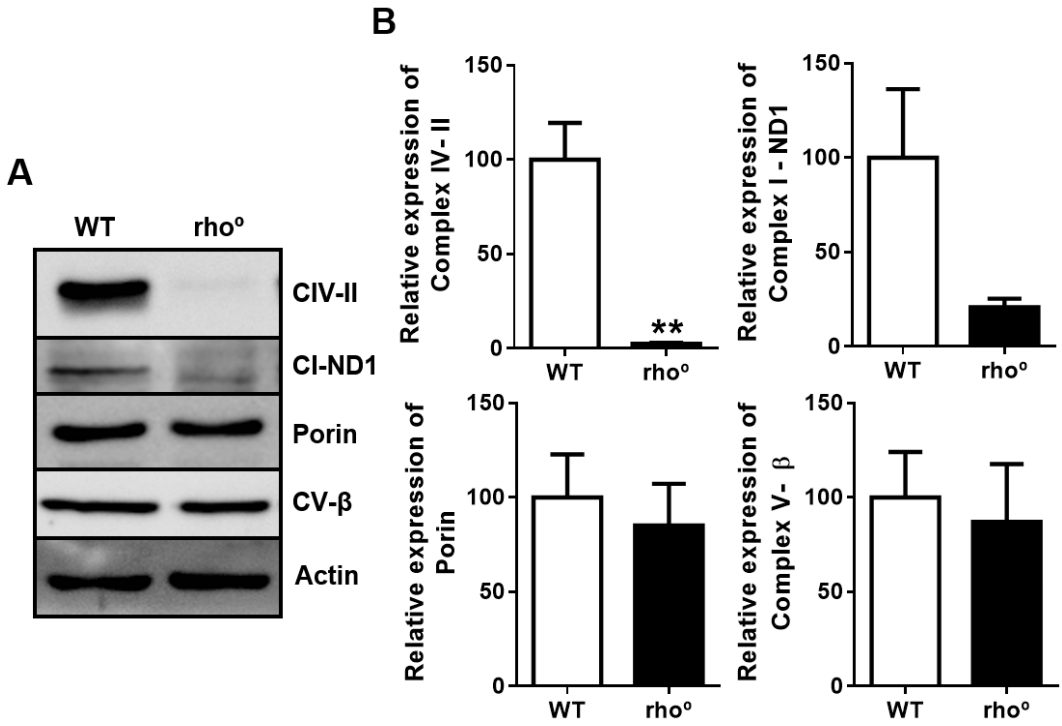

Figure IV.2. WB analysis of mtDNA and nDNA-encoded proteins in Hep3B rho$^+$ and rho^o cells. (A) Representative WB image and (B) histograms expressing quantification of Complex IV subunit II, Complex I subunit ND1, Complex V subunit β and Porin expression in total cell extracts; β-actin was used as a loading control. Data represent mean ± SEM, n = 4, and were analysed by Student's *t*-test ($P < 0.01$ vs. WT cells).**

2. Mitochondrial effect of EFV on respiration-deficient hepatic cells

After generation of rho^o cells and confirmation of their phenotype, we evaluated the effect of EFV on mitochondria after 24 h of treatment in WT and mtDNA-depleted cells through three parameters indicative of mitochondrial function: mitochondrial superoxide ($O_2^{\cdot-}$) production, $\Delta\Psi_m$ and mitochondrial morphology/mass.

2.1. Mitochondrial superoxide production

Rho^o cells under basal conditions display a slightly higher mitochondrial $O_2^{\cdot-}$ production (MitoSOX fluorescence) than WT cells. After 24 h of treatment, all three stimuli (EFV, TG and Rot) induced an increase in mitochondrial $O_2^{\cdot-}$ production in Hep3B WT cells that was significantly lower (with TG and Rot) or even absent (with EFV) in cells lacking normal mitochondria (Fig.IV.3).

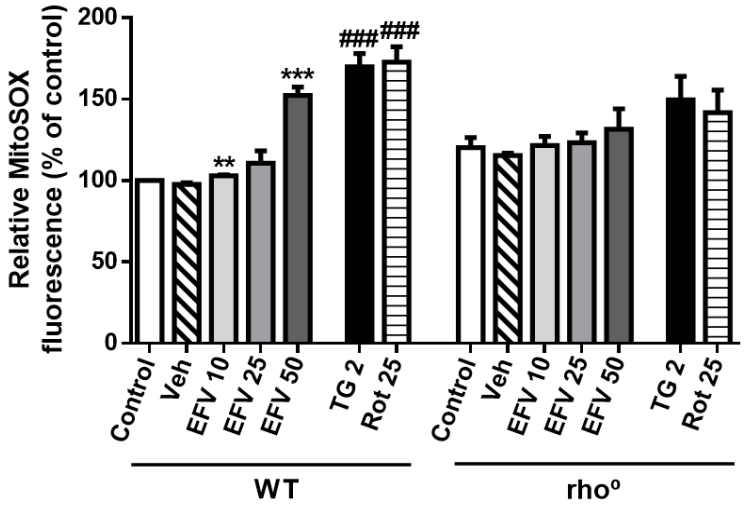

Figure IV.3. Analysis of superoxide production ($O_2^{\cdot -}$, MitoSOX fluorescence) in Hep3B WT and rho^o cells treated for 24 h with increasing concentrations of EFV, vehicle, TG 2 µM or Rot 25 µM. Data represent mean ± SEM, n = 4-6, and were calculated as % of control value (untreated WT cells considered 100%) and analysed by Student's *t*-test (P < 0.01, ***P < 0.001 for EFV vs. vehicle and $^{###}P$ < 0.001 for Rot and TG vs. untreated cells).**

2.2. Analysis of mitochondrial membrane potential ($\Delta\Psi_m$)

Assessment of $\Delta\Psi_m$ (TMRM fluorescence) revealed a decrease in this parameter in untreated rho^o cells compared to rho$^+$ under basal conditions (Fig.IV.4A). Cells exposed to EFV or Rot exhibited a similar drop in $\Delta\Psi_m$ to that observed with 10 µM of the uncoupler of OxPhos CCCP, which was employed as a positive control. Importantly, this effect was present in rho^o cells and was even more pronounced with EFV 50 µM and Rot. Unlike EFV and Rot, TG provoked an increase in TMRM fluorescence in WT cells, an effect that was absent in rho^o cells.

Many cell types have the ability to maintain $\Delta\Psi_m$ under conditions of diminished mitochondrial respiration or OxPhos uncoupling through the reverse (ATP spending) activity of ATP synthase (complex V of ETC) (Faccenda D. and Campanella M., 2012). Taking this into account, we also assessed the effect of EFV on cells where glycolysis had been inhibited (by addition of 10 mM 2-DG). All three stimuli (EFV, TG and Rot) provoked a similar response although slightly more pronounced in cells treated with 2-DG compared to WT. Moreover, while rho^o cells under basal conditions displayed only a slightly lower $\Delta\Psi_m$ in comparison to WT cells, this difference was greater (about 50% reduction) when both cell populations were exposed to 2-DG. Both EFV and Rot, as

well as CCCP, were able to induce a similar $\Delta\Psi_m$ decrease in 2-DG-exposed rho^o cells compared to the WT counterpart, whereas interestingly, in 2-DG-exposed rho^o cells the increase triggered by TG was absent (Fig.IV.4B).

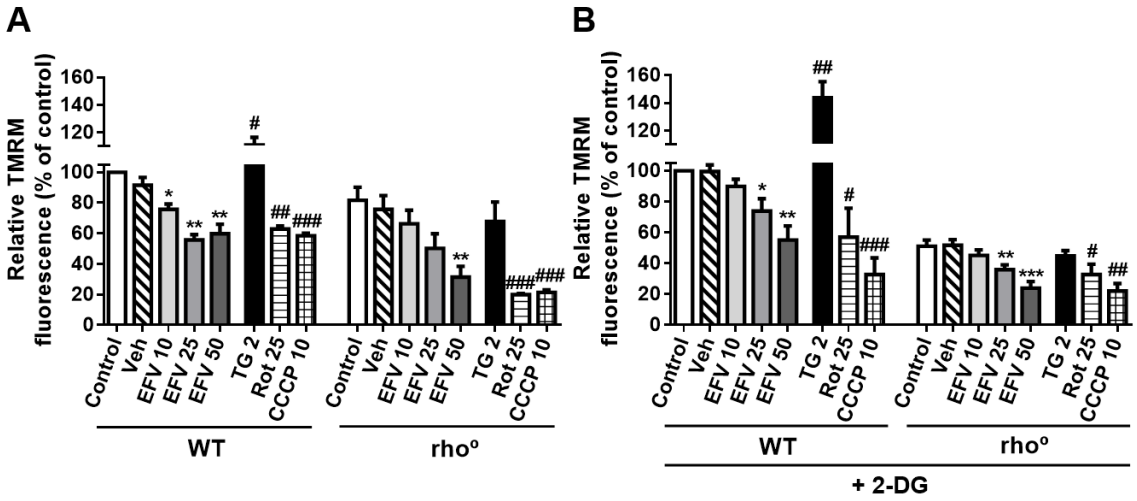

Figure IV.4. Analysis of mitochondrial membrane potential ($\Delta\Psi_m$, TMRM fluorescence) in Hep3B WT and rho^o cells. (A) Cells were treated for 24 h with increasing concentrations of EFV, vehicle, Rot 25 µM or TG 2 µM, or (B) a combination of each one of these treatments with 2-DG 10 mM. CCCP 10 µM was used as a positive control. Data represent mean ± SEM, n = 4-6, and were calculated as % of control value (untreated WT cells considered 100%) and analysed by Student's *t*-test (P* < 0.05, ***P* < 0.01, ****P* < 0.001 for EFV vs. vehicle and $^{\#}P$ < 0.05, $^{\#\#}P$ < 0.01, $^{\#\#\#}P$ < 0.001 for Rot, TG and CCCP vs. untreated cells).**

2.3. Determination of intracellular ATP levels

In parallel to the above experiments, we evaluated the intracellular ATP levels after 24 h of treatment and this assessment revealed several interesting results. Firstly, in rho$^+$ cells, all three stimuli led to an increase in the ATP level and clearly this effect was due to activation of glycolysis as it was abolished when cells were co-treated with 2-DG (Fig.IV.5A). In the case of EFV, we observed a concentration-dependent decrease in ATP in 2-DG-exposed WT cells. Rot provoked an even greater drop in the ATP level in these cells, whereas ATP levels were preserved in TG-treated cells. Secondly, the changes in intracellular ATP were generally less pronounced in rho^o cells compared to WT (Fig.IV.5B). Both EFV and Rot did not seem to induce an increase in ATP in cells with active glycolysis and the reduction in ATP levels previously described in 2-DG exposed cells was much smaller (or even absent). TG-treated cells seem to be less

affected by the rho^o phenotype in accordance to the action of this drug being primarily on ER and not mitochondria.

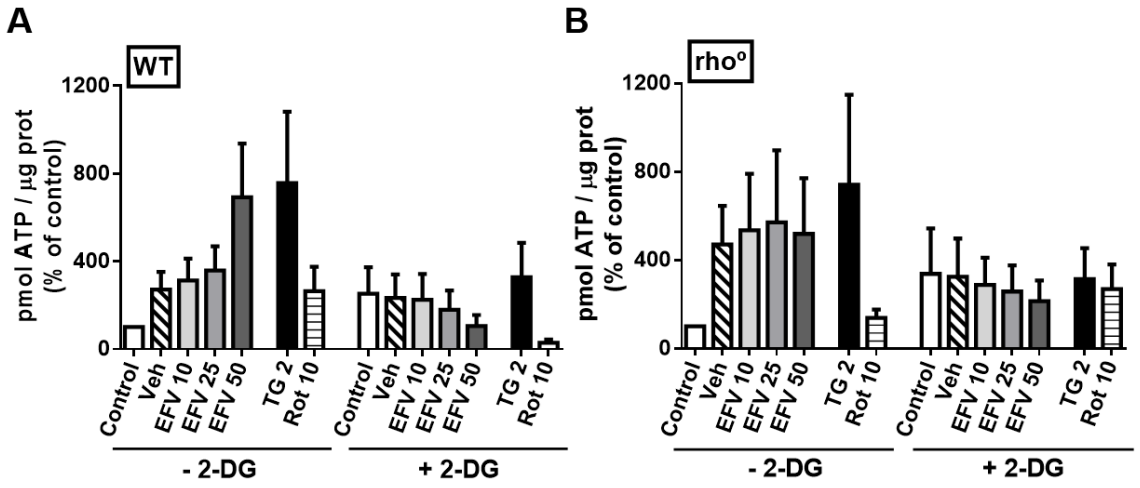

Figure IV.5. Measurement of intracellular ATP levels with or without 2-DG 10 mM in Hep3B cells. (A) WT and (B) rho^o cells treated for 24 h with increasing concentrations of EFV, vehicle, Rot 10 µM or TG 2 µM. Data represent mean ± SEM, n = 4-6, and were calculated as % of control (untreated cells without 2-DG considered 100%) and analysed by Student's *t*-test.

In accordance with its potential to produce lactic acidosis in human toxicology, methanol (the vehicle of EFV) by itself led to an increase in intracellular ATP, an effect that seem to be due to glycolysis as it was absent when cells were co-treated with 2-DG.

2.4. Analysis of mitochondrial mass and morphology

In order to evaluate the mitochondrial mass and morphology, after 24 h-treatment cells were stained with the mitochondria-specific fluorochrome NAO. An increase in NAO fluorescence has been associated with mitochondrial damage in this model (Apostolova N. *et al*., 2010), and in the present study, we observed an increase in NAO fluorescence in WT cells exposed for 24 h to EFV (25 and 50 µM, but not 10 µM), TG or Rot (Fig.IV.6). In the case of rho^o cells, only the highest concentration of EFV increased NAO fluorescence and the effect of TG was lower in rho^o than in WT cells.

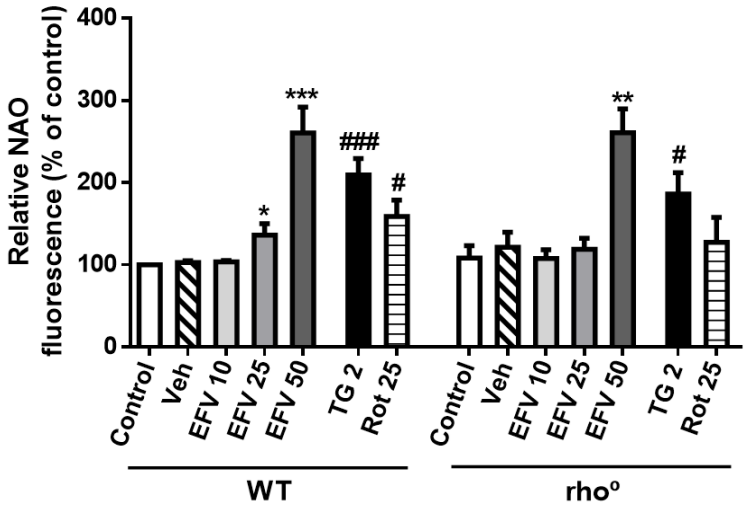

Figure IV.6. Analysis of mitochondrial mass (NAO fluorescence) in Hep3B WT and rho° cells treated for 24 h with increasing concentrations of EFV, vehicle, Rot 25 µM or TG 2 µM. Data represent mean ± SEM, n = 4-6, and were calculated as % of control value (untreated WT cells considered 100%) and analysed by Student's *t*-test (P* < 0.05, ***P* < 0.01, ****P* < 0.001 for EFV vs. vehicle and $^{\#}P$ < 0.05, $^{\#\#\#}P$ < 0.001 for Rot and TG vs. untreated cells).**

All three stimuli induced clear changes in the mitochondrial network, as shown in Fig.IV.7. While mitochondria in untreated cells were dispersed, EFV- and TG-treated cells emitted a more compact mitochondrial signal. Rot-exposed cells exhibited a granulated mitochondrial network with an intense signal around the nucleus. Importantly, the alterations in NAO fluorescence were less prominent in rho° cells. In sharp contrast to WT cells, Hep3B cells lacking normal mitochondria showed either no increase or a lower increase in mean NAO fluorescence intensity when exposed to Rot and TG respectively. In the case of EFV, NAO fluorescence revealed a major difference between the different concentrations of the drug evaluated. As shown in Fig.IV.6, both EFV 25 and 50 µM increased NAO fluorescence in WT cells, whereas such an increase was detected in rho° cells only with EFV 50 µM, which points to a more severe degree of mitochondrial damage that exceeded a certain threshold.

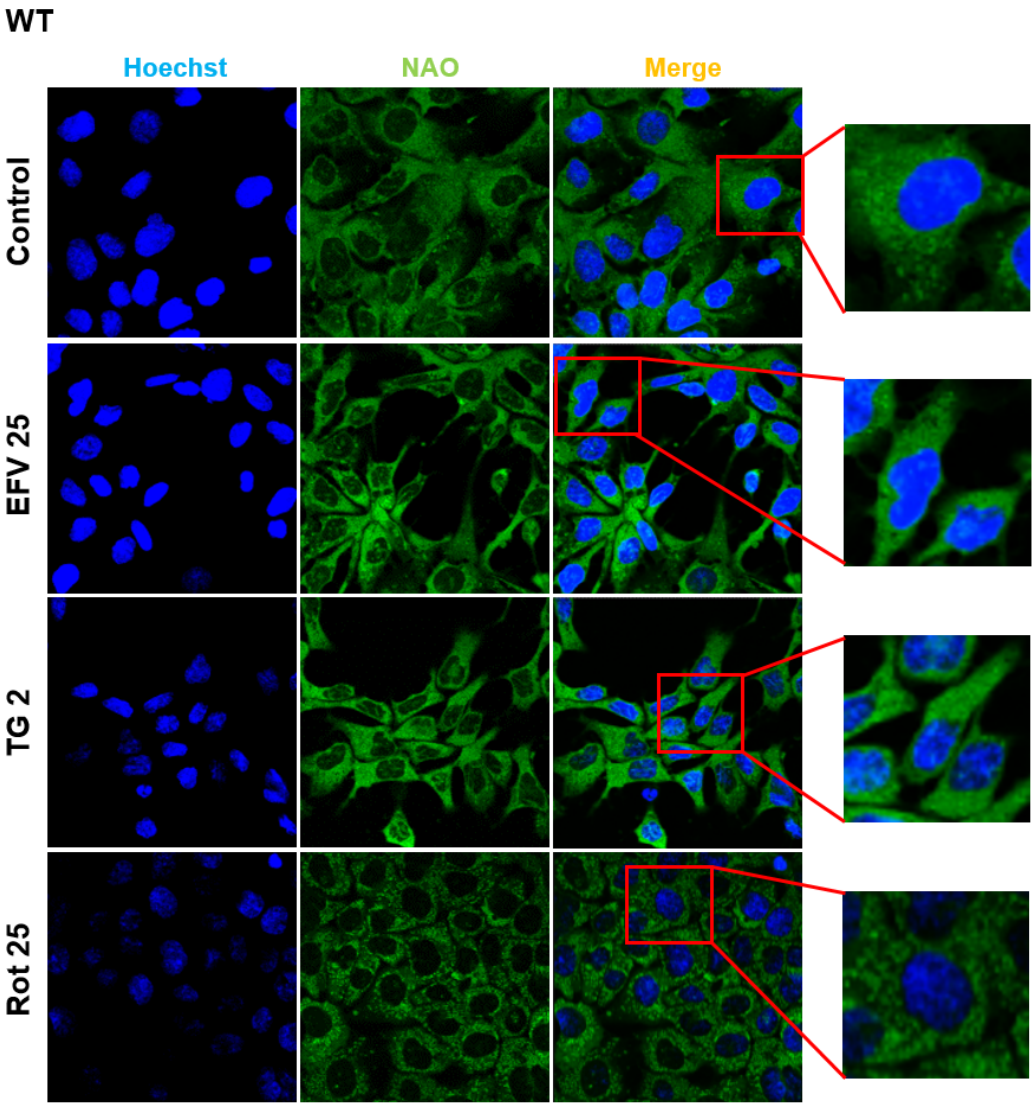
WT
Hoechst
NAO
Merge
Control
EFV 25
TG 2
Rot 25

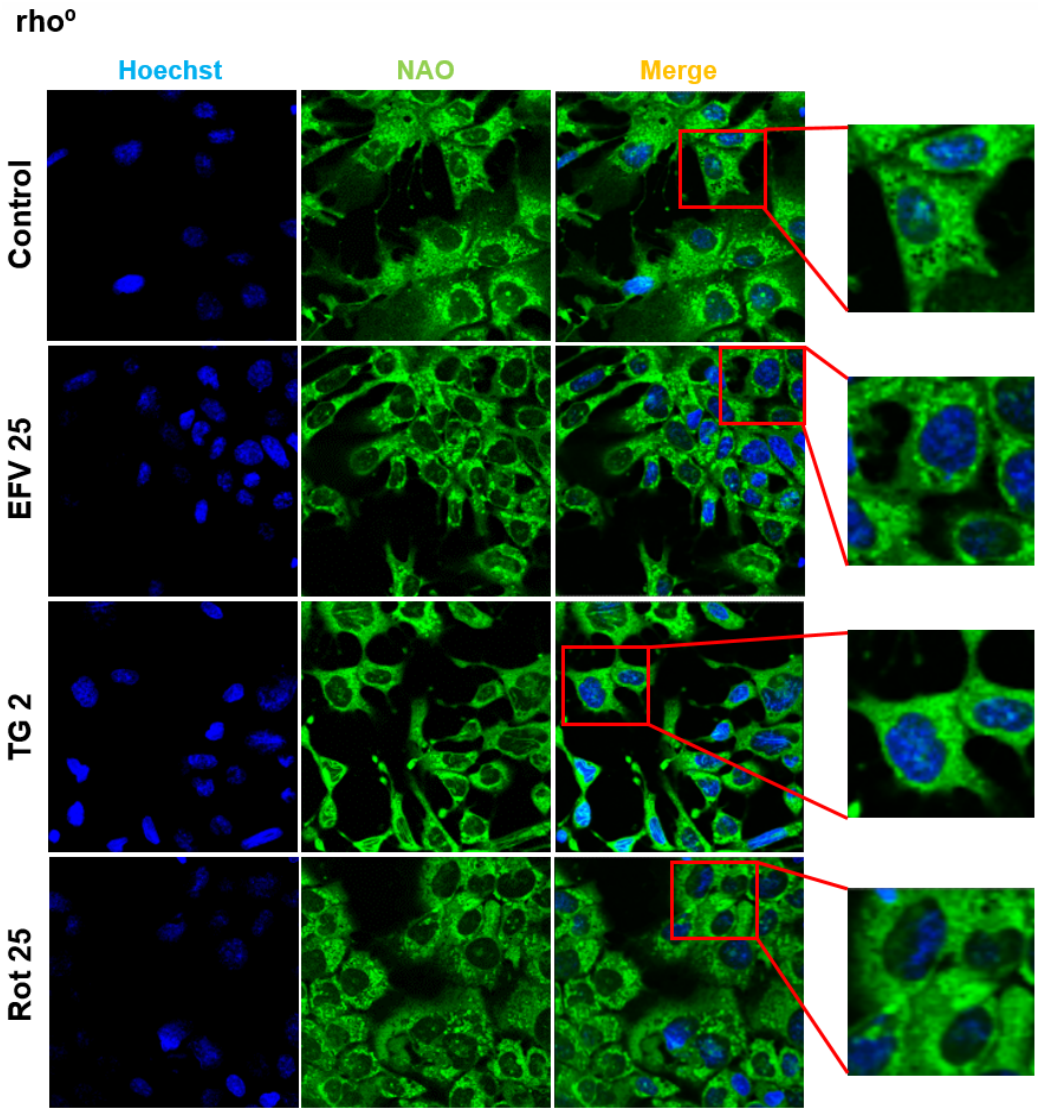

Fig.IV.7. Analysis of mitochondrial morphology in Hep3B WT and rho^0 cells. Representative confocal microscopy images (63×) of cells treated for 24 h with EFV 25 µM, TG 2 µM or Rot 25 µM and stained with Hoechst 33342 (blue, nuclei) and NAO (green, mitochondria).

3. Effect of EFV treatment on the viability of rho^0 cells

3.1. Study of cell morphology

After studying the mitochondrial effect of EFV on respiration-deficient hepatic cells, we analysed the effect of the drug on the viability of rho^0 cells. Light microscopy images of WT cells obtained after 24 h of treatment with EFV 25 µM, EFV 50 µM, TG 2 µM or Rot 25 µM revealed alterations in cell size and morphology with all three stressors, with major differences between the treatments (Fig.IV.8). EFV 25 µM-treated cells were thinner than controls; this “spider net” appearance was particularly evident in cells

treated with TG, whereas Rot-treated cells were bigger, had a rounder shape and exhibited a high amount of aggregates (lipofuscin golden brown finely granular pigment granules). Moreover, cell number was markedly reduced in Rot- and TG-treated samples.

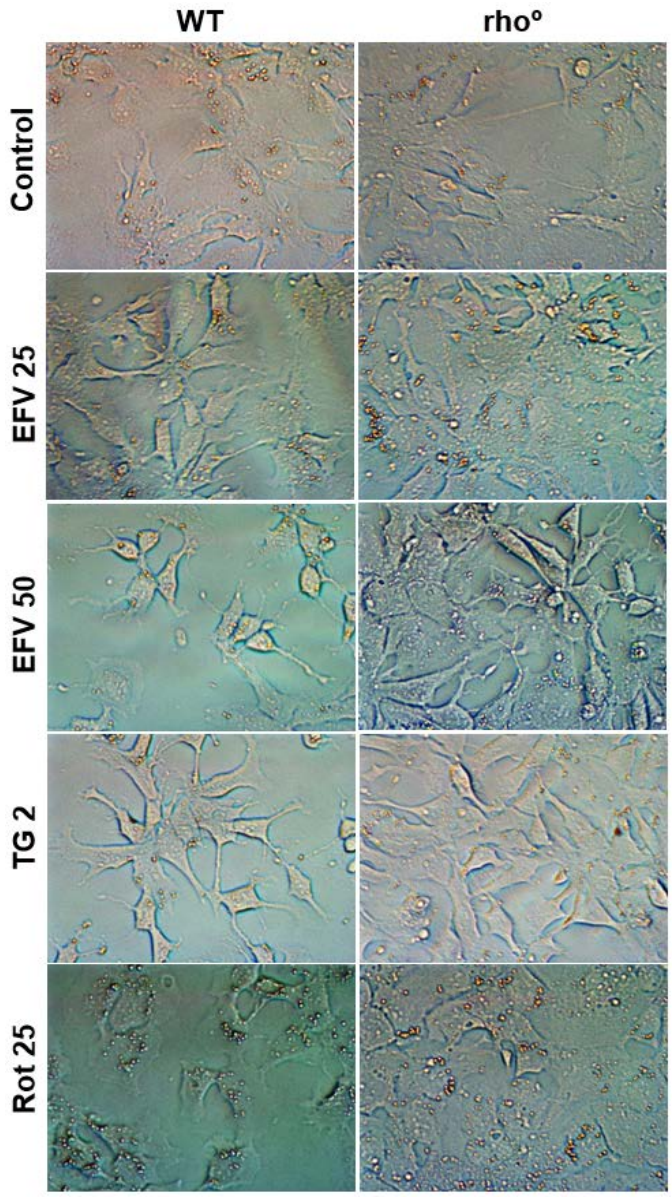

Figure IV.8. Study of cell morphology. Representative inverted light microscopy images (40×) of Hep3B WT and rho^{o} cells treated for 24 h with EFV 25 µM, EFV 50 µM, TG 2 µM or Rot 25 µM.

3.2. Analysis of cell number, nuclear area and nuclear signal

Previous studies by our group have shown that EFV exerts a cytotoxic effect on Hep3B cells. When a range of clinically relevant concentrations was evaluated (10-50 µM), the highest concentration (50 µM) was clearly associated with a major drop in cell viability,

expressed as a dramatic decrease in cell number, altered cell cycle and induction of apoptosis. Very importantly, the present study revealed that all these effects are less pronounced in rho^{o} cells; 24 h of treatment of Hep3B WT cells with EFV 50 μM led to a marked drop in cell number (a reduction of 60% with respect to vehicle-treated cells), whereas only a slight decrease (approximately 20%) was observed in rho^{o} cells undergoing the same treatment (Fig.IV.9A). A similar phenomenon was observed when chromatin condensation was assessed (mean nuclear fluorescence intensity and nuclear area through Hoechst 33342 fluorescence; Fig.IV.9B and C). WT cells exposed to EFV displayed increased Hoechst fluorescence and decreased nuclear area, modifications that were less evident or absent, respectively, in cells lacking functional mitochondria. A similar behaviour regarding both cell number and nuclear size/morphology was recorded with TG. In the case of exposure to Rot 25 μM, the increase in Hoechst fluorescence was absent in rho^{o} cells and the reduction in cell number was lower than that of WT cells. Unlike EFV and TG, Rot produced an increase in the nuclear area, a phenomenon also present in rho^{o} cells (Fig.IV.9C).

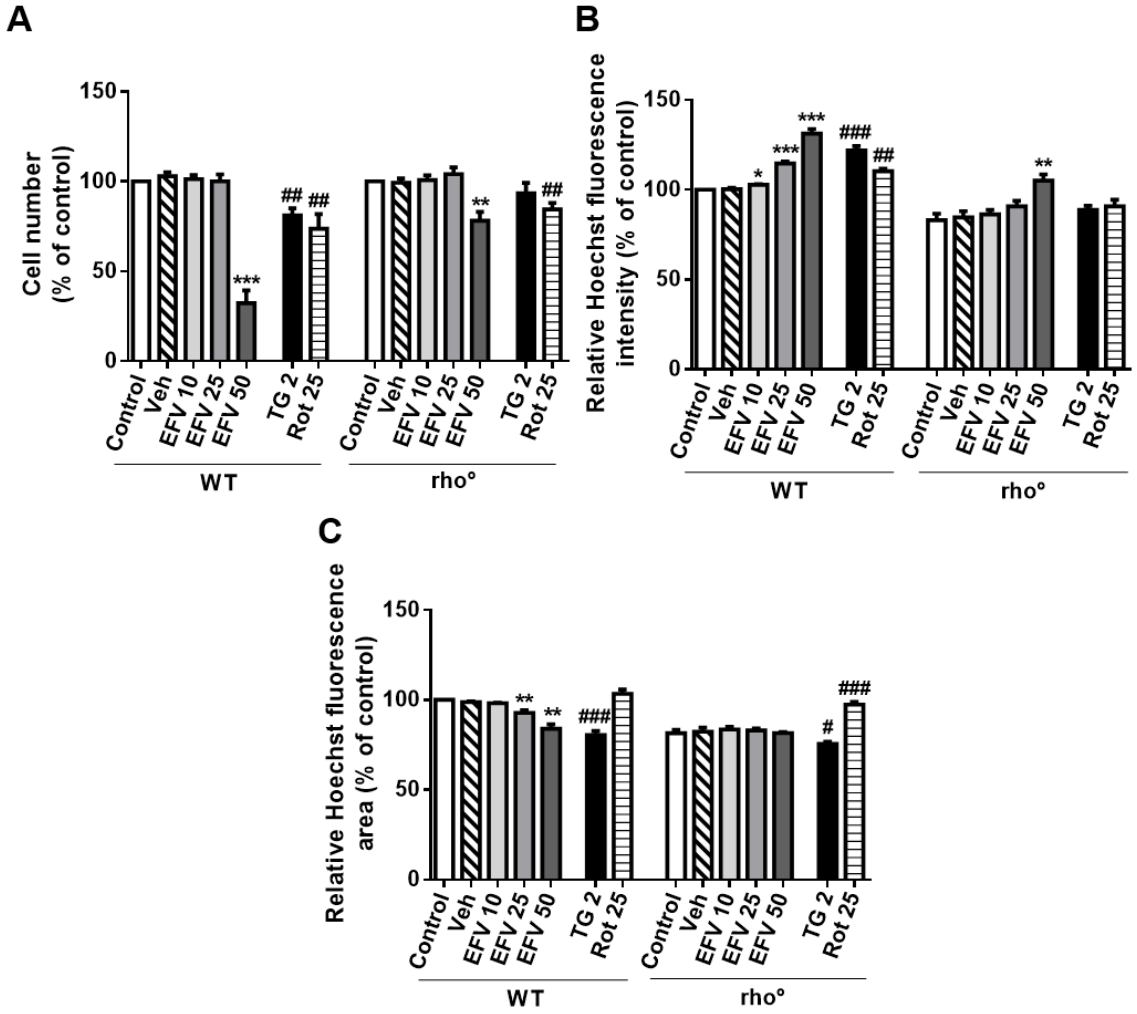

Figure IV.9. Cell viability analysis of Hep3B WT and rho^{o} cells treated for 24 h with increasing concentrations of EFV, vehicle, Rot 25 µM or TG 2 µM. Hoechst fluorescence data: (A) cell number, (B) nuclear signal and (C) nuclear area. Data represent mean ± SEM, n = 3-6, and were calculated as % of control fluorescence value (untreated WT cells considered 100%) and analysed by Student's *t*-test (P* < 0.05, ***P* < 0.01, ****P* < 0.001 for EFV vs. vehicle and $^{\#}P$ < 0.05, $^{\#\#}P$ < 0.01, $^{\#\#\#}P$ < 0.001 for Rot and TG vs. untreated cells). The cell number of untreated cells in both cellular backgrounds (rho^{o} and rho^{+}) was considered to be 100%.**

3.3. Cell cycle analysis

The above results were supported by cell cycle analysis (Fig.IV.10). Firstly, Hep3B rho^{o} cells displayed slight differences in their cell cycle pattern compared to WT cells, expressed as decreased S and G2M populations with an increase in both subG1 and G1. All three stimuli - EFV (only 50 µM), TG and Rot - induced a change in the cell cycle of WT cells. EFV- and TG-exposed WT cells manifested an increase in their G2M cellular

population and a decrease in the S phase, modifications that were absent in rho^o cells. On the other hand, the effect of Rot was present in both rho^o cells and rho$^+$ cells.

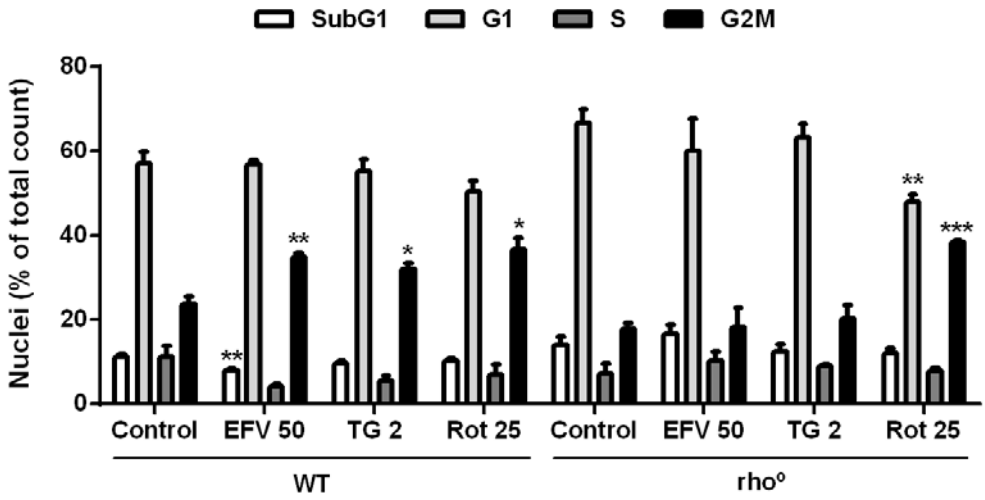

Figure IV.10. Cell cycle analysis by static cytometry (Hoescht fluorescence) in Hep3B WT and rho^o cells treated for 24 h with EFV 50 µM, TG 2 µM or Rot 25 µM. Data represent mean ± SEM, n = 3, and were analysed by Student's *t*-test (P* < 0.05, ***P* < 0.01, ****P* < 0.001 vs. the corresponding value of the cell cycle phase in control cells).**

3.4. Cell death analysis

In order to delve more deeply in the effect of EFV on cell viability, we assessed the presence of apoptotic and necrotic cells, in both parental cells and cells lacking functional mitochondria, after 24 h of treatment. The inducer of apoptosis STS (1 µM) was used as positive control. As expected, these experiments revealed that under basal conditions, rho^o cells have a higher percentage of all three cell death subpopulations: early or typically apoptotic (Ann$^+$/PI$^-$), late apoptotic and/or necrotic (Ann$^+$/PI$^+$) and typically necrotic or damaged (Ann$^-$/PI$^+$). As previously published, in Hep3B WT cells, EFV (particularly the highest concentration, EFV 50 µM) induced apoptosis and perhaps slightly also necrosis, effects that were shown to be largely diminished (apoptosis) or absent (necrosis) in respiration-deficient cells (Fig.IV.11). Interestingly, the effects of Rot and TG were somewhat different; they triggered apoptosis in WT cells and this effect seemed to be diminished in rho^o cells; however, their ability to induce necrosis seemed to be enhanced.

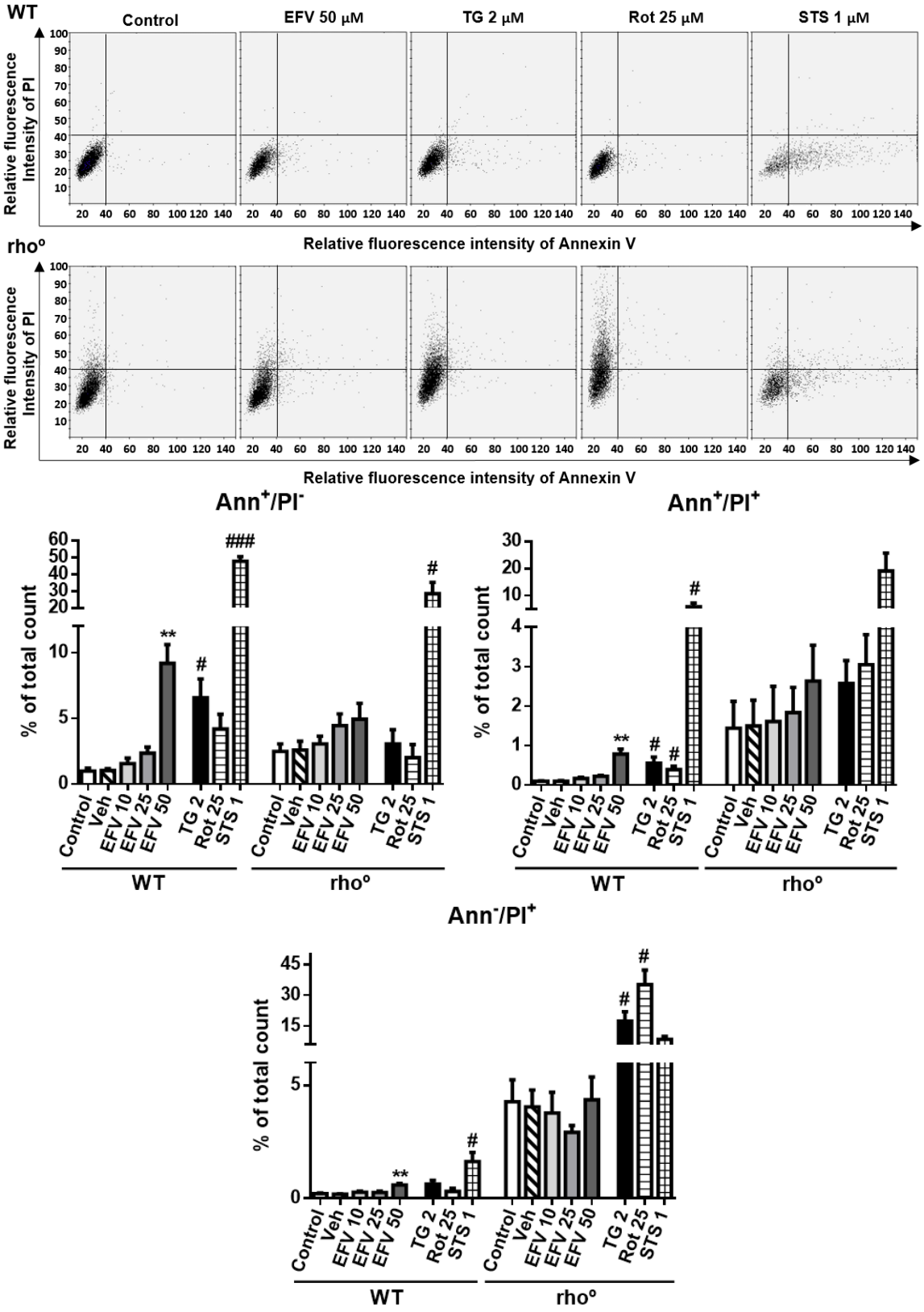

Figure IV.11. Cell death analysis of Hep3B WT and rho° cells. Representative cytograms (bivariate Annexin V/PI analysis) of cells treated for 24 h with EFV 50 µM, vehicle, TG 2 µM, Rot 25 µM or staurosporine (STS 1 µM, used as a positive control), showing the existence of four cellular populations: AnnV⁻/PI⁻, AnnV⁺/PI⁻, AnnV⁻/PI⁺ and AnnV⁺/PI⁺ (upper panel). Histograms expressing quantification of AnnV⁺/PI⁻, AnnV⁻/PI⁺ and AnnV⁺/PI⁺ cellular populations in rho⁺ and rho° cells

treated with increasing concentrations of EFV, TG 2 µM, Rot 25 µM and STS 1 µM (lower panel). Data represent mean ± SEM, n = 3, and were calculated as % of total number of nuclei counted and analysed by Student's *t*-test (*P* < 0.01 for EFV vs. vehicle and #*P* < 0.05, ###*P* < 0.001 for Rot, TG and STS vs. untreated cells).**

4. Effect of EFV treatment on HepaRG cells

In order to confirm that despite its cancerous nature, Hep3B cells were an appropriate model for these pharmacological analyses, several experiments were also performed in WT HepaRG, a terminally differentiated hepatic cell line derived from human hepatic progenitor cells. Importantly, the responses observed in parental Hep3B and WT HepaRG cells were similar in the parameters studied. As shown in Fig.IV.12A and B, 24 h-treatment with EFV led to a concentration-dependent increase in mitochondrial ROS production (MitoSOX fluorescence) paralleled by a decrease in cell number (nuclei stained with Hoechst 33342), although the effect was less pronounced in HepaRG than on Hep3B cells. Also, in comparison to Hep3B, HepaRG cells seemed to be particularly susceptible to Rot, in both parameters, and less susceptible to TG and EFV regarding mitochondrial ROS production.

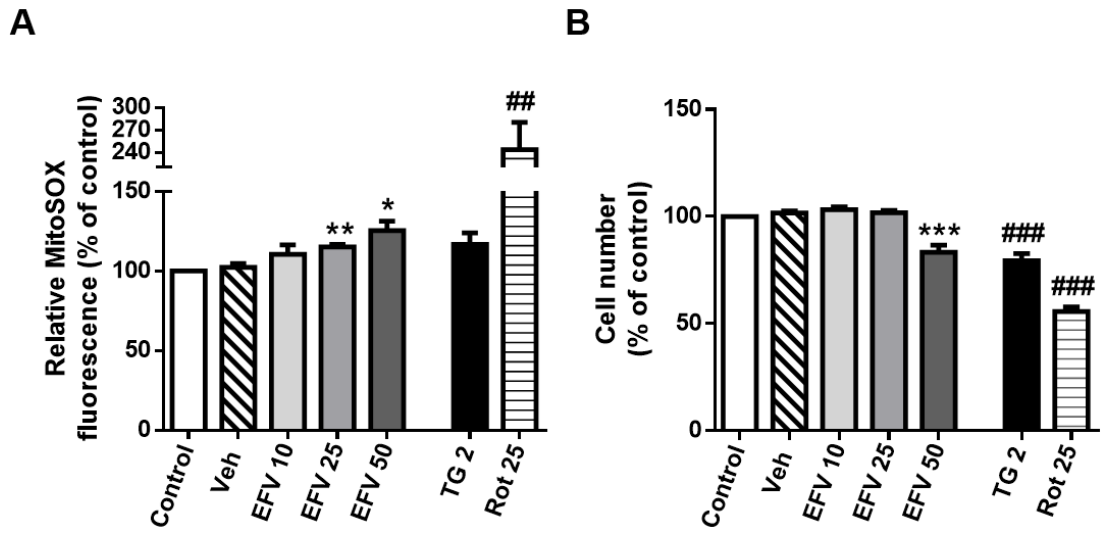

Figure IV.12. Effect of EFV treatment on HepaRG cells. Cells were treated for 24 h with increasing concentrations of EFV, vehicle, Rot 25 µM or TG 2 µM. (A) Mitochondrial $O_2^{\cdot-}$ production (MitoSOX fluorescence). (B) Cell viability expressed as cell number (nuclei according to Hoechst fluorescence). Data represent mean ± SEM, n = 4-6, and were calculated as % of control value (untreated cells considered 100%) and analysed by Student's *t*-test (P* < 0.05, ***P* < 0.01, ****P* < 0.001 for EFV vs. vehicle and ##*P* < 0.01, ###*P* < 0.001 for Rot and TG vs. untreated cells).**

5. Analysis of LONP1 protein expression

The induction of ER stress and UPR in EFV-treated hepatic cells is dependent on mitochondria as several markers of this stress response were found to be diminished in Hep3B cells lacking functional mitochondria (Apostolova N. *et al*., 2013). In order to further link the two effects of EFV (mitochondria and ER), we wanted to analyse the expression of LONP1, whose activation is thought to be an adaptive mechanism in both oxidative and ER stress, in WT and rho^{o} Hep3B cells. As shown in Fig.IV.13A, 24 h-treatment with EFV led to a modest but consistent and concentration-dependent increase in LONP1 protein expression. TG and Rot also increased LONP1 expression but to a much lesser extent than EFV. The basal expression of LONP1 in rho^{o} cells was slightly higher than in rho^{+} cells. Importantly, in cells lacking functional mitochondria the level of LONP1 was not enhanced by any of the stressors (EFV, TG or Rot). In addition, the EFV-induced concentration-dependent increase in LONP1 protein levels detected in wild-type Hep3B cells was confirmed in HepaRG cells (Fig.IV.13B).

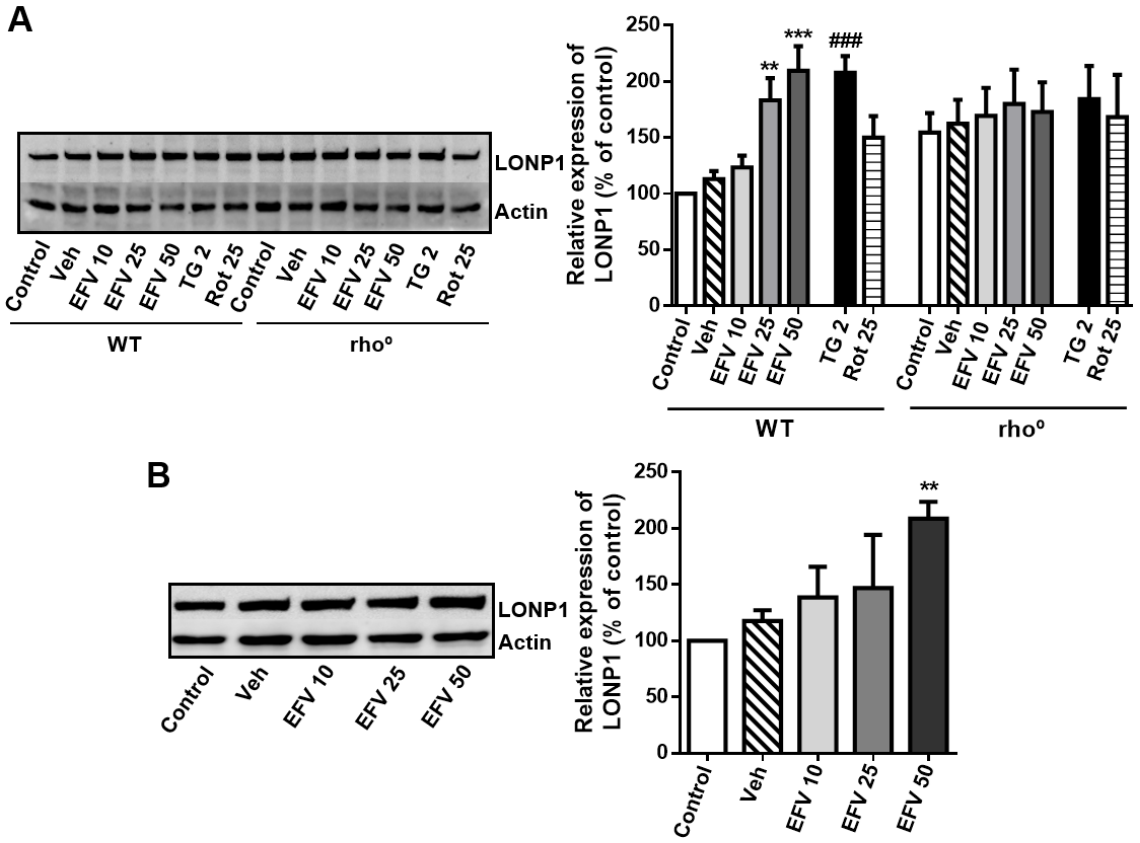

Figure IV.13. Western blot analysis of LONP1 expression in total cell extracts. Representative WB image and histogram expressing quantification of protein expression in (A) Hep3B rho^{+} and rho^{o} cells, treated for 24 h with increasing concentrations of EFV, vehicle, Rot 25 µM or TG 2 µM, or (B) HepaRG cells treated for 24 h with increasing concentrations of EFV or vehicle. Results are expressed as relative protein expression in relation to WT untreated cells (Hep3B), or untreated cells (HepaRG), which were considered 100%. Data represent mean ± SEM, n = 4-8, and were analysed by Student's *t*-test ($P < 0.01$, ***$P < 0.001$ for EFV vs. vehicle and $^{\#\#\#}P < 0.001$ for Rot and TG vs. untreated cells).**

SECTION 2: ANALYSIS OF MITOCHONDRIAL DYNAMICS

After studying the involvement of mitochondria in the development of EFV-induced toxicity in Hep3B cells (24h-treatment), we also analysed the mitochondrial dynamics in this model of dual mitochondrial/ER stress and compared it to TG, Rot and CCCP.

1. Gene and protein expression of main regulators of mitochondrial dynamics

Firstly, we analysed the gene and protein expression of several markers of mitochondrial fusion (Mfn1, Mfn2 and OPA1) and fission (Drp1 and Fis1) in cells treated with EFV, TG, Rot or CCCP for 24 h. As shown in Fig.IV.14A, immunoblot analysis using whole-cell extracts revealed no changes in the level of total Drp1 under any of the conditions assayed, whereas the effect in the case of p-Drp1 (Ser^{616}) was differential. Moderate mitochondrial/ER stress, such as that triggered by EFV 10 and 25 µM, incremented p-Drp1 levels, an increase that was not observed with severe stress (EFV 50 µM). In sharp contrast, a decrease in p-Drp1 expression was detected in cells exposed to TG, Rot or CCCP. Regarding OPA1, a concentration-dependent increase in the expression of its 80 kDa (s-OPA1) form was recorded with all stimuli (including EFV) manner. Unlike this effect, the expression of 100 kDa OPA1 (l-OPA1) showed no alterations with TG, Rot or the moderate concentrations of EFV (10 and 25 µM), while a marked down-regulation was observed with treatment with EFV 50 µM or CCCP. Finally, the expression of Mfn2 was severely diminished with Rot and CCCP treatment, while no significant changes were recorded with either TG or EFV. Importantly, quantitative RT-PCR analysis showed that ER stress (TG treatment) is related to a major increase in the expression of several genes employed as markers of mitochondrial dynamics - *MFN1, MFN2, OPA1, FIS1* and *DRP1* (Fig.IV.14B). With the exception of DRP1, the expression of these genes was also enhanced with EFV in a concentration-dependent manner, whereas the classical mitochondrial stressors Rot and CCCP not only failed to trigger upregulation (*MFN2*, *OPA1*) but actually provoked the contrary effect (*MFN1*, *FIS1* and *DRP1*). Considered together, these data provide

evidence of a differential expression of mitochondrial fusion and fission markers under conditions of ER stress and/or different types of mitochondrial dysfunction.

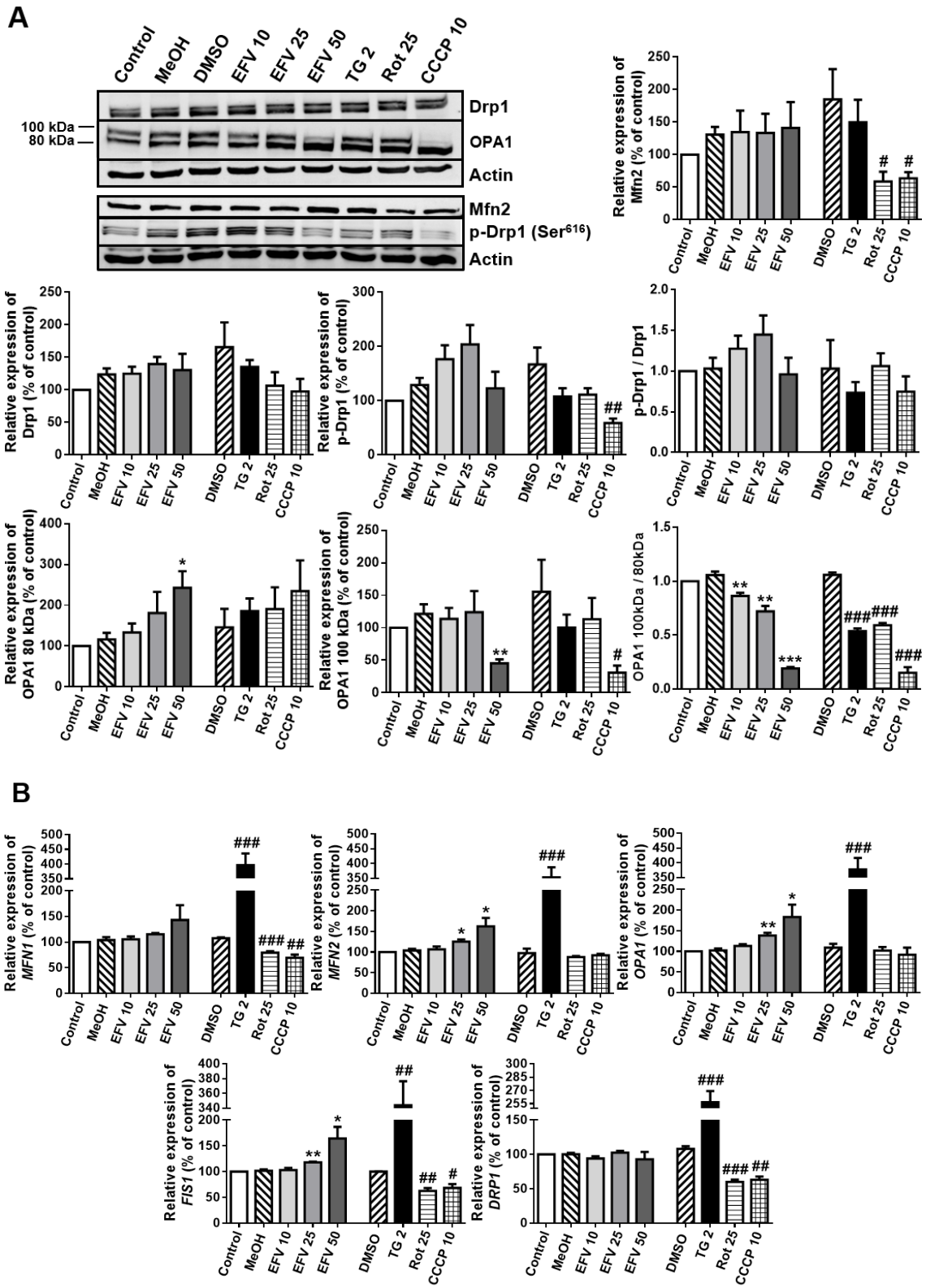

Figure IV.14. Expression of main molecular mediators of mitochondrial dynamics in Hep3B cells. These were treated for 24 h with increasing concentrations of EFV, vehicles (MeOH or DMSO), TG 2 µM, Rot 25 µM or CCCP 10 µM. (A) Immunoblot analysis showing representative WB image and histograms

expressing quantification of the main regulators of mitochondrial fusion and fission. (B) Gene expression analysed by quantitative RT-PCR. mRNA content was normalized with the expression of the housekeeping gene *ACTB* (β-actin). Data represent mean ± SEM, n = 4-8, and were calculated as % of control value (untreated cells considered 100%) and analysed by Student's *t*-test (P* < 0.05, ***P* < 0.01, ****P* < 0.001 for EFV vs. MeOH and $^{\#}P$ < 0.05, $^{\#\#}P$ < 0.01, $^{\#\#\#}P$ < 0.001 for TG, Rot or CCCP vs. DMSO).**

2. Location of proteins involved in mitochondrial fusion and fission

Several proteins involved in mitochondrial dynamics have been related to mitochondria-associated ER membranes (MAMs), including p-Drp1 and Mfn2. In this regard, we determined their specific location by studying their presence in mitochondria-enriched and cytosolic protein extracts.

2.1. Purity analysis of mitochondria-enriched and cytosolic protein extracts

Firstly, we confirmed the purity of the extracts obtained by assessment of several mitochondrial (TOM20 (translocase of OMM 20), CIV-II and Porin) and cytosolic (LDH (lactate dehydrogenase), Tubulin and β-actin) proteins under basal conditions and after 24 h-treatments (Fig.IV.15).

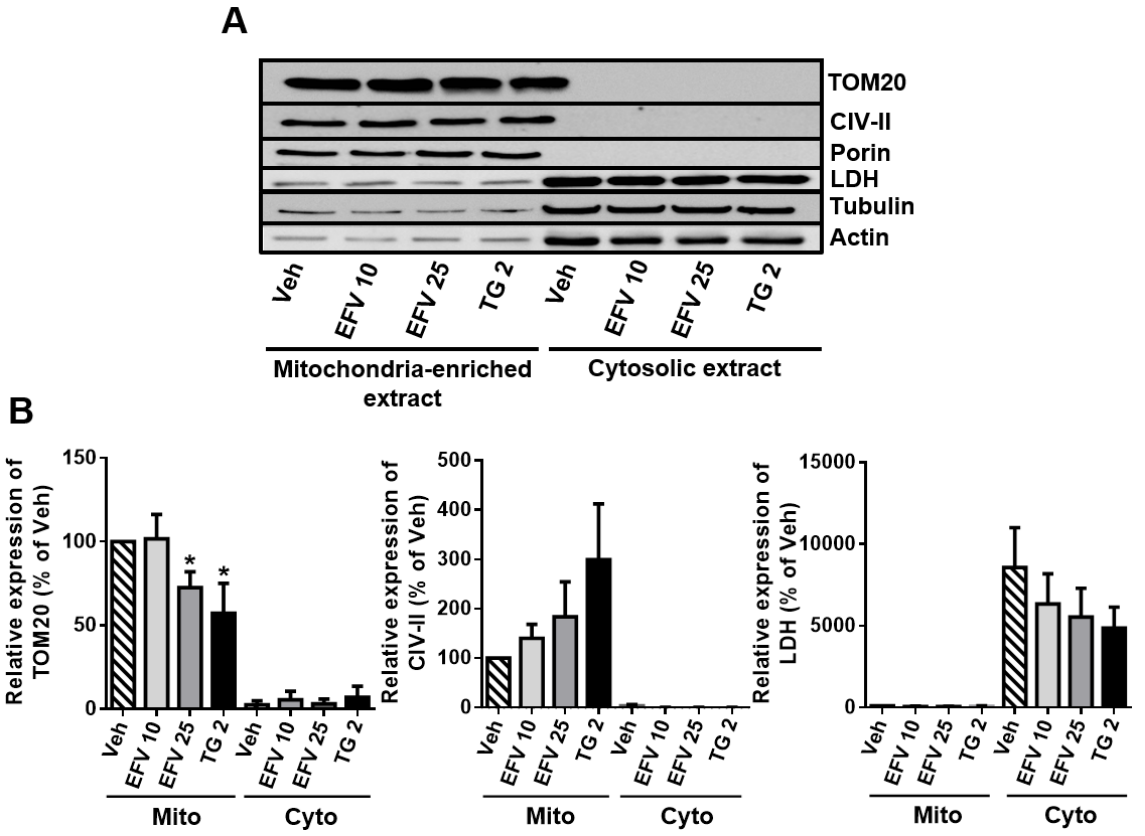

Figure IV.15. Analysis of the purity of mitochondria-enriched and cytosolic protein extracts. (A) Representative WB image and (B) histograms expressing quantification of several mitochondrial (TOM20, CIV-II and Porin) and cytosolic (LDH, Tubulin and β-actin) proteins after 24 h of treatment. Data represent mean ± SEM, n = 3, and were calculated as % of vehicle in mitochondria-enriched extracts considered 100% and analysed by Student's *t*-test (P* < 0.05 vs. vehicle).**

2.2. Protein analysis of p-Drp1 and Mfn2 in mitochondria-enriched and cytosolic extracts

We then analysed the abundance of specific proteins related to mitochondrial dynamics. Intriguingly, cells under EFV treatment tend to exhibit a slightly increased expression of p-Drp1 and Mfn2 in the cytosolic fraction, while a clear decrease is seen in cells treated with classical mitochondrial (Rot and CCCP) or ER stressors (TG) (Fig.IV.16).

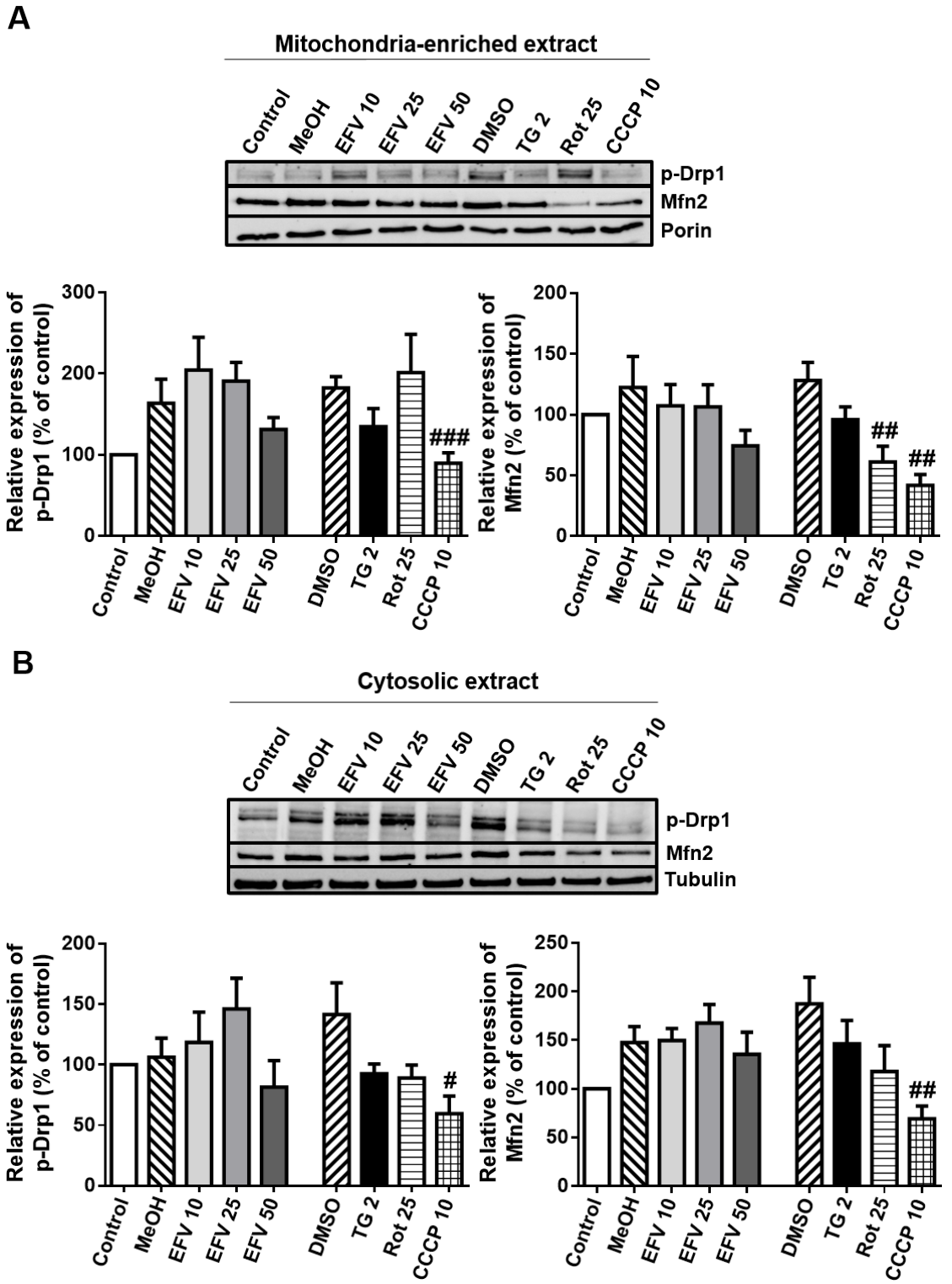

Figure IV.16. Study of p-Drp1 and Mfn2 protein expression in Hep3B cells. WB analysis in (A) mitochondria-enriched and (B) cytosolic extracts in cells treated for 24 h with increasing concentrations of EFV, vehicles (MeOH or DMSO), TG 2 µM, Rot 25 µM or CCCP 10 µM. A representative image and histograms of the data quantification are shown. Data represent mean ± SEM, n = 6, and were calculated as % of control (untreated cells considered 100%) and analysed by Student's *t*-test ($^{\#}P < 0.05$, $^{\#\#}P < 0.01$, $^{\#\#\#}P < 0.001$ for TG, Rot or CCCP vs. DMSO).

We considered that a possible explanation for the observed response was that EFV triggered *de novo* synthesis of these proteins and the time frame of 24 h may not have been ample enough to have the protein inside mitochondria. However, this possibility was ruled out with the analysis of the expression of p-Drp1 after prolonged treatment (48 h), which revealed that a differential response continued to be present as can be seen in Fig.IV.17. The level of cell stress was crucial for this response; the highest concentration of EFV, which triggered severe mitochondrial damage, failed to produce the same effects as EFV 10 and 25 µM and exerted similar actions to those of the rest of the stimuli.

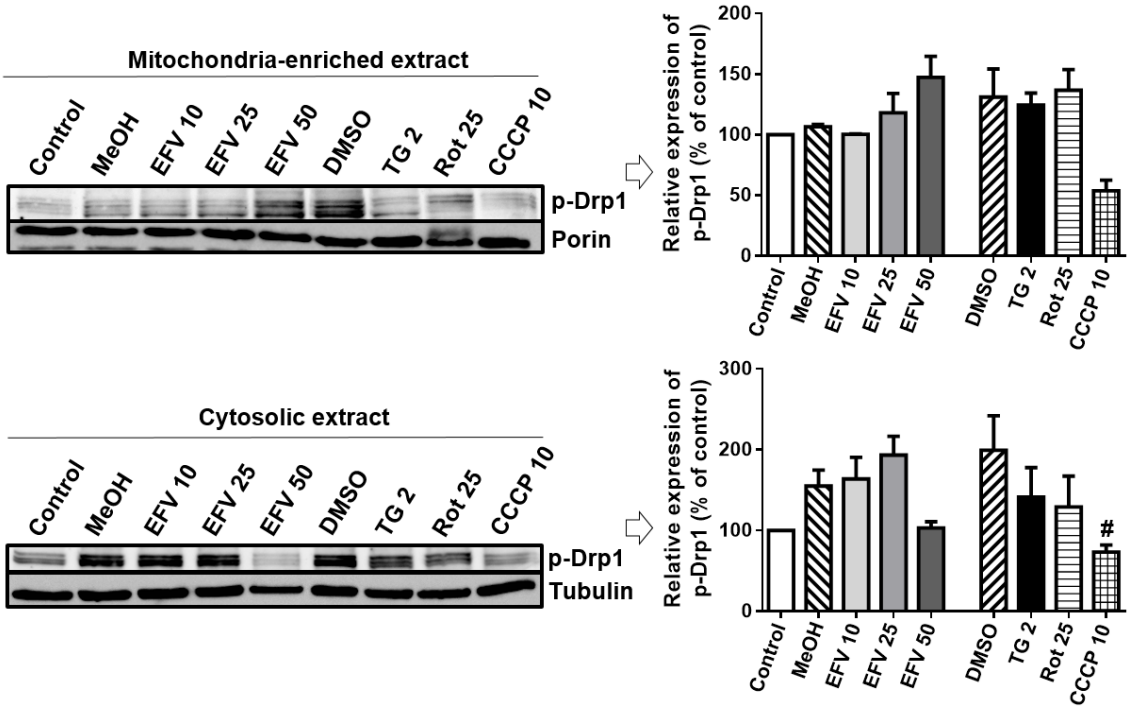

Figure IV.17. Analysis of p-Drp1 protein expression after 48 h of treatment. Hep3B cells were treated with increasing concentrations of EFV, vehicles (MeOH or DMSO), TG 2 µM, Rot 25 µM or CCCP 10 µM. Representative WB images and histograms showing quantification of p-Drp1 in mitochondria-enriched and cytosolic protein extracts. Data represent mean ± SEM, n = 4, and were calculated as % of control (untreated cells considered 100%) and analysed by Student's *t*-test ($^{\#}P < 0.05$ for TG, Rot or CCCP vs. DMSO).

2.3. Analysis of the translocation of p-Drp1 to mitochondria

The differential effect exerted by EFV in comparison to the rest of the stimuli was also confirmed by confocal microscopy experiments; there was an increase in the colocalization of p-Drp1 with the mitochondrial protein TOM20 in 10 or 25 μM EFV-treated cells, which was absent with the rest of the treatments (Fig.IV.18).

This experiment confirmed our previous findings of altered mitochondrial morphology. Using the expression of the OMM protein TOM20 as a marker, we detected enhanced presence of “fragmented” mitochondria (small rod-like or spherical mitochondria) in all treatments (Fig.IV.18A), an effect indicative of increased fission relative to fusion.

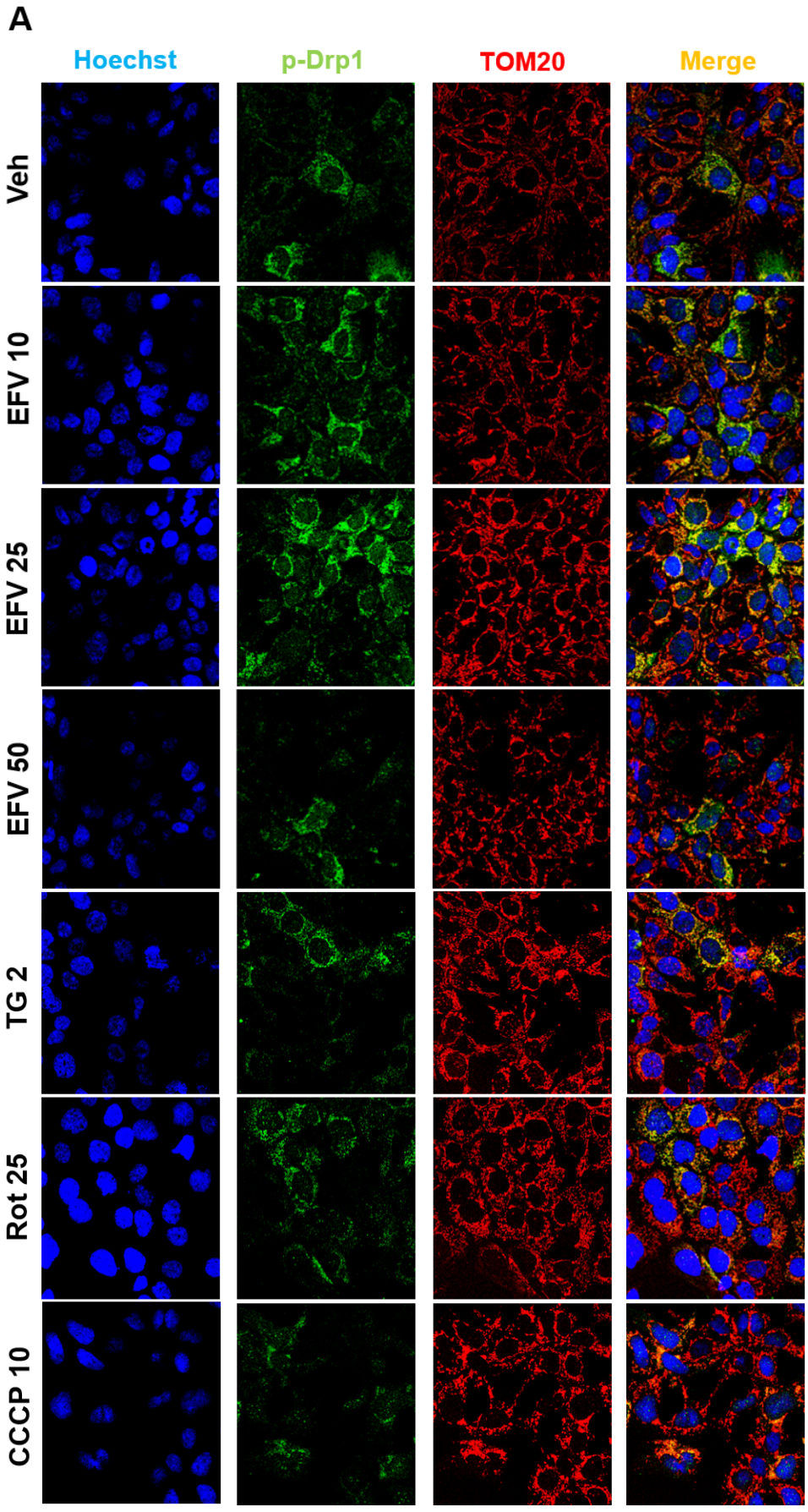
A
Hoechst
p-Drp1
TOM20
Merge
Veh
EFV 10
EFV 25
EFV 50
TG 2
Rot 25
CCCP 10

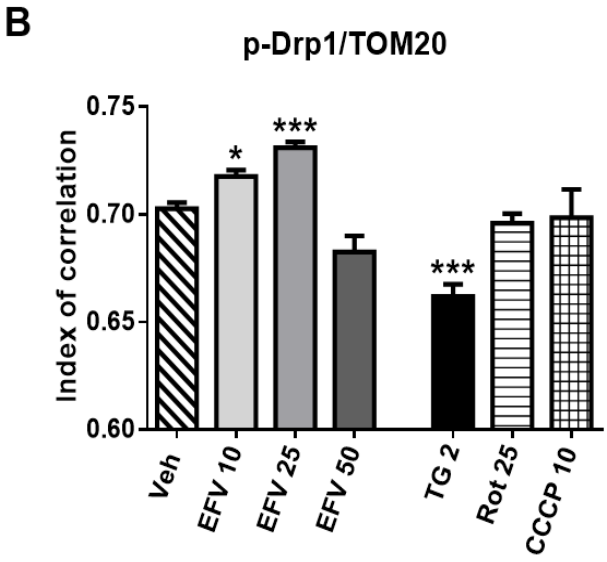

Figure IV.18. Translocation of p-Drp1 to mitochondria in Hep3B cells. (A) Representative confocal microscopy images (63x) and (B) histogram showing the index of correlation between p-Drp1 and mitochondria. Cells were treated for 24 h with increasing concentrations of EFV, vehicle, TG 2 µM, Rot 25 µM or CCCP 10 µM, and labelled with Hoechst 33342 (blue, nuclei), anti-p-Drp1 Ser616 (green) and anti-TOM20 (red, mitochondria). Data represent mean ± SEM, n = 3, and were analysed by Student's *t*-test (P* < 0.05, ****P* < 0.001 vs. vehicle).**

SECTION 3: ANALYSIS OF MITOCHONDRIAL/ER CONTACT

1. Study of mitochondria-associated ER membranes (MAMs)

Mitochondria-associated membranes (MAMs) are specific domains of the ER that enable its direct interaction with mitochondria. As stated previously, several proteins involved in mitochondrial dynamics have been related to MAMs and we have observed that markers of mitochondrial dynamics (Drp1, OPA1 and Mfn2) are expressed differentially with the stimuli used, which points to specificity of the dual ER/mitochondrial stress in this model.

1.1. Analysis of contacts between specific MAMs protein partners: PTPIP51-VAP B/C and Porin-Grp75

In order to analyse the contact between specific MAMs protein partners, we performed coimmunoprecipitation experiments in this model of dual mitochondrial/ER stress and compared it to TG, Rot and CCCP. We assessed two protein pairs: i) PTPIP51 and VAP B/C; and ii) Porin and Grp75. In both cases, the contact was enhanced in EFV-treated cells, while no increase or a significant decrease were observed with the rest of the treatments (Fig.IV.19).

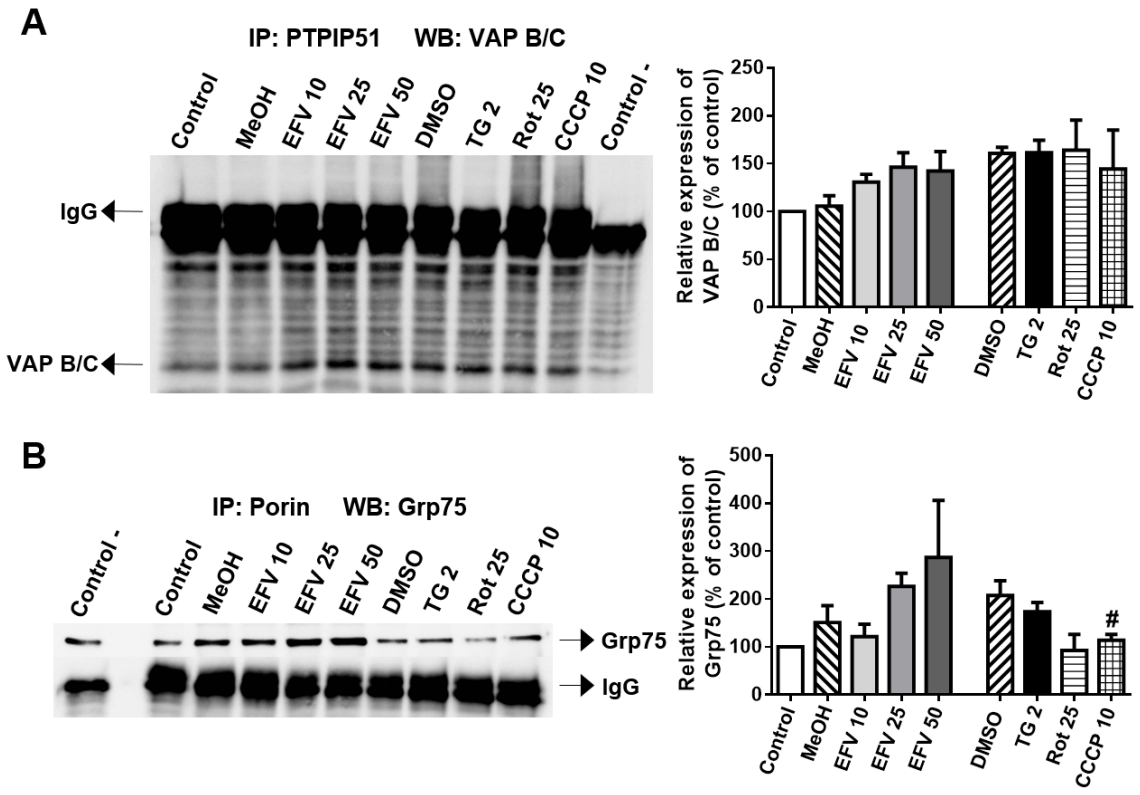

Figure IV.19. Study of Mitochondria-associated ER membranes (MAMs). Hep3B cells were treated for 24 h with increasing concentrations of EFV, vehicles (MeOH or DMSO), TG 2 µM, Rot 25 µM or CCCP 10 µM. (A, B) Analysis of contact between specific MAMs protein partners by coimmunoprecipitation using protein A sepharose beads. Representative WB images and histograms expressing quantification of (A) VAP B/C after immunoprecipitation of PTPIP51 and (B) Grp75 after immunoprecipitation of Porin. A negative control (without primary antibody) was used as control of the immunoprecipitation. Data represent mean ± SEM, n = 3-4, and were calculated as % of control (untreated cells considered 100%) and analysed by Student's *t*-test ($^{\#}P < 0.05$ for CCCP vs. DMSO).

1.2. Analysis of protein expression of several MAMs participants

In order to assess the general expression of several MAMs proteins (PTPIP51, VAP B/C and SIG-1R), we used whole cell extracts of cells treated for 24 h with EFV, TG, Rot or CCCP. Interestingly, the mitochondrial protein PTPIP51 displayed a major enhancement in EFV-exposed cells (Fig.IV.20A), an effect that was not evident with the rest of the stressors. In the case of VAP B/C protein expression, the effect was much less pronounced with EFV treatment and lacked concentration-dependence while TG also induced a slight increment (Fig.IV.20B). As can be seen in Fig.IV.20C, only TG increased the expression of SIG-1R. In summary, these data point to an enhancement of MAMs in cells exposed to combined ER stress/mitochondrial dysfunction.

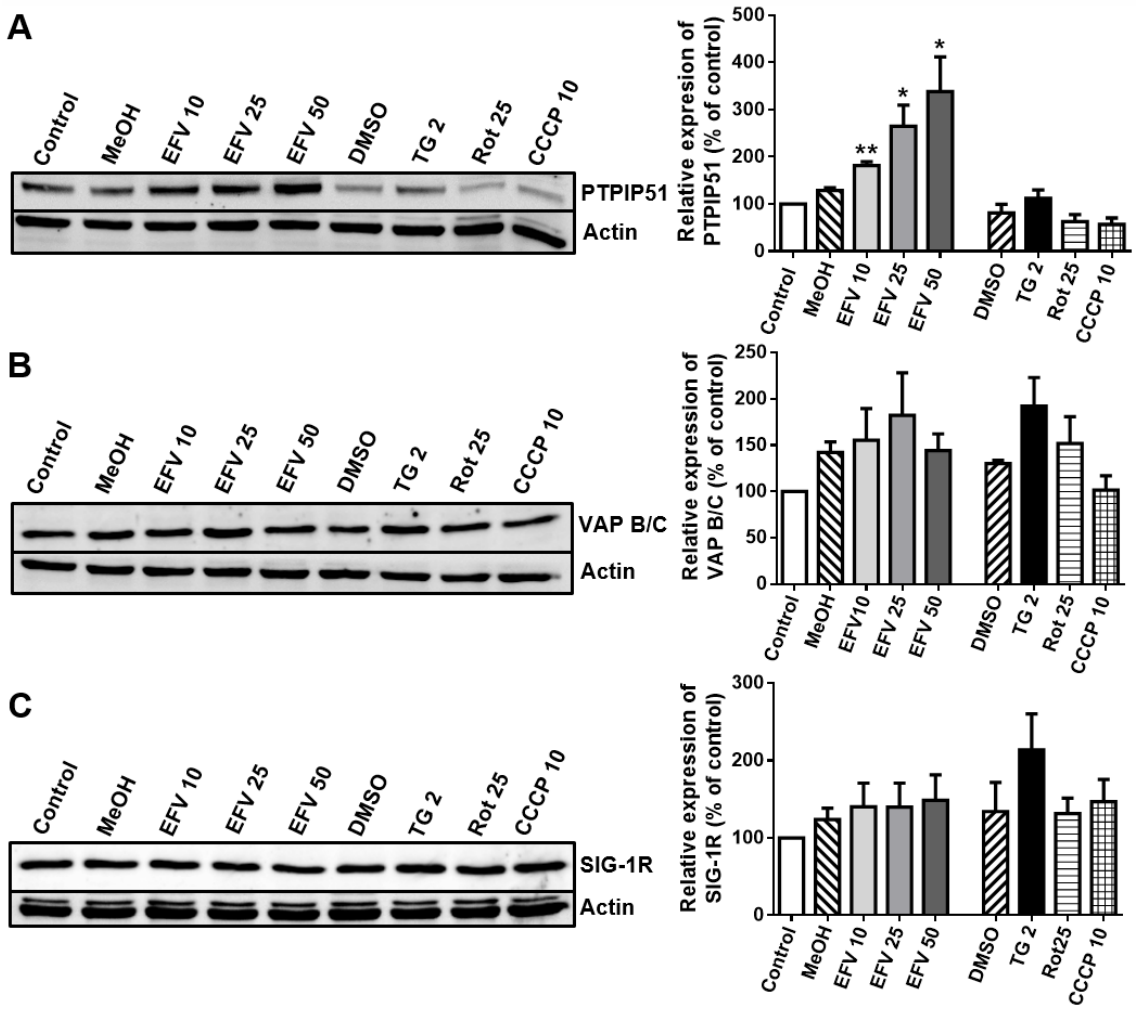

Figure IV.20. Analysis of protein expression of several MAMs components in Hep3B cells. WB analysis of (A) PTPIP51, (B) VAP B/C and (C) SIG-1R expression in whole cell extracts after treatment for 24 h with increasing concentrations of EFV, vehicles (MeOH or DMSO), TG 2 µM, Rot 25 µM or CCCP 10 µM. A representative image and histograms of the data quantification are shown. Data represent mean ± SEM, n = 3-4, and were calculated as % of control (untreated cells considered 100%) and analysed by Student's *t*-test (P* < 0.05, ***P* < 0.01, for EFV vs. MeOH).**

Next, we analysed the protein expression and specific location of another MAMs participant, Grp75 (mitochondrial HSP70), by studying its presence in mitochondria-enriched and cytosolic protein extracts of cells treated for 24 h with EFV, TG, Rot or CCCP. In this case, EFV treatment showed a similar pattern as that observed for p-Drp1 and Mfn2, with increased cytosolic content and a tendency towards a drop in mitochondrial content. In contrast, upon treatment with the other three stimuli, levels of Grp75 inside mitochondria did not diminish (Fig.IV.21).

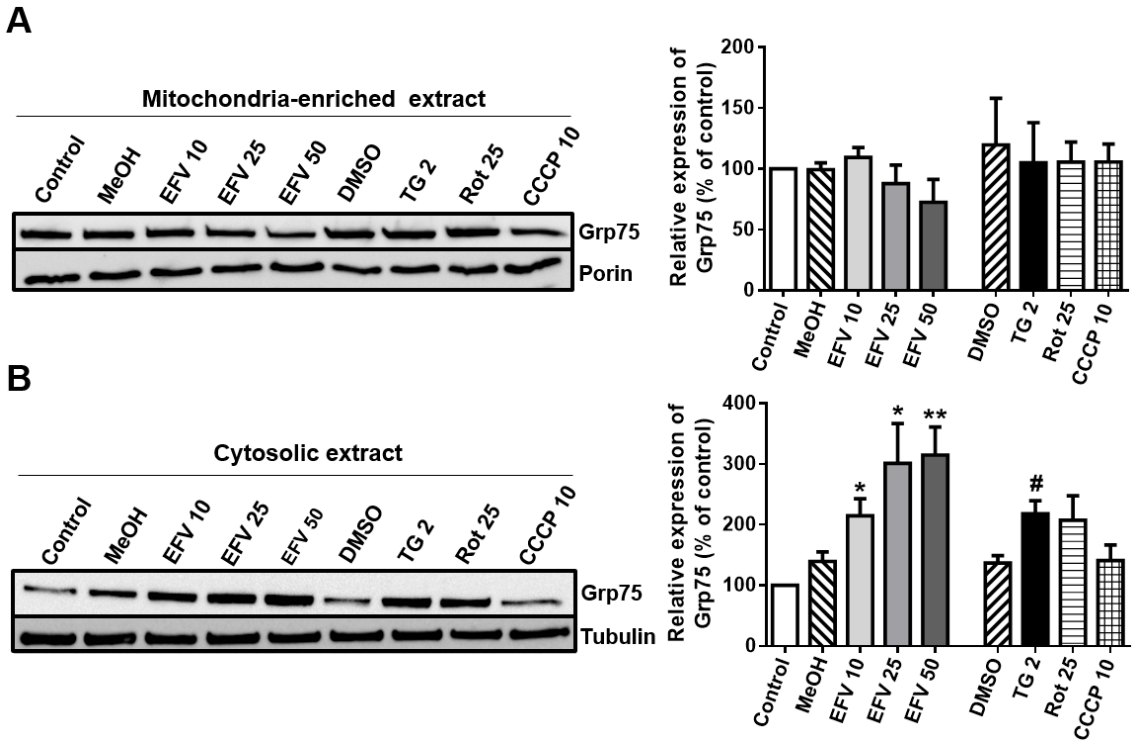

Figure IV.21. Study of protein expression and specific location of Grp75 in Hep3B cells. Representative WB images and histograms expressing quantification of Grp75 in (A) mitochondria-enriched and (B) cytosolic protein extracts. Cells were treated for 24 h with increasing concentrations of EFV, vehicles (MeOH or DMSO), TG 2 µM, Rot 25 µM or CCCP 10 µM. Data represent mean ± SEM, n = 4, and were calculated as % of control (untreated cells considered 100%) and analysed by Student's *t*-test (P* < 0.05, ***P* < 0.01 for EFV vs. MeOH and $^{\#}P$ < 0.05 for TG vs. DMSO).**

SECTION 4: ANALYSIS OF MITOCHONDRIAL LON PROTEASE

Knowing that Grp75 is involved in mitochondrial proteostasis, we were interested to know whether a similar effect would be observed with another mitochondrial protein in charge of protein maintenance in this organelle, LONP1.

1. Analysis of LONP1 in mitochondria-enriched and cytosolic extracts

Firstly, we analysed LONP1 expression in cytosolic and mitochondria-enriched fractions of Hep3B cells treated with EFV, TG, Rot and CCCP for 24 h. This study revealed a very similar result to that exerted by Grp75: a decrease in the mitochondrial fraction and an increase in the extramitochondrial fraction (Fig.IV.22). Once again, this was not the case with the rest of the stimuli; while TG and Rot treatment enhanced lightly LONP1 expression in both fractions, CCCP produced a drop or no change in mitochondria-enriched and cytosolic extract, respectively.

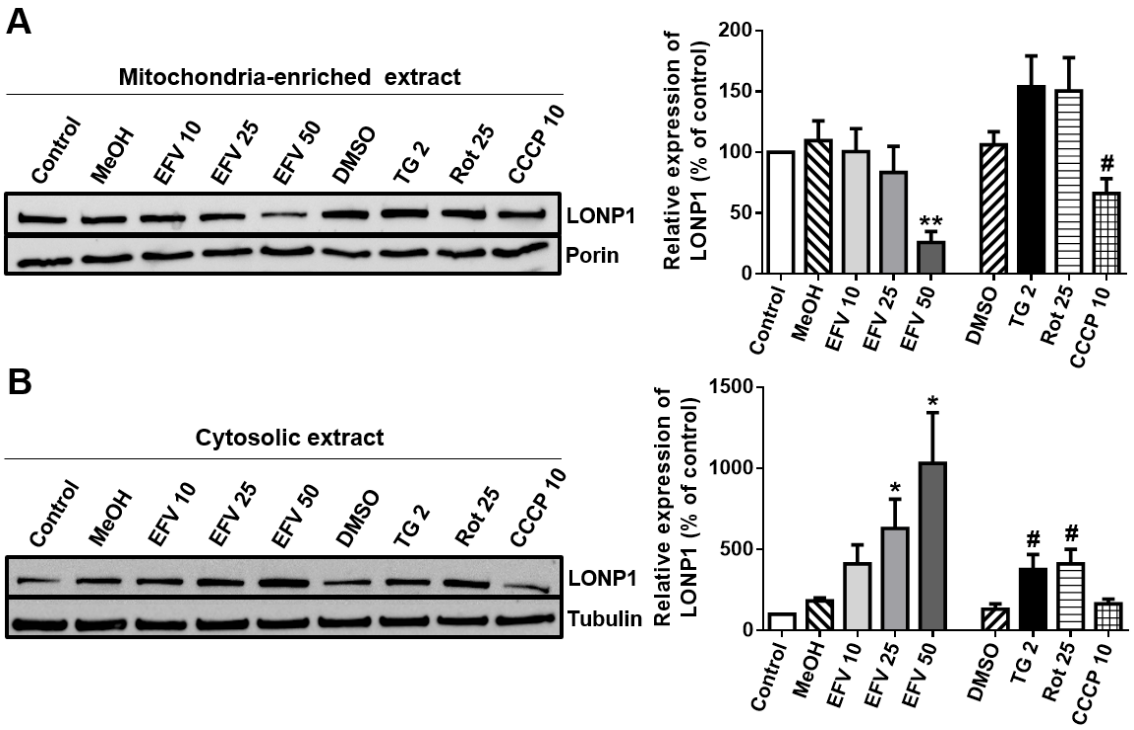

Figure IV.22. Analysis of LONP1 presence in mitochondria and cytosol. Representative WB images and histograms expressing quantification of LONP1 protein expression in (A) mitochondria-enriched and (B) cytosolic protein extracts. Hep3B cells were treated for 24 h with increasing concentrations of EFV, vehicles (MeOH or DMSO), TG 2 µM, Rot 25 µM or CCCP 10 µM. Data represent mean ± SEM, n = 4, and were calculated as % of control (untreated cells considered 100%) and analysed by Student's *t*-test (P* < 0.05, ***P* < 0.01 for EFV vs. MeOH and #*P* < 0.05 for TG, Rot or CCCP vs. DMSO).**

2. Gene and protein expression of LONP1

2.1. Hep3B cells

As shown in Fig.IV.13, 24 h of treatment with EFV led to a modest but consistent and concentration-dependent increase in LONP1 expression in both wild-type Hep3B and HepaRG cells. We then compared this effect to that exerted by TG, Rot or CCCP and found a similar upregulation with these three stimuli (Fig.IV.23A). Moreover, we assessed the gene expression of *LONP1* and observed that all 4 stimuli produced an increment of *LONP1* mRNA, although to varying extents: while the increase in the case of Rot and CCCP was modest, that induced by TG was remarkable (Fig.IV.23B).

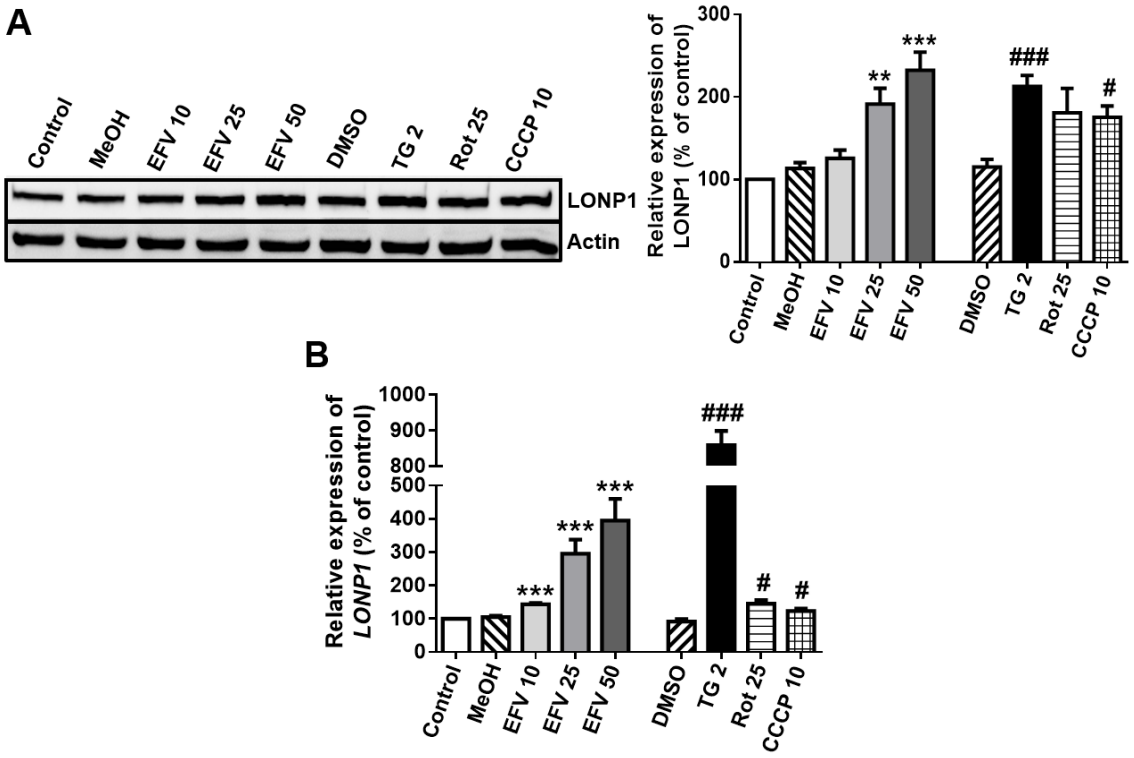

Figure IV.23. Analysis of protein and gene expression of LONP1 in Hep3B cells. Cells were treated for 24 h with increasing concentrations of EFV, vehicles (MeOH or DMSO), TG 2 µM, Rot 25 µM or CCCP 10 µM. (A) Representative WB image and histogram expressing quantification of LONP1 in whole cell protein extracts. (B) Quantitative RT-PCR analysis of *LONP1*. Data represent mean ± SEM, n = 4, and were calculated as % of control (untreated cells considered 100%) and analysed by Student's *t*-test (*P* < 0.01, ****P* < 0.001 for EFV vs. MeOH and $^{\#}P$ < 0.05, $^{\#\#\#}P$ < 0.001 for TG, Rot or CCCP vs. DMSO).**

Next, we wished to study the expression of a LONP1 substrate, Aco2 (MM protein which is preferentially degraded by LONP1 after oxidative modification). As can be seen in Fig.IV.24, no changes were observed with EFV, Rot and CCCP, while in the case of TG, an increase, albeit statistically non-significant, could be observed.

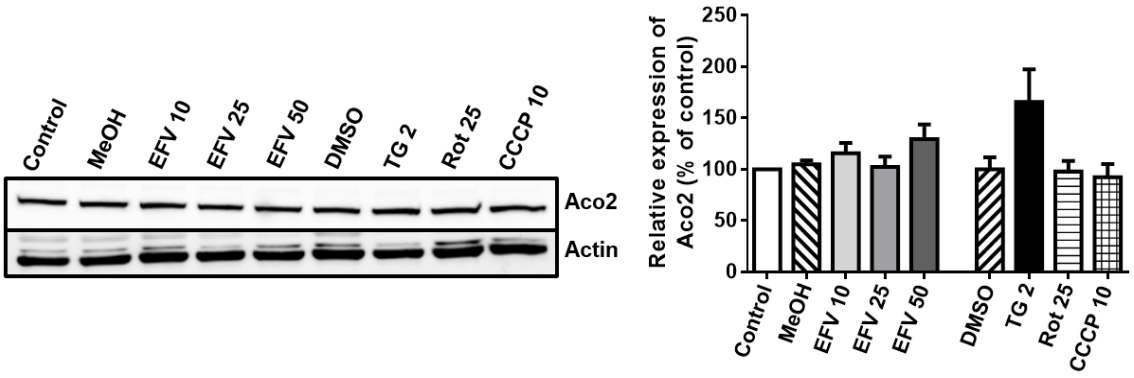

Figure IV.24. WB analysis of Aco2 expression in whole cell protein extracts. Hep3B cells were treated for 24 h with increasing concentrations of EFV, vehicles (MeOH or DMSO), TG 2 µM, Rot 25 µM or CCCP 10 µM. A representative image and histogram of the data quantification are shown. Data represent mean ± SEM, n = 5, and were calculated as % of control (untreated cells considered 100%) and analysed by Student's *t*-test.

2.2. U-251MG cells

Our group has reported that EFV also alters mitochondrial function in cultured neurons and glial cells (Funes H.A. *et al*., 2014). To confirm that EFV affects cellular respiration as it does in Hep3B, we studied the O_2 consumption and mitochondrial $O_2^{\cdot -}$ production in the glial cell line U-251MG exposed to EFV 25 µM for 6 h. Given that EFV induces nitric oxide (NO) generation in U-251MG cells, we performed the same assessments in cells co-treated with EFV and an inhibitor of NO production (L-NAME 50 µM). We observed that EFV compromised O_2 consumption and induced mitochondrial $O_2^{\cdot -}$ production and that both effects were alleviated in cells where NO generation was pharmacologically inhibited (Fig.IV.25).

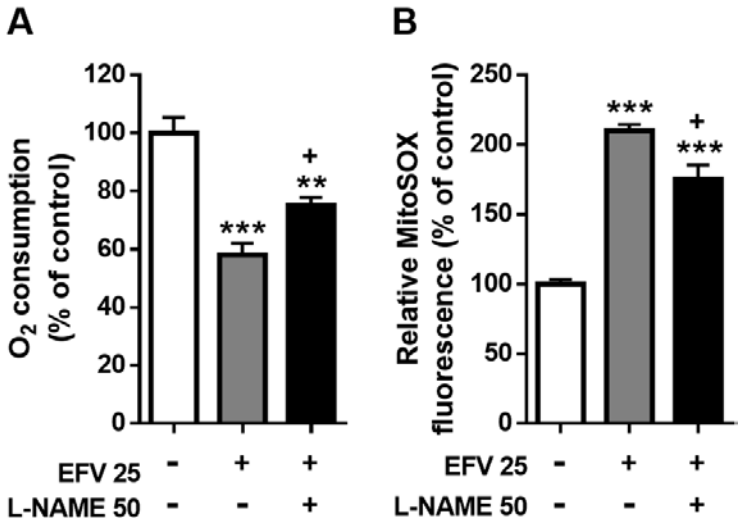

Figure IV.25. Analysis of mitochondrial function in U-251MG (glioblastoma) cells. Cells were exposed to EFV 25 µM or a combined treatment of EFV 25 µM + L-N^G-nitroarginine methyl ester (L-NAME) 50 µM for 6 h. (A) O_2 consumption in intact cells (Clark-type O_2 electrode). (B) Determination of $O_2^{\cdot-}$ production (MitoSOX fluorescence). Data represent mean ± SEM, n = 3-5, and were calculated as % of control (untreated cells considered 100%) and analysed by Student's *t*-test ($P < 0.01$, ***$P < 0.001$ vs. vehicle). $^{+}P < 0.05$ represent the significance of the data obtained with EFV 25 µM vs. EFV 25 µM + L-NAME.**

Next we studied the expression of LONP1 in U-251MG cells treated for 24 h with EFV, TG 2 µM, Rot 25 µM or CCCP 10 µM. This experiment revealed a similar result to that observed in Hep3B cells. EFV treatment concentration-dependently increased *LONP1* expression and enhanced presence on *LONP1* mRNA was also detected with the other three stimuli however, to a different extent - in the case of Rot and CCCP the increase was modest, but that induced by TG was remarkable (Fig.IV.26).

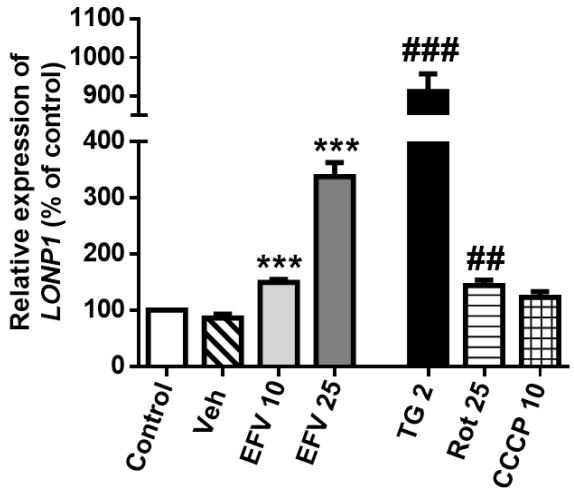

Figure IV.26. Quantitative RT-PCR analysis of *LONP1* in U-251MG cells. U251MG cells were treated for 24 h with increasing concentrations of EFV, vehicle, TG 2 µM, Rot 25 µM or CCCP 10 µM. Data represent mean ± SEM, n = 4, and were calculated as % of control (untreated cells considered 100%) and analysed by Student's *t*-test (*$P < 0.001$ for EFV vs. vehicle and $^{\#\#}P < 0.01$, $^{\#\#\#}P < 0.001$ for TG, Rot or CCCP vs. untreated cells).**

3. Regulation of LONP1 upregulation

Our group has already reported that EFV and TG increase CHOP expression in Hep3B cells treated for 24 h (Apostolova N. *et al*., 2013). In order to assess the regulation of LONP1 upregulation by CHOP, we transiently silenced this transcription factor and examined the protein level of LONP1 in whole cell extracts by WB. We confirmed the expected increase in CHOP with all three stimuli (in accordance with the previously published work) and found out that siCHOP cells exhibited similar LONP1 levels as siControl, which would suggest that this transcription factor is not involved in the regulation of LONP1 expression (Fig.IV.27).

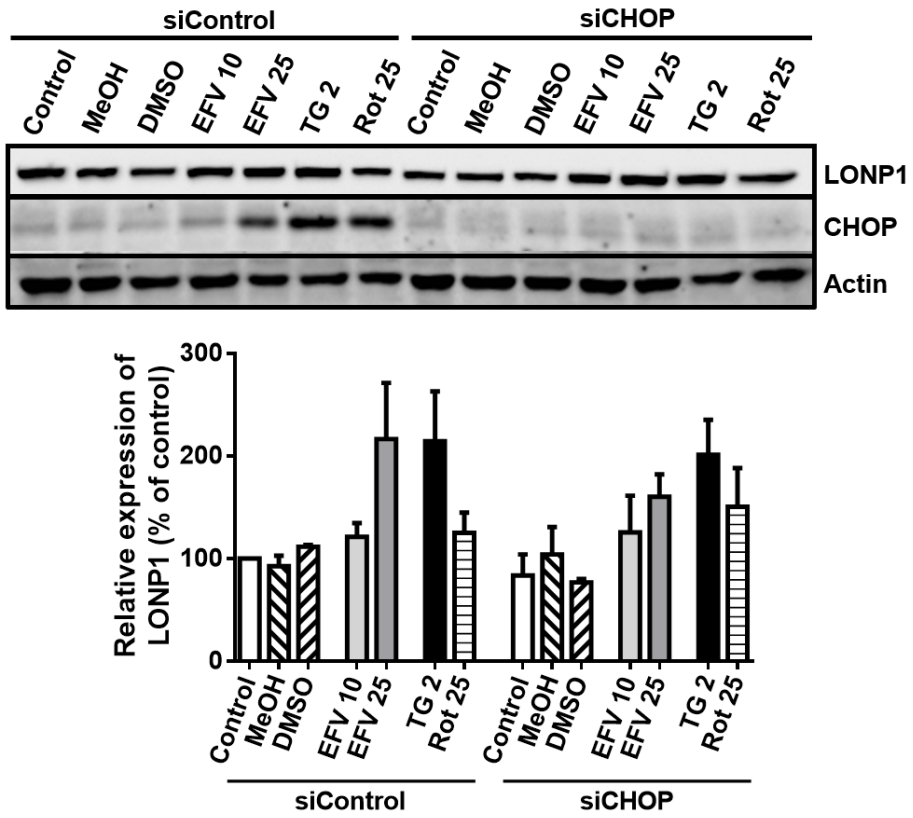

Figure IV.27. Analysis of LONP1 expression in Hep3B cells where *CHOP/DDIT3* has been silenced by siRNA. Representative WB image and histogram expressing quantification of LONP1 expression in cells transfected with siRNA Control or siCHOP and treated for 24 h with EFV, vehicle (MeOH or DMSO), TG 2 μM or Rot 25 μM. Data represent mean ± SEM, n = 5, and were calculated as % of control of siControl cells (considered 100%) and analysed by Student's *t*-test.

Another transcription factor that we speculated could be involved in upregulation of *LONP1* expression in our model was NF-κB. In order to test this possibility, we performed ChIP assay, a technique used for probing protein-DNA interactions within the natural chromatin context of the cell. These experiments revealed that EFV treatment concentration-dependently increased the contact between NF-κB and the promoter of *LONP1* (Fig.IV.28).

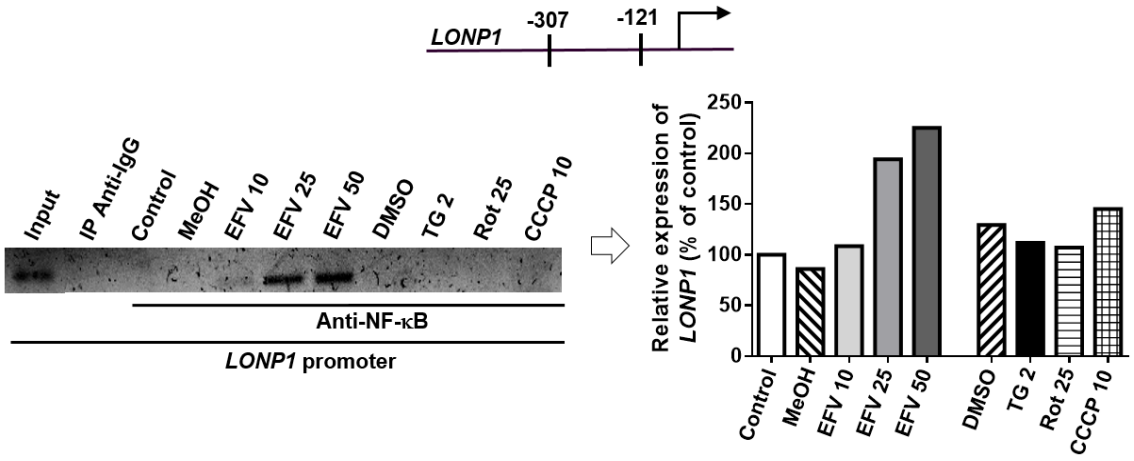

Figure IV.28. Analysis of the recruitment of NF-κB to the promoter of *LONP1*. Representative image of semiquantitative PCR after chromatin immunoprecipitation (ChIP) with anti-NF-κB; a non-related antibody anti-IgG and a sample of the input chromatin were used as controls. Hep3B cells were treated for 24 h with EFV, vehicle (MeOH or DMSO), TG 2 µM, Rot 25 µM or CCCP 10 µM. Data were calculated as % of control (untreated cells considered 100%).

Knowing that EFV (similarly to TG) also induces a concentration-dependent increase in cytosolic Ca^{2+} concentration in hepatic cells (Apostolova N. *et al*., 2013), we aimed to assess the expression of LONP1 in cells pre-treated with the Ca^{2+} chelator BAPTA 10 µM. As can be observed in Fig.IV.29, after 24 h-treatment all 4 stimuli produced an increment of *LONP1* mRNA but this effect was significantly lower in cells treated with BAPTA, which suggests that Ca^{2+} is involved in the upregulation of *LONP1* expression induced by EFV, TG and Rot.

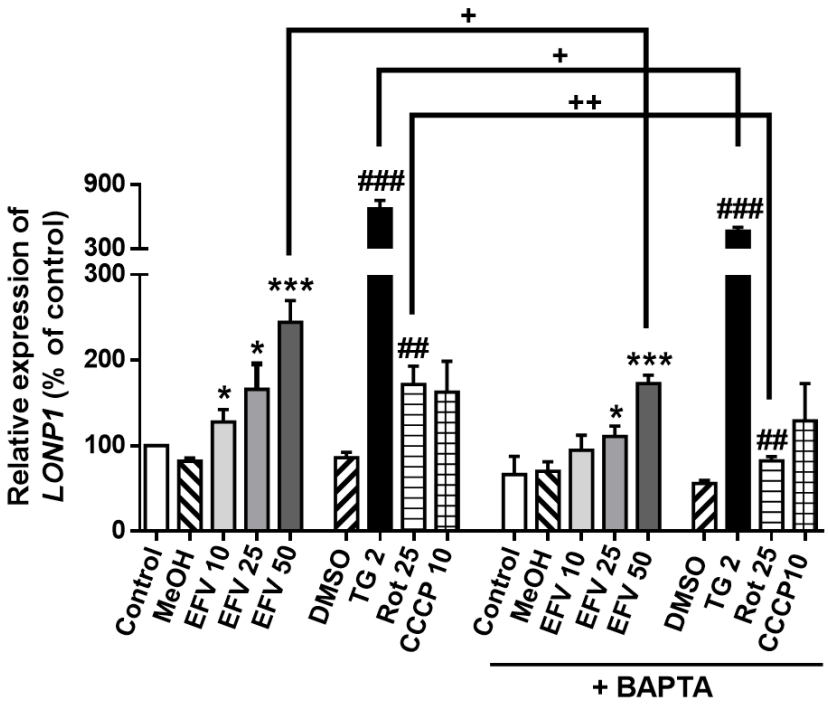

Figure IV.29. Quantitative RT-PCR analysis of *LONP1* in cells treated in the presence or absence of BAPTA. Hep3B cells were treated with BAPTA 10 µM for 1 h followed by treatment with increasing concentrations of EFV, vehicles (MeOH or DMSO), TG 2 µM, Rot 25 µM or CCCP 10 µM for 24 h. Data represent mean ± SEM, n = 3, and were calculated as % of control of cells without BAPTA (considered 100%) and analysed by Student's *t*-test (P* < 0.05, ***P* < 0.01 for EFV vs. MeOH and $^{\#\#}P$ < 0.01, $^{\#\#\#}P$ < 0.001 for TG vs. DMSO). ^{+}P < 0.05, ^{++}P < 0.01 represent the significance of the data comparing the corresponding treatment with vs. without BAPTA.**

4. Analysis of the expression of mitochondrial ClpX protease and several HSP90 chaperones

In order to assess the specificity of LONP1 upregulation, we analysed the expression of several other proteins involved in cellular proteostasis. ClpX, another ATP-dependent protease located in the MM, was assessed with WB in whole cell extracts of Hep3B cells treated for 24 h with all 4 stimuli. As can be observed in Fig.IV.30, neither of the treatments altered the expression of ClpX.

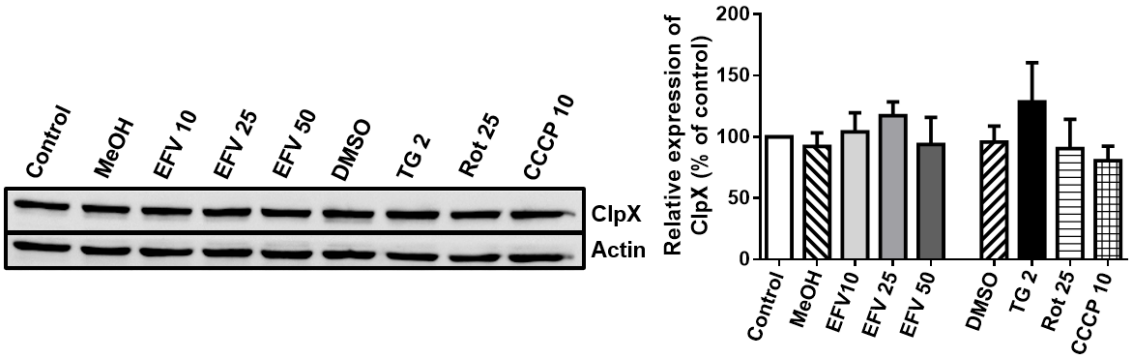

Figure IV.30. WB analysis of ClpX expression in total cell extracts. Hep3B cells were treated for 24 h with increasing concentrations of EFV, vehicles (MeOH or DMSO), TG 2 µM, Rot 25 µM or CCCP 10 µM. A representative image and histogram of data quantification are shown. Data represent mean ± SEM, n = 4, and were calculated as % of control (untreated cells considered 100%) and analysed by Student's *t*-test.

We also studied the gene expression of HSP90 chaperones (*HSP90AA1*, *HSP90AB1* and *HSP90B1*) which also have key role in protein quality control. After 24 h-treatment, EFV 25 µM induced a slightly increase in *HSP90AB1* expression while TG increased remarkably the expression of all *HSP90s* (Fig.IV.31).

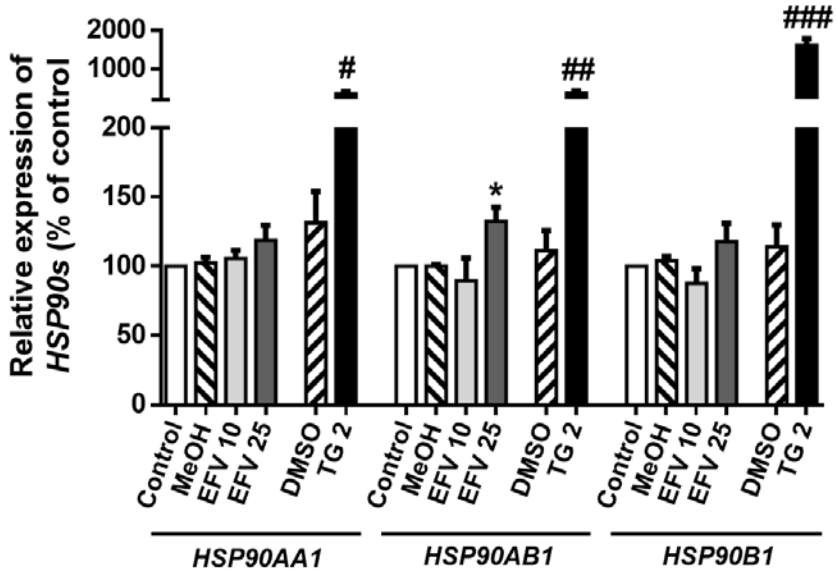

Figure IV.31. Gene expression of HSP90 chaperones analysed by quantitative RT-PCR. Hep3B cells were treated for 24 h with increasing concentrations of EFV, vehicles (MeOH or DMSO) and TG 2 µM. Data represent mean ± SEM, n = 4. They were calculated as mRNA content in relation to that of control (untreated cells considered 100%), after normalization with the expression of the housekeeping gene *ACTB* (β-actin), and analysed by Student's *t*-test (P* < 0.05 for EFV vs. MeOH and $^{\#}P < 0.05$, $^{\#\#}P < 0.01$, $^{\#\#\#}P < 0.001$ for TG vs. DMSO).**

Given this result, we wished to analyse the effect of EFV on several stress-related chaperones as part of PrimePCR assay in which we studied the expression of different genes involved in inflammation and cellular stress. Data obtained with Hep3B were below the limit of detection and therefore the results obtained in individual RT-PCRs could not be corroborated. However, this experiment was also performed in human hepatic stellate cells (HSCs) LX2 and U937-derived macrophages. As can be seen in Fig.IV.32, EFV 25 µM induced an increase in the expression of *HSP90AA1* and *HSP90AB1* in LX2 cells and, in the expression of *HSP90B1,* in the case of macrophages. The effect of EFV on these stress-related chaperones is more pronounced in LX2 cells and U937-derived macrophages than in Hep3B.

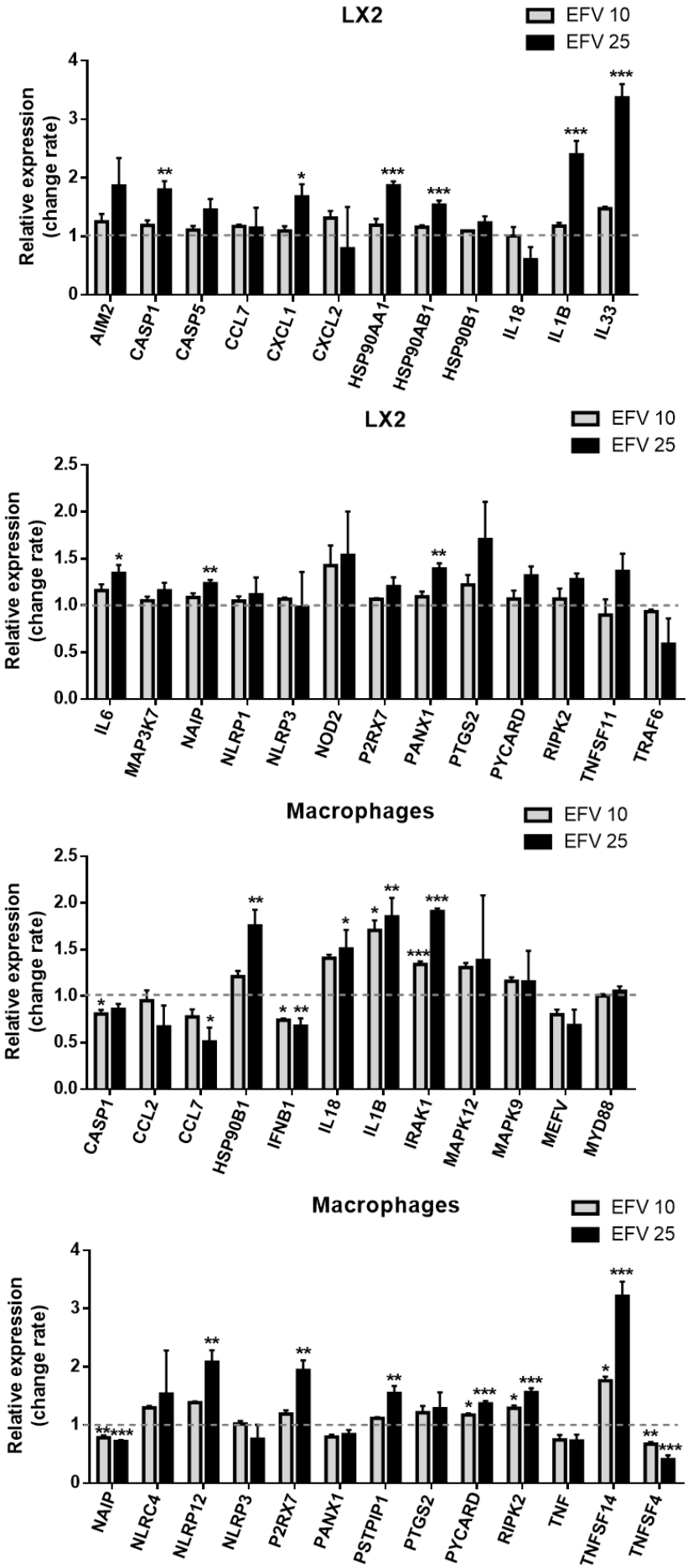
LX2
EFV 10
EFV 25
Relative expression (change rate)
AIM2
CASP1
CASP5
CCL7
CXCL1
CXCL2
HSP90AA1
HSP90AB1
HSP90B1
IL18
IL1B
IL33
LX2
EFV 10
EFV 25
Relative expression (change rate)
IL6
MAP3K7
NAIP
NLRP1
NLRP3
NOD2
P2RX7
PANX1
PTGS2
PYCARD
RIPK2
TNFSF11
TRAF6
Macrophages
EFV 10
EFV 25
Relative expression (change rate)
CASP1
CCL2
CCL7
HSP90B1
IFNB1
IL18
IL1B
IRAK1
MAPK12
MAPK9
MEFV
MYD88
Macrophages
EFV 10
EFV 25
Relative expression (change rate)
NAIP
NLRC4
NLRP12
NLRP3
P2RX7
PANX1
PSTPIP1
PTGS2
PYCARD
RIPK2
TNF
TNFSF14
TNFSF4

Figure IV.32. Relative expression of different genes involved in inflammation and cellular stress analysed by real time RT-PCR assays. LX2 cells and U937-derived macrophages were treated with vehicle, EFV 10 or 25 μM for 24 h. Data represent mean ± SEM, n = 3, and were calculated as relative-fold change with respect to vehicle, set to one, and analysed by one-way ANOVA multiple comparison test followed by a Newman-Keuls test (P* < 0.05, ***P* < 0.01, ****P* < 0.001 vs. vehicle).**

5. Role of LONP1 in the effects induced by EFV on Hep3B cells

As stated previously, our group has already reported that EFV disrupts mitochondrial function, activates the adaptive response of autophagy and induces ER stress/UPR in hepatic cells (Blas-García A. *et al*., 2010; Apostolova N. *et al*., 2011c; 2013). After observing that the expression of LONP1 increases with ER stress (TG), mitochondrial dysfunction (CCCP or Rot) or both (EFV), we aimed to study the role of this protein in the effects induced by EFV by means of transiently silencing *LONP1* by siRNA. For this, Hep3B cells were transfected with *LONP1* siRNA and then treated for 24 h with EFV, TG or Rot.

5.1. Autophagy and ER stress

We assessed the protein levels of CHOP, LC3 and p62 in whole cell extracts by WB. Firstly, we verified the efficacy of *LONP1* silencing in siLONP1 cells by analysing LONP1 protein expression. Also, we confirmed the expected increase of CHOP and LONP1 with all three stimuli, as well as LC3-II and p62 with EFV and TG in siControl cells (in accordance with our previously published work). We found that siLONP1 cells exhibited similar CHOP levels as siControl. However, the effect of all three stimuli on p62 expression was slightly lower in siLONP1 cells than siControl. Regarding LC3-II, no changes were observed in the effect of TG when we silenced *LONP1* but, surprisingly, the effect of EFV treatment on LC3-II expression was absent when *LONP1* was silenced (Fig.IV.33). This result suggests that LONP1 could be involved in autophagy regulation under dual ER/mitochondrial stress.

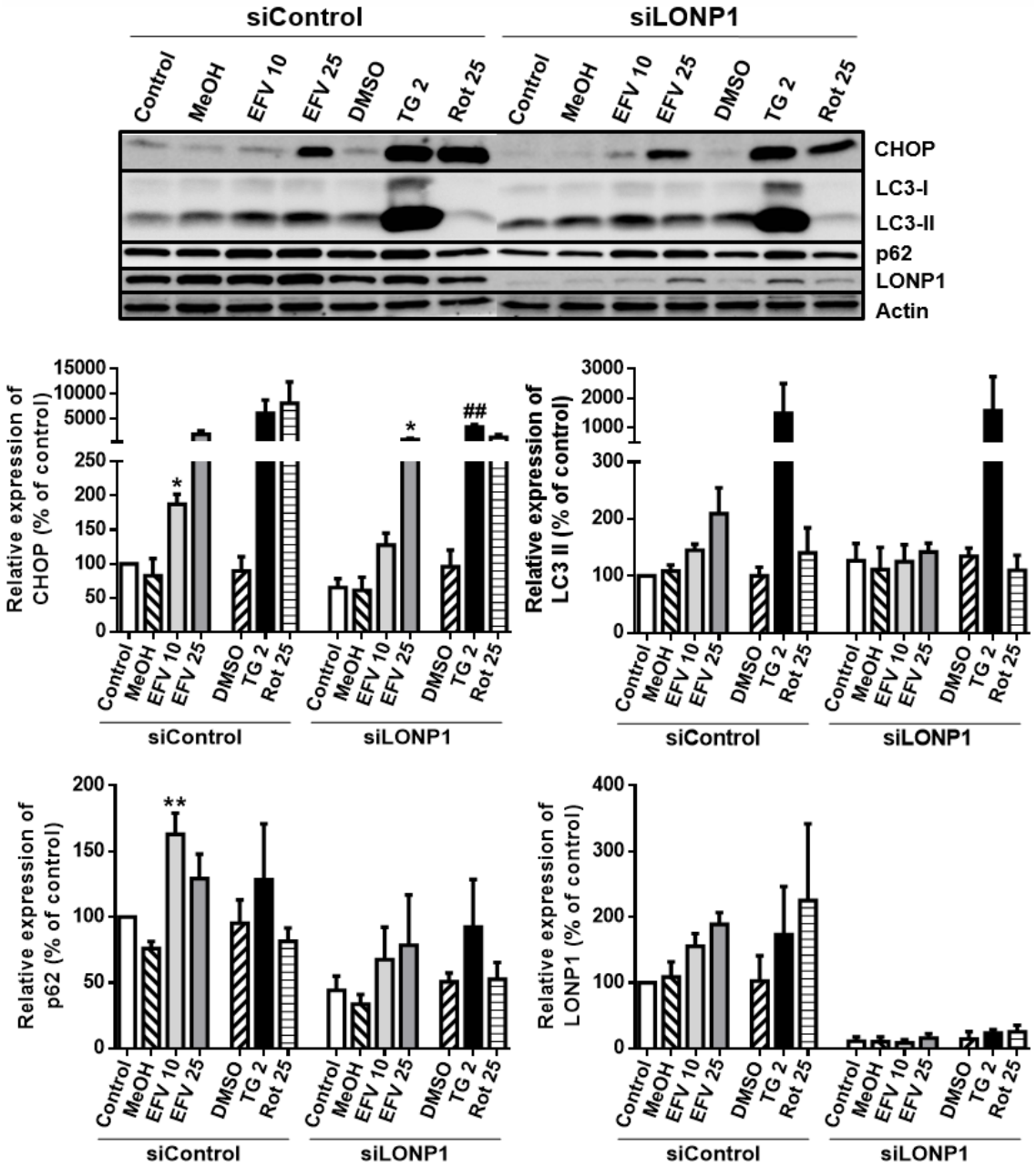

Figure IV.33. Role of LONP1 in the effects of EFV on hepatic cells. Representative WB images and histograms expressing quantification of the expression of CHOP, LC3, p62 and LONP1 in cells transfected with siRNA Control or siLONP1 and treated for 24 h with increasing concentrations of EFV, vehicles (MeOH or DMSO), TG 2 µM or Rot 25 µM. Data represent mean ± SEM, n = 4, and were calculated as % of control (untreated siControl cells considered 100%) and analysed by Student's *t*-test (P* < 0.05, ***P* < 0.01 for EFV vs. MeOH and $^{\#\#}P$ < 0.01 for TG vs. DMSO).**

5.2. Mitochondrial function

Mitochondria function was studied through three parameters: $O_2^{\cdot -}$ production, $\Delta\Psi_m$ and mitochondrial mass. As can be seen in Fig.IV.34, no changes were observed in $\Delta\Psi_m$ (TMRM fluorescence) and mitochondrial morphology/mass (NAO fluorescence) when *LONP1* was silenced. In contrast, EFV 25 µM induced a significantly higher increase in mitochondrial $O_2^{\cdot -}$ production (MitoSOX fluorescence) in siLONP1 cells. This result confirms the protective role of LONP1 under oxidative stress.

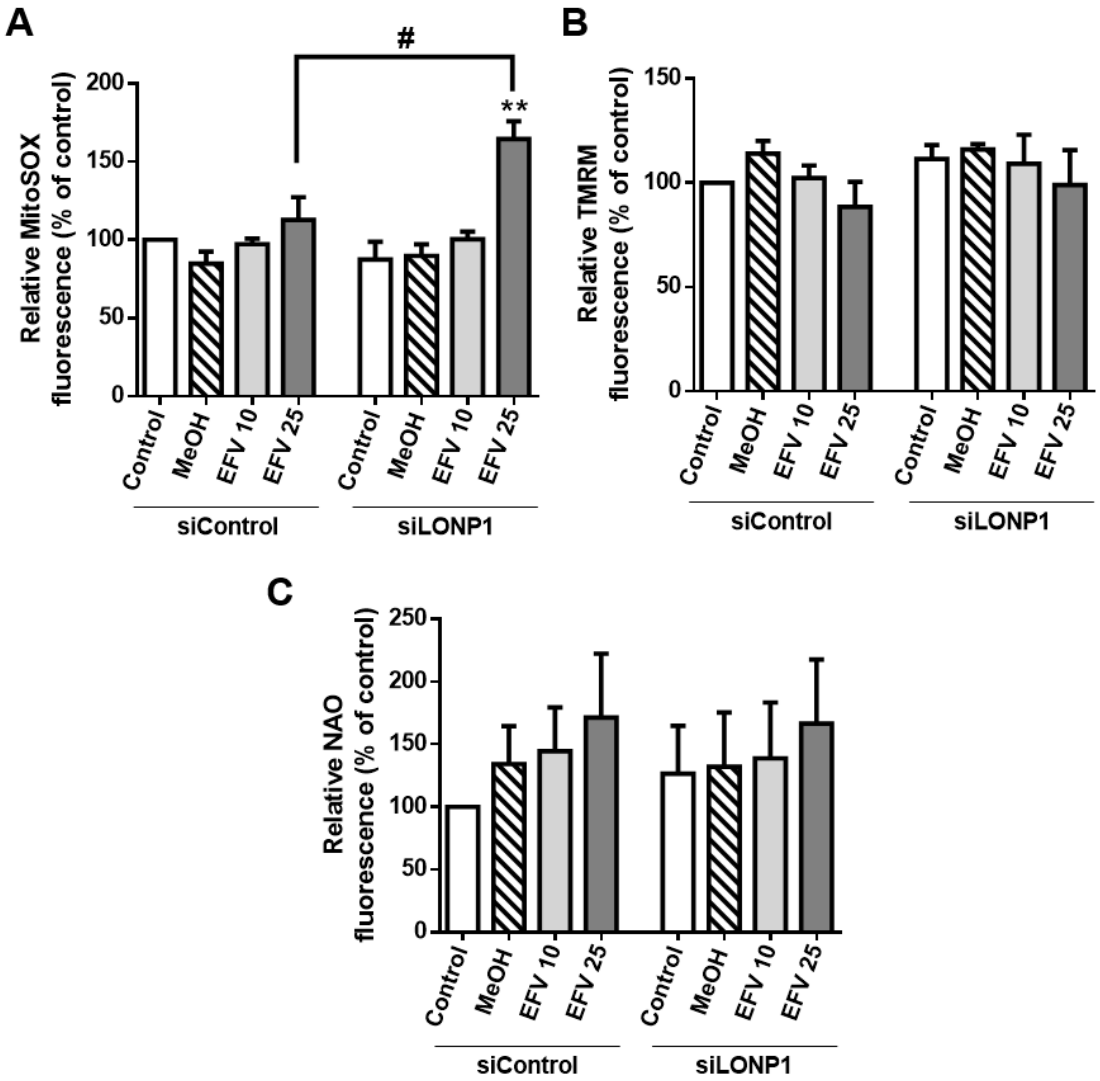

Figure IV.34. Role of LONP1 in mitochondrial function. Analysis of (A) $O_2^{\cdot -}$ production (MitoSOX fluorescence), (B) $\Delta\Psi_m$ (TMRM fluorescence) and (C) mitochondrial mass (NAO fluorescence) in Hep3B cells transfected with siRNA Control or siLONP1 and treated for 24 h with increasing concentrations of EFV and vehicle (MeOH). Data represent mean ± SEM, n = 4, and were calculated as % of control (untreated siControl cells considered 100%) and analysed by Student's *t*-test ($P < 0.01$ for EFV vs. MeOH and $^{\#}P < 0.05$ for siLONP1 vs. siControl cells).**

6. Effect of other antiretroviral drugs on LONP1 expression

6.1. Newer antiretroviral drugs: DRV, RAL and RPV

EFV excellence has been challenged by the arrival of newer antiretrovirals, such as the IP darunavir (DRV), the II raltegravir (RAL) and the NNRTI rilpivirine (RPV). They have a better toxicological profile than EFV while producing similar levels of efficacy and virological suppression. In view of our previous report that EFV induces mitochondrial toxicity in hepatic cells, we wished to assess the effect of these drugs on mitochondria through the $O_2^{\cdot -}$ production and $\Delta\Psi_m$, for which we used a range of clinically relevant concentrations of each drug and compared the effect to that produced by EFV 25 µM.

As can be seen in Fig.IV.35, none of the newer compounds induced significant changes in $O_2^{\cdot -}$ production (MitoSOX fluorescence) or $\Delta\Psi_m$ (TMRM fluorescence) at 24 h of treatment, although a slight reduction of $\Delta\Psi_m$ was produced by RAL.

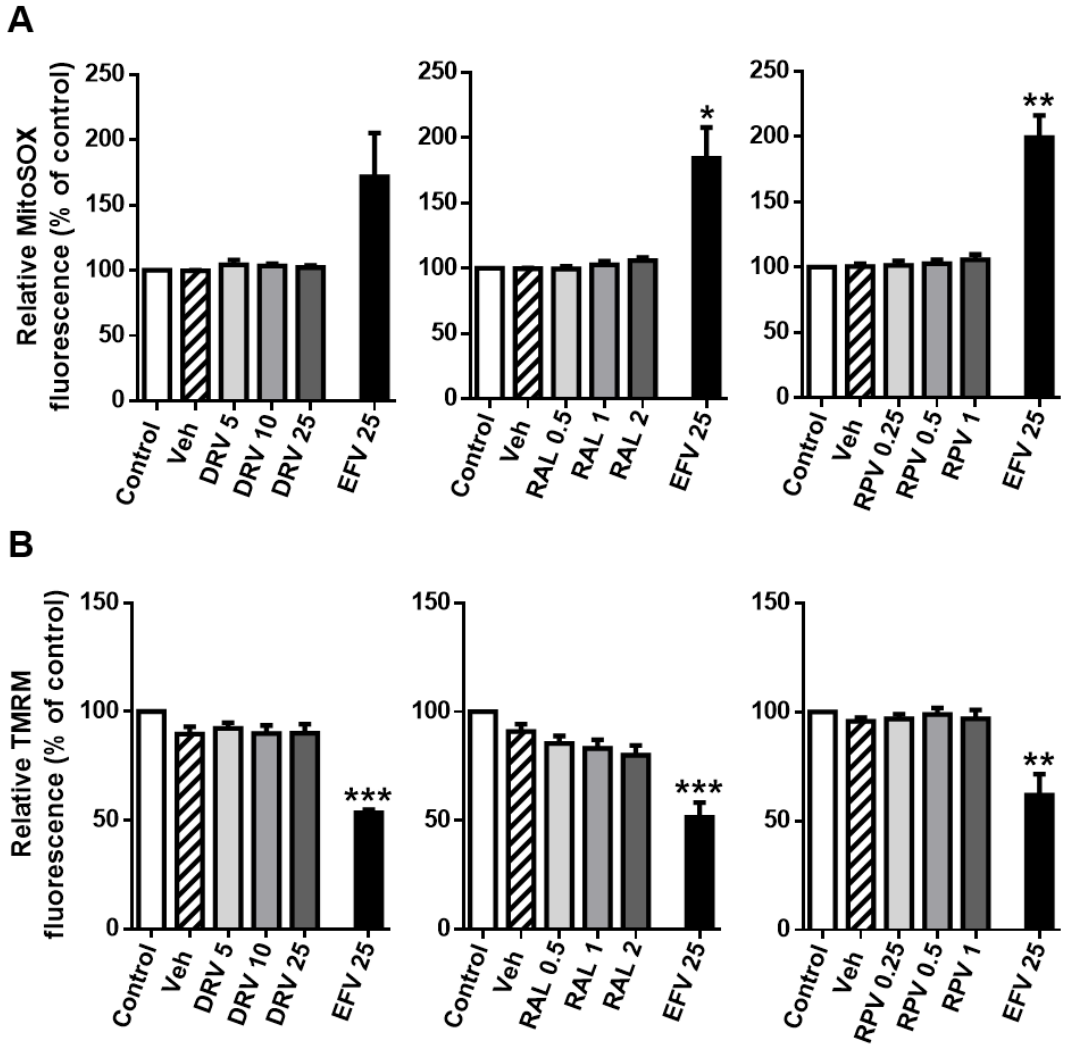

Figure IV.35. Effect of newer antiretroviral drugs (DRV, RAL and RPV) on mitochondrial function in hepatic cells. Quantitative analysis of (A) mitochondrial $O_2^{\cdot-}$ production (MitoSOX fluorescence) and (B) $\Delta\Psi_m$ (TMRM fluorescence) by fluorescence microscopy, after 24 h of treatment with increasing concentrations of each drug, vehicle or EFV 25 µM. Data represent mean ± SEM, n = 4-6, and were calculated as % of control (untreated cells considered 100%) and analysed by Student's *t*-test (P* < 0.05, ***P* < 0.01, ****P* < 0.001 vs. untreated cells).**

In order to examine into more detail the specificity of the effect of EFV, we also assessed the expression of LONP1 in Hep3B cells treated for 24 h with clinically relevant concentrations of each drug and compared the effect to that induced by EFV 25 µM. In contrast to EFV that produced a significant increase as expected, none of the newer antiretrovirals altered the expression of LONP1 (Fig.IV.36).

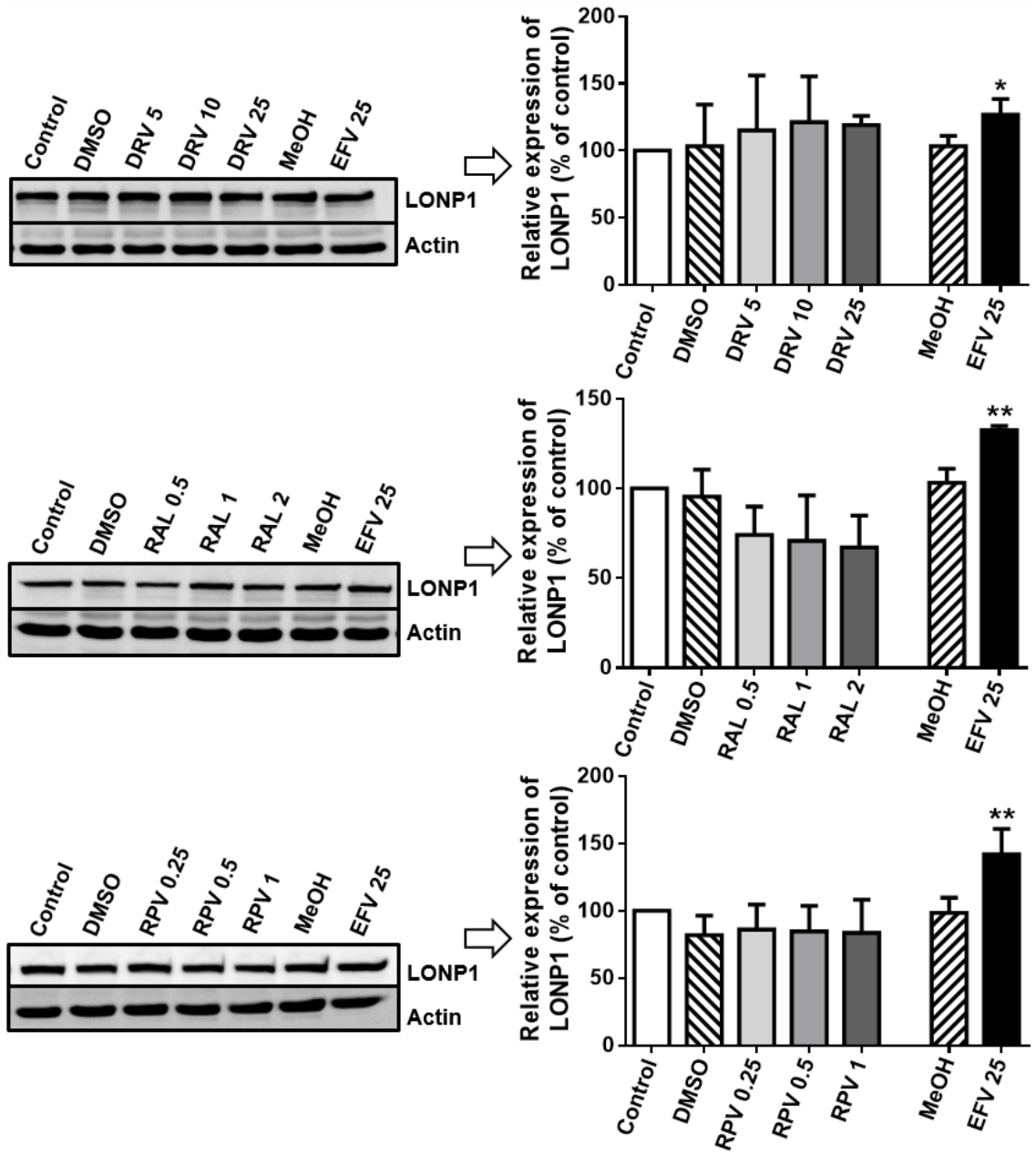

Figure IV.36. Effect of newer antiretroviral drugs (DRV, RAL and RPV) on LONP1 expression in hepatic cells. Representative WB images and histograms expressing quantification of protein expression in total cell extracts after 24 h of treatment with increasing concentrations of each drug, vehicles (MeOH or DMSO) or EFV 25 µM. Data represent mean ± SEM, n = 4, and were calculated as % of control (untreated cells considered 100%) and analysed by Student's *t*-test (P* < 0.05, ***P* < 0.01 for EFV vs. MeOH).**

6.2. Purine analogues ABC and ddI

NRTIs are essential components of HIV therapy with well-documented long-term mitochondrial toxicity in hepatic cells. We evaluated the acute effects of clinically relevant concentrations of the widely used NRTIs (ABC and ddI) on mitochondrial function after 1 h of treatment. The purine analogues ABC and ddI produced an immediate and concentration-dependent reduction of $\Delta\Psi_m$ in Hep3B cells (Fig.IV.37). While ddI produced a profound reduction of $\Delta\Psi_m$ at all the concentrations evaluated, ABC influenced this parameter, but to a lesser extent, reaching statistical significance only at the highest concentration.

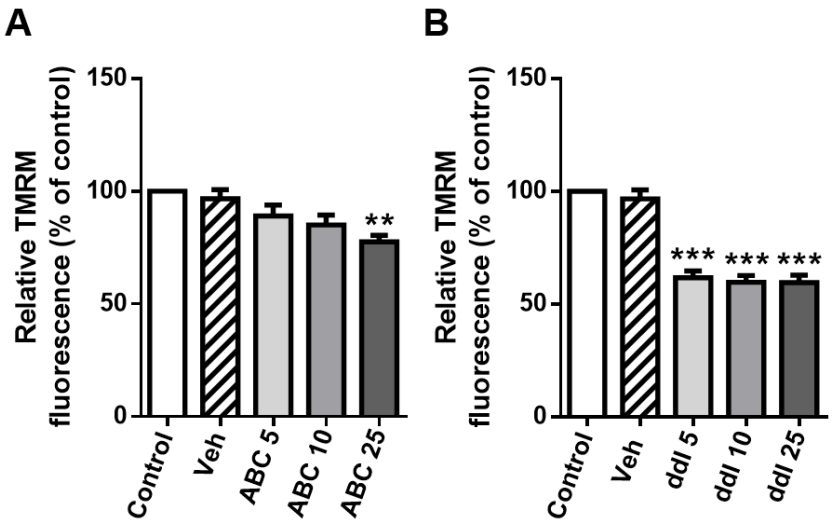

Figure IV.37. Analysis of $\Delta\Psi_m$ in Hep3B cells treated with increasing concentrations of the purine analogues ABC and ddI. $\Delta\Psi_m$ was assessed by measuring TMRM fluorescence after 1 h of treatment with increasing concentrations of (A) ABC and (B) ddI. Data represent mean + SEM, n = 5, and were calculated as % of control (untreated cells considered 100%) and analysed by Student's t-test (P < 0.01, ***P < 0.001 vs. vehicle).**

Secondly, we studied the effect of ABC and ddI on LONP1 expression in Hep3B cells. Purine analogues did not alter the expression of LONP1 after 24 h of treatment (Fig.IV.38).

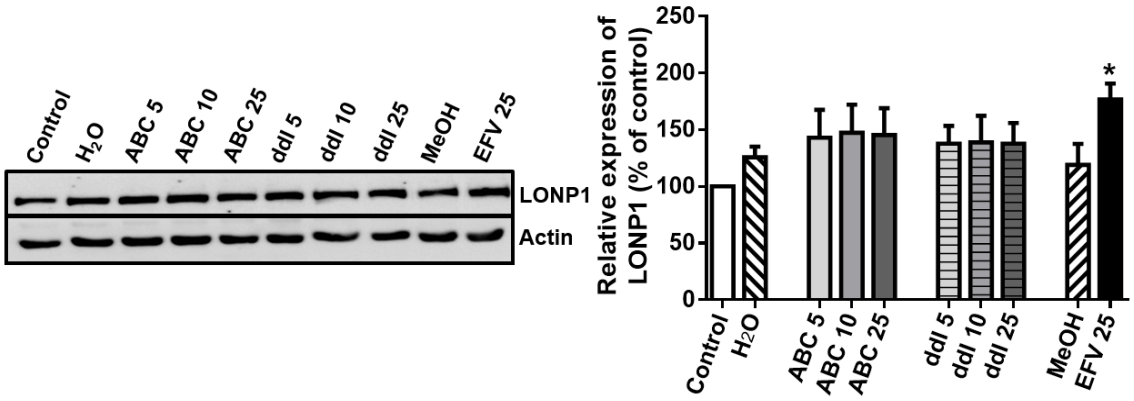

Figure IV.38. Effect of ABC and ddI on LONP1 expression. Representative WB image and histogram expressing quantification of protein expression in total cell extracts in Hep3B cells treated for 24 h with increasing concentrations of ABC or ddI, vehicles (H_2O or MeOH) or EFV 25. Data represent mean ± SEM, n = 6, and were calculated as % of control (untreated cells considered 100%) and analysed by Student's *t*-test (P* < 0.05 for EFV vs. MeOH).**

6.3. Analysis of LONP1 expression with LPV and RTV

Our group has already reported that LPV and RTV, two widely used PI in HIV therapy, induce ER stress without evident mitotoxicity in Hep3B cells (Apostolova N. *et al*., 2013). In order to study the effect of these drugs on LONP1 expression, cells were treated for 24 h with increasing concentrations of LPV or RTV, EFV 25 µM or TG 2 µM. As can be seen in Fig.IV.39, LPV produced a concentration-dependent increase of LONP1 protein and gene expression, similar to that produced by EFV and TG, whereas RTV lacked any effect.

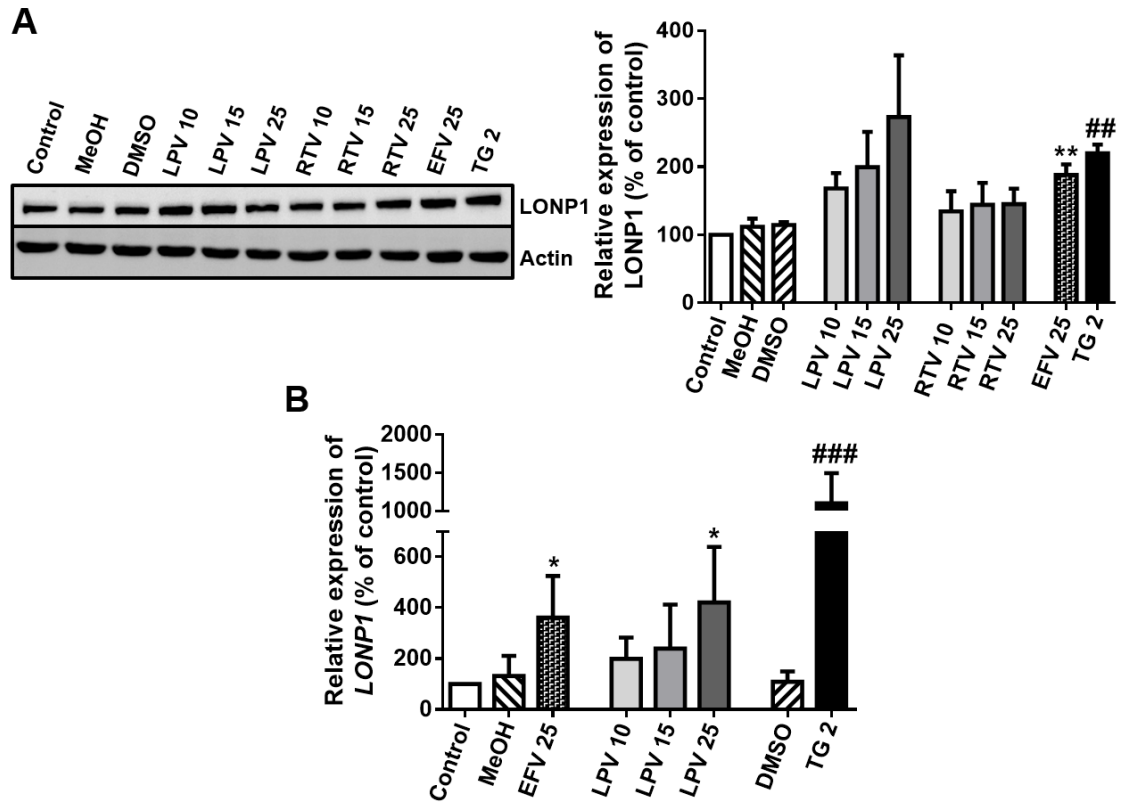

Figure IV.39. Effect of LPV and RTV on LONP1 expression. Hep3B cells were treated for 24 h with increasing concentrations of LPV or RTV, vehicles (MeOH or DMSO), EFV 25 µM or TG 2 µM. (A) Representative WB image and histogram expressing quantification of LONP1 in whole cell protein extracts. (B) Quantitative RT-PCR analysis of *LONP1* expression. Data represent mean ± SEM, n = 4, and were calculated as % of control (untreated cells considered 100%) and analysed by Student's *t*-test (P* < 0.05, ***P* < 0.01 for EFV and LPV vs. MeOH and $^{\#\#}P$ < 0.01, $^{\#\#\#}P$ < 0.001 for TG vs. DMSO).**

7. Analysis of extramitochondrial location of LONP1

Having observed that LONP1 presence in the extramitochondrial fraction increases following EFV treatment (Fig.IV.22), we sought to analyse its intracellular location.

7.1. Analysis of LONP1 presence in mitochondria and ER

As stated previously, the activation of LONP1 is thought to be an adaptive mechanism in both oxidative and ER stress. For this reason, firstly, we wanted to study the presence of LONP1 in mitochondria and ER. We performed double-staining immunocytochemistry experiments by confocal fluorescence microscopy using the chaperone Calnexin as a protein marker for ER and TOM20 for mitochondria. On the one hand, confocal microscopy analysis for LONP1 and TOM20 revealed an increased

overlapping between these two signals in Hep3B cells treated with EFV 10 and 25 µM, while a decrease was observed in cells treated with TG and no changes were produced with Rot and CCCP (Fig.IV.40). On the other hand, colocalization analysis between the LONP1 signal and the ER revealed an increased, concentration-dependent overlapping in cells exposed to EFV, while TG induced a significant decrease, and no changes were observed with Rot and CCCP (Fig.IV.41).

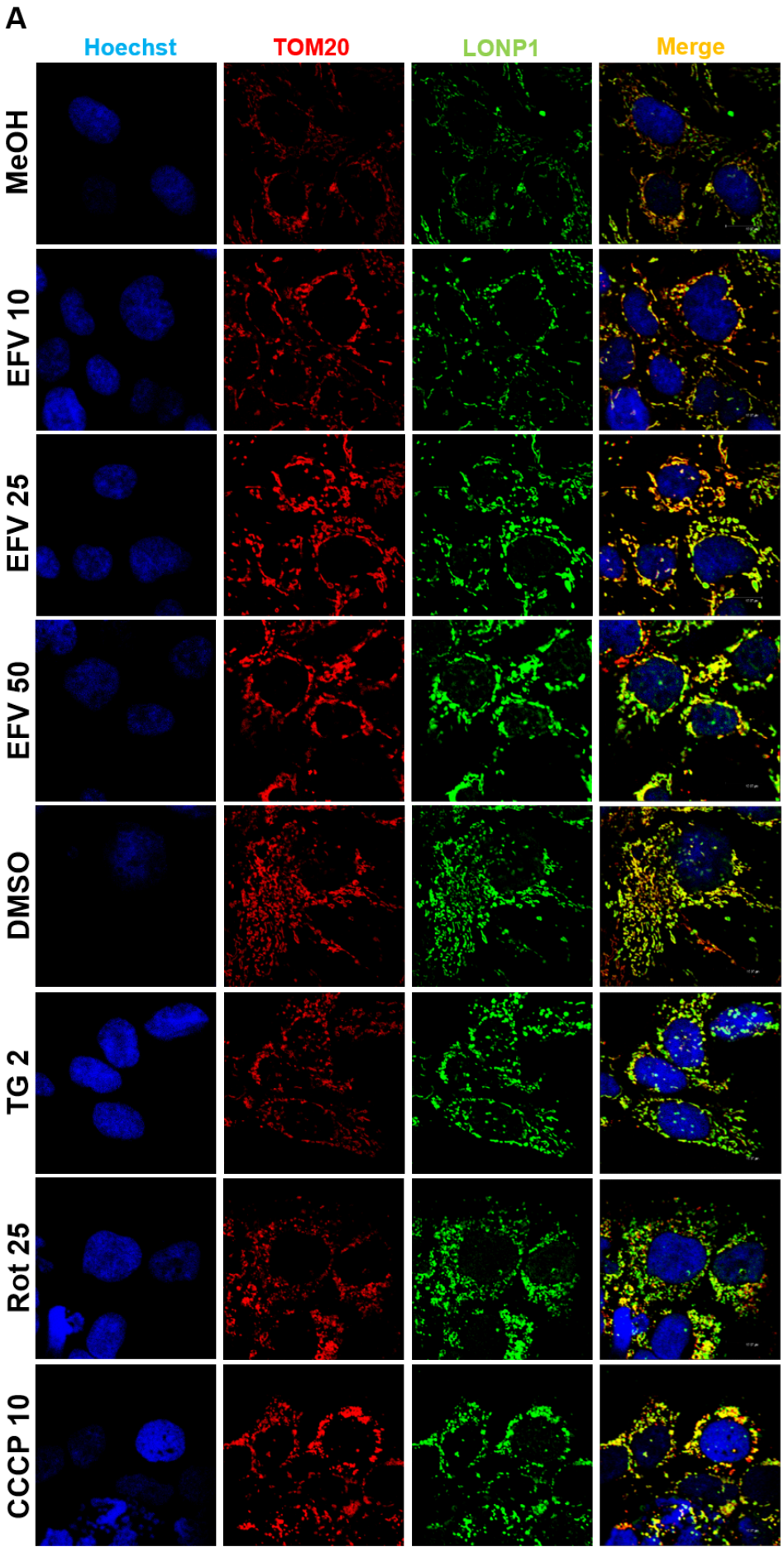
A
Hoechst
TOM20
LONP1
Merge
MeOH
EFV 10
EFV 25
EFV 50
DMSO
TG 2
Rot 25
CCCP 10

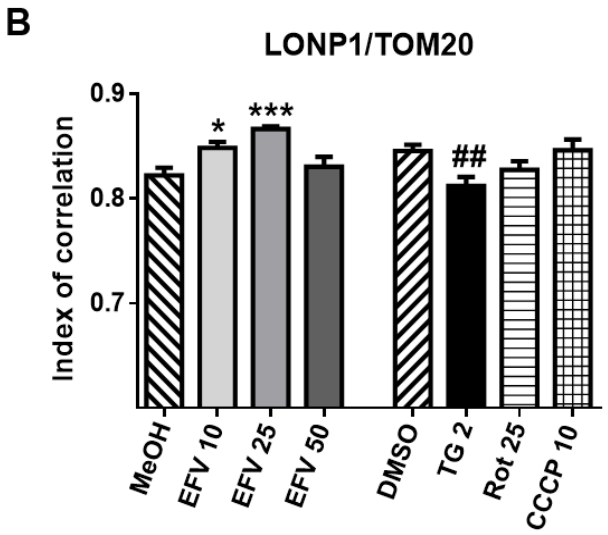

Figure IV.40. Analysis of LONP1 presence in mitochondria by confocal microscopy. Hep3B cells were treated for 24 h with increasing concentrations of EFV, vehicles (MeOH or DMSO), TG 2 µM, Rot 25 µM or CCCP 10 µM, and stained with Hoechst 33342 (blue, nuclei), anti-TOM20 (red, mitochondria) and anti-LONP1 (green) antibodies. (A) Representative confocal microscopy images (63x with 3x optical zoom) and (B) histogram showing the index of correlation between LONP1 and mitochondria. Data represent mean ± SEM, n = 3, and were analysed by Student's *t*-test (P* < 0.05, ****P* < 0.001 for EFV vs. MeOH and $^{\#\#}P$ < 0.01 for TG vs. DMSO).**

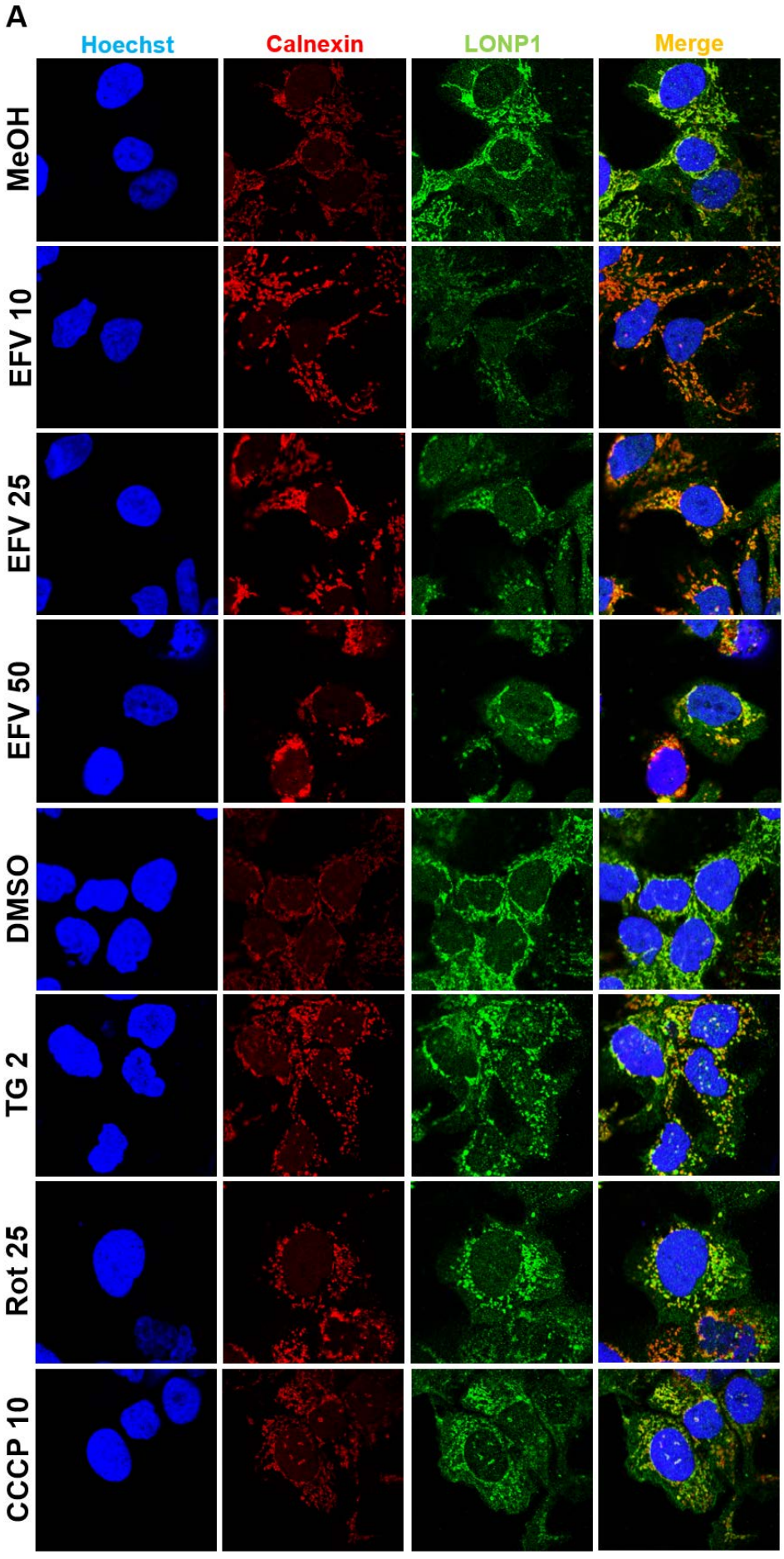
A
Hoechst
Calnexin
LONP1
Merge
MeOH
EFV 10
EFV 25
EFV 50
DMSO
TG 2
Rot 25
CCCP 10

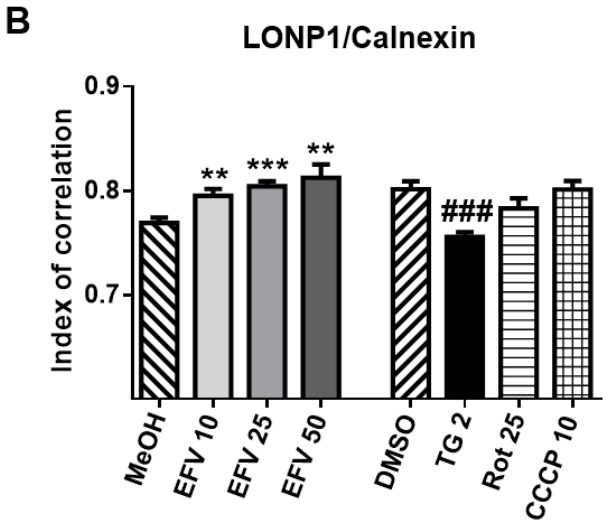

Figure IV.41. Analysis of LONP1 presence in ER by confocal microscopy. Hep3B cells were treated for 24 h with increasing concentrations of EFV, vehicles (MeOH or DMSO), TG 2 µM, Rot 25 µM or CCCP 10 µM, and stained with Hoechst 33342 (blue, nuclei), anti-Calnexin (red, ER) and anti-LONP1 (green) antibodies. (A) Representative confocal microscopy images (63x with 3x optical zoom) and (B) histogram showing the index of correlation between LONP1 and Calnexin. Data represent mean ± SEM, n = 3, and were analysed by Student's *t*-test (***P*** **< 0.01, ******P*** **< 0.001 for EFV vs. MeOH and** $^{###}$***P*** **< 0.001 for TG vs. DMSO).**

7.2. Assessment of the purity of different cell fractions

LONP1 presence in mitochondria is depleted under dual ER stress/mitochondrial dysfunction such as that induced by EFV (Fig.IV.22) while its presence in extramitochondrial location (cytosol and ER) is increased (Fig.IV.22 and Fig.IV.41). These results and knowing that Calnexin itself is considered a MAMs protein, made us speculate about LONP1´s location in MAMs. In order to assess this possibility, we next obtained subcellular fractions (crude mitochondria, ER, cytosol and MAMs) of Hep3B cells treated with EFV, TG or CCCP and explored the presence of several marker proteins. The grade of purity of the samples was assessed by studying the abundance of specific proteins in the untreated cell extracts (Fig.IV.42) and the obtained results were similar to those reported elsewhere (Wieckowski M.R. *et al*., 2009). While Porin, a MAMs protein was detected both in crude mitochondria and MAMs fractions, MAMs lacked Cytochrome *c*, a MM protein, as expected. Also, the OMM protein TOM20 was especially detected in crude mitochondria and a small amount could also be found in MAMs fraction. The mitochondrial protein and reported MAMs component FACL4 was

highly abundant in crude mitochondria and MAMs, but was also detected in the ER and the cytosol. Virtually all LONP1 was located in the mitochondria, as anticipated (Fig.IV.42).

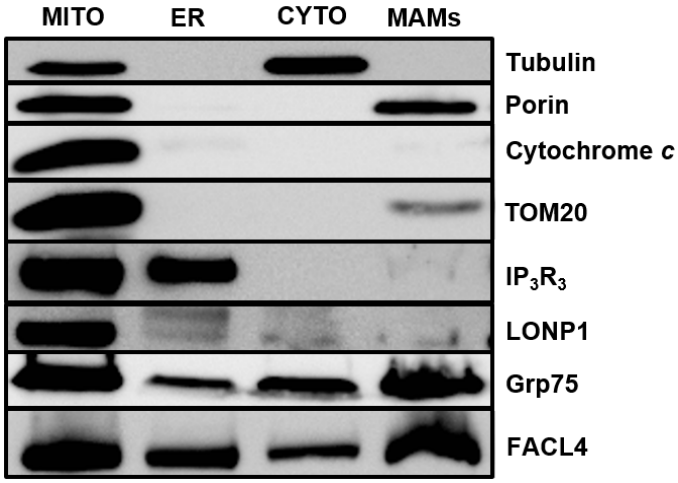

Figure IV.42. Analysis of the purity of different cell fractions (mitochondrial, ER, cytosolic and MAMs) in untreated Hep3B cells. Representative WB image showing the expression of several mitochondrial (Porin, Cytochrome *c*, TOM20, LONP1), ER (IP_3R_3), cytosolic (Tubulin) and MAMs (FACL4, Grp75) proteins in basal conditions.

7.3. Protein analysis of LONP1, Grp75 and PTPIP51 in cytosolic, ER, mitochondrial and MAMs fraction

Subsequently, we compared the presence of two mitochondrial proteins recognized as MAMs members (Grp75 and PTPIP51) under different pharmacological treatments and contrasted this with the expression of LONP1 (Fig.IV.43). PTPIP51 was detected only in the crude mitochondria fraction, while EFV induced a major increment in its expression, in accordance with the experiments using whole cell extracts (Fig.IV.20A). Grp75 was present in all four fractions, as shown in Fig.IV.43, and EFV increased its presence notably in the cytosol, ER and MAMs. Interestingly, the pattern of LONP1 expression was very similar to that of Grp75, pointing to the possibility that LONP1 is itself a MAMs protein whose presence in MAMs is greatly incremented under combined ER/mitochondrial stress.

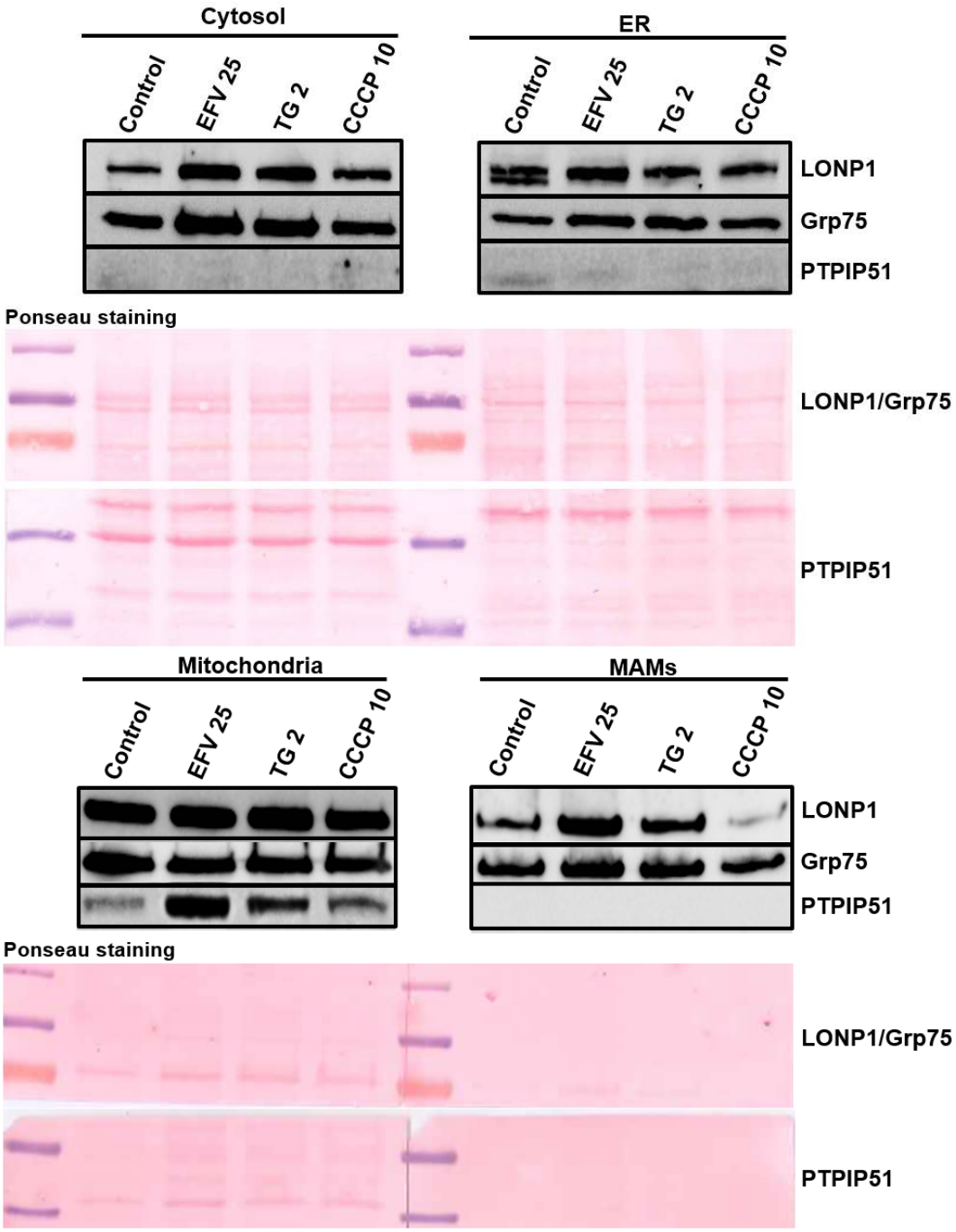

Figure IV.43. WB analysis of LONP1, Grp75 and PTPIP51 in cytosolic, ER, mitochondrial and MAMs fractions obtained from Hep3B cells treated for 24 h with EFV 25 µM, TG 2 µM or CCCP 10 µM. Ponceau staining of proteins was used as a loading control to normalize the results.

V. DISCUSSION

The current pharmacological approach for treatment of HIV infection, cART, has significantly prolonged the survival of HIV-infected people in developed countries, transforming AIDS into a chronic illness. Compared to previous combined regimens, current options are associated with increased viral suppression and lower rates of treatment discontinuation due to their improved convenience and tolerability. However, some of the agents used in this treatment have also been responsible for the emergence and development of side effects, some of which can be severe. This, together with the fact that the treatment once started has to be taken throughout life, has generated a growing interest in the long-term adverse effects and in the mechanisms responsible for them. EFV is among the most widely used drugs in this therapeutic combination. Although generally considered safe, there is a concern about the side effects induced by EFV-containing therapies, such as rash, neuropsychiatric disturbances, lipid and metabolic alterations and hepatotoxicity (Tashima K.T. *et al.*, 2003; Gutiérrez F. *et al.*, 2005; Maggiolo F., 2009; Loko M.A. *et al.*, 2011; Echenique I.A. and Rich J.D., 2013; Patil R. *et al*., 2015). In particular, a positive association between plasma concentrations of EFV and the appearance of liver side effects is logical and well documented (Kappelhoff B.S. *et al*., 2005; Brück S. *et al*., 2008; Pandit A. *et al*., 2012; Echenique I.A. and Rich J.D., 2013; Patil R. *et al*., 2015). In addition, there is a higher risk of this adverse effect in patients with already elevated liver enzymes levels and/or coinfected with HBV and/or HCV (Brück S. *et al*., 2008; Núñez M., 2010; Hernandez M.D. and Sherman K.E., 2011; Joshi D. *et al*., 2011; Healy S.A. *et al*., 2013).

Due to the properties of cART and the interindividual variability among patients, it is very difficult to assess the adverse effects induced by each drug separately; for this reason, *in vitro* studies have become a key tool. Although an *in vitro* cellular model, as the one employed in the present study, cannot fully reflect the hepatic alterations induced by the drug in a living organism and particularly those related to systemic effects, cultured cells can provide relevant knowledge regarding specific drug-induced subcellular responses and provide a starting point for *in vivo* studies or clinical approximations. In this work, the experimental parameters used were as similar as possible to the physiological conditions. The human hepatoma cell line Hep3B was chosen due to the fact that it has an active P450 system (Zhu X.H. *et al*., 2007),

necessary for the metabolism of EFV. To determine if the observed effects were dependent on the cell line used, some experiments were performed using HepaRG cells, terminally differentiated hepatic cells derived from a human hepatic progenitor cell line with many characteristics of primary human hepatocytes. In some experiments, we also used the human glioma cell line U-251MG, human hepatic stellate cells (HSCs) LX2 and U937 human monocytes, in which our group had previously studied the effect of EFV. The concentrations of EFV used (10, 25 and 50 µM) were chosen taking into account the significant interindividual variability described for its pharmacokinetics. The recommended daily dose of EFV for adults (600 mg) usually results in a C_{max} of 12.9 ± 3.7 µM and a C_{min} of 5.6 ± 3.2 µM in plasma (Staszewski S. *et al*., 1999), although several clinical studies have shown that 20%-40% of patients exhibit higher levels, even up to 73.6 µM (Burger D. *et al*., 2006; Carr D.F. *et al*., 2010; Gounden V. *et al*., 2010). In addition, analysis of plasma EFV concentration of 843 patients included in the EuroSIDA trial revealed that 14.1% of them had supratherapeutic plasma concentrations and that the highest EFV concentration recorded was 80.75 µM (van Luin M. *et al*., 2009). In addition, there are numerous publications that describe interactions with certain drugs coadministered during cART, which result in a significant increase in EFV C_{max} (Sustiva Technical Data Sheet, endorsed by the European Medicines Agency, 2012). It has also been described that patients with HIV-HCV coinfections present up to twice the plasma concentrations present in patients infected with HIV alone (Dominguez S. *et al*., 2010).

In vitro studies have attributed a hepatotoxic action to EFV that involves (i) interference with mitochondrial function resembling that induced by the pharmacological inhibitor of mitochondrial complex I rotenone (Rot) and (ii) presence of ER stress with activation of UPR, manifestations triggered by the classic ER stressor thapsigargin (TG) (Apostolova N. *et al*., 2010; 2011c; Blas-García A. *et al*., 2010; Apostolova N. *et al.*, 2013). However, several studies have reported differences in the actions of the aforementioned compounds that imply specificity for EFV. In this context, it has seen that TG not only affects the ER but also undermines mitochondrial function in rat liver cells (Korge P. and Weiss J.N., 1999; Hom J.R. *et al*., 2007), which is confirmed by the present findings. In contrast, Rot does not mimic the actions of EFV

or TG regarding ER stress/UPR in hepatic cells (Apostolova N. *et al.*, 2013).

In this work, firstly, we wished to investigate the implication of the mitochondria in EFV-induced effects by evaluating the action of this drug (24 h-treatment) on cells significantly depleted of functional mitochondria ("rho^o" throughout the manuscript), and comparing it to the effect of Rot and TG on the same model. Rho^o cells are respiration-deficient and display an aberrant mitochondrial phenotype with distorted cristae. It is evident that rho^o cells are an artificial cellular model of non-respiring mitochondria; however, despite certain limitations, rho^o cells are still used as a robust approach to generate a respiration-deficient model in culture, which enables the evaluation of the mitochondrial dependence or independence of the interference exerted by different stimuli including drugs. Of note, quantitative PCR analysis revealed that 30% of the mtDNA remained meaning that the established phenotype was not fully "rho^o". Depletion of mtDNA is a characteristic of the so-called mitochondrial diseases, although the amount of remaining mtDNA and its correlation with the severity of these diseases present great variations among patients. A minimum critical proportion of mtDNAs is necessary (a threshold level) before biochemical defects and tissue dysfunction become apparent and it varies in the range of 60-90% mutant to wild-type mtDNA. Although the threshold level can partly explain the disease phenotypes and clinical severity observed in patients, an exact correlation is lacking. Mitochondrial diseases with a major hepatic component (hepatocerebral mtDNA depletion syndromes or isolated hepatic disease) display a significant decrease in liver mtDNA content with most cases usually presenting 20% or less mtDNA compared to age-matched healthy control individuals (Dimmock D.P. *et al.*, 2008; Müller-Höcker J. *et al.*, 2011). It is generally assumed that in mtDNA-depleted cells, the reduced abundance of mtDNA-encoded proteins mirrors the replicative failure of mtDNA. However, liver mitochondrial proteins are soon degraded when they are not properly assembled; therefore, the expression of mtDNA-encoded proteins may be relatively low compared to the depletion in mtDNA, which seems to be the case in our model. Moreover, the number of mtDNA copies relative to nDNA does not always reflect the degree of mitochondrial dysfunction; therefore, functional assays such as measurements of the activity of the specific ETC complexes or evaluation of the overall

respiration deficit are needed. The depletion of mtDNA-encoded proteins in the present work was confirmed by studying the protein expression of two mtDNA-encoded proteins, subunit II of cytochrome *c* oxidase (complex IV) and subunit ND1 of complex I; rho^o cells, however, maintain an intact nuclear genome, which conferred a comparable protein expression of the β subunit of complex V, β-actin and Porin in the parental and mitochondrial DNA-depleted cells. The presence of mitochondria with severely diminished respiration resulted in a differential cellular response to EFV in all the parameters studied. When exposed to EFV, rho^o cells did not display a significant increase in ROS generation, and the increase in the mitochondrial signal (NAO fluorescence) was absent in cells treated with EFV 25 μM and only visible in those treated with 50 μM, presumably due to the crossing of a threshold in the stress response. Such a threshold may also account for the effect observed regarding $\Delta\Psi_m$ where, interestingly, exposure to EFV induced a slightly less evident reduction in rho^o cells than in WT, with the exception of treatment with 50 μM. Importantly, the deleterious effect of EFV 50 μM on cell number, its triggering of cell cycle arrest and induction of cell death (via apoptosis) was, once again, largely ameliorated in rho^o cells. Fluorescence microscopy experiments confirmed that the cell morphology and specifically mitochondrial appearance were less modified in cells lacking functional mitochondria. Many cell types have the ability to maintain $\Delta\Psi_m$ under condition of diminished mitochondrial respiration through the reverse activity of ATP synthase, and it was the case of our model. While rho^o cells under basal conditions displayed only a slightly lower $\Delta\Psi_m$ than WT cells, about 50% reduction was observed when glycolysis was inhibited.

TG induced similar changes as EFV in WT cells with the exception of $\Delta\Psi_m$. We found not a decrease but an increase in it, which is in keeping with the results of other studies showing a lack of $\Delta\Psi_m$ dissipation during ER stress triggered by TG (Zhdanov A.V. *et al*., 2011; Jipu R. *et al*., 2012). However, to our knowledge ours is the first study to address the mitochondrial action of TG in cells with greatly diminished respiration. As with EFV, the overall effect of TG on mitochondria and cell viability was largely reduced in rho^o cells. However, the effect of TG on cell survival in respiration-depleted cells is more complex as these cells exhibit a higher percentage of necrotic/damaged

(but not apoptotic) cells compared to WT.

The effects of Rot on WT cells were similar to those of EFV, except for that concerning the nuclear area (Hoechst fluorescence), which in the case of Rot was found to increase. Diminished nuclear area (chromatin condensation and nuclear fragmentation) is a hallmark of apoptosis, and the precise relevance of this slight increment in Rot-treated cells is unknown. An increase in nuclear area after treatment with Rot was also present in rho^{o} cells but it was higher than in WT cells. Another singularity of Rot treatment was observed in the cell cycle analysis. Unlike EFV and TG, which altered the cell cycle in rho^{+} but not rho^{o} cells, Rot produced a similar alteration in both populations. These effects point to the presence of a mitochondria-independent action of Rot in this cell line used, which may also be concentration related. Rot at concentrations similar to those employed in the present work has been shown to arrest mammalian cells in metaphase by binding directly to tubulin and preventing microtubule assembly (Meisner H.M. and Sorensen L., 1966). Alternatively, the interference with the cell cycle may be due to the cancerous nature of the cell line in question, as completion of the cell division in cells with a high metabolic drive and high proliferation rate, such as cancer cells, is particularly sensitive to inhibition of mitochondrial function. This result is related to the fact that in a similar manner to TG, the percentage of Ann^{-}/PI^{+} cells in the Rot-treated samples is enhanced in rho^{o} cells. In summary, the stress response triggered by clinical concentrations of EFV is diminished in cells lacking functional mitochondria and this effect shows certain differences when compared to that elicited by other cytotoxic compounds that compromise mitochondria.

Mitochondria play a pivotal role in the development of drug-induced toxicity. The fact that the deleterious effects of drugs can be alleviated in cells with diminished mitochondrial respiration opens a new horizon for understanding mitochondria's involvement in cellular survival. It is tempting to speculate on the concept of a mtDNA threshold and the level of drug-induced or mediated injury. This idea is endorsed by the data obtained in a rho subline of human hepatoma SK-Hep-1 cells showing resistance to bile acid-induced concentration-dependent activation of apoptosis (Marin J.J. *et al.*, 2013). Similar phenomena have been described, such as a protective

effect of membrane depolarization of isolated rat liver mitochondria, which was shown to attenuate permeability transition pore opening and oxidant production induced by *tert*-butyl hydroperoxide (Aronis A. *et al.*, 2002). Effects such as these, which involve alterations in basal mitochondrial function, may account for the idiosyncratic hepatic reactions triggered by anti-HIV drugs and may also explain the different degrees of susceptibility to liver damage seen in patients undergoing antiretroviral therapy. In the case of EFV, its mitochondrial effects in the clinic may be directly affected by several factors. Firstly, the concomitant administration of other mitochondriotropic drugs may have a crucial role in the effects of EFV on mitochondria. Indeed, EFV is never administered individually but as an element within cART together with two NRTIs; importantly, these drugs are known to possess mitotoxic potential due to their ability to inhibit mitochondrial DNA polymerase γ (Pol-γ hypothesis) and therefore their administration may generate a different type of mitochondria with a distinct susceptibility to EFV. Secondly, the intrinsic genetic variability such as that induced by the mtDNA haplogroup may account for the drug-induced mitotoxicity both under basal or stress conditions. Mitochondrial haplogroups and subhaplogroups have been associated with certain toxicities of NRTI drugs (Hendrickson S.L. *et al*., 2009; Hulgan T. *et al*., 2011; Kampira E. *et al.*, 2013); however, to the best of our knowledge, no such correlations have been made with EFV. In all, a very intriguing picture is emerging of patient-specific mitochondrial function as a factor that influences the mitotoxic potential of anti-HIV drugs.

In order to understand the role of mitochondria in the ER stress induced by EFV, we studied the mitochondrial dynamics that depends among other processes on the interaction between these organelles. Regulation of mitochondrial dynamics/morphology is paramount for proper mitochondrial functioning (Vannuvel K. *et al*., 2013). While mitochondrial fusion facilitates the exchange of vital metabolites and mtDNA between different mitochondria to ensure their functional maintenance (Nakada K. *et al*., 2009), mitochondrial fission is required to ensure biogenesis, to respond to changes in local energy demands and to separate/eliminate damaged or old mitochondria through a selective autophagic process called mitophagy (Archer S.L., 2013). Mitochondrial fusion and fission are tightly controlled processes that require

several highly evolutionary conserved GTPases: mitofusins, anchored in the OMM (Santel A. and Fuller M.T., 2001); OPA1, located in the IMM (Smirnova E. *et al*., 1998); and Drp1 (Otera H. and Mihara K., 2011). During the import of OPA1 into the MM, the MTS domain is cleaved to form the mature OPA1 isoform (l-OPA1), which undergoes further processing events generating shorter isoforms (s-OPA1) (Ishihara N. *et al*., 2006). L-isoform has a mitochondrial fusion-stimulating activity, a feature that is lost following proteolytic cleavage into the s-isoform (Ishihara N. *et al*., 2006). There is evidence that mitochondrial dysfunction, characterized by low mitochondrial ATP production and $\Delta\Psi_m$ dissipation, is associated with loss of the long isoform (Vannuvel K. *et al*., 2013). This is in line with our results, which demonstrate that mitochondrial/ER stressors reduce the l-OPA1/s-OPA1 ratio, which is particularly evident under the conditions that cause massive $\Delta\Psi_m$ loss. The master regulator of mitochondrial division in most eukaryotic organisms, Drp1, is mostly cytosolic, with only approximately 3% associated to the OMM (Smirnova E. *et al*., 2001). In order to promote fission, Drp1 is recruited to mitochondria, where it oligomerizes around the mitochondrion, thus constricting it. Many studies have failed to report an increase in fission through the alteration of protein levels of Drp1, which is in line with the results shown here. On the contrary, it seems that post-translational modifications target Drp1 to mitochondria and enable it to mediate fission. One such regulation is phosphorylation at Ser^{616}, which occurs through cyclin B1/CDK1 (Taguchi N. *et al*., 2007) and triggers mitotic Drp1-dependent mitochondrial fission. Under oxidative stress conditions, it has been seen that Ser^{579} in human Drp1 isoform 3 (corresponding to Ser^{616} in the human Drp1 isoform 1) is phosphorylated, leading to mitochondrial fragmentation and impaired mitochondrial function (Qi X. *et al*., 2011). Since this modification does not directly affect its GTPase activity, the increase in fission may be mediated by alterations in Drp1 interactions with other proteins. In the present model, the dual effect of ER stress/mitochondrial dysfunction led to an increase in p-Drp1 expression, its colocalization with mitochondria, as well as in the expression of the recruitment protein Fis1, effects that were not achieved with the rest of the stimuli (except TG that only increased Fis1 expression). In conclusion, it is crucial to understand that different stimuli which produce ER stress and/or different types of mitochondrial dysfunction regulate markers of mitochondrial dynamics in a differential

way. These results reveal that EFV induce mitochondrial fission and decrease fusion in hepatic cells, and it is in accordance with a recent *in vitro* study in human T lymphocyte cells incubated with plasma, which show that EFV-containing therapy leads to a decrease in mitochondrial fusion (Morén C. *et al*., 2015).

In recent years, it has become evident that mitochondria and ER are spatially connected through specific and tightly regulated contact sites, MAMs. The composition and function of these structures are still far from being understood; however, current knowledge suggests that MAMs enable a two-way supply of fundamental metabolites/messengers, such as lipids or Ca^{2+}, while modulating the bioenergetic fate of the cell (Giorgi C. *et al*., 2009; van Vliet A.R. *et al*., 2014). Many proteins have been shown to participate in MAMs, and it is evident that the composition of these structures adapts in response to multiple internal and external stimuli (Bui M. *et al*., 2010). One of the most widely described complexes involves VDAC1 (Porin) and IP_3R, which physically interact through the chaperone Grp75 (Szabadkai G. *et al*., 2006). Another MAMs protein partner that regulate Ca^{2+} homeostasis is that formed by VAP B/C and PTPIP51 (De Vos K.J. *et al*., 2012). In addition, abundant evidence points to the fact that the dynamics of both ER and mitochondria depend on the formation and dissolution of ER–mitochondrial contacts (Scorrano L., 2013). In line with this, several studies have shown that ER tubule wraps around mitochondria and recruits Drp1 locally to form a tight ring around the OMM and constrict it at that site (Friedman J.R. *et al*., 2011). Also, Mfn2 - present at both the ER and mitochondrial surface - (de Brito O.M. and Scorrano L., 2008), not only enables intermitochondrial contacts, but also regulates ER shape and ER-mitochondrial tethering (Chen H. *et al*., 2003; De Brito O.M. and Scorrano L., 2008; Munoz J.P. *et al*., 2013). In this regard, we have observed that cells under combined mitochondrial/ER stress (EFV treatment) tend to exhibit a slightly increased expression of p-Drp1 and Mfn2 in the cytosolic fraction. Intriguingly, a clear decrease was seen in cells treated with Rot, TG and CCCP. These results confirm that mitochondrial dynamics is regulated in a differential way by the stimuli used. In addition, we have seen that VAP B/C-PTPIP51 and Porin-Grp75 complexes are enhanced with EFV, while no increase or a significant decrease were observed with the rest of the stimuli (TG, Rot and CCCP).

Also, the mitochondrial protein PTPIP51 displayed a major enhancement in EFV-exposed cells, an effect that was not evident with the rest of the stressors. In the case of VAP B/C protein expression, the effect was much less pronounced with EFV treatment while TG also induced a slight increment. These data are in line with the finding that EFV treatment increases cytosolic content of Grp75 and lightly decreases its mitochondrial content. In contrast, the other stimuli did not diminish the levels of Grp75 inside mitochondria. Therefore, these data together point to an enhancement of MAMs in cells exposed to combined ER stress/mitochondrial dysfunction.

Very importantly, the fact that EFV exerts an effect on both mitochondria and ER creates a new scenario for understanding liver toxicity. The induction of ER stress and UPR in EFV-treated hepatic cells is dependent on mitochondria as several markers of this stress response (increased expression of protein markers such as Grp78 and CHOP, and higher content of ER) were found to be diminished in Hep3B cells lacking functional mitochondria (Apostolova N. *et al.*, 2013). In order to further link the two effects of EFV (mitochondria and ER), we analysed the expression of LONP1, whose activation is thought to be an adaptive mechanism in both oxidative and ER stress. The present work is the first to describe the upregulation of this protein by EFV. This is relevant, as an upregulation of LONP1 has been associated with HIV treatment, in particular with the development of lipodystrophy in patients receiving cART (Pinti M. *et al.*, 2010), but has not been related to EFV until now. As expected, in line with the rest of the mitochondrial parameters evaluated, EFV-triggered LONP1 upregulation was absent in respiration-deficient cells, which supports the involvement of mitochondria in the onset of EFV-induced ER stress. We also found an upregulation of LONP1 gene and protein expression with the other three stimuli, although to varying extents: while the increase in the case of Rot and CCCP was modest, that induced by TG was remarkable. Of note, the upregulation of LONP1 induced by all four stimuli in Hep3B cells was also seen in human glial cells.

LONP1 is located in the MM, and has been implicated in numerous processes, including degradation of oxidatively damaged mitochondrial proteins (Bota D.A. and Davies K.J., 2002), assembly of ETC complexes (Fukuda R. *et al*., 2007) and regulation of mtDNA maintenance, transcription and replication (Matsushima Y. *et al*., 2010).

Although the role of LONP1 in protein quality control is one of its best demostrated physiological functions, interestingly, it does not appear to be required for mediating the UPRmt (Fig.V.1). In cultured mammalian cells and worms, ClpXP plays a central role in controlling and responding to the UPRmt (Zhao Q. *et al*., 2002; Aldridge J.E. *et al*., 2007; Haynes C.M. *et al*., 2007; 2010; Haynes C.M. and Ron D., 2010). By contrast, LONP1 does not appear to be an essential participant in this stress response pathway (Yoneda T. *et al*., 2004; Horibe T. and Hoogenraad N.J., 2007; Aldridge J.E. *et al*., 2007). In cultured mammalian cells, the accumulation of an aggregation-prone protein within the MM leads to the transcriptional upregulation of ClpP (Zhao Q. *et al*., 2002; Aldridge J.E. *et al*., 2007; Horibe T. and Hoogenraad N.J., 2007). The *CLPP* gene carries UPRmt elements (MURE1 and MURE2) in its promoter region, whereas the *LONP1* gene lacks these promoter sequences. In *C. elegans*, studies show that ClpXP is required to initiate the UPRmt stress response pathway leading to the transcriptional upregulation of UPRmt genes in the nucleus such as ClpP and the mitochondrial DnaJ-like protein Tid1 (Haynes C.M. *et al*., 2007; 2010; Haynes C.M. and Ron D., 2010). By contrast, LONP1 does not play a notable role in UPRmt, as knocking down the worm homolog has no effect on this cell stress response pathway (Yoneda T. *et al*., 2004).

Although LONP1 does not appear to have a major function in the UPRmt, its role in the ER stress-induced UPR (UPRER) has been suggested (Fig.V.1). LONP1 expression is upregulated in response to protein misfolding or increased protein burden in the ER, induced by agents that activate the UPRER such as tunicamycin (a glycosylation inhibitor), TG (as we have seen in this work) or brefeldin A (an inducer of retrograde traffic of Golgi proteins to the ER) (Hori O. *et al*., 2002). Results show that UPRER-stimulated LONP1 overexpression is dependent on PERK, which is specifically activated by UPRER (Hori O. *et al*., 2002). In addition, hypoxia, which also induces ER stress, has been shown to upregulate LONP1. When O_2 availability is low, HIF-1α binds to hypoxia response elements (HRE) in the promoter of the *LONP1* gene leading to LONP1 upregulation and Cox4-1 degradation (Fukuda R. *et al*., 2007). Although the UPRER is traditionally viewed as a signaling pathway responsible for regulating ER proteostasis, it is becoming increasingly clear that PERK can also regulate mitochondrial proteostasis and function in response to pathologic insults that induce ER stress (Han J. *et al*., 2013;

Rainbolt T.K. *et al*., 2014). It is well known that PERK is enriched in MAMs, localizing this ER stress sensor to ER-mitochondrial contact sites (Verfaillie T. *et al*., 2012; Liu Z.W. *et al*., 2013). Studies show that PERK-deficient cells display defects in regulating ETC, abnormal increase in ROS and defects in mtDNA biogenesis (Rainbolt T.K. *et al*., 2014). Regulation of intrinsic apoptosis is also impaired in PERK-deficient cells. In addition, PERK activation induces the downstream expression of mitochondrial quality control factors such as LONP1 (Hori O. *et al*., 2002; Venkatesh S. *et al*., 2012; Han J. *et al*., 2013) and it has been seen that this process requires the activity of ATF4. This transcription factor induces the expression of cellular proteostasis genes such as CHOP (Zinszner H. *et al*., 1998). In line with this, we have observed that CHOP does not seem to be involved in the regulation of *LONP1* expression, but it seems to be controlled by NF-κB, as suggested by other studies (Pinti M. *et al*., 2011). Our group has recently reported that EFV (similarly to TG) increase cytosolic Ca^{2+} concentration in hepatic cells (Apostolova N. *et al*., 2013) and in this context, Ca^{2+} seems to be also involved in the upregulation of *LONP1* under these treatments.

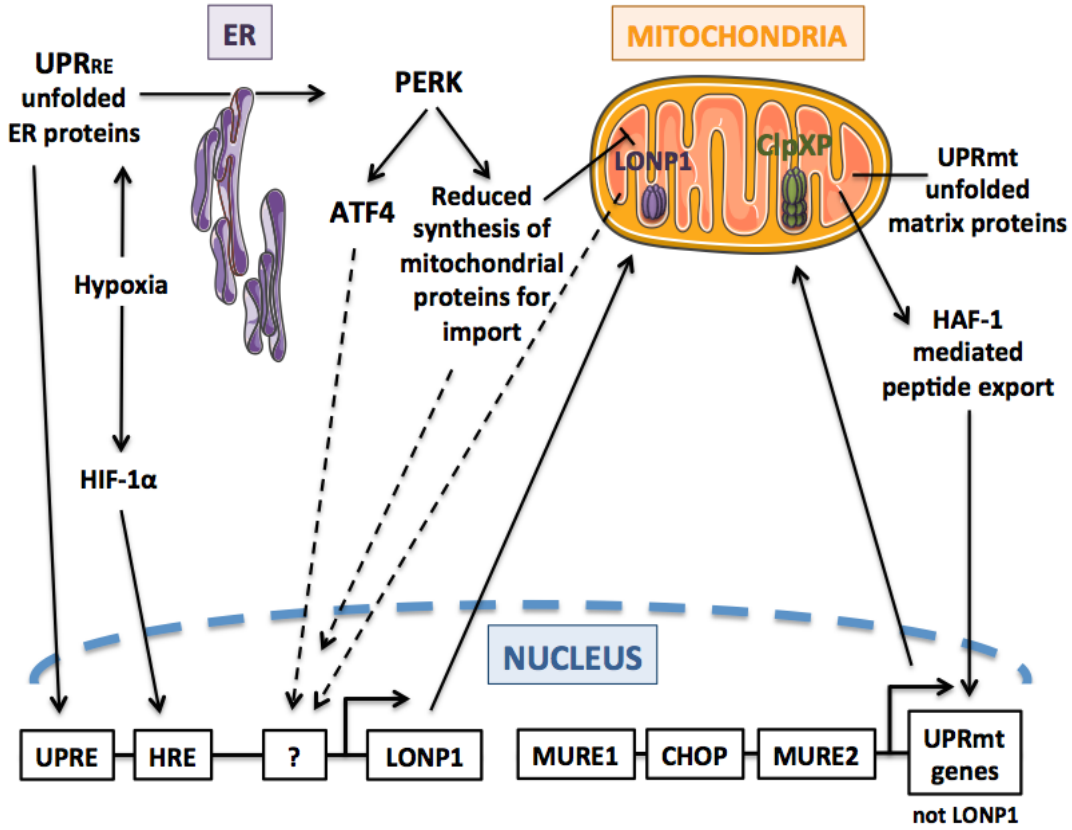

Figure V.1. Regulation of LONP1 in the ER and mitochondrial unfolded protein responses. On the one hand, the consequences of the unfolded protein response in the ER (UPRER). The accumulation of

unfolded or misfolded proteins in the ER lumen activates PERK which leads to the selective reduction of cytosolic protein synthesis, which includes proteins imported into mitochondria. The reduction in proteins imported into the MM may result in a stoichiometric imbalance of mitochondrial proteins that must assemble to form functional complexes. PERK activation also induces the expression of *LONP1* through ATF4, but the transcription factors implicated remain to be identified. In addition, signals from the cytosol or the mitochondrion may transcriptionally upregulate the *LONP1* gene by an unknown mechanism. Alternatively, accumulation of unfolded proteins in the ER may activate *LONP1* expression by binding to a putative UPRE (unfolded protein response element), which has yet to be identified. Hypoxia is a physiological inducer of ER stress that has been shown to upregulate *LONP1* expression by the activation of HIF-1α, which binds to HREs (hypoxia response element) within the promoter of *LONP1*. Finally, the resulting increase of LONP1 may function to re-establish mitochondrial homeostasis. On the other hand, the consequences of the unfolded protein response in the mitochondria (UPRmt). Accumulation of unfolded or misfolded proteins lead to the UPRmt, which is initiated by ClpXP-dependent degradation of protein substrates thereby generating peptides that are effluxed from the MM to the cytosol by the HAF-1 transporter located in IMM. These peptides activate transcription factors which, binding to MURE and CHOP sequences, upregulate the expression of UPRmt-related genes such as *CLPP*, but not *LONP1*. The increased expression of *CLPP* relieves mitochondrial stress and re-establishes mitochondrial homeostasis. Figure modified from Venkatesh S. *et al*., 2012.

Abundant evidence demonstrates that mitochondria function in close collaboration with the ER, but precisely how this is affected by distinct pathophysiological conditions remains to be determined. On examining the role of LONP1 we have found that its content in the mitochondrion is depleted upon dual ER stress/mitochondrial dysfunction, while its extramitochondrial presence is increased. Having observed that LONP1 presence is increased in the cytosol and that this protease colocalize with the ER protein calnexin, which is considered a MAMs component, we speculated about LONP1's location in MAMs. The analysis of subcellular fractions (cytosol, ER, mitochondria and MAMs) revealed that LONP1 is mainly present in mitochondria in basal conditions but, under ER stress and/or different types of mitochondrial dysfunction, it is present in all four fractions and notably in the cytosol, ER and MAMs with EFV treatment. In summary, surprisingly, LONP1 presence decreased in mitochondria in parallel with an increase in ER and MAMs under dual ER stress/mitochondrial dysfunction. This, however, is not the case when cells are exposed to classical mitotoxic stimuli such as Rot or CCCP, which underlines, once

more, the importance of the role of ER stress in this phenomenon. In addition, interestingly, the pattern of LONP1 expression was very similar to that of Grp75, pointing to the possibility that LONP1 is itself a MAMs protein whose presence in MAMs is greatly incremented in our model. The fact that the ER stress sensor PERK is enriched in MAMs and induces LONP1 expression, supports the novel function of LONP1 in the interconnection between mitochondrial dysfunction and ER stress. In addition, the evidence presented here is in line with a recent proteomic analysis of MAMs during RNA virus infection, which identified LONP1 as a mitochondrial antiviral-signaling protein (MAVS)-interacting protein (Horner S.M. *et al*., 2015). MAVS, itself considered a MAMs component, is recognized as a crucial participant in the innate immune response to RNA virus infection in mammalian cells. The fact that LONP1 regulation occurs in the presence of an antiretroviral drug, as shown by our results, significantly bolsters the findings of said study and opens a new and very promising route for research.

There is a growing body of evidence that pinpoints LONP1 as a human stress protein whose levels increase after exposure to multiple independent stressors. In light of our results, it is tempting to speculate on LONP1´s location during these specific cellular insults. Moreover, LONP1 is regarded as MM protease hence its upregulation upon the mentioned stress stimuli would be assumed to enhance its canonical mitochondrial function. What exactly is its putative role in the MAMs is unknown and remains to be explored.

Based on our results, we analysed the specificity of the LONP1 upregulation under dual ER stress/mitochondrial dysfunction studying the expression of another protein involved in the mitochondrial proteostasis, ClpX. Neither of the treatments altered the expression of this protease, while the expression of HSP90 chaperones was increased with both EFV and TG in hepatic cells. In this work we have also studied the role of LONP1 in the effects induced by EFV. Besides confirming the protective role of LONP1 under oxidative stress, we have also seen that this protease could be involved in the autophagy regulation under dual ER/mitochondrial stress. These results are similar to that observed with the protease HTRA2 (localized in the IMS) whose loss in HeLa and murine cells results in ROS increase, higher frequency of mtDNA mutations,

accumulation of unfolded elements of ETC and OxPhos impairment (Moisoi N. *et al*., 2009, Goo H.G. *et al*., 2013). Interestingly, HTRA2 proteolytic activity also contributes to regulate both basal and ER stress-induced autophagy activation (Li B. *et al*., 2010). It is known that beyond UPRmt, mitochondrial fusion and mitophagy provide additional levels of quality control in the mitochondrial stress response however, the connection between them remains unclear. The expression of unfolded proteins in the MM causes the accumulation of PINK1 on energetically healthy mitocondria in mammalian cells, resulting in mitophagy and subsequent reduction of unfolded protein load (Jin S.M. and Youle R.J., 2013). Also, PINK1 accumulation is greatly enhanced by the knockdown of the LONP1 protease. It suggests that the accumulation of unfolded proteins in mitochondria is a physiological trigger of mitophagy. In conclusion, our result suggests that LONP1 could be involved in the autophagy activation under dual ER/mitochondrial stress, pointing out the specificity and complexity of EFV's actions.

On the other hand, the primacy of EFV is being challenged by newer drugs that, although not significantly more effective at lowering viral load and restoring immune function, are claimed to have a better toxicological profile and to result, consequently, in greater patient tolerance and adherence, critical factors to the success of any ART in an age when HIV has become a lifelong illness. In accordance with this, we set out to study the expression of LONP1 in cultured hepatic cells exposed to short term treatment with clinically relevant concentrations of the newer antiretroviral drugs (RAL, DRV and RPV). Firstly, we analysed their mitochondrial toxicity and we observed that none altered mitochondrial function (superoxide production and $\Delta\Psi_m$ were not significantly affected) in contrast to EFV. In addition, it has been seen that they do not alter protein expression of LC3-II and CHOP, in contrast to EFV (Blas-García A. *et al*., 2014). In line with this, as expected, they did not increase the expression of LONP1 either. The effect of the widely used NRTIs (ABC and ddI) on LONP1 expression was also studied in this work. These drugs are known to possess mitotoxic potential due to their ability to inhibit mitochondrial DNA Pol-γ (Martin J.L *et al*., 1994; Walker U.A. *et al*., 2002; Apostolova N. *et al*., 2011b). They did not alter LONP1, while they produced a reduction of $\Delta\Psi_m$, which underlines, once more, the importance of the role of ER stress in this phenomenon. It has been reported that the widely used PIs (LPV and RTV)

induce ER stress without evident mitotoxicity in Hep3B cells (Apostolova N. *et al.*, 2013). Our results show that LPV induced a concentration-dependent increase of LONP1 protein and gene expression, similar to that produced by EFV and TG. In summary, in contrast to EFV, neither of the antiretrovirals used increased the expression of LONP1, except LPV. These results support the involvement of ER stress in the upregulation of LONP1 in our model of dual ER stress/mitochondrial dysfunction. Alterations of LONP1 levels have been associated with HIV treatment (Pinti M. *et al.*, 2010), however, it has been difficult to attribute the effect observed on LONP1 expression to a single drug, since cART is a very complex therapy. Pinti and colleagues have shown that NRTIs, and in particular stavudine, determine LONP1 upregulation in SW872 liposarcoma cells; this increase is caused by higher levels of ROS (Pinti M. *et al.*, 2010). To our knowledge, ours is the first study to assess the effect of these anti-HIV drugs on the expression of LONP1.

Our results lead to several conclusions: firstly, the stress response triggered by clinical concentrations of EFV in hepatic cells is diminished in those lacking functional mitochondria. These findings (i) highlight the participation of this organelle in the effects induced by EFV on hepatic cells and (ii) reveal both similarities and differences when compared to the responses invoked by two other distinct mitochondrial stressors, pointing out the specificity and complexity of EFV's actions. Secondly, mitochondrial dynamics and mitochondria/ER contact are differentially regulated upon different types of mitochondrial and ER stress. Thirdly, LONP1 is transcriptionally upregulated under these conditions; and, fourthly, and most importantly, LONP1 plays a role in the interorganellar crosstalk between the ER and mitochondria as a MAMs component itself (Fig.V.2). We believe that these findings contribute in a considerable way to the growing knowledge regarding mitochondria-ER inter-regulations. Indeed, we hope they are a starting point for a more comprehensive understating of the role of LONP1 under complex stressful conditions. Also, the effects of EFV described here may throw light on the hepatic stress induced by its clinical use.

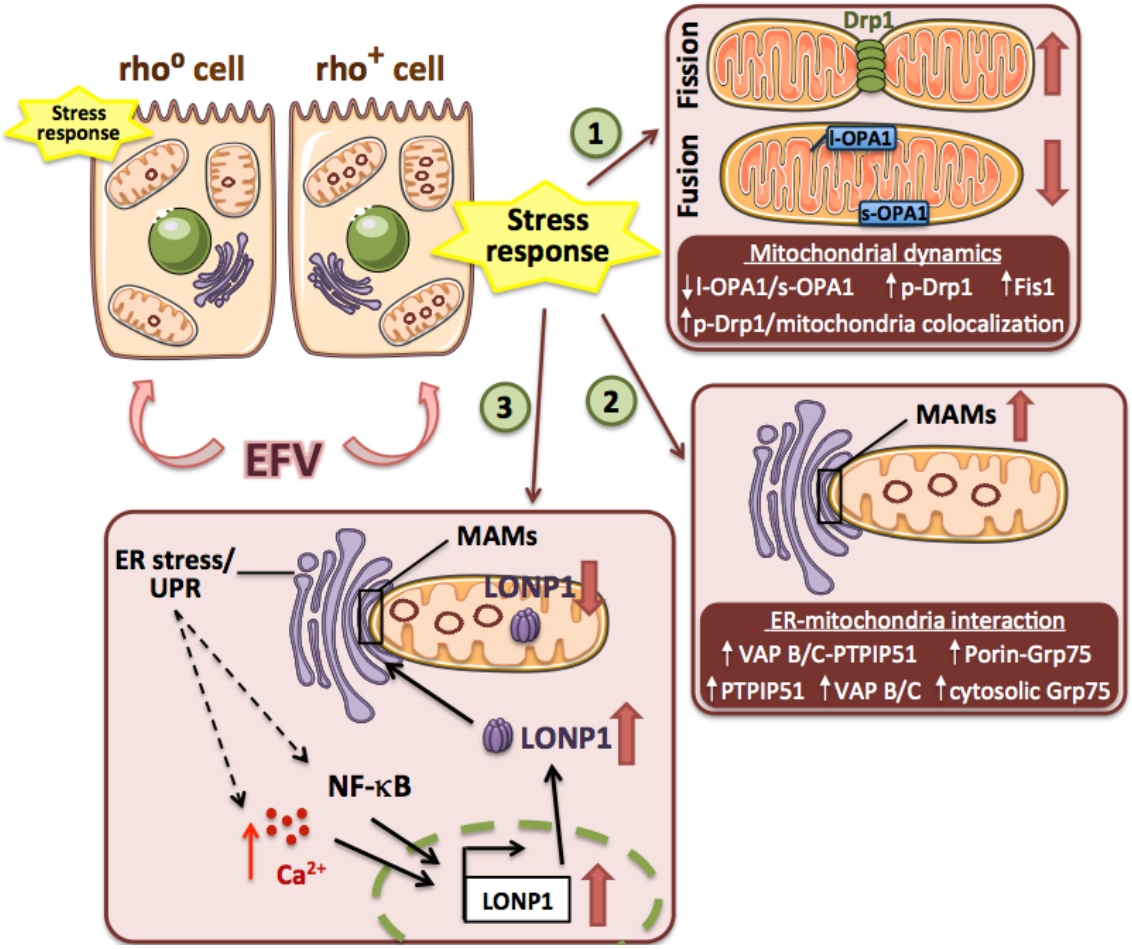

Figure V.2. Mitochondria and ER interplay at the core of EFV-induced hepatic effects. The stress response (altered mitocondrial function and cell viability) triggered by EFV in hepatic cells is diminished in those lacking functional mitocondria (rho^0 cells), which supports the participation of this organelle in the dual ER stress/mitochondrial dysfunction induced by EFV. In this context, our study reveals several findings: (1) EFV alters mitochondrial dynamics, induce mitochondrial fission (increasing Fis1, p-Drp1 and its translocation to mitochondria) and decrease fusion (decrease l-OPA1/s-OPA1 ratio) in hepatic cells; (2) EFV enhances mitochondria/ER interaction, as shown by increasing MAMs protein partners (VAP B/C-PTPIP51 and Porin-Grp75) and expression of them; and (3) EFV upregulates LONP1 expression, while its content in the mitochondrion is depleted upon dual ER stress/mitochondrial dysfunction, its extramitochondrial presence (ER and MAMs) is increased. This finding suggests that LONP1 plays a role in the interorganellar crosstalk between the ER and mitochondria as a MAMs component itself. The upregulation of LONP1 could be regulated by NF-κB and the increased cytosolic Ca^{2+} concentration, both ER stress outcomes.

VI. CONCLUSIONS

1. **The stress response triggered by clinical concentrations of EFV in cultured human hepatic cells is diminished in those lacking functional mitochondria. EFV-treated rho^{o} cells exhibited a substantial reduction in the parameters indicative of mitochondrial interference and the cytotoxic effect was less pronounced than in wild-type cells. The effect of EFV was both similar and different from those of two distinct mitochondrial stressors, TG and Rot, depending on the parameter studied. These findings suggest that the hepatic action of EFV involves acute interference with mitochondria.**

2. **EFV alters mitochondrial dynamics, induces mitochondrial fission and decreases fusion in cultured human hepatic cells. Markers of mitochondrial dynamics were expressed differentially upon different types of mitochondrial and ER stress, which points to a specificity of the dual ER/mitochondrial stress induced by EFV.**

3. **Mitochondria/ER contact is enhanced in cultured human hepatic cells exposed to EFV as shown by co-immunoprecipitation experiments of MAMs protein partners. This effect was not observed with other distinct mitochondrial/ER stressors supporting, once more, the specificity of EFV's effects.**

4. **The highly conserved mitochondrial protease LONP1 is upregulated at mRNA and protein levels in cultured human hepatic cells under different types of mitochondrial and ER stress. Upon treatment with EFV, its content in the mitochondrion is depleted while its extramitochondrial presence (ER and MAMs) is increased, which suggests that LONP1 plays a role in the interorganellar crosstalk between the ER and mitochondria as a MAMs component itself.**

5. **NF-κB and cytosolic Ca^{2+} seem to regulate *LONP1* gene expression in cultured human hepatic cells treated with EFV. Neither of the distinct mitochondrial/ER stressors alters the expression of the mitochondrial protease ClpX, while the expression of HSP90 chaperones is increased with EFV and TG.**

6. **LONP1 is involved in the EFV-induced autophagy activation in hepatic cells since the effect of EFV treatment in LC3-II expression was absent when *LONP1* was silenced.**

7. **Neither of the newer antiretroviral drugs (RAL, DRV and RPV) or the widely used NRTIs (ABC and ddI), which possess mitotoxic potential, increases the expression of LONP1. In contrast, the PI LPV, that induces ER stress without evident mitotoxicity in hepatic cells, increases LONP1 expression, which underlines the importance of the role of ER stress in this phenomenon.**

VII. CONCLUSIONES

1. **La respuesta a estrés provocada por concentraciones clínicas de EFV en células hepáticas humanas cultivadas disminuye en aquellas que carecen de mitocondrias funcionales. Las células rho^{o} tratadas con EFV mostraron una reducción importante en los parámetros indicativos de interferencia mitocondrial y el efecto citotóxico fue menos pronunciado que en las células *wild-type*. El efecto de EFV fue tanto similar como diferente de aquellos producidos por dos factores estresantes mitocondriales distintos, TG y Rot, dependiendo del parámetro estudiado. Estos hallazgos sugieren que la acción hepática de EFV implica una interferencia aguda con la mitocondria.**

2. **EFV altera la dinámica mitocondrial, induce la fisión mitocondrial y disminuye la fusión en células hepáticas humanas cultivadas. Los marcadores de la dinámica mitocondrial se expresaron diferencialmente ante diferentes tipos de estrés mitocondrial y de RE, lo que apunta a una especificidad del doble estrés mitocondrial/RE inducido por EFV.**

3. **El contacto mitocondria/RE aumenta en células hepáticas humanas cultivadas expuestas a EFV, como demuestran los experimentos de co-inmunoprecipitación de complejos proteicos de las MAMs. Este efecto no se observó con otros factores distintos de estrés mitocondrial/RE apoyando, una vez más, la especificidad de los efectos de EFV.**

4. **La proteasa mitocondrial altamente conservada LONP1 es regulada positivamente a nivel de ARNm y de proteína en células hepáticas humanas cultivadas bajo diferentes tipos de estrés mitochondrial y de RE. Tras el tratamiento con EFV, disminuye su contenido en la mitocondria, mientras que su presencia extramitocondrial (RE y MAMs) aumenta, lo que sugiere que LONP1 juega un papel en la comunicación entre el RE y la mitocondria como componente en sí de las MAMs.**

5. **El NF-κB y el Ca^{2+} citosólico parecen regular la expresión génica de *LONP1* en células hepáticas humanas cultivadas tratadas con EFV. Ninguno de los distintos factores de estrés mitocondrial/RE altera la expresión de la proteasa mitocondrial ClpX, mientras que la expresión de las chaperonas HSP90 aumenta con EFV y TG.**

6. **LONP1 participa en la activación de la autofagia inducida por EFV en células hepáticas, ya que no se observó el efecto del tratamiento con EFV en la expresión de LC3-II cuando se silenció *LONP1*.**

7. **Ninguno de los nuevos fármacos antirretrovirales (RAL, DRV y RPV) o de los ampliamente utilizados ITIAN (ABC y ddI), que poseen potencial mitotóxico, aumenta la expresión de LONP1. Por el contrario, el IP LPV, que induce estrés de RE sin evidente mitotoxicidad en células hepáticas, aumenta la expresión de LONP1, lo que destaca la importancia del papel del estrés de RE en este fenómeno.**

VIII. BIBLIOGRAPHY

Abdul-Ghani M.A., DeFronzo R.A. Mitochondrial dysfunction, insulin resistance, and type 2 diabetes mellitus. *Curr Diab Rep* 2008; 8(3):173-8.

Achleitner G., Gaigg B., Krasser A., Kainersdorfer E., Kohlwein S.D., Perktold A., Zellnig G., Daum G. Association between the endoplasmic reticulum and mitochondria of yeast facilitates interorganelle transport of phospholipids through membrane contact. *Eur J Biochem* 1999; 264(2):545-53.

AIDS Study Group (GESIDA) of the Spanish Society of Infectious Diseases, Clinical Microbiology, the National AIDS Plan. Executive summary of the GESIDA/National AIDS Plan Consensus Document on Antiretroviral Therapy in Adults Infected by the Human Immunodeficiency Virus (Updated January 2016). *Enferm Infecc Microbiol Clin* 2016; 34(7):439-51.

AIDSinfo (a service of the U.S. Department of Health and Human Services). Guidelines for the use of antiretroviral agents in HIV-1-infected adults and adolescents. Available at: https://aidsinfo.nih.gov/guidelines/html/1/adult-and-adolescent-arv-guidelines/31/adverse-effects-of-arv (accessed November 2016).

Al-Furoukh N., Ianni A., Nolte H., Hölper S., Krüger M., Wanrooij S., Braun T. ClpX stimulates the mitochondrial unfolded protein response (UPR(mt)) in mammalian cells. *Biochim Biophys Acta* 2015; 1853(10 Pt A):2580-91.

Aldridge J.E., Horibe T., Hoogenraad N.J. Discovery of genes activated by the mitochondrial unfolded protein response (mtUPR) and cognate promoter elements. *PLoS One* 2007; 2(9):e874.

Allbritton N.L., Meyer T., Stryer L. Range of messenger action of calcium ion and inositol 1,4,5-trisphosphate. *Science* 1992; 258(5089):1812-5.

Amacher D.E. Drug-associated mitochondrial toxicity and its detection. *Curr Med Chem* 2005; 12(16):1829-39.

Anand R., Wai T., Baker M.J., Kladt N., Schauss A.C., Rugarli E., Langer T. The i-AAA protease YME1L and OMA1 cleave OPA1 to balance mitochondrial fusion and fission. *J Cell Biol* 2014; 204(6):919-29.

Anderson G.R., Brenner B.M, Swede H., Chen N., Henry W.M., Conroy J.M., Karpenko M.J., Issa J.P., Bartos J.D., Brunelle J.K., Jahreis G.P, Kahlenberg M.S., Basik M., Sait S., Rodriguez-Bigas M.A., Nowak N.J., Petrelli N.J., Shows T.B., Stoler D.L. Intrachromosomal genomic instability in human sporadic colorectal cancer measured by genome-wide allelotyping and inter-(simple sequence repeat) PCR. *Cancer Res* 2001; 61(22):8274-83.

Anderson S., Bankier A.T., Barrell B.G., de Bruijn M.H., Coulson A.R., Drouin J., Eperon I.C., Nierlich D.P., Roe B.A., Sanger F., Schreier P.H., Smith A.J., Staden R., Young I.G. Sequence and organization of the human mitochondrial genome. *Nature* 1981; 290(5806):457-65.

Anelli T., Bergamelli L., Margittai E., Rimessi A., Fagioli C., Malgaroli A., Pinton P., Ripamonti M., Rizzuto R., Sitia R. Ero1alpha regulates Ca(2+) fluxes at the endoplasmic reticulum-mitochondria interface (MAM). *Antioxid Redox Signal* 2012; 16(10):1077-87.

Anthérieu S., Chesné C., Li R., Camus S., Lahoz A., Picazo L., Turpeinen M., Tolonen A., Uusitalo J., Guguen-Guillouzo C., Guillouzo A. Stable expression, activity, and inducibility of cytochromes P450 in differentiated HepaRG cells. *Drug Metab Dispos* 2010; 38(3):516-25.

Apostolova N., Blas-Garcia A., Esplugues J.V. Mitochondria sentencing about cellular life and death: a matter of oxidative stress. *Curr Pharm Des* 2011(a); 17(36):4047-60.

Apostolova N., Blas-García A., Esplugues J.V. Mitochondrial interference by anti-HIV drugs: mechanisms beyond Pol-γ inhibition. *Trends Pharmacol Sci* 2011(b); 32(12):715-25.

Apostolova N., Gomez-Sucerquia L.J., Alegre F., Funes H.A., Victor V.M., Barrachina M.D., Blas-Garcia A., Esplugues J.V. ER stress in human hepatic cells treated with Efavirenz: mitochondria again. *J Hepatol* 2013; 59(4):780-9.

Apostolova N., Gomez-Sucerquia L.J., Gortat A., Blas-Garcia A., Esplugues J.V. Compromising mitochondrial function with the antiretroviral drug efavirenz induces cell survival-promoting autophagy. *Hepatology* 2011(c); 54(3):1009-19.

Apostolova N., Gomez-Sucerquia L.J., Moran A., Alvarez A., Blas-Garcia A., Esplugues J.V. Enhanced oxidative stress and increased mitochondrial mass during efavirenz-induced apoptosis in human hepatic cells. *Br J Pharmacol* 2010; 160(8):2069-84.

Archer S.L. Mitochondrial dynamics–mitochondrial fission and fusion in human diseases. *N Engl J Med* 2013; 369(23):2236-51.

Argilés J.M., Busquets S., López-Soriano F.J. The role of uncoupling proteins in pathophysiological states. *Biochem Biophys Res Commun* 2002; 293(4):1145-52.

Aronis A., Komarnitsky R., Shilo S., Tirosh O. Membrane depolarization of isolated rat liver mitochondria attenuates permeability transition pore opening and oxidant production. *Antioxid Redox Signal* 2002; 4(4):647-54.

Arruda A.P., Pers B.M., Parlakgül G., Güney E., Inouye K., Hotamisligil G.S. Chronic enrichment of hepatic ER-mitochondria contact sites leads to calcium dependent mitochondrial dysfunction in obesity. *Nat Med* 2014; 20(12):1427-35.

Auman J.T., Chou J., Gerrish K., Huang Q., Jayadev S., Blanchard K., Paules R.S. Identification of genes implicated in methapyrilene- induced hepatotoxicity by comparing differential gene expression in target and nontarget tissue. *Environ Health Perspect* 2007; 115(4):572-8.

Autran B., Carcelain G., Li T.S., Blanc C., Mathez D., Tubiana R., Katlama C., Debre P., Leibowitch J. Positive effects of combined antiretroviral therapy on CD4+ T cell homeostasis and function in advanced HIV disease. *Science* 1997; 277(5322):112-6.

Bahat A., Perlberg S., Melamed-Book N., Isaac S., Eden A., Lauria I., Langer T., Orly J. Transcriptional activation of LON gene by a new form of mitochondrial stress: A role for the nuclear respiratory factor 2 in StAR overload response (SOR). *Mol Cell Endocrinol* 2015; 408:62-72.

Baker T.A, Sauer R.T. ClpXP, an ATP-powered unfolding and protein-degradation machine. *Biochim Biophys Acta* 2012; 1823(1):15-28.

Balzarini J. Metabolism and mechanism of antiretroviral action of purine and pyrimidine derivatives. *Pharm World Sci* 1994; 16(2):113-26.

Barre-Sinoussi F., Chermann J.C., Rey F., Nugeyre M.T., Chamaret S., Gruest J., Dauguet C., Axler-Blin C., Vézinet-Brun F., Rouzioux C., Rozenbaum W., Montagnier L. Isolation of a T- Lymphotropic retrovirus from a patient at risk for acquired immune deficiency síndrome (AIDS). *Science* 1983; 220(4599):868-71.

Beaver J.P., Waring P. Thapsigargin induces mitochondrial dysfunction and apoptosis in the mastocytoma P815 cell line and in mouse thymocytes. *Cell Death Differ* 1996; 3(4):415-24.

Bell R.M, Ballas L.M., Coleman R.A. Lipid topogenesis. *J Lipid Res* 1981; 22(3):391-403.

Bereiter-Hahn J. Behavior of mitochondria in the living cell. *Int Rev Cytol* 1990; 122:1-63.

Bernales S., McDonald K.L., Walter P. Autophagy counterbalances endoplasmic reticulum expansion during the unfolded protein response. *PLoS Biol* 2006; 4(12):e423.

Bernstein S.H., Venkatesh S., Li M., Lee J., Lu B., Hilchey S.P., Morse K.M., Metcalfe H.M., Skalska J., Andreeff M., Brookes P.S., Suzuki C.K. The mitochondrial ATP-dependent Lon protease: a novel target in lymphoma death mediated by the synthetic triterpenoid CDDO and its derivatives. *Blood* 2012; 119(14):3321-9.

Bezprozvanny I., Watras J., Ehrlich B.E. Bell-shaped calcium-response curves of Ins(1,4,5)P3- and calcium-gated channels from endoplasmic reticulum of cerebellum. *Nature* 1991; 351(6329):751-4.

Birner R., Burgermeister M., Schneiter R., Daum G. Roles of phosphatidylethanolamine and of its several biosynthetic pathways in Saccharomyces cerevisiae. *Mol Biol Cell* 2001; 12(4):997-1007.

Blas-García A., Apostolova N., Ballesteros D., Monleón D., Morales J.M., Rocha M., Victor V.M., Esplugues J.V. Inhibition of mitochondrial function by efavirenz increases lipid content in hepatic cells. *Hepatology* 2010; 52(1):115-25.

Blas-García A., Esplugues J.V., Apostolova N. Twenty years of HIV-1 non-nucleoside reverse transcriptase inhibitors: time to reevaluate their toxicity. *Curr Med Chem* 2011; 18(14):2186-95.

Blas-García A., Polo M., Alegre F., Funes H.A., Martínez E., Apostolova N., Esplugues J.V. Lack of mitochondrial toxicity of darunavir, raltegravir and rilpivirine in neurons and hepatocytes: a comparison with efavirenz. *J Antimicrob Chemother* 2014; 69(11):2995-3000.

Boehning D., Patterson R.L., Sedaghat L., Glebova N.O., Kurosaki T., Snyder S.H. Cytochrome c binds to inositol (1,4,5) trisphosphate receptors, amplifying calcium-dependent apoptosis. *Nat Cell Biol* 2003; 5(12):1051-61.

Bonfanti P., Valsecchi L., Parazzini F., Carradori S., Pusterla L., Fortuna P., Timillero L., Alessi F., Ghiselli G., Gabbuti A., Di Cintio E., Martinelli C., Faggion I., Landonio S., Quirino T. Incidence of adverse reactions in HIV patients treated with protease inhibitors: a cohort study. Coordinamento Italiano Studio Allergia e Infezione da HIV (CISAI) Group. *J Acquir Immune Defic Syndr* 2000; 23(3):236-45.

Bononi A., Bonora M., Marchi S., Missiroli S., Poletti F., Giorgi C., Pandolfi P.P., Pinton P. Identification of PTEN at the ER and MAMs and its regulation of Ca(2+) signaling and apoptosis in a protein phosphatase-dependent manner. *Cell Death Differ* 2013; 20(12):1631-43.

Bosch M., Marí M., Gross S.P., Fernández-Checa J.C, Pol A. Mitochondrial cholesterol: a connection between caveolin, metabolism, and disease. *Traffic* 2011; 12(11):1483-9.

Bota D.A., Davies K.J. Lon protease preferentially degrades oxidized mitochondrial aconitase by an ATP-stimulated mechanism. *Nat Cell Biol* 2002; 4(9):674-80.

Bota D.A., Davies K.J. Mitochondrial Lon protease in human disease and aging: Including an etiologic classification of Lon-related diseases and disorders. *Free Radic Biol Med* 2016. pii:S0891-5849(16)30319-7.

Boveris A., Cadenas E. Cellular sources and steady-state levels of reactive oxygen species. In: L.B. Clerch, D.J. Massaro (eds.). Oxygen, Gene Expression and Cellular Function. Marcel Dekker, New York, 1997; 1-25.

Bozidis P., Williamson C.D., Wong D.S., Colberg-Poley A.M. Trafficking of UL37 proteins into mitochondrion-associated membranes during permissive human cytomegalovirus infection. *J Virol* 2010; 84(15):7898-903.

Bravo R., Vicencio J.M., Parra V., Troncoso R., Munoz J.P., Bui M., Quiroga C., Rodriguez A.E., Verdejo H.E., Ferreira J., Iglewski M., Chiong M., Simmen T., Zorzano A., Hill J.A., Rothermel B.A., Szabadkai G., Lavandero S. Increased ER-mitochondrial coupling promotes mitochondrial respiration and bioenergetics during early phases of ER stress. *J Cell Sci* 2011; 124(Pt 13):2143-52.

Bravo-Sagua R., Rodriguez A.E., Kuzmicic J., Gutierrez T., Lopez-Crisosto C., Quiroga C., Díaz-Elizondo J., Chiong M., Gillette T.G., Rothermel B.A., Lavandero S. Cell death and survival through the endoplasmic reticulum-mitochondrial axis. *Curr Mol Med* 2013; 13(2):317-29.

Brück S., Witte S., Brust J., Schuster D., Mosthaf F., Procaccianti M., Rump J.A., Klinker H., Petzold D., Hartmann M. Hepatotoxicity in patients prescribed efavirenz or nevirapine. *Eur J Med* 2008; 13(7):343-8.

Bui M., Gilady S.Y., Fitzsimmons R.E., Benson M.D., Lynes E.M., Gesson K., Alto N.M., Strack S., Scott J.D., Simmen T. Rab32 modulates apoptosis onset and mitochondria-associated membrane (MAM) properties. *J Biol Chem* 2010; 285(41):31590-602.

Bumpus N.N., Kent U.M., Hollenberg P.F. Metabolism of efavirenz and 8-hydroxyefavirenz by P450 2B6 leads to inactivation by two distinct mechanisms. *J Pharmacol Exp Ther* 2006; 318(1):345-51.

Burger D., van der Heiden I., la Porte C., van der Ende M., Groeneveld P., Richter C., Koopmans P., Kroon F., Sprenger H., Lindemans J., Schenk P., van Schaik R. Interpatient variability in the pharmacokinetics of the HIV non-nucleoside reverse transcriptase inhibitor efavirenz: the effect of gender, race, and CYP2B6 polymorphism. *Br J Clin Pharmacol* 2006; 61(2):148-54.

Cadenas E., Davies K.J. Mitochondrial free radical generation, oxidative stress, and aging. *Free Radic Biol Med* 2000; 29(3-4):222-30.

Caron-Debarle M., Lagathu C., Boccara F., Vigouroux C., Capeau J. HIV-associated lipodystrophy: from fat injury to premature aging. *Trends Mol Med* 2010; 16(5):218-29.

Carr D.F., la Porte C.J., Pirmohamed M., Owen A., Cortes C.P. Haplotype structure of CYP2B6 and association with plasma efavirenz concentrations in a Chilean HIV cohort. *J Antimicrob Chemother* 2010; 65(9):1889-93.

Cartoni R., Martinou J.C. Role of mitofusin 2 mutations in the physiopathology of Charcot–Marie–Tooth disease type 2A. *Exp Neurol* 2009; 218(2):268-73.

Chan D.C. Fusion and fission: interlinked processes critical for mitochondrial health. *Annu Rev Genet* 2012; 46:265-87.

Chan D.C. Mitochondria: dynamic organelles in disease, aging, and development. *Cell* 2006; 125(7):1241-52.

Chang C.R., Blackstone C. Cyclic AMP-dependent protein kinase phosphorylation of Drp1 regulates its GTPase activity and mitochondrial morphology. *J Biol Chem* 2007; 282(30):21583-7.

Chen B., Piel W.H., Gui L., Bruford E., Monteiro A. The HSP90 family of genes in the human genome: insights into their divergence and evolution. *Genomics* 2005; 86(6):627-37.

Chen H., Chomyn A., Chan D.C. Disruption of fusion results in mitochondrial heterogeneity and dysfunction. *J Biol Chem* 2005; 280(28):26185-92.

Chen H., Detmer S.A., Ewald A.J., Griffin E.E., Fraser S.E., Chan D.C. Mitofusins Mfn1 and Mfn2 coordinately regulate mitochondrial fusion and are essential for embryonic development. *J Cell Biol* 2003; 160(2):189-200.

Chiao S.K., Romero D.L., Johnson D.E. Current HIV therapeutics: mechanistic and chemical determinants of toxicity. *Curr Opin Drug Discov Devel* 2009; 12(1):53-60.

Chin K.T., Kang G., Qu J., Gardner L.B., Coetzee W.A., Zito E., Fishman G.I., Ron D. The sarcoplasmic reticulum luminal thiol oxidase ERO1 regulates cardiomyocyte excitation-coupled calcium release and response to hemodynamic load. *FASEB J* 2011; 25(8):2583-91.

Clapham D.E. Calcium signaling. *Cell* 2007; 131(6):1047-58.

Clark L.C., Wolf R., Granger D., Taylor Z. Continuous recording of blood oxygen tensions by polarography. *J Appl Physiol* 1953; 6(3):189-93.

Clumeck N., Pozniak A., Raffi F. EACS Executive Committee. European AIDS Clinical Society (EACS) guidelines for the clinical management and treatment of HIV-infected adults. *HIV Med* 2008; 9(2):65-71.

Cnop M., Foufelle F., Velloso L.A. Endoplasmic reticulum stress, obesity and diabetes. *Trends Mol Med* 2012; 18(1):59-68.

Corydon T.J., Bross P., Holst H.U., Neve S., Kristiansen K., Gregersen N., Bolund L. A human homologue of Escherichia coli ClpP caseinolytic protease: recombinant expression, intracellular processing and subcellular localization. *Biochem J* 1998; 331(Pt1):309-16.

Craig A., Sidaway J., Holmes E., Orton T., Jackson D., Rowlinson R., Nickson J., Tonge R., Wilson I., Nicholson J. Systems toxicology: integrated genomic, proteomic and metabonomic analysis of methapyrilene induced hepatotoxicity in the rat. *J Proteome Res* 2006; 5(7):1586-601.

Crandall K.A. Human Immunodeficiency Viruses (HIV). In: eLS-John Wiley & Sonds Ltd, Chichester, 2001. http://www. esl. net [doi:10. 1038/npg. els. 0000417].

Cribbs J.T., Strack S. Reversible phosphorylation of Drp1 by cyclic AMP-dependent protein kinase and calcineurin regulates mitochondrial fission and cell death. *EMBO Rep* 2007; 8(10):939-44.

Crutchley R.D., Guduru R.C., Cheng A.M. Evaluating the role of atazanavir/cobicistat and darunavir/cobicistat fixed-dose combinations for the treatment of HIV-1 infection. *HIV AIDS (Auckl)* 2016; 8:47-65.

Csordas G., Varnai P., Golenar T., Roy S., Purkins G., Schneider T.G., Balla T., Hajnoczky G. Imaging interorganelle contacts and local calcium dynamics at the ER–mitochondrial interface. *Mol Cell* 2010; 39(1):121-32.

De Brito O.M., Scorrano L. Mitofusin 2 tethers endoplasmic reticulum to mitochondria. *Nature* 2008; 456(7222):605-10.

De Clercq E. Anti-HIV drugs: 25 compounds approved within 25 years after the discovery of HIV. *Int J Antimicrob Agents* 2009; 33(4):307-20.

De Clercq E. Strategies in the design of antiviral drugs. *Nat Rev Drug Discov* 2002; 1(1):13-25.

De Cock K.M., Adjorlolo G., Ekpini E., Sibailly T., Kouadio J., Maran M., Brattegaard K., Vetter K.M., Doorly R., Gayle H.D. Epidemiology and transmission of HIV-2. Why there is no HIV-2 pandemic. *JAMA* 1993; 270(17):2083-6.

De Duve C., Wattiaux R. Functions of lysosomes. *Annu Rev Physiol* 1966; 28:435-92.

De Vos K.J., Mórotz G.M., Stoica R., Tudor E.L., Lau K.F., Ackerley S., Warley A., Shaw C.E., Miller C.C. VAPB interacts with the mitochondrial protein PTPIP51 to regulate calcium homeostasis. *Hum Mol Genet* 2012; 21(6):1299-311.

Deegan S., Saveljeva S., Gorman A.M., Samali A. Stress-induced self-cannibalism: on the regulation of autophagy by endoplasmic reticulum stress. *Cell Mol Life Sci* 2013; 70(14):2425-41.

Dennis E.A., Kennedy E.P. Intracellular sites of lipid synthesis and the biogenesis of mitochondria. *J Lipid Res* 1972; 13(2):263-7.

Desta Z., Saussele T., Ward B., Blievernicht J., Li L., Klein K., Flockhart D.A., Zanger U.M. Impact of CYP2B6 polymorphism on hepatic efavirenz metabolism in vitro. *Pharmacogenomics* 2007; 8(6):547-58.

Dikoglu E., Alfaiz A., Gorna M., Bertola D., Chae J.H., Cho T.J., Derbent M., Alanay Y., Guran T., Kim O.H., Llerenar J.C. Jr., Yamamoto G., Superti-Furga G., Reymond A., Xenarios I., Stevenson B., Campos-Xavier B., Bonafé L., Superti-Furga A., Unger S. Mutations in LONP1, a mitochondrial matrix protease, cause CODAS syndrome. *Am J Med Genet A* 2015; 167(7):1501-9.

Dimmock D.P., Zhang Q., Dionisi-Vici C., Carrozzo R., Shieh J., Tang L.Y., Truong C., Schmitt E., Sifry-Platt M., Lucioli S., Santorelli F.M., Ficicioglu C.H., Rodriguez M., Wierenga K., Enns G.M., Longo N., Lipson M.H., Vallance H., Craigen W.J., Scaglia F., Wong L.J. Clinical and molecular features of mitochondrial DNA depletion due to mutations in deoxyguanosine kinase. *Hum Mutat* 2008; 29(2):330-1.

Dixit E., Boulant S., Zhang Y., Lee A.S., Odendall C., Shum B., Hacohen N., Chen Z.J., Whelan S.P., Fransen M., Nibert M.L., Superti-Furga G., Kagan J.C. Peroxisomes are signaling platforms for antiviral innate immunity. *Cell* 2010; 141(4):668-81.

Dobson C.M. Protein folding and misfolding. *Nature* 2003; 426(6968):884-90.

Domingo P., Lozano F. [Management of antiretroviral drug toxicity]. *Enferm Infecc Microbiol Clin* 2011; 29(7):535-44.

Dominguez S., Ghosn J., Peytavin G., Guiguet M., Tubiana R., Valantin M.A., Murphy R., Bricaire F., Benhamou Y., Katlama C. Impact of hepatitis C and liver fibrosis on antiretroviral plasma drug concentrations in HIV-HCV co-infected patients: the HEPADOSE study. *J Antimicrob Chemother* 2010; 65(11):2445-9.

Dostert C., Petrilli V., Van Bruggen R., Steele C., Mossman B.T., Tschopp J. Innate immune activation through Nalp3 inflammasome sensing of asbestos and silica. *Science* 2008; 320(5876):674-7.

Dragic T., Trkola A., Thompson D.A., Cormier E.G., Kajumo F.A., Maxwell E., Lin S.W., Ying W., Smith S.O., Sakmar T.P., Moore J.P. A binding pocket for a small molecule inhibitor of HIV-1 entry within the transmembrane helices of CCR5. *Proc Natl Acad Sci* 2000; 97(10):5639-44.

Duchen M.R., Szabadkai G. Roles of mitochondria in human disease. *Essays Biochem* 2010; 47:115-37.

Dunn W.A. Jr., Cregg J.M., Kiel J.A., van der Klei I.J., Oku M., Sakai Y., Sibirny A.A., Stasyk O.V., Veenhuis M. Pexophagy: the selective autophagy of peroxisomes. *Autophagy* 2005; 1(2):75-83.

Echenique I.A., Rich J.D. EFV/FTC/TDF-associated hepatotoxicity: a case report and review. *AIDS Patient Care STDS* 2013; 27(9):493-7.

Ehses S., Raschke I., Mancuso G., Bernacchia A., Geimer S., Tondera D., Martinou J.C., Westermann B., Rugarli E.I., Langer T. Regulation of OPA1 processing and mitochondrial fusion by m-AAA protease isoenzymes and OMA1. *J Cell Biol* 2009; 187(7):1023-36.

Ekert P.G., Vaux D.L. The mitochondrial death squad: hardened killers or innocent bystanders? *Curr Opin Cell Biol* 2005; 17(6):626-30.

Elmore S. Apoptosis: A review of programmed cell death. *Toxicol Pathol* 2007; 35(4):495-516.

Evans W.E., McLeod H.L. Pharmacogenomics--drug disposition, drug targets, and side effects. *N Engl J Med* 2003; 348(6):538-49.

Faccenda D., Campanella M. Molecular regulation of the mitochondrial F(1)F(o)-ATPsynthase: physiological and pathological significance of the inhibitory factor 1 (IF(1)). *Int J Cell Biol* 2012; 2012:367934.

Fassan M., D'Arca D., Letko J., Vecchione A., Gardiman M.P., McCue P., Wildemore B., Rugge M., Shupp-Byrne D., Gomella L.G., Morrione A., Iozzo R.V., Baffa R. Mitostatin is down-regulated in human prostate cancer and suppresses the invasive phenotype of prostate cancer cells. *PLoS One* 2011; 6(5):e19771.

Feeney E.R., Mallon P.W. HIV and HAART-Associated Dyslipidemia. *Open Cardiovasc Med J* 2011; 5:49-63.

Feeney E.R., Mallon P.W. Impact of mitochondrial toxicity of HIV-1 antiretroviral drugs on lipodystrophy and metabolic dysregulation. *Curr Pharm Des* 2010; 16(30):3339-51.

Felk S., Ohrt S., Kussmaul L., Storch A., Gillardon F. Activation of the mitochondrial protein quality control system and actin cytoskeletal alterations in cells harbouring the MELAS mitochondrial DNA mutation. *J Neurol Sci* 2010; 295(1-2):46-52.

Fischl M.A., Richman D.D., Grieco M.H., Gottlieb M.S., Volberding P.A., Laskin O.L., Leedom J.M., Groopman J.E., Mildvan D., Schooley R.T. The efficacy of azidothymidine (AZT) in the treatment of patients with AIDS and AIDS-related complex. A double-blind, placebo-controlled trial. *N Engl J Med* 1987; 317(4):185-91.

Flint O.P., Noor M.A., Hruz P.W., Hylemon P.B., Yarasheski K., Kotler D.P., Parker R.A., Bellamine A. The role of protease inhibitors in the pathogenesis of HIV-associated lipodystrophy: cellular mechanisms and clinical implications. *Toxicol Pathol* 2009; 37(1):65-77.

Franchi L., Munoz-Planillo R., Reimer T., Eigenbrod T., Nunez G. Inflammasomes as microbial sensors. *Eur J Immunol* 2010; 40(3):611-5.

Frank P.G., Pavlides S., Cheung M.W., Daumer K., Lisanti M.P. Role of caveolin-1 in the regulation of lipoprotein metabolism. *Am J Physiol Cell Physiol* 2008; 295(1):C242-8.

Frank S., Gaume B., Bergmann-Leitner E.S., Leitner W.W., Robert E.G., Catez F., Smith C.L., Youle R.J. The role of dynamin-related protein 1, a mediator of mitochondrial fission, in apoptosis. *Dev Cell* 2001; 1(4):515-25.

Fransson S., Ruusala A., Aspenstrom P. The atypical Rho GTPases Miro-1 and Miro-2 have essential roles in mitochondrial trafficking. *Biochem Biophys Res Commun* 2006; 344(2):500-10.

Friedman J.R., Lackner L.L., West M., DiBenedetto J.R., Nunnari J., Voeltz G.K. ER tubules mark sites of mitochondrial division. *Science* 2011; 334(6054):358-62.

Fukuda R., Zhang H., Kim J.W., Shimoda L., Dang C.V., Semenza G.L. HIF-1 regulates cytochrome oxidase subunits to optimize efficiency of respiration in hypoxic cells. *Cell* 2007; 129(1):111-22.

Funes H.A., Apostolova N., Alegre F., Blas-Garcia A., Alvarez A., Marti-Cabrera M., Esplugues J.V. Neuronal bioenergetics and acute mitochondrial dysfunction: a clue to understanding the central nervous system side effects of efavirenz. *J Infect Dis* 2014; 210(9):1385-95.

Furuichi T., Yoshikawa S., Miyawaki A., Wada K., Maeda N., Mikoshiba K. Primary structure and functional expression of the inositol 1,4,5-trisphosphate-binding protein P400. Nature 1989; 342(6245):32-8.

Gandre-Babbe S., van der Bliek A.M. The novel tail-anchored membrane protein Mff controls mitochondrial and peroxisomal fission in mammalian cells. *Mol Biol Cell* 2008; 19(6):2402-12.

Garcia-Nafria J., Ondrovicova G., Blagova E., Levdikov V.M., Bauer J.A., Suzuki C.K., Kutejová E., Wilkinson A.J., Wilson K.S. Structure of the catalytic domain of the human mitochondrial Lon protease: proposed relation of oligomer formation and activity. *Protein Sci* 2010; 19(5):987-99.

Geisler S., Holmstrom K.M., Skujat D., Fiesel F.C., Rothfuss O.C., Kahle P.J., Springer W. PINK1/Parkin-mediated mitophagy is dependent on VDAC1 and p62/SQSTM1. *Nat Cell Biol* 2010; 12(2):119-31.

Gellerich F.N., Gizatullina Z., Trumbeckaite S., Nguyen H.P., Pallas T., Arandarcikaite O., Vielhaber S., Seppet E., Striggow F. The regulation of OXPHOS by extramitochondrial calcium. *Biochim Biophys Acta* 2010; 1797(6-7):1018-27.

Gething M.J., Sambrook J. Protein folding in the cell. *Nature* 1992; 355(6355):33-45.

Ghebremedhin B. Maraviroc in Antiretroviral-Naïve HIV-1 Patients. *Infectious Diseases: Research and Treatment* 2012; 5:1-13.

Giacomello M., Drago I., Bortolozzi M., Scorzeto M., Gianelle A., Pizzo P., Pozzan T. Ca^{2+} hot spots on the mitochondrial surface are generated by Ca^{2+} mobilization from stores, but not by activation of store-operated Ca^{2+} channels. *Mol Cell* 2010; 38(2):280-90.

Gibellini L., De Biasi S., Nasi M., Iannone A., Cossarizza A., Pinti M. Mitochondrial proteases as emerging pharmacological targets. *Curr Pharm Des* 2016; 22(18):2679-88.

Gibellini L., Pinti M., Beretti F., Pierri C.L., Onofrio A., Riccio M., Carnevale G., De Biasi S, Nasi M., Torelli F., Boraldi F., De Pol A., Cossarizza A. Sirtuin 3 interacts with Lon protease and regulates its acetylation status. *Mitochondrion* 2014(a); 18:76-81.

Gibellini L., Pinti M., Boraldi F., Giorgio V., Bernardi P., Bartolomeo R., Nasi M., De Biasi S., Missiroli S., Carnevale G., Losi L., Tesei A., Pinton P., Quaglino D., Cossarizza A. Silencing of mitochondrial Lon protease deeply impairs mitochondrial proteome and function in colon cancer cells. *FASEB J* 2014(b); 28(12):5122-35.

Giorgi C., De Stefani D., Bononi A., Rizzuto R., Pinton P. Structural and functional link between the mitochondrial network and the endoplasmic reticulum. *Int J Biochem Cell Biol* 2009; 41(10):1817-27.

Goo H.G., Jung M.K., Han S.S., Rhim H., Kang S. HtrA2/Omi deficiency causes damage and mutation of mitochondrial DNA. *Biochim Biophys Acta* 2013; 1833(8):1866-75.

Gounden V., van Niekerk C., Snyman T., George J.A. Presence of the CYP2B6 516G>T polymorphism, increased plasma efavirenz concentrations and early neuropsychiatric side effects in South African HIV-infected patients. *AIDS Res Ther* 2010; 7:32.

Grad I., Cederroth C.R., Walicki J., Grey C., Barluenga S., Winssinger N., De Massy B., Nef S., Picard D. The molecular chaperone Hsp90alpha is required for meiotic progression of spermatocytes beyond pachytene in the mouse. *PloS One* 2010; 5(12):e15770.

Granot Z., Kobiler O., Melamed-Book N., Eimerl S., Bahat A., Lu B., Braun S., Maurizi M.R., Suzuki C.K., Oppenheim A.B., Orly J. Turnover of mitochondrial steroidogenic acute regulatory (StAR) protein by Lon protease: the unexpected effect of proteasome inhibitors. *Mol Endocrinol* 2007; 21(9):2164-77.

Guillon B., Bulteau A.L., Wattenhofer-Donze M., Schmucker S., Friguet B., Puccio H., Drapier J.C., Bouton C. Frataxin deficiency causes upregulation of mitochondrial Lon and ClpP proteases and severe loss of mitochondrial Fe-S proteins. *FEBS J* 2009; 276(4):1036-47.

Gutiérrez F., Navarro A., Padilla S., Antón R., Masiá M., Borrás J., Martín-Hidalgo A. Prediction of neuropsychiatric adverse events associated with long-term efavirenz therapy, using plasma drug level monitoring. *Clin Infect Dis* 2005; 41(11):1648-53.

Hailey D.W., Rambold A.S., Satpute-Krishnan P., Mitra K., Sougrat R., Kim P.K., Lippincott-Schwartz J. Mitochondria supply membranes for autophagosome biogenesis during starvation. *Cell* 2010; 141(4):656-67.

Halliwell B., Cross C.E. Oxygen-derived species: their relation to human disease and environmental stress. *Environ Health Perspect* 1994; 102(10):5-12.

Hamasaki M., Furuta N., Matsuda A., Nezu A., Yamamoto A., Fujita N., Oomori H., Noda T., Haraguchi T., Hiraoka Y., Amano A., Yoshimori T. Autophagosomes form at ER- mitochondria contact sites. *Nature* 2013; 495(7441):389-93.

Hammer S.M., Eron J.J. Jr., Reiss P., Schooley R.T., Thompson M.A., Walmsley S., Cahn P., Fischl M.A., Gatell J.M., Hirsch M.S., Jacobsen D.M., Montaner J.S., Richman D.D., Yeni P.G., Volberding P.A. International AIDS Society-USA. Antiretroviral treatment of adult HIV infection: recommendations of the International AIDS Society-USA panel. *JAMA* 2008; 300(5):555-70.

Han J., Back S.H., Hur J., Lin Y.H., Gildersleeve R., Shan J., Yuan C.L., Krokowski D., Wang S., Hatzoglou M., Kilberg M.S., Sartor M.A., Kaufman R.J. ER-stress-induced transcriptional regulation increases protein synthesis leading to cell death. *Nat Cell Biol* 2013; 15(5):481-90.

Hansen J., Corydon T.J., Palmfeldt J., Durr A., Fontaine B., Nielsen M.N., Christensen J.H., Gregersen N., Bross P. Decreased expression of the mitochondrial matrix proteases Lon and ClpP in cells from a patient with hereditary spastic paraplegia (SPG13). *Neuroscience* 2008; 153(2):474-482.

Hansford R.G., Hogue B.A., Mildaziene V. Dependence of H2O2 formation by rat heart mitochondria on substrate availability and donor age. *J Bioenerg Biomembr* 1997; 29(1):89-95.

Hao Z., Cooney D.A., Farquhar D., Perno C.F., Zhang K., Masood R., Wilson Y., Hartman N.R., Balzarini J., Johns D.G. Potent DNA chain termination activity and selective inhibition of human immunodeficiency virus reverse transcriptase by 2', 3'-dideoxyuridine-5'- triphosphate. *Mol. Pharmacol* 1990; 37(2):157-63.

Harding H.P., Zhang Y., Ron D. Protein translation and folding are coupled by an endoplasmic- reticulum-resident kinase. *Nature* 1999; 397(6716):271-4.

Hartl F.U., Bracher A., Hayer-Hartl M. Molecular chaperones in protein folding and proteostasis. *Nature* 2011; 475(7356):324-32.

Hatch A.L., Gurel P.S., Higgs H.N. Novel roles for actin in mitochondrial fission. *J Cell Sci* 2014; 127(Pt 21):4549-60.

Hayashi T., Su T.P. Sigma-1 receptor chaperones at the ER-mitochondrion interface regulate Ca(2+) signaling and cell survival. *Cell* 2007; 131(3):596-610.

Hayashi T., Su T.P. Sigma-1 receptors (sigma(1) binding sites) form raft-like microdomains and target lipid droplets on the endoplasmic reticulum: roles in endoplasmic reticulum lipid compartmentalization and export. *J Pharmacol Exp Ther* 2003; 306(2):718-25.

Haynes C.M., Petrova K., Benedetti C., Yang Y., Ron D. ClpP mediates activation of a mitochondrial unfolded protein response in C. elegans. *Dev Cell* 2007; 13(4):467-80.

Haynes C.M., Ron D. The mitochondrial UPR-protecting organelle protein homeostasis. *J Cell Sci* 2010; 123(Pt 22):3849-55.

Haynes C.M., Yang Y., Blais S.P., Neubert T.A., Ron D. The matrix peptide exporter HAF-1 signals a mitochondrial UPR by activating the transcription factor ZC376.7 in C. elegans. *Mol Cell* 2010; 37(4):529-40.

He C., Klionsky D.J. Regulation mechanisms and signaling pathways of autophagy. *Annu Rev Genet* 2009; 43:67-93.

Healy S.A., Gupta S., Melvin A.J. HIV/HBV coinfection in children and antiviral therapy. *Expert Rev Anti Infect Ther* 2013; 11(3):251-63.

Hendrickson S.L., Kingsley L.A., Ruiz-Pesini E., Poole J.C., Jacobson L.P., Palella F.J., Bream J.H., Wallace D.C., O'Brien S.J. Mitochondrial DNA Haplogroups influence lipoatrophy after Highly Active Anti-retroviral Therapy. *J Acquir Immune Defic Syndr* 2009; 51(2):111-6.

Hernandez M.D., Sherman K.E. HIV/hepatitis C coinfection natural history and disease progression. *Curr Opin HIV AIDS* 2011; 6(6):478-82.

Hetz C., Bernasconi P., Fisher J., Lee A.H., Bassik M.C., Antonsson B., Brandt G.S., Iwakoshi N.N., Schinzel A., Glimcher L.H., Korsmeyer S.J. Proapoptotic bax and bak modulate the unfolded protein response by a direct interaction with ire1alpha. *Science* 2006; 312(5773):572-6.

Hofman P., Nelson A.M. The pathology induced by highly active antiretroviral therapy against human immunodeficiency virus: an update. *Curr Med Chem* 2006; 13(26):3121-32.

Hom J.R., Gewandter J.S., Michael L., Sheu S.S., Yoon Y. Thapsigargin induces biphasic fragmentation of mitochondria through calcium-mediated mitochondrial fission and apoptosis. *J Cell Physiol* 2007; 212(2):498-508.

Hoppins S., Nunnari J. Cell Biology. Mitochondrial dynamics and apoptosis--the ER connection. *Science* 2012; 337(6098):1052-54.

Hori O., Ichinoda F., Tamatani T., Yamaguchi A., Sato N., Ozawa K., Kitao Y., Miyazaki M., Harding H.P., Ron D., Tohyama M., Stern D., Ogawa S. Transmission of cell stress from endoplasmic reticulum to mitochondria: enhanced expression of Lon protease. *J Cell Biol* 2002; 157(7):1151-60.

Horibe T., Hoogenraad N.J. The chop gene contains an element for the positive regulation of the mitochondrial unfolded protein response. *PLoS One* 2007; 2(9):e835.

Horner S.M. Activation and evasion of antiviral innate immunity by hepatitis C virus. *J Mol Biol* 2014; 426(6):1198-209.

Horner S.M., Liu H.M., Park H.S., Briley J., Gale M. Mitochondrial-associated endoplasmic reticulum membranes (MAM) form innate immune synapses and are targeted by hepatitis C virus. *PNAS* 2011; 108(35):14590-95.

Horner S.M., Wilkins C., Badil S., Iskarpatyoti J., Gale M. Jr. Proteomic analysis of mitochondrial-associated ER membranes (MAM) during RNA virus infection reveals dynamic changes in protein and organelle trafficking. *PLoS One* 2015; 10(3):e0117963.

Huang C.Y., Chiang S.F., Lin T.Y., Chiou S.H., Chow K.C. HIV-1 Vpr triggers mitochondrial destruction by impairing Mfn2-mediated ER–mitochondria interaction. *PLoS One* 2012; 7(3):e33657.

Hulgan T., Haubrich R., Riddler S.A., Tebas P., Ritchie M.D., McComsey G.A., Haas D.W., Canter J.A. European Mitochondrial DNA Haplogroups and Metabolic Changes during Antiretroviral Therapy in AIDS Clinical Trials Group Study A5142. *AIDS* 2011; 25(1):37-47.

Hussain S.G., Ramaiah K.V. Endoplasmic reticulum: Stress, signalling and apoptosis. *Current science* 2007; 93(12):1684-96.

Ishihara N., Fujita Y., Oka T., Mihara K. Regulation of mitochondrial morphology through proteolytic cleavage of OPA1. *EMBO J* 2006; 25(13):2966-77.

Ishihara N., Nomura M., Jofuku A., Kato H., Suzuki S.O., Masuda K., Otera H., Nakanishi Y., Nonaka I., Goto Y. Mitochondrial fission factor Drp1 is essential for embryonic development and synapse formation in mice. *Nat Cell Biol* 2009; 11(8):958-66.

Iwasawa R., Mahul-Mellier A.L., Datler C., Pazarentzos E., Grimm S. Fis1 and Bap31 bridge the mitochondria-ER interface to establish a platform for apoptosis induction. *EMBO J* 2011; 30(3):556-68.

Iwawaki T., Hosoda A., Okuda T., Kamigori Y., Nomura-Furuwatari C., Kimata Y., Tsuru A., Kohno K. Translational control by the er transmembrane kinase/ribonuclease ire1 under er stress. *Nat Cell Biol* 2001; 3(2):158-64.

Jackson S.E. Hsp90: structure and function. *Top Curr Chem* 2013; 328:155-240.

Jelsema C.L., Morre D.J. Distribution of phospholipid biosynthetic enzymes among cell components of rat liver. *J Biol Chem* 1978; 253(21):7960-71.

Ji C. Dissection of endoplasmic reticulum stress signaling in alcoholic and non-alcoholic liver injury. *J Gastroenterol Hepatol* 2008; 23(1):S16-S24.

Jin C., Flavell R.A. Molecular mechanism of NLRP3 inflammasome activation. *J Clin Immunol* 2010; 30(5):628-31.

Jin S.M., Youle R.J. The accumulation of misfolded proteins in the mitochondrial matrix is sensed by PINK1 to induce PARK2/Parkin- mediated mitophagy of polarized mitochondria. *Autophagy* 2013; 9(11):1750-7.

Jipu R., Amititeloaie C., Zonda G.I., Iancu R.I., Carasevici E., Costuleanu M. Thapsigargin-induced endoplasmic reticulum stress is not accompanied by mitochondrial membrane potential dissipation in murine pro-B cells. *Rev Med Chir Soc Med Nat Iasi* 2012; 116(2):557-62.

John L.M., Lechleiter J.D., Camacho P. Differential modulation of SERCA2 isoforms by calreticulin. *J Cell Biol* 1998; 142(4):963-73.

Jones D.P. Radical-free biology of oxidative stress. *Am J Physiol Cell Physiol* 2008; 295(4):C849-68.

Jones M., Núñez M. Liver toxicity of antiretroviral drugs. *Semin Liver Dis* 2012; 32(2):167-76.

Joshi D., O'Grady J., Dieterich D., Gazzard B., Agarwal K. Increasing burden of liver disease in patients with HIV infection. *Lancet* 2011; 377(9772):1198-209.

Kadowaki H., Nishitoh H. Signaling pathways from the endoplasmic reticulum and their roles in disease. *Genes (Basel)* 2013; 4(3):306-33.

Kampira E., Kumwenda J., van Oosterhout J.J., Dandara C. Mitochondrial DNA subhaplogroups L0a2 and L2a modify susceptibility to peripheral neuropathy in Malawian adults on stavudine containing highly active antiretroviral therapy. *J Acquir Immune Defic Syndr* 2013; 63(5):647-52.

Kang S.G., Dimitrova M.N., Ortega J., Ginsburg A., Maurizi M.R. Human mitochondrial ClpP is a stable heptamer that assembles into a tetradecamer in the presence of ClpX. *J Biol Chem* 2005; 280(42):35424-32.

Kann O., Kovacs R. Mitochondria and neuronal activity. *Am J Physiol Cell Physiol* 2007; 292(2):C641-57.

Kappelhoff B.S., van L.F., Robinson P.A., MacGregor T.R., Baraldi E., Montella F., Uip D.E., Thompson M.A., Russell D.B., Lange J.M., Beijnen J.H., Huitema A.D. Are adverse events of nevirapine and efavirenz related to plasma concentrations? *Antivir Ther* 2005; 10(4):489-98.

Kaufman R.J. Orchestrating the unfolded protein response in health and disease. *J Clin Invest* 2002; 110(10):1389-98.

Kim I., Rodriguez-Enriquez S., Lemasters J.J. Selective degradation of mitochondria by mitophagy. *Arch Biochem Biophys* 2007; 462(2):245-53.

Kim I., Xu W., Reed J.C. Cell death and endoplasmic reticulum stress: disease relevance and therapeutic opportunities. *Nat Rev Drug Discov* 2008; 7(12):1013-30.

King J., Aberg J.A. Clinical impact of patient population differences and genomic variation in efavirenz therapy. *AIDS* 2008; 22(14):1709-17.

King M.P., Attardi G. Human cells lacking mtDNA: repopulation with exogenous mitochondria by complementation. *Science* 1989; 246(4929):500-3.

Kita K., Suzuki T., Ochi T. Diphenylarsinic acid promotes degradation of glutaminase C by mitochondrial Lon protease. *J Biol Chem* 2012; 287(22):18163-72.

Klionsky D.J. Autophagy: from phenomenology to molecular understanding in less than a decade. *Nat Rev Mol Cell Biol* 2007; 8(11):931-7.

Klionsky D.J., Cuervo A.M., Dunn W.A. Jr., Levine B., van der Klei I., Seglen P.O. How shall I eat thee? *Autophagy* 2007; 3(5):413-6.

Knott A.B., Bossy-Wetzel E. Impairing the mitochondrial fission and fusion balance: a new mechanism of neurodegeneration. *Ann N Y Acad Sci* 2008; 1147:283-92.

Knott A.B., Perkins G., Schwarzenbacher R., Bossy-Wetzel E. Mitochondrial fragmentation in neurodegeneration. *Nat Rev Neurosci* 2008; 9(7):505-18.

Kohler J.J., Lewis W. A brief overview of mechanisms of mitochondrial toxicity from NRTIs. *Environ Mol Mutagen* 2007; 48(3-4):166-72.

Komanduri K.V., Viswanathan M.N., Wieder E.D., Schmidt D.K., Bredt B.M., Jacobson M.A., McCune J.M. Restoration of cytomegalovirus-specific CD4+ T-lymphocyte responses after ganciclovir and highly active antiretroviral therapy in individuals infected with HIV-1. *Nat Med* 1998; 4(8):953-6.

Korge P., Weiss J.N. Thapsigargin directly induces the mitochondrial permeability transition. *Eur J Biochem* 1999; 265(1):273-80.

Kraft C., Deplazes A., Sohrmann M., Peter M. Mature ribosomes are selectively degraded upon starvation by an autophagy pathway requiring the Ubp3p/Bre5p ubiquitin protease. *Nat Cell Biol* 2008; 10(5):602-10.

Kumar H., Kawai T., Kato H., Sato S., Takahashi K., Coban C., Yamamoto M., Uematsu S., Ishii K.J., Takeuchi O., Akira S. Essential role of IPS-1 in innate immune responses against RNA viruses. *J Exp Med* 2006; 203(7):1795-1803.

Kuo C.Y., Chiu Y.C., Lee A.Y., Hwang T.L. Mitochondrial Lon protease controls ROS-dependent apoptosis in cardiomyocyte under hypoxia, *Mitochondrion* 2015; 23:7-16.

Kwara A., Lartey M., Sagoe K.W., Rzek N.L., Court M.H. CYP2B6 (c.516G→T) and CYP2A6 (*9B and/or *17) polymorphisms are independent predictors of efavirenz plasma concentrations in HIV-infected patients. *Br J Clin Pharmacol* 2009; 67(4):427-36.

Labbe G., Pessayre D., Fromenty B. Drug-induced liver injury through mitochondrial dysfunction: mechanisms and detection during preclinical safety studies. *Fundam Clin Pharmacol* 2008; 22(4):335-53.

Laemmli U.K. Cleavage of structural proteins during the assembly of the head of bacteriophage T4. *Nature* 1970; 227(5259):680-5.

Lakhani S.A., Masud A., Kuida K., Porter G.A. Jr., Booth C.J., Mehal W.Z., Inayat I., Flavell R.A. Caspases 3 and 7: key mediators of mitochondrial events of apoptosis. *Science* 2006; 311(5762):847-51.

Lancel S., Qin F., Lennon S.L., Zhang J., Tong X., Mazzini M.J., Kang Y.J., Siwik D.A., Cohen R.A., Colucci W.S. Oxidative posttranslational modifications mediate decreased SERCA activity and myocyte dysfunction in Galphaq-overexpressing mice. *Circ Res* 2010; 107(2):228-32.

Lancel S., Zhang J., Evangelista A., Trucillo M.P., Tong X., Siwik D.A., Cohen R.A., Colucci W.S. Nitroxyl activates SERCA in cardiac myocytes via glutathiolation of cysteine 674. *Circ Res* 2009; 104(6):720-3.

Laskey S.B., Siliciano R.F. A mechanistic theory to explain the efficacy of antiretroviral therapy. *Nat Rev Microbiol* 2014; 12(11):772-80.

Le Bras M., Clément M.V., Pervaiz S., Brenner C. Reactive oxygen species and the mitochondrial signaling pathway of cell death. *Histol Histopathol* 2005; 20(1):205-19.

Lecoeur H., Langonné A., Baux L., Rebouillat D., Rustin P., Prévost M.C., Brenner C., Edelman L., Jacotot E. Real-time flow cytometry analysis of permeability transition in isolated mitochondria. *Exp Cell Res* 2004; 294(1):106-17.

Lederman M.M., Connick E., Landay A., Kuritzkes D.R., Spritzler J., St Clair M., Kotzin B.L., Fox L., Chiozzi M.H., Leonard J.M., Rousseau F., Wade M., Roe J.D. Immunologic responses associated with 12 weeks of combination antiretroviral therapy consisting of zidovudine, lamivudine, and ritonavir: Results of AIDS Clinical Trials Group Protocol 315. *J Infect Dis* 1998; 178(1):70-9.

Lee S., Park Y.Y., Kim S.H., Nguyen O.T., Yoo Y.S., Chan G.K., Sun X., Cho H. Human mitochondrial Fis1 links to cell cycle regulators at G2/M transition. *Cell Mol Life Sci* 2014; 71(4):711-25.

Lemasters J.J. Selective mitochondrial autophagy, or mitophagy, as a targeted defense against oxidative stress, mitochondrial dysfunction, and aging. *Rejuvenation Res* 2005; 8(1):3-5.

Li B., Hu Q., Wang H., Man N., Ren H., Wen L., Nukina N., Fei E., Wang G. Omi/HtrA2 is a positive regulator of autophagy that facilitates the degradation of mutant proteins involved in neurodegenerative diseases. *Cell Death Differ* 2010; 17(11):1773-84.

Li N., Ragheb K., Lawler G., Sturgis J., Rajwa B., Melendez J.A., Robinson J.P. Mitochondrial complex I inhibitor rotenone induces apoptosis through enhancing mitochondrial reactive oxygen species production. *J Biol Chem* 2003; 278(10):8516-25.

Li Z., Srivastava P. Heat-shock proteins. *Curr Protoc Immunol* 2004; Appendix 1:Appendix 1T.

Lièvremont J.P., Rizzuto R., Hendershot L., Meldolesi J. BiP, a major chaperone protein of the endoplasmic reticulum lumen, plays a direct and important role in the storage of the rapidly exchanging pool of Ca2+. *J Biol Chem* 1997; 272(49):30873-9

Lin J., Schyschka L., Mühl-Benninghaus R., Neumann J., Hao L., Nussler N., Dooley S., Liu L., Stöckle U., Nussler A.K., Ehnert S. Comparative analysis of phase I and II enzyme activities in 5 hepatic cell lines identifies Huh-7 and HCC-T cells with the highest potential to study drug metabolism. *Arch Toxicol* 2012; 86(1):87-95.

Liu X., Kim C.N., Yang J., Jemmerson R., Wang X. Induction of apoptotic program in cell-free extracts: requirement for dATP and cytochrome c. *Cell* 1996; 86(1):147-57.

Liu Y., Lan L., Huang K., Wang R., Xu C., Shi Y., Wu X., Wu Z., Zhang J., Chen L., Wang L., Yu X., Zhu H., Lu B. Inhibition of Lon blocks cell proliferation, enhances chemosensitivity by promoting apoptosis and decreases cellular bioenergetics of bladder cancer: potential roles of Lon as a prognostic marker and therapeutic target in baldder cancer. *Oncotarget* 2014; 5(22):11209-24.

Liu Z.W., Zhu H.T., Chen K.L., Dong X., Wei J., Qiu C., Xue J.H. Protein kinase RNA-like endoplasmic reticulum kinase (PERK) signaling pathway plays a major role in reactive oxygen species (ROS)-mediated endoplasmic reticulum stress-induced apoptosis in diabetic cardiomyopathy. *Cardiovasc Diabetol* 2013; 12:158.

Lodish H., Berk A., Zipursky S.L., Matsudaira P., Baltimore D., Darnell J. Molecular Cell Biology. New York: W. H. Freeman. 5th edition. 2003.

Loko M.A., Bani-Sadr F., Winnock M., Lacombe K., Carrieri P., Neau D., Morlat P., Serfaty L., Dabis F., Salmon D. ANRS CO 13 HEPAVIH Study Group. Impact of HAART exposure and associated lipodystrophy on advanced liver fibrosis in HIV/HCV-coinfected patients. *J Viral Hepat* 2011; 18(7):e307-14.

Loson O.C., Song Z., Chen H., Chan D.C. Fis1, Mff, MiD49, and MiD51 mediate Drp1 recruitment in mitochondrial fission. *Mol Biol Cell* 2013; 24(5):659-67.

Lou P.H., Hansen B.S., Olsen P.H., Tullin S., Murphy M.P., Brand M.D. Mitochondrial uncouplers with an extraordinary dynamic range. *Biochem J* 2007; 407(1):129-40.

Lu B., Lee J., Nie X., Li M., Morozov Y.I., Venkatesh S., Bogenhagen D.F., Temiakov D., Suzuki C.K. Phosphorylation of human TFAM in mitochondria impairs DNA binding and promotes degradation by the AAA+ Lon protease. *Mol Cell* 2013; 49(1):121-32.

Ly J.D., Grubb D.R., Lawen A. The mitochondrial membrane potential (deltapsi(m)) in apoptosis; an update. *Apoptosis* 2003; 8(2):115-28.

Lynes E.M., Bui M., Yap M.C., Benson M.D., Schneider B., Ellgaard L., Berthiaume L.G., Simmen T. Palmitoylated TMX and calnexin target to the mitochondria-associated membrane *EMBO J* 2012; 31(2):457-70.

Maagaard A., Kvale D. Long term adverse effects related to nucleoside reverse transcriptase inhibitors: clinical impact of mitochondrial toxicity. *Scand J Infect Dis* 2009; 41(11-12):808-17.

Maggiolo F. Efavirenz: a decade of clinical experience in the treatment of HIV. *J Antimicrob Chemother* 2009; 64(5):910-28.

Malhi H., Kaufman R.J. Endoplasmic reticulum stress in liver disease. *J Hepatol* 2011; 54(4):795-809.

Marchi S., Patergnani S., Pinton P. The endoplasmic reticulum-mitochondria connection: one touch, multiple functions. *Biochim Biophys Acta* 2014; 1837(4):461-9.

Marin J.J., Hernandez A., Revuelta I.E., Gonzalez-Sanchez E., Gonzalez-Buitrago J.M., Perez M.J. Mitochondrial genome depletion in human liver cells abolishes bile acid-induced apoptosis: role of the Akt/mTOR survival pathway and Bcl-2 family proteins. *Free Radic Biol Med* 2013; 61:218-28.

Marsboom G., Toth P.T., Ryan J.J., Hong Z., Wu X., Fang Y.H., Thenappan T., Piao L., Zhang H.J., Pogoriler J. Chen Y., Morrow E., Weir E.K., Rehman J., Archer S.L. Dynamin-related protein 1-mediated mitochondrial mitotic fission permits hyperproliferation of vascular smooth muscle cells and offers a novel therapeutic target in pulmonary hypertension. *Circ Res* 2012; 110(11):1484-97.

Martin J.L., Brown C.E., Matthews-Davis N., Reardon J.E. Effects of antiviral nucleoside analogs on human DNA polymerases and mitochondrial DNA synthesis. *Antimicrob Agents Chemother* 1994; 38(12):2743-9.

Marzolini C., Gibbons S., Khoo S., Back D. Cobicistat versus ritonavir boosting and differences in the drug-drug interaction profiles with co-medications. *J Antimicrob Chemother* 2016; 71(7):1755-8.

Marzolini C., Telenti A., Decosterd L.A., Greub G., Biollaz J., Buclin T. Efavirenz plasma levels can predict treatment failure and central nervous system side effects in HIV-1-infected patients. *AIDS* 2001; 15(1):71-5.

Matsushima Y., Goto Y., Kaguni L.S. Mitochondrial Lon protease regulates mitochondrial DNA copy number and transcription by selective degradation of mitochondrial transcription factor A (TFAM). *Proc Natl Acad Sci U S A* 2010; 107(43):18410-5.

Matsushima Y., Kaguni L.S. Matrix proteases in mitochondrial DNA function. *Biochim Biophys Acta* 2012; 1819(9-10):1080-7.

Matthews T., Salgo M., Greenberg M., Chung J., DeMasi R., Bolognesi D. Enfuvirtide: the first therapy to inhibit the entry of HIV-1 into host CD4 lymphocytes. *Nat Rev Drug Discov* 2004; 3(3):215-25.

McQuibban G.A., Saurya S., Freeman M. Mitochondrial membrane remodelling regulated by a conserved rhomboid protease. *Nature* 2003; 423(6939):537-41.

Meeusen S., DeVay R., Block J., Cassidy-Stone A., Wayson S., McCaffery J.M., Nunnari J. Mitochondrial inner-membrane fusion and crista maintenance requires the dynamin-related GTPase Mgm1. *Cell* 2006; 127(2):383-95.

Meijer A.J., Codogno P. Autophagy: regulation and role in disease. *Crit Rev Clin Lab Sci* 2009; 46(4):210-40.

Meisner H.M., Sorensen L. Metaphase arrest of Chinese hamster cells with rotenone. *Exp Cell Res* 1966; 42(2):291-5.

Meylan E., Curran J., Hofmann K., Moradpour D., Binder M., Bartenschlager R., Tschopp J. Cardif is an adaptor protein in the RIG-I antiviral pathway and is targeted by hepatitis C virus. *Nature* 2005; 437(7062):1167-72.

Michalak M., Robert Parker J.M., Opas M. Ca^{2+} signaling and calcium binding chaperones of the endoplasmic reticulum. *Cell Calcium* 2002; 32(5-6):269-78.

Mikoshiba K. Inositol 1,4,5-trisphosphate IP(3) receptors and their role in neuronal cell function. *J Neurochem* 2006; 97(6):1627-33.

Mishra P. Interfaces between mitochondrial dynamics and disease. *Cell Calcium* 2016; 60(3):190-8.

Mishra P., Carelli V., Manfredi G., Chan D.C. Proteolytic cleavage of Opa1 stimulates mitochondrial inner membrane fusion and couples fusion to oxidative phosphorylation. *Cell Metab* 2014; 19(4):630-41.

Mishra P., Chan D.C. Mitochondrial dynamics and inheritance during cell division, development and disease. *Nat Rev Mol Cell Biol* 2014; 15(10):634-46.

Misko A., Jiang S., Wegorzewska I., Milbrandt J., Baloh R.H. Mitofusin 2 is necessary for transport of axonal mitochondria and interacts with the Miro/Milton complex. *J Neurosci* 2010; 30(12):4232-40.

Mitra K., Wunder C., Roysam B., Lin G., Lippincott-Schwartz J. A hyperfused mitochondrial state achieved at G1-S regulates cyclin E buildup and entry into S phase. *Proc Natl Acad Sci U S A* 2009; 106(29):11960-5.

Mitsuya H., Weinhold K.J., Furman P.A., St Clair M.H., Lehrman S.N., Gallo R.C., Bolognesi D., Barry D.W., Broder S. 3'-Azido-3'-deoxythymidine (BW A509U): an antiviral agent that inhibits the infectivity and cytopathic effect of human T-lymphotropic virus type III/lymphadenopathy-associated virus in vitro. *Proc Natl Acad Sci U S A* 1985; 82(20):7096-100.

Mizushima N., Levine B., Cuervo A.M., Klionsky D.J. Autophagy fights disease through cellular self-digestion. *Nature* 2008; 451(7182):1069-75.

Mocroft A., Ledergerber B., Katlama C., Kirk O., Reiss P., d'Arminio Monforte A., Knysz B., Dietrich M., Phillips A.N., Lundgren J.D. Decline in the AIDS and death rates in the EuroSIDA study: an observational study. *Lancet* 2003; 362(9377):22-9.

Mogk A., Huber D., Bukau B. Integrating protein homeostasis strategies in prokaryotes. *Cold Spring Harb Perspect Biol* 2011; 3(4), pii:a004366.

Moisoi N., Klupsch K., Fedele V., East P., Sharma S., Renton A., Plun-Favreau H., Edwards R.E., Teismann P., Esposti M.D., Morrison A.D., Wood N.W., Downward J., Martins L.M. Mitochondrial dysfunction triggered by loss of HtrA2 results in the activation of a brain- specific transcriptional stress response. *Cell Death Differ* 2009; 16(3):449-64.

Morén C., Bañó M., González-Casacuberta I., Catalán-Garcia M., Guitart-Mampel M., Tobías E., Cardellach F., Pedrol E., Peraire J., Vidal F., Domingo P., Miró Ò., Gatell J.M., Martínez E., Garrabou G. Mitochondrial and apoptotic in vitro modelling of differential HIV-1 progression and antiretroviral toxicity. J *Antimicrob Chemother* 2015; 70(8):2330-6.

Mori K. Tripartite management of unfolded proteins in the endoplasmic reticulum. *Cell* 2000; 101(5):451-4.

Müller-Höcker J., Horvath R., Schäfer S., Hessel H., Müller-Felber W., Kühr J., Copeland W.C., Seibel P. Mitochondrial DNA depletion and fatal infantile hepatic failure due to mutations in the mitochondrial polymerase γ (POLG) gene: a combined morphological/enzyme histochemical and immunocytochemical/biochemical and molecular genetic study. *J Cell Mol Med* 2011; 15(2):445-56.

Munoz J.P., Ivanova S., Sánchez-Wandelmer J., Martínez-Cristóbal P., Noguera E., Sancho A., Díaz-Ramos A., Hernández-Alvarez M.I., Sebastián D., Mauvezin C., Palacín M., Zorzano A. Mfn2 modulates the UPR and mitochondrial function via repression of PERK. *EMBO J* 2013; 32(17):2348-61.

Nagy G., Kardon T., Wunderlich L., Szarka A., Kiss A., Schaff Z., Banhegyi G., Mandl J. Acetaminophen induces ER dependent signaling in mouse liver. *Arch Biochem Biophys* 2007; 459(2):273-9.

Nagy G., Szarka A., Lotz G., Doczi J., Wunderlich L., Kiss A., Jemnitz K., Veres Z., Banhegyi G., Schaff Z., Sumegi B., Mandl J. BGP-15 inhibits caspase-independent programmed cell death in acetaminophen- induced liver injury. *Toxicol Appl Pharmacol* 2010; 243(1):96-103.

Nakada K., Sato A., Hayashi J. Mitochondrial functional complementation in mitochondrial DNA-based diseases. *Int J Biochem Cell Biol* 2009; 41(10):1907-13.

Nakahira K., Haspel J.A., Rathinam V.A., Lee S.J., Dolinay T., Lam H.C., Englert J.A., Rabinovitch M., Cernadas M., Kim H.P., Fitzgerald K.A., Ryter S.W., Choi A.M. Autophagy proteins regulate innate immune responses by inhibiting the release of mitochondrial DNA mediated by the NALP3 inflammasome. *Nat Immunol* 2011; 12(3):222-30.

Nargund A.M., Pellegrino M.W., Fiorese C.J., Baker B.M., Haynes C.M. Mitochondrial import efficiency of ATFS-1 regulates mitochondrial UPR activation. *Science* 2012; 337(6094):587-90.

Ngo J.K., Davies K.J. Mitochondrial Lon protease is a human stress protein. *Free Radic Biol Med* 2009; 46(8):1042-8.

Nie X., Li M., Lu B., Zhang Y., Lan L., Chen L., Lu J. Downregulating overexpressed human Lon in cervical cancer suppresses cell proliferation and bioenergetics. *PLoS One* 2013; 8(11):e81084.

Nishitoh H., Matsuzawa A., Tobiume K., Saegusa K., Takeda K., Inoue K., Hori S., Kakizuka A., Ichijo H. Ask1 is essential for endoplasmic reticulum stress-induced neuronal cell death triggered by expanded polyglutamine repeats. *Genes Dev* 2002; 16(11):1345-55.

Novo E., Parola M. Redox mechanisms in hepatic chronic wound healing and fibrogenesis. *Fibrogenesis Tissue Repair* 2008; 1(1):5.

Núñez M. Clinical syndromes and consequences of antiretroviral-related hepatotoxicity. *Hepatology* 2010; 52(3):1143-55.

Ohsumi Y. Molecular dissection of autophagy: two ubiquitin-like systems. *Nat Rev Mol Cell Biol* 2001; 2(3):211-6.

Orrenius S., Gogvadze V., Zhivotovsky B. Mitochondrial oxidative stress: implications for cell death. *Annu Rev Pharmacol Toxicol* 2007; 47:143-83.

Oslowski C.M., Hara T., O'Sullivan-Murphy B., Kanekura K., Lu S., Hara M., Ishigaki S., Zhu L.J., Hayashi E., Hui S.T., Greiner D., Kaufman R.J., Bortell R., Urano F. Thioredoxin- interacting protein mediates ER stress-induced beta cell death through initiation of the inflammasome. *Cell Metab* 2012; 16(2):265-73.

Otera H., Mihara K. Discovery of the membrane receptor for mitochondrial fission GTPase Drp1. *Small GTPases* 2011; 2(3):167-72.

Oyadomari S., Koizumi A., Takeda K., Gotoh T., Akira S., Araki E., Mori M. Targeted disruption of the chop gene delays endoplasmic reticulum stress-mediated diabetes. *J Clin Invest* 2002; 109(4):525-32.

Palade G.E. An electron microscope study of the mitochondrial structure. *J Histochem Cytochem* 1953; 1(4):188-211.

Pandey K.K. Raltegravir in HIV-1 infection: Safety and Efficacy in Treatment-naïve Patients. *Clin Med Rev Ther* 2011; 2012(4):13-30.

Pandit A., Sachdeva T., Bafna P. Drug-Induced Hepatotoxicity: A Review. *JAPS* 2012; 02(05):233-43.

Panos G., Samonis G., Alexiou V.G., Kavarnou G.A., Charatsis G., Falagas M.E. Mortality and morbidity of HIV infected patients receiving HAART: a cohort study. *Curr HIV Res* 2008; 6(3):257-60.

Pantaleo G., Graziosi C., Fauci A.S. The role of lymphoid organs in the pathogenesis of HIV infection. *Semin Immunol* 1993; 5(3):157-63.

Parker I., Yao Y. Ca^{2+} transients associated with openings of inositol trisphosphate-gated channels in Xenopus oocytes. *J Physiol* 1996; 491(Pt 3):663-8.

Parker R.A., Flint O.P., Mulvey R., Elosua C., Wang F., Fenderson W., Wang S., Yang W.P., Noor M.A. Endoplasmic reticulum stress links dyslipidemia to inhibition of proteasome activity and glucose transport by HIV protease inhibitors. *Mol Pharmacol* 2005; 67(6):1909-19.

Patel S., Joseph S.K., Thomas A.P. Molecular properties of inositol 1,4,5-trisphosphate receptors. *Cell Calcium* 1999; 25(3):247-64.

Patergnani S., Suski J.M., Agnoletto C., Bononi A., Bonora M., De Marchi E., Giorgi C., Marchi S., Missiroli S., Poletti F., Rimessi A., Duszynski J., Wieckowski M.R., Pinton P. Calcium signaling around mitochondria associated membranes (MAMs). *Cell Commun Signal* 2011; 9:19.

Patil R., Ona M.A., Papafragkakis H., Carey J., Moshenyat Y., Alhaddad A., Anand S. Acute Liver Toxicity due to Efavirenz/Emtricitabine/Tenofovir. *Case Reports Hepatol* 2015; 2015:280353.

Patterson R.L., Boehning D., Snyder S.H. Inositol 1,4,5-trisphosphate receptors as signal integrators. *Annu Rev Biochem* 2004; 73:437-65.

Perl M., Chung C.S., Ayala A. Apoptosis. *Crit Care Med* 2005; 33(12):S526-9.

Perry S.W., Norman J.P., Barbieri J., Brown E.B., Gelbard H.A. Mitochondrial membrane potential probes and the proton gradient: a practical usage guide. *Biotechniques* 2011; 50(2):98-115.

Petit F., Fromenty B., Owen A., Estaquier J. Mitochondria are sensors for HIV drugs. *Trends Pharmacol Sci* 2005; 26(5):258-64.

Pineda J.A., Macias J., Mira J.A., Merchante N., del Valle J., Neukam K.I. HAART and the liver: friend or foe? *Eur J Med Res* 2010; 15(3):93-6.

Pinti M., Gibellini L., De Biasi S., Nasi M., Roat E., O'Connor J.E., Cossarizza A. Functional characterization of the promoter of the human Lon protease gene. *Mitochondrion* 2011; 11(1):200-6.

Pinti M., Gibellini L., Guaraldi G., Orlando G., Gant T.W., Morselli E., Nasi M., Salomoni P., Mussini C., Cossarizza A. Upregulation of nuclear- encoded mitochondrial LON protease in HAART-treated HIV- positive patients with lipodystrophy: implications for the pathogenesis of the disease. *AIDS* 2010; 24(6):841-50.

Pinti M., Gibellini L., Liu Y., Xu S., Lu B., Cossarizza A. Mitochondrial Lon protease at the crossroads of oxidative stress, ageing and cancer. *Cell Mol Life Sci* 2015; 72(24):4807-24.

Pinton P., Giorgi C., Pandolfi P.P. The role of PML in the control of apoptotic cell fate: a new key player at ER-mitochondria sites. *Cell Death Differ* 2011; 18(9):1450-6.

Pinton P., Giorgi C., Siviero R., Zecchini E., Rizzuto R. Calcium and apoptosis: ER-mitochondria Ca2+ transfer in the control of apoptosis. *Oncogene* 2008; 27(50):6407-18.

Pizzo P., Drago I., Filadi R., Pozzan T. Mitochondrial Ca(2)(+) homeostasis: mechanism, role, and tissue specificities. *Pflugers Arch* 2012; 464(1):3-17.

Pizzo P., Pozzan T. Mitochondria-endoplasmic reticulum choreography: structure and signaling dynamics. *Trends Cell Biol* 2007; 17(10):511-17.

Pomatto L.C., Raynes R., Davies K.J. The peroxisomal Lon protease LonP2 in aging and disease: functions and comparisons with mitochondrial Lon protease LonP1. *Biol Rev Camb Philos Soc* 2016. doi:10.1111/brv.12253.

Powers E.T., Balch W.E. Diversity in the origins of proteostasis networks–a driver for protein function in evolution. *Nat Rev Mol Cell Biol* 2013; 14(4):237-48.

Poyton R.O., Ball K.A., Castello P.R. Mitochondrial generation of free radicals and hypoxic signaling. *Trends Endocrinol Metab* 2009; 20(7):332-40.

Price J.C., Thio C.L. Liver disease in the HIV-infected individual. *Clin Gastroenterol Hepatol* 2010; 8(12):1002-12.

Qi X., Disatnik M.H., Shen N., Sobel R.A., Mochly-Rosen D. Aberrant mitochondrial fission in neurons induced by protein kinase C{delta} under oxidative stress conditions in vivo. *Mol Biol Cell* 2011; 22(2):256-65.

Quiros P.M., Espanol Y., Acin-Perez R., Rodriguez F., Barcena C., Watanabe K., Calvo E., Loureiro M., Fernandez-Garcia M.S., Fueyo A., Vazquez J., Enriquez J.A., Lopez-Otin C. ATP- dependent Lon protease controls tumor bioenergetics by reprogramming mitochondrial activity. *Cell reports* 2014; 8(2):542-556.

Quiros P.M., Langer T., Lopez-Otin C. New roles for mitochondrial proteases in health, ageing and disease. *Nat Rev Mol Cell Biol* 2015; 16(6):345-59.

Raffi F., Esser S., Nunnari G., Pérez-Valero I., Waters L. Switching regimens in virologically suppressed HIV-1-infected patients: evidence base and rationale for integrase strand transfer inhibitor (INSTI)-containing regimens. *HIV Med* 2016; 17(5):3-16.

Rainbolt T.K., Atanassova N., Genereux J.C., Wiseman R.L. Stress-regulated translational attenuation adapts mitochondrial protein import through Tim17A degradation. *Cell Metab* 2013; 18(6):908-19.

Rainbolt T.K., Saunders J.M., Wiseman R.L. Stress-responsive regulation of mitochondria through the ER unfolded protein response. *Trends Endocrinol Metab* 2014; 25(10):528-37.

Rambold A.S., Kostelecky B., Elia N., Lippincott-Schwartz J. Tubular network formation protects mitochondria from autophagosomal degradation during nutrient starvation. *Proc Natl Acad Sci U S A* 2011; 108(25):10190-5.

Randow F., Seed B. Endoplasmic reticulum chaperone gp96 is required for innate immunity but not cell viability. *Nat Cell Biol* 2001; 3(10):891-6.

Rao R.V., Ellerby H.M., Bredesen D.E. Coupling endoplasmic reticulum stress to the cell death program. *Cell Death Differ* 2004; 11(4):372-80.

Rehman J., Zhang H.J., Toth P.T., Zhang Y., Marsboom G., Hong Z., Salgia R., Husain A.N., Wietholt C., Archer S.L. Inhibition of mitochondrial fission prevents cell cycle progression in lung cancer. *FASEB J* 2012; 26(5):2175-86.

Rizzuto R., Pinton P., Carrington W., Fay F.S., Fogarty K.E., Lifshitz L.M., Tuft R.A., Pozzan T. Close contacts with the endoplasmic reticulum as determinants of mitochondrial Ca2+ responses. *Science* 1998; 280(5370):1763-6.

Rodríguez-Nóvoa S., Barreiro P., Jiménez-Nacher I., Rendón A., Soriano V. Pharmacogenetics in HIV therapy. *AIDS Rev* 2005; 7(2):103-12.

Rojo M., Legros F., Chateau D., Lombes A. Membrane topology and mitochondrial targeting of mitofusins, ubiquitous mammalian homologs of the transmembrane GTPase Fzo. *J Cell Sci* 2002; 115(Pt 8):1663-74.

Rotanova T.V., Melnikov E.E., Khalatova A.G., Makhovskaya O.V., Botos I., Wlodawer A., Gustchina A. Classification of ATP-dependent proteases Lon and comparison of the active sites of their proteolytic domains. *Eur J Biochem* 2004; 271(23-24):4865-71.

Rowland A.A., Voeltz G.K. Endoplasmic reticulum-mitochondria contacts: function of the junction. *Nat Rev Mol Cell Biol* 2012; 13(10):607-25.

Ruby J.R., Dyer R.F., Skalko R.G. Continuities between mitochondria and endoplasmic reticulum in the mammalian ovary. *Z Zellforsch Mikrosk Anat* 1969; 97(1):30-7.

Rusinol A.E., Cui Z., Chen M.H., Vance J.E. A unique mitochondria-associated membrane fraction from rat liver has a high capacity for lipid synthesis and contains pre-Golgi secretory proteins including nascent lipoproteins. *J Biol Chem* 1994; 269(44):27494-502.

Rutkowski D.T., Arnold S.M., Miller C.N., Wu J., Li J., Gunnison K.M., Mori K., Sadighi Akha A.A., Raden D., Kaufman R.J. Adaptation to er stress is mediated by differential stabilities of pro-survival and pro-apoptotic mrnas and proteins. *PLoS Biol* 2006; 4(11):e374.

Saito T., Owen D.M., Jiang F., Marcotrigiano J., Gale M. Innate immunity induced by composition-dependent RIG-I recognition of hepatitis C virus RNA. *Nature* 2008; 454(7203):523-7.

Sala-Vila A., Navarro-Lérida I., Sánchez-Alvarez M., Bosch M., Calvo C., López J.A., Calvo E., Ferguson C., Giacomello M., Serafini A., Scorrano L., Enriquez J.A., Balsinde J., Parton R.G., Vázquez J., Pol A., Del Pozo M.A. Interplay between hepatic mitochondria-associated membranes, lipid metabolism and caveolin-1 in mice. *Sci Rep* 2016; 6:27351.

Sano R., Annunziata I., Patterson A., Moshiach S., Gomero E., Opferman J., Forte M., d'Azzo A. GM1-ganglioside accumulation at the mitochondria- associated ER membranes links ER stress to Ca(2+)-dependent mitochondrial apoptosis. *Mol Cell* 2009; 36(3):500-11.

Santel A., Frank S., Gaume B., Herrler M., Youle R.J., Fuller M.T. Mitofusin-1 protein is a generally expressed mediator of mitochondrial fusion in mammalian cells. *J Cell Sci* 2003; 116(Pt 13):2763-74.

Santel A., Fuller M.T. Control of mitochondrial morphology by a human mitofusin. *J Cell Sci* 2001; 114(Pt 5):867-74.

Saotome M., Safiulina D., Szabadkai G., Das S., Fransson A., Aspenstrom P., Rizzuto R., Hajnoczky G. Bidirectional Ca2+-dependent control of mitochondrial dynamics by the Miro GTPase. *PNAS* 2008; 105(52):20728-33.

Sato N. Central role of mitochondria in metabolic regulation of liver pathophysiology. *J Gastroenterol Hepatol* 2007; 22(1):S1-6.

Sauer H., Wartenberg M., Hescheler J. Reactive oxygen species as intracellular messengers during cell growth and differentiation. *Cell Physiol Biochem* 2001; 11(4):173-86.

Saxena G., Chen J., Shalev A. Intracellular shuttling and mitochondrial function of thioredoxin-interacting protein. *J Biol Chem* 2010; 285(6):3997-4005.

Scarpulla R.C. Nuclear activators and coactivators in mammalian mitochondrial biogenesis. *Biochim Biophys Acta* 2002; 1576(1-2):1-14.

Schapira A.H. Mitochondrial involvement in Parkinson's disease, Huntington's disease, hereditary spastic paraplegia and Friedreich's ataxia. *Biochim Biophys Acta* 1999; 1410(2):159-70.

Schild H., Rammensee H.G. gp96--the immune system's Swiss army knife. *Nat Immunol* 2000; 1(2):100-1.

Schon E.A., Area-Gomez E. Is Alzheimer's disease a disorder of mitochondria-associated membranes? *J Alzheimers Dis* 2010; 20(2):281-92.

Schroder K., Tschopp J. The inflammasomes. *Cell* 2010; 140(6):821-32.

Scorrano L. Keeping mitochondria in shape: a matter of life and death. *Eur J Clin Invest* 2013; 43(8):886-93.

Scorrano L., Oakes S.A., Opferman J.T., Cheng E.H., Sorcinelli M.D., Pozzan T., Korsmeyer S.J. Bax and bak regulation of endoplasmic reticulum Ca2+: A control point for apoptosis. *Science* 2003; 300(5616):135-9.

Sebastian D., Hernandez-Alvarez M.I., Segales J., Sorianello E., Munoz J.P., Sala D., Waget A., Liesa M., Paz J.C., Gopalacharyulu P., Oresic M., Pich S., Burcelin R., Palacin M., Zorzano A. Mitofusin 2 (Mfn2) links mitochondrial and endoplasmic reticulum function with insulin signaling and is essential for normal glucose homeostasis. *Proc Natl Acad Sci U S A* 2012; 109(14):5523-8.

Seth R.B., Sun L., Ea C.K., Chen Z.J. Identification and characterization of MAVS, a mitochondrial antiviral signaling protein that activates NF-kappaB and IRF 3. *Cell* 2005; 122(5):669-82.

Severinghaus J.W., Astrup P.B. History of blood gas analysis. VI. Oximetry. *J Clin Monit* 1986; 2(4):270-88.

Shen H.M., Codogno P. Autophagic cell death: Loch Ness monster or endangered species? *Autophagy* 2011; 7(5):457-65.

Shiao Y.J., Balcerzak B., Vance J.E. A mitochondrial membrane protein is required for translocation of phosphatidylserine from mitochondria-associated membranes to mitochondria. *Biochem J* 1998; 331(Pt 1):217-23.

Simmen T., Aslan J.E., Blagoveshchenskaya A.D., Thomas L., Wan L., Xiang Y., Feliciangeli S.F., Hung C.H., Crump C.M., Thomas G. PACS-2 controls endoplasmic reticulum–mitochondria communication and Bid-mediated apoptosis. *EMBO J* 2005; 24(4):717-29.

Simmen T., Lynes E.M., Gesson K., Thomas G. Oxidative protein folding in the endoplasmic reticulum: tight links to the mitochondria-associated membrane (MAM). *Biochim Biophys Acta* 2010; 1798(8):1465-73.

Smirnova E., Griparic L., Shurland D.L., van der Bliek A.M. Dynamin-related protein Drp1 is required for mitochondrial division in mammalian cells. *Mol Biol Cell* 2001; 12(8):2245-56.

Smirnova E., Shurland D.L., Ryazantsev S.N., van der Bliek A.M. A human dynamin-related protein controls the distribution of mitochondria. *J Cell Biol* 1998; 143:351-8.

Smith J.A., Daniel R. Following the path of the virus: the exploitation of host DNA repair mechanisms by retroviruses. *ACS Chem Biol* 2006; 1(4):217-26.

Smith P.F., DiCenzo R., Morse G.D. Clinical pharmacokinetics of non-nucleoside reverse transcriptase inhibitors. *Clin Pharmacokinet* 2001; 40(12):893-905.

Smith P.K., Krohn R.I., Hermanson G.T., Mallia A.K., Gartner F.H., Provenzano M.D., Fujimoto E.K., Goeke N.M., Olson B.J., Klenk D.C. Measurement of protein using bicinchoninic acid. *Anal Biochem* 1985; 150(1):76-85.

Smith R.A., Hartley R.C., Cochemé H.M., Murphy M.P. Mitochondrial pharmacology. *Trends Pharmacol Sci* 2012; 33(6):341-52.

Song Z., Chen H., Fiket M., Alexander C., Chan D.C. OPA1 processing controls mitochondrial fusion and is regulated by mRNA splicing, membrane potential, and Yme1L. *J Cell Biol* 2007; 178(5):749-55.

Song Z., Ghochani M., McCaffery J.M., Frey T.G., Chan D.C. Mitofusins and OPA1 mediate sequential steps in mitochondrial membrane fusion. *Mol Biol Cell* 2009; 20(15):3525-32.

Soriano V., Puoti M., Garcia-Gasco P., Rockstroh J.K., Benhamou Y., Barreiro P., McGovern B. Antiretroviral drugs and liver injury. *AIDS* 2008; 22(1):1-13.

St-Pierre J., Buckingham J.A., Roebuck S.J., Brand M.D. Topology of superoxide production from different sites in the mitochondrial electron transport chain. *J Biol Chem* 2002; 277(47):44784-90.

Starr S.E., Fletcher C.V., Spector S.A., Yong F.H., Fenton T., Brundage R.C., Manion D., Ruiz N., Gersten M., Becker M., McNamara J., Mofenson L.M., Purdue L., Siminski S., Graham B., Kornhauser D.M., Fiske W., Vincent C., Lischner H.W., Dankner W.M., Flynn P.M. Combination therapy with efavirenz, nelfinavir, and nucleoside reverse-transcriptase inhibitors in children infected with human immunodeficiency virus type 1. Pediatric AIDS Clinical Trials Group 382 Team. *N Engl J Med* 1999; 341(25):1874-81.

Staszewski S., Morales-Ramirez J., Tashima K.T., Rachlis A., Skiest D., Stanford J., Stryker R., Johnson P., Labriola D.F., Farina D., Manion D.J., Ruiz N.M. Efavirenz plus zidovudine and lamivudine, efavirenz plus indinavir, and indinavir plus zidovudine and lamivudine in the treatment of HIV-1 infection in adults. Study 006 Team. *N Engl J Med* 1999; 341(25):1865-73.

Steenbergen R., Nanowski T.S., Beigneux A., Kulinski A., Young S.G., Vance J.E. Disruption of the phosphatidylserine decarboxylase gene in mice causes embryonic lethality and mitochondrial defects. *J Biol Chem* 2005; 280(48):40032-40.

Stern J.O., Robinson P.A., Love J., Lanes S., Imperial M.S., Mayers D.L. A comprehensive hepatic safety analysis of nevirapine in different populations of HIV infected patient. *J Acquir Immune Defic Syn dr* 2003; 34(1):S21-33.

Strauss K.A., Jinks R.N., Puffenberger E.G., Venkatesh S., Singh K., Cheng I., Mikita N., Thilagavathi J., Lee J., Sarafianos S., Benkert A., Koehler A., Zhu A., Trovillion V., McGlincy M., Morlet T., Deardorff M., Innes A.M., Prasad C., Chudley A.E., Lee I.N., Suzuki C.K. CODAS syndrome is associated with mutations of LONP1, encoding mitochondrial AAA+ Lon protease. *Am J Hum Genet* 2015; 96(1):121-35.

Sulkowski M.S. Drug-induced liver injury associated with antiretroviral therapy that include HIV-1 protease inhibitors. *Clin Infect Dis* 2004; 38:S90-7.

Sulkowski M.S., Thomas D.L., Mehta S.H., Chaisson R.E., Moore R.D. Hepatotoxicity associated with nevirapine or efavirenz-containing antiretroviral therapy: role of hepatitis C and B infections. *Hepatology* 2002; 35(1):182-9.

Szabadkai G., Bianchi K., Várnai P., De Stefani D., Wieckowski M.R., Cavagna D., Nagy A.I., Balla T., Rizzuto R. Chaperone-mediated coupling of endoplasmic reticulum and mitochondrial Ca2+ channels. J Cell Biol 2006; 175(6):901-11.

Szklarczyk R., Nooteboom M., Osiewacz H.D. Control of mitochondrial integrity in ageing and disease. *Philos Trans R Soc Lond B Biol Sci* 2014; 369(1646):20130439.

Tabas I., Ron D. Integrating the mechanisms of apoptosis induced by endoplasmic reticulum stress. *Nat Cell Biol* 2011; 13(3):184-90.

Taguchi N., Ishihara N., Jofuku A., Oka T., Mihara K. Mitotic phosphorylation of dynamin-related GTPase Drp1 participates in mitochondrial fission. *J Biol Chem* 2007; 282(15):11521-9.

Tashima K.T., Bausserman L., Alt E.N., Aznar E., Flanigan T.P. Lipid changes in patients initiating efavirenz- and indinavir-based antiretroviral regimens. *HIV Clin Trials* 2003; 4(1):29-36.

Taylor S., Reynolds H., Sabin C.A., Drake S.M., White D.J., Back D.J., Pillay D. Penetration of efavirenz into the male genital tract: drug concentrations and antiviral activity in semen and blood of HIV-1-infected men. *AIDS* 2001; 15(15):2051-3.

Teng H., Wu B., Zhao K., Yang G., Wu L., Wang R. Oxygen-sensitive mitochondrial accumulation of cystathionine beta-synthase mediated by Lon protease. *Proc Natl Acad Sci U S A* 2013; 110(31):12679-84.

Thastrup O., Cullen P.J., Drøbak B.K., Hanley M.R., Dawson A.P. Thapsigargin, a tumor promoter, discharges intracellular Ca2+ stores by specific inhibition of the endoplasmic reticulum Ca2+-ATPase. *Proc Natl Acad Sci U S A* 1990; 87(7):2466-70.

Tian Q., Li T., Hou W., Zheng J., Schrum L.W., Bonkovsky H.L. Lon peptidase 1 (LONP1)-dependent breakdown of mitochondrial 5-aminolevulinic acid synthase protein by heme in human liver cells. *J Biol Chem* 2011; 286(30):26424-30.

Tsamis F., Gavrilov S., Kajumo F., Seibert C., Kuhmann S., Ketas T., Trkola A., Palani A., Clader J.W., Tagat J.R., McCombie S., Baroudy B., Moore J.P., Sakmar T.P., Dragic T. Analysis of the mechanism by which the small-molecule CCR5 antagonists SCH-351125 and SCH-350581 inhibit human immunodeficiency virus type 1 entry. *J Virol* 2003; 77(9):5201-8.

Tschopp J. Mitochondria: sovereign of inflammation? *Eur J Immunol* 2011; 41(5):1196-202.

Turner C., Schapira A.H. Mitochondrial dysfunction in neurodegenerative disorders and ageing. *Adv Exp Med Biol* 2001; 487:229-51.

Twig G., Elorza A., Molina A.J., Mohamed H., Wikstrom J.D., Walzer G., Stiles L., Haigh S.E., Katz S., Las G., Alroy J., Wu M., Py B.F., Yuan J., Deeney J.T., Corkey B.E., Shirihai O.S. Fission and selective fusion govern mitochondrial segregation and elimination by autophagy. *EMBO J* 2008; 27(2):433-46.

Urano F., Wang X., Bertolotti A., Zhang Y., Chung P., Harding H.P., Ron D. Coupling of stress in the er to activation of jnk protein kinases by transmembrane protein kinase ire1. *Science* 2000; 287(5453):664-6.

Van Luin M., Bannister W.P., Mocroft A., Reiss P., Di Perri G., Peytavin G., Molto J., Karlson A., Castagna A., Beniowski M., Lundgren J.D., Burger D.M. EuroSIDA Study Group. Absence of a relation between efavirenz plasma concentrations and toxicity-driven efavirenz discontinuations in the EuroSIDA study. *Antivir Ther* 2009; 14(1):75-83.

van Vliet A.R., Verfaillie T., Agostinis P. New functions of mitochondria associated membranes in cellular signaling. *Biochim Biophys Acta* 2014; 1843(10):2253-62.

Vance J.E. Phospholipid synthesis in a membrane fraction associated with mitochondria. *J Biol Chem* 1990; 265(13):7248-56.

Vangheluwe P., Raeymaekers L., Dode L., Wuytack F. Modulating sarco(endo) plasmic reticulum Ca^{2+} ATPase 2 (SERCA2) activity: cell biological implications. *Cell Calcium* 2005; 38(3-4):291-302.

Vannuvel K., Renard P., Raes M., Arnould T. Functional and morphological impact of ER stress on mitochondria. *J Cell Physiol* 2013; 228(9):1802-18.

Vecchione A., Fassan M., Anesti V., Morrione A., Goldoni S., Baldassarre G., Byrne D., D'Arca D., Palazzo J.P., Lloyd J., Scorrano L., Gomella L.G., Iozzo R.V., Baffa R. MITOSTATIN, a putative tumor suppressor on chromosome 12q24.1, is downregulated in human bladder and breast cancer. *Oncogene* 2009; 28(2):257-69.

Venkatesh S., Lee J., Singh K., Lee I., Suzuki C.K. Multitasking in the mitochondrion by the ATP-dependent Lon protease. *Biochim Biophys Acta* 2012; 1823(1):56-66.

Verfaillie T., Rubio N., Garg A.D., Bultynck G., Rizzuto R., Decuypere J.P., Piette J., Linehan C., Gupta S., Samali A., Agostinis P. PERK is required at the ER–mitochondrial contact sites to convey apoptosis after ROS-based ER stress. *Cell Death Differ* 2012; 19(11):1880-91.

Voelker D.R. Bridging gaps in phospholipid transport. *Trends Biochem Sci* 2005; 30(7):396-404.

Voss A.K., Thomas T., Gruss P. Mice lacking HSP90beta fail to develop a placental labyrinth. *Development* 2000; 127(1):1-11.

Walker U.A., Setzer B., Venhoff N. Increased long-term mitochondrial toxicity in combinations of nucleoside analogue reverse-transcriptase inhibitors. *AIDS* 2002; 16(16):2165-73.

Wallace D.C. Mitochondrial diseases in man and mouse. *Science* 1999; 283(5407):1482-8.

Wang N., Gottesman S., Willingham M.C., Gottesman M.M., Maurizi M.R. A human mitochondrial ATP-dependent protease that is highly homologous to bacterial Lon protease. *Proc Natl Acad Sci U S A* 1993; 90(23):11247-51.

Wang N., Maurizi M.R., Emmert-Buck L., Gottesman M.M. Synthesis, processing, and localization of human Lon protease. *J Biol Chem* 1994; 269(46):29308-13.

Wang X. The expanding role of mitochondria in apoptosis. *Genes Dev* 2001; 15(22):2922-33.

Wang X., Winter D., Ashrafi G., Schlehe J., Wong Y.L., Selkoe D., Rice S., Steen J., Lavoie M.J., Schwarz T.L. PINK1 and Parkin target Miro for phosphorylation and degradation to arrest mitochondrial motility. *Cell* 2011; 147(4):893-906.

Ward B.A., Gorski J.C., Jones D.R., Hall S.D., Flockhart D.A., Desta Z. The cytochrome P450 2B6 (CYP2B6) is the main catalyst of efavirenz primary and secondary metabolism: implication for HIV/AIDS therapy and utility of efavirenz as a substrate marker of CYP2B6 catalytic activity. *J Pharmacol Exp Ther* 2003; 306(1):287-300.

Wasiak S., Zunino R., Mcbride H.M. Bax/Bak promote SUMOylation of Drp1 and its stable association with mitochondria during apoptotic cell death. *J Cell Biol* 2007; 177(3):439-50.

Weber R., Sabin C.A., Friis-Moller N., Reiss P., El-Sadr W.M., Kirk O., Dabis F., Law M.G., Pradier C., De W.S., Akerlund B., Calvo G., Monforte A., Rickenbach M., Ledergerber B., Phillips A.N., Lundgren J.D. Liver-related deaths in persons infected with the human immunodeficiency virus: the D:A:D study. *Arch Intern Med* 2006; 166(15):1632-41.

Wei M.C., Zong W.X., Cheng E.H., Lindsten T., Panoutsakopoulou V., Ross A.J., Roth K.A., MacGregor G.R., Thompson C.B., Korsmeyer S.J. Proapoptotic bax and bak: A requisite gateway to mitochondrial dysfunction and death. *Science* 2001; 292(5517):727-30.

Wensing A.M., van Maarseveen N.M., Nijhuis M. Fifteen years of HIV Protease Inhibitors: raising the barrier to resistance. *Antiviral Res* 2010; 85(1):59-74.

Westermann B. Mitochondrial fusion and fission in cell life and death. *Nat Rev Mol Cell Biol* 2010; 11(12):872-84.

WHO and UNAIDS, 2016. In http://www.who.int/features/qa/71/en/index.html.

Wick A.N., Drury D.R., Nakada H.I., Wolfe J.B. Localization of the primary metabolic block produced by 2-deoxyglucose. *J Biol Chem* 1957; 224(2):963-9.

Wieckowski M.R., Giorgi C., Lebiedzinska M., Duszynski J., Pinton P. Isolation of mitochondria-associated membranes and mitochondria from animal tissues and cells. *Nat Protoc* 2009; 4(11):1582-90.

Williamson C.D., Colberg-Poley A.M. Access of viral proteins to mitochondria via mitochondria-associated membranes. *Rev Med Virol* 2009; 19(3):147-64.

Williamson C.D., Colberg-Poley A.M. Intracellular sorting signals for sequential trafficking of human cytomegalovirus UL37 proteins to the endoplasmic reticulum and mitochondria. J Virol 2010; 84(13):6400-9.

Wit F.W., Weverling G.J., Weel J., Jurriaans S., Lange J.M. Incidence of and risk factors for severe hepatotoxicity associated with antiretroviral combinationtherapy. *J Infect Dis* 2002; 186(1):23-31.

Wu C.W., Ping Y.H., Yen J.C., Chang C.Y., Wang S.F., Yeh C.L., Chi C.W., Lee H.C. Enhanced oxidative stress and aberrant mitochondrial biogenesis in human neuroblastoma SH-SY5Y cells during methamphetamine induced apoptosis. *Toxicol Appl Pharmacol* 2007; 220(3):243-51.

Wu S.B., Ma Y.S., Wu Y.T., Chen Y.C., Wei Y.H. Mitochondrial DNA mutation-elicited oxidative stress, oxidative damage, and altered gene expression in cultured cells of patients with MERRF syndrome. *Mol Neurobiol* 2010; 41(2-3):256-66.

Xu C., Bailly-Maitre B., Reed J.C. Endoplasmic reticulum stress: cell life and death decisions. *J Clin Invest* 2005; 115(10):2656-64.

Yang J., Liu X., Bhalla K., Kim C.N., Ibrado A.M., Cai J., Peng T.I., Jones D.P., Wang X. Prevention of apoptosis by Bcl-2: release of cytochrome c from mitochondria blocked. *Science* 1997; 275(5303):1129-32.

Yang Y., Liu B., Dai J., Srivastava P.K., Zammit D.J., Lefrançois L., Li Z. Heat shock protein gp96 is a master chaperone for toll-like receptors and is important in the innate function of macrophages. *Immunity* 2007; 26(2):215-26.

Yen W.L., Klionsky D.J. How to live long and prosper: autophagy, mitochondria, and aging. *Physiology (Bethesda)* 2008; 23:248-62.

Yi M., Weaver D., Hajnoczky G. Control of mitochondrial motility and distribution by the calcium signal: a homeostatic circuit. *J Cell Biol* 2004; 167(4):661-72.

Yoneda T., Benedetti C., Urano F., Clark S.G., Harding H.P., Ron D. Compartment-specific perturbation of protein handling activates genes encoding mitochondrial chaperones. *J Cell Sci* 2004; 117(Pt 18):4055-66.

Youle R.J., van der Bliek A.M. Mitochondrial fission, fusion, and stress. *Science* 2012; 337(6098):1062-5.

Yu W., Sun Y., Guo S., Lu B. The PINK1/Parkin pathway regulates mitochondrial dynamics and function in mammalian hippocampal and dopaminergic neurons. *Hum Mol Genet* 2011; 20(16):3227-40.

Zampese E., Fasolato C., Kipanyula M.J., Bortolozzi M., Pozzan T., Pizzo P. Presenilin 2 modulates endoplasmic reticulum (ER)–mitochondria interactions and Ca2+ cross-talk. *Proc Natl Acad Sci U S A* 2011(a); 108(7):2777-82

Zampese E., Fasolato C., Pozzan T., Pizzo P. Presenilin-2 modulation of ER–mitochondria interactions: FAD mutations, mechanisms and pathological consequences. *Commun Integr Biol* 2011(b); 4(3):357-60.

Zhang A., Williamson C.D., Wong D.S., Bullough M.D., Brown K.J., Hathout Y., Colberg-Poley A.M. Quantitative proteomic analyses of human cytomegalovirus-induced restructuring of endoplasmic reticulum–mitochondrial contacts at late times of infection. *Mol Cell Proteomics* 2011; 10(10):M111.009936.

Zhang Z., Liu L., Wu S., Xing D. Drp1, Mff, Fis1, and MiD51 are coordinated to mediate mitochondrial fission during UV irradiation-induced apoptosis. *FASEB J* 2016; 30(1):466-76.

Zhao Q., Wang J., Levichkin I.V., Stasinopoulos S., Ryan M.T., Hoogenraad N.J. A mitochondrial specific stress response in mammalian cells. *EMBO J* 2002; 21(17):4411-9.

Zhdanov A.V., Dmitriev R.I., Papkovsky D.B. Bafilomycin A1 activates respiration of neuronal cells via uncoupling associated with flickering depolarization of mitocondria. *Cell Mol Life Sci* 2011; 68(5):903-17.

Zheng Y.H., Lovsin N., Peterlin B.M. Newly identified host factors modulate HIV replication. *Immunol Lett* 2005; 97(2):225-34.

Zhou H., Gurley E.C., Jarujaron S., Ding H., Fang Y., Xu Z., Pandak W.M. Jr., Hylemon P.B. HIV protease inhibitors activate the unfolded protein response and disrupt lipid metabolism in primary hepatocytes. *Am J Physiol Gastrointest Liver Physiol* 2006; 291(6):G1071-80.

Zhou R., Yazdi A.S., Menu P., Tschopp J. A role for mitochondria in NLRP3 inflammasome activation. *Nature* 2011; 469(7329):221-5.

Zhu P.P., Patterson A., Stadler J., Seeburg D.P., Sheng M., Blackstone C. Intra- and intermolecular domain interactions of the C-terminal GTPase effector domain of the multimeric dynamin-like GTPase Drp1. *J Biol Chem* 2004; 279(34):35967-74.

Zhu X.H., Wang C.H., Tong Y.W. Growing tissue-like constructs with Hep3B/HepG2 liver cells on PHBV microspheres of different sizes. *J Biomed Mater Res B Appl Biomater* 2007; 82(1):7-16.

Zick M., Rabl R., Reichert A.S. Cristae formation-linking ultrastructure and function of mitochondria. *Biochim Biophys Acta* 2009; 1793(1):5-19.

Zinszner H., Kuroda M., Wang X., Batchvarova N., Lightfoot R.T., Remotti H., Stevens J.L., Ron D. Chop is implicated in programmed cell death in response to impaired function of the endoplasmic reticulum. *Genes Dev* 1998; 12(7):982-95.

Zorzano A., Liesa M., Palacin M. Role of mitochondrial dynamics proteins in the pathophysiology of obesity and type 2 diabetes. *Int J Biochem Cell Biol* 2009; 41(10):1846-54.

Zuchner S., Vance J.M. Mechanisms of disease: a molecular genetic update on hereditary axonal neuropathies. *Nat Clin Pract Neurol* 2006; 2(1):45-53.

Zuehlke A.D., Beebe K., Neckers L., Prince T. Regulation and function of the human HSP90AA1 gene. *Gene* 2015; 570(1):8-16.

ANNEX

BIBLIOGRAPHIC PRODUCTION RELATED TO THIS THESIS

- Authors: BLAS-GARCIA A., **POLO M**., ALEGRE F., FUNES H.A., MARTINEZ E., APOSTOLOVA N., ESPLUGUES J.V. Title: Lack of mitochondrial toxicity of darunavir, raltegravir and rilpivirine in neurons and hepatocytes: a comparison with efavirenz. *Journal of Antimicrobial Chemotherapy* 2014; 69(11):2995-3000.
- Authors: **POLO M**., ALEGRE F., FUNES H.A., BLAS-GARCIA A., VICTOR V.M., ESPLUGUES J.V., APOSTOLOVA N. Title: Mitochondrial (dys)function-a factor underlying the variability of EFV-induced hepatotoxicity? *British Journal of Pharmacology* 2015; 172(7):1713-1727.
- Authors: APOSTOLOVA N., FUNES H.A., BLAS-GARCIA A., ALEGRE F., **POLO M**., ESPLUGUES J.V. Title: Involvement of nitric oxide in the mitochondrial action of efavirenz: a differential effect on neurons and glial cells. *Journal of Infectious Diseases* 2015; 211(12):1953-1958.
- Authors: BLAS-GARCIA A., MARTI-RODRIGO A. **POLO M**., ALEGRE F., FUNES H.A., VICTOR V.M., APOSTOLOVA N., ESPLUGUES J.V. Title: The purine analogues abacavir and didanosine increase acetaminophen-induced hepatotoxicity by enhancing mitochondrial dysfunction. *Journal of Antimicrobial Chemotherapy* 2016; 71(4):916-926.
- Authors: **POLO M**., ALEGRE F., GIBELLINI L., MARTI-RODRIGO A., BLAS-GARCIA A., ESPLUGUES J.V., APOSTOLOVA N. Title: Lon protease: a novel function in the interconnection between mitochondrial dysfunction and ER stress. *British Journal of Pharmacology*. Under review.
- Authors: ALEGRE F., MARTI-RODRIGO A., **POLO M**., ORTIZ-MASIA D., PINTI M., APOSTOLOVA N., ESPLUGUES J.V., BLAS-GARCIA A. Title: Modulation by macrophages of hepatic injury involving NLRP3 inflammasome activation: the example of Efavirenz. *Hepatology.* Under review.